LAMS-2526

27

LOS ALAMOS SCIENTIFIC LABORATORY

OF THE UNIVERSITY OF CALIFORNIA o LOS ALAMOS NEW MEXICO

S-4 REPORT SECTION

REPRODUCTION COPY

BIOLOGICAL AND MEDICAL RESEARCH GROUP (H-4)
OF THE HEALTH DIVISION - SEMIANNUAL REPORT
JULY THROUGH DECEMBER 1960

LEGAL NOTICE

This report was prepared as an account of Government sponsored work. Neither the United States, nor the Commission, nor any person acting on behalf of the Commission:

A. Makes any warranty or representation, expressed or implied, with respect to the accuracy, completeness, or usefulness of the information contained in this report, or that the use of any information, apparatus, method, or process disclosed in this report may not infringe privately owned rights; or

B. Assumes any liabilities with respect to the use of, or for damages resulting from the use of any information, apparatus, method, or process disclosed in this report.

As used in the above, "person acting on behalf of the Commission" includes any employee or contractor of the Commission, or employee of such contractor, to the extent that such employee or contractor of the Commission, or employee of such contractor prepares, disseminates, or provides access to any information pursuant to his employment or contract with the Commission, or his employment with such contractor.

LAMS-2526
BIOLOGY AND MEDICINE
(TID-4500, 16th Ed.)

LOS ALAMOS SCIENTIFIC LABORATORY
OF THE UNIVERSITY OF CALIFORNIA LOS ALAMOS NEW MEXICO

REPORT WRITTEN: January 1961

REPORT DISTRIBUTED: April 24, 1961

BIOLOGICAL AND MEDICAL RESEARCH GROUP (H-4) OF THE HEALTH DIVISION - SEMIANNUAL REPORT JULY THROUGH DECEMBER 1960

Group Leader, W. H. Langham
Division Leader, T. L. Shipman

Contract W-7405-ENG. 36 with the U. S. Atomic Energy Commission

CONTENTS

CHAPTER 1

INTRODUCTION

This document is the third semiannual report of the activities of the Biological and Medical Research Group of the Los Alamos Scientific Laboratory's Health Division. The previous reports were LAMS-2445 and LAMS-2455.

The format of the present report is essentially the same as in the past with the Group's activities divided into biochemistry, low-level counting, organic chemistry, radiobiology, radiopathology, and veterinary services, each constituting a chapter. A more complete table of contents, however, has been added.

For several years, the Group has been pioneering in the development and use of organic scintillators for the measurement of low-level radioactivity. During the present report period, the Group had its second opportunity to make a major contribution to the planning and conducting of an international symposium on the subject. As in 1957, when Group personnel were involved in organizing the Northwestern University

Conference on Scintillation Counting, E. C. Anderson, D. G. Ott, and F. N. Hayes worked on the Program and Arrangements Committees for the International Conference held at the University of New Mexico on August 15-17, 1960. In attendance were 223 delegates from 9 countries. Twenty-two papers were presented, and the proceedings will be published by the AEC's Office of Technical Information in Oak Ridge with Elizabeth Sullivan and F. N. Hayes on the editorial staff.

During this report period, the Group also participated in Nevada tests of the prototype nuclear rocket propulsion reactors, Kiwi-A Prime and Kiwi-A Three. Participation consisted of fallout measurements and measurements of neutron and gamma ray dose rates and integral doses, under shielded and free air conditions.

As of December 31, 1960, the personnel of the Group, their qualifications, classification, and Group and Section affiliations were as shown in the following table of organization.

GROUP H-4
BIOMEDICAL RESEARCH

W. H. Langham, Ph.D., Leader
O. S. Johnson, Alt. Ldr. for Administration
E. M. Sullivan, Group Secretary

MOLECULAR RADIOBIOLOGY

F. N. Hayes, Ph.D., Leader

Staff Members

V. N. Kerr, M.A.
A. Murray, M.S.
D. G. Ott, Ph.D.
D. F. Petersen, Ph.D.
D. L. Williams, M.S.

Research Assistants

L. B. Cole, M.S.
E. Hansbury, M.A.
E. H. Lilly, B.S.

Technical Staff

M. Magee
V. E. Mitchell

CELLULAR RADIOBIOLOGY

I. U. Boone, M.D., Leader

Staff Member

H. Foreman, M.D., Ph.D.

Research Assistants

L. T. Rivera, B.S.
P. C. Sanders, M.S.

CLINICAL INVESTIGATIONS

C. C. Lushbaugh, M.D., Leader

Research Assistants

D. B. Hale, B.S.
G. L. Humason, M.S.
J. M. Wellnitz, A.B.

Technical Staff

N. J. Basmann

LOW-LEVEL COUNTING

E. C. Anderson, Ph.D., Leader

Staff Members

*J. H. Larkins, B.S.
J. D. Perrings
R. L. Schuch
M. A. Van Dilla, Ph.D.
G. M. Ward, Ph.D.

Research Assistant

M. W. Rowe, B.S.

*Casual employee.

TABLE OF ORGANIZATION GROUP H-4 AS OF DECEMBER 31, 1960

GROUP H-4 (continued)

MAMMALIAN METABOLISM

C. R. Richmond, Ph.D., Leader

Staff Member

J. E. Furchner, Ph.D.

Research Assistant

G. A. Trafton, B.S.

MAMMALIAN RADIOBIOLOGY

J. F. Spalding, Ph.D., Leader

Staff Members

J. A. Sayeg, Ph.D.
T. T. Trujillo, B.S.

Technical Staff

R. F. Archuleta
V. G. Strang

VETERINARY SERVICES

O. S. Johnson, B.S., Leader

Animal Caretakers

J. M. Alire
F. Archuleta
S. E. Cordova
J. Lovato
R. Martinez
L. Ortiz
A. Trujillo
D. Valdez
F. Valdez

CHAPTER 2

BIOCHEMISTRY SECTION

Long-Term Retention of Zinc^{65} by Man (C. R. Richmond, J. E. Furchner, and W. H. Langham)

INTRODUCTION

A previous report (1) from this Laboratory summarized the results of experiments on the retention of $Zn^{65}Cl_2$ by 4 species of mammals. Retention functions covering a period of approximately 1 yr were obtained for 2 human subjects and were resolved into 3 exponential components by a 704 computer method. The parameters which described the retention functions were used to calculate equilibrium levels and maximum permissible concentration values. The data strongly suggested that additional components were not needed to describe retention for times in excess of 1 yr. It was decided to continue retention measurements for both subjects until the body activities approached the lower limits of the detecting system. The entire time-course of Zn^{65} retention

could then be compared with the retention patterns previously reported.

METHODS AND RESULTS

Whole body retention experiments were terminated at 664 and 579 days following acute oral administration for [redacted] and [redacted], respectively. Differences in gastrointestinal absorption and size of the administered dose were the major factors which determined the duration of the experiments. The biological retention was calculated from the relation

$$\text{Biological Retention} = \left(\frac{\text{Subj. } Zn^{65} \text{ Activity}}{\text{Std. } Zn^{65} \text{ Activity}}\right)_t \Big/ \left(\frac{\text{Subj. } Zn^{65} \text{ Activity}}{\text{Std. } Zn^{65} \text{ Activity}}\right)_o$$

where the subscripts t and o refer to the times after Zn^{65} administration. An iterative least square 704 computer procedure was used to obtain the best fit to the experimental data. Each value of Y (per cent retention) was weighted by a factor proportional to 1/Y (statistical weighting). Use of this weighting procedure simply assures that the points with the larger variances will have a smaller influence on the final fit, while those with the smaller variances will have more influence (2).

Each biological retention curve was fitted by a function of the form

$$Y = \sum_i^3 \left[a_i e^{-(k_i t)} \right]$$

Retention parameters calculated from data collected from [redacted] over 664 days agree well with those from data obtained during the first 387 days of the experiment (Table 1). Similarly, good agreement was found between the values derived for [redacted] from data collected during the first 344 days and those collected during the entire retention period of 579 days (Table 2), i.e.,

$$\text{Effective Retention} = \sum_{1}^{3} \left[a_i e^{-k_i} + \lambda t \right]$$

from t_o to t_∞. Total area under the retention curve corresponds to the equilibrium level, expressed as per cent of the daily intake, which would be attained during conditions of chronic exposure.

Equilibrium levels are important as, in most cases, estimates of $(MPC)_w$ are based on a model which assumes a constant intake of P μc/day and exponential loss from the body (3). Because a maximum permissible body burden (q, μc) is also recommended, the $(MPC)_w$ value is simply the maximum permissible concentration (μc/ml water) which can be taken in continuously without exceeding q, when conditions of equilibrium are established.

Tables 1 and 2 show that the equilibrium level for each subject is essentially unchanged. The values obtained from the short-term data were within 1 per cent of those obtained

TABLE 1. COMPARISON OF SHORT-TERM (0 TO 387 DAYS) AND LONG-TERM (0 TO 664 DAYS) ZINC^{65} RETENTION IN A HUMAN SUBJECT [redacted]

Component	a (per cent)	k (fraction per day)	k + λ (fraction per day)	T (days)	Area, Effective* (per cent days)	Area, Effective* (per cent of total)
1	38.50 (38.80) **	2.520122 (2.471285)	2.522972 (2.474135)	0.27 (0.28)	--	0.14 (0.14)
2	11.36 (11.37)	0.154890 (0.142755)	0.157740 (0.145605)	4.39 (4.86)	--	0.64 (0.69)
3	50.15 (49.84)	0.001638 (0.001580)	0.004488 (0.004430)	154.3 (156.39)	--	99.22 (99.17)
Total	100.01 (100.01)	--	--	--	11,255 (11,337)	100.00 (100.00)

*Effective area (per cent days) = $\sum_i \left[\frac{a_i}{k_i + \lambda}\right]$.

**Values in parentheses were obtained from the function which described retention of Zn^{65} by [redacted] from 0 to 387 days (1).

TABLE 2. COMPARISON OF SHORT-TERM (0 TO 344 DAYS) AND LONG-TERM (0 TO 579 DAYS) ZINC^{65} RETENTION IN A HUMAN SUBJECT [redacted]

Component	a (per cent)	k (fraction per day)	k + λ (fraction per day)	T (days)	Area, Effective* (per cent days)	Area, Effective* (per cent of total)
1	9.26 (8.89)**	0.745224 (0.787739)	0.748077 (0.790591)	0.93 (0.88)	--	0.08 (0.07)
2	24.37 (22.80)	0.027742 (0.031581)	0.030594 (0.034433)	22.66 (20.13)	--	4.89 (4.10)
3	66.63 (68.57)	0.001452 (0.001584)	0.004304 (0.004437)	161.04 (156.25)	--	95.03 (95.83)
Total	100.26 (100.26)	--	--	--	16,290 (16,131)	100.00 (100.00)

*Effective area (per cent days) = $\sum_{1}^{3}\left[\frac{a_i}{k_i + \lambda}\right]$.

**Values in parentheses were obtained from the function which described retention of Zn^{65} by [redacted] from 0 to 344 days (1).

from the long-term data. This agreement is virtually the same for all parameters.

DISCUSSION

The observation that retention of Zn^{65} by mice, rats, and dogs could be expressed by a 3 component exponential function, when measured to $\sim$ 1 per cent of the initial burden, suggested that a similar function would describe the retention of Zn^{65} by human subjects. This report shows that no more than 3 components seem necessary to describe Zn^{65} retention by human subjects.

In addition, the precision of the interspecific relation between "effective area" and species weight (1) has not been affected by the long-term data. Additional subjects are currently being measured to obtain more information on the variations among people and to test further the interspecies relation.

REFERENCES

(1) C. R. Richmond, J. E. Furchner, and G. A. Trafton, Los Alamos Scientific Laboratory Report LAMS-2445 (1960), p. 80.

(2) R. H. Moore and R. K. Zeigler, Los Alamos Scientific Laboratory Report LA-2367 (1960), p. 12.

(3) Report of the International Commission on Radiological Protection, Committee II, on Permissible Dose for Internal Radiation (1959), Health Phys. 3, 16 (1960).

Modification of Zinc^{65} Absorption by Dietary Zinc Intake

(J. E. Furchner, C. R. Richmond, and G. A. Trafton)

INTRODUCTION

Although much is known about the metabolism of the essential trace element zinc, factors which affect its absorption from the gut are relatively unknown (1). Mager et al. (2) suggested that fecal excretion of Zn^{65} by man may depend on saturation of the intestinal epithelial tissue. Previous work at this Laboratory (3) showed that in 2 humans, 1 absorbed ~ 60 per cent and the other ~ 90 per cent of an oral dose. Work presently in progress shows absorption in humans may range between 30 and 90 per cent. The present experiment was designed to test the effect of differing levels of zinc in the diet on the absorption of orally administered Zn^{65}.

METHODS AND RESULTS

Fifty-four male Sprague-Dawley rats, 112 days of age, were randomly assigned to 6 groups of 9 rats each and placed on normal ground Purina Lab Chow and water ad libitum for a conditioning period of 2 weeks. The Purina Lab Chow was pulverized in a meat grinder to facilitate subsequent mixing with powdered zinc acetate in a Patterson-Kelley twin-shell laboratory blender. The Ralston-Purina Company gives the

normal zinc content of Purina Lab Chow as 58.6 ppm. The acetate was added to the pulverized Purina Lab Chow in quantities sufficient to make diets containing 1 (control), 2, 3, 5, 7, and 11 times the normal zinc content. After 28 days of feeding groups of animals on each of these diets, each animal was given 1.2 μc of $Zn^{65}Cl$ by gastric gavage. The individual rats were assayed for radioactivity by whole body counting techniques 30 min after administration and 1, 2, 4, 7, and 11 days thereafter. The results are given in Fig. 1, where the retention on the various days after administration is plotted as a function of the dietary level of zinc. The points represent group averages. One series of measurements (293 ppm) lie above the eye-fit lines drawn for days 2, 4, 7, and 11. This displacement is due to 1 animal in that group whose retention was, for unknown reasons, between 2 and 3 times the mean retention of the group. The data show that per cent retention on the first day decreased slowly with increasing level of dietary zinc. Retention on the second day, however, decreased greatly as the level of dietary zinc increased and retention levels on subsequent days paralleled that of the second day. These observations strongly suggest that zinc absorption from the gut is modified by the level in the diet. Extrapolation to zero zinc levels suggests increased retention at subnormal levels of zinc intake.

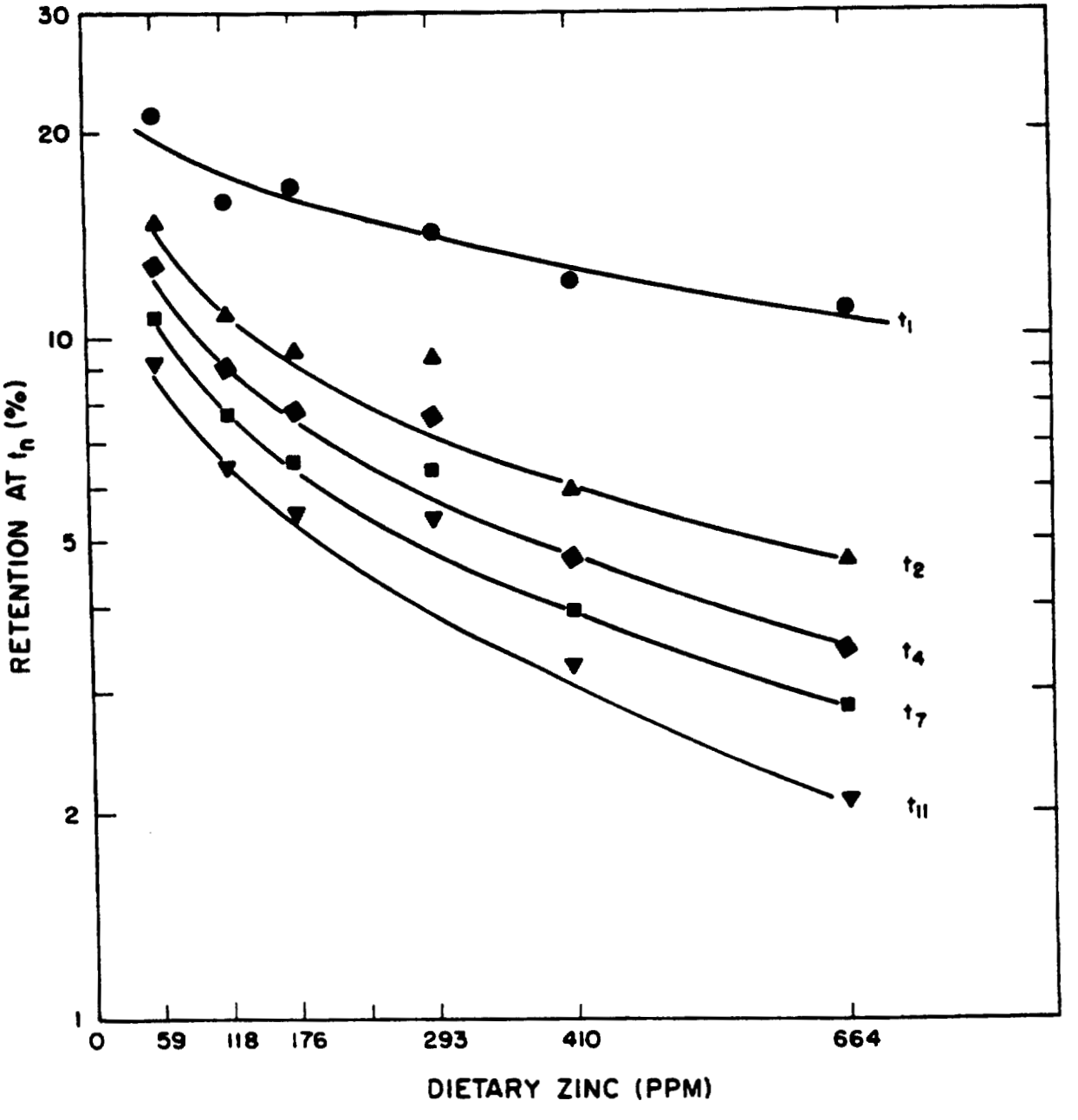

Fig. 1. The effect of dietary zinc on the retention of orally administered Zn^{65} by rats at various times after administration.

DISCUSSION

Elevated levels of dietary zinc apparently affect the absorption of orally administered Zn^{65} in rats. Although this experiment does not test subnormal levels of zinc intake, it does indicate that such dietary levels may enhance the absorption of tracer doses of Zn^{65}. This aspect of the problem will be investigated.

It is possible that differences in dietary zinc levels may contribute to the wide range of absorption observed in humans. Recent work (4) indicates that absorption of Mg^{28} by man is also influenced by the load presented to the intestinal mucosa, but is not linearly related to the load. At present there are no experimental data available to evaluate the effect of dietary zinc on gastrointestinal absorption of zinc in humans.

REFERENCES

(1) E. J. Underwood, Trace Elements in Human and Animal Nutrition, Academic Press, New York (1956).

(2) M. Mager, F. M. McNary, Jr., and F. Lionetti, J. Histochem. Cytochem. 1, 493 (1953).

(3) C. R. Richmond, J. E. Furchner, and G. A. Trafton, Los Alamos Scientific Laboratory Report LAMS-2445 (1960), p. 80.

(4) L. A. Graham, J. J. Caesar, and A. S. V. Burgen, Metabolism 9, 646 (1960).

Estimation of Maximum Permissible Concentrations of Radioisotopes in Water $(MPC)_w$ from Interspecies Correlations. I. Comparison of Estimated and Measured Values for Zinc^{65} and Tritium

(C. R. Richmond, J. E. Furchner, and W. H. Langham)

INTRODUCTION

In essence, the maximum permissible concentration of a radioactive material is that amount of activity per cubic centimeter of air or water which may be taken into the body continuously without exceeding a recommended activity (q) in a specific tissue, when conditions of equilibrium are reached. Integration of the effective retention function from t_o to t_∞ gives the total area under the curve. The area is an estimate of the equilibrium level in terms of multiples of the daily intake. Estimates of $(MPC)_w$ values can then be obtained from the following relation:

$$(MPC)_w = \frac{q}{(A)\ (I)} \qquad \text{(Eq. 1)}$$

where q is the maximum permissible body burden, I is the daily intake of water, and A is the equilibrium level or the area under the retention function. This report shows how A can be estimated from interspecies correlations.

METHODS AND RESULTS

The areas under the effective retention functions for mice,

rats, dogs, and humans given an acute dose of Zn^{65} were shown to be a power function of species weight (1). Similarly, experiments with HTO in mice, rats, rabbits, dogs, horses, and human subjects (2) have yielded the necessary retention parameters from which equilibrium levels may be calculated.

Figure 1 shows the relationship between equilibrium level and species weight for Zn^{65}. The regression line, calculated from mouse, rat, and dog data, is shown as a broken line over the extrapolated range to man. Measured equilibrium values shown for the 2 human subjects were not used in calculating the line. When the whole body is the critical organ, the value of q for Zn^{65} is 60 μc (3). If a value of 2200 ml is assigned as the daily water intake for man, $(MPC)_w$ for Zn^{65} can be estimated from Eq. 1 and the equilibrium level for man (A) determined by the extrapolation shown in Fig. 1. Table 1 gives the $(MPC)_w$ value most recently recommended by the International Commission on Radiological Protection (3) and those obtained from the interspecies correlation.

Figure 2 shows the interspecific correlation between equilibrium level and species weight for HTO. The value for the human subjects was not included in the calculation of the line. Table 2 gives the most recent I. C. R. P. $(MPC)_w$ for

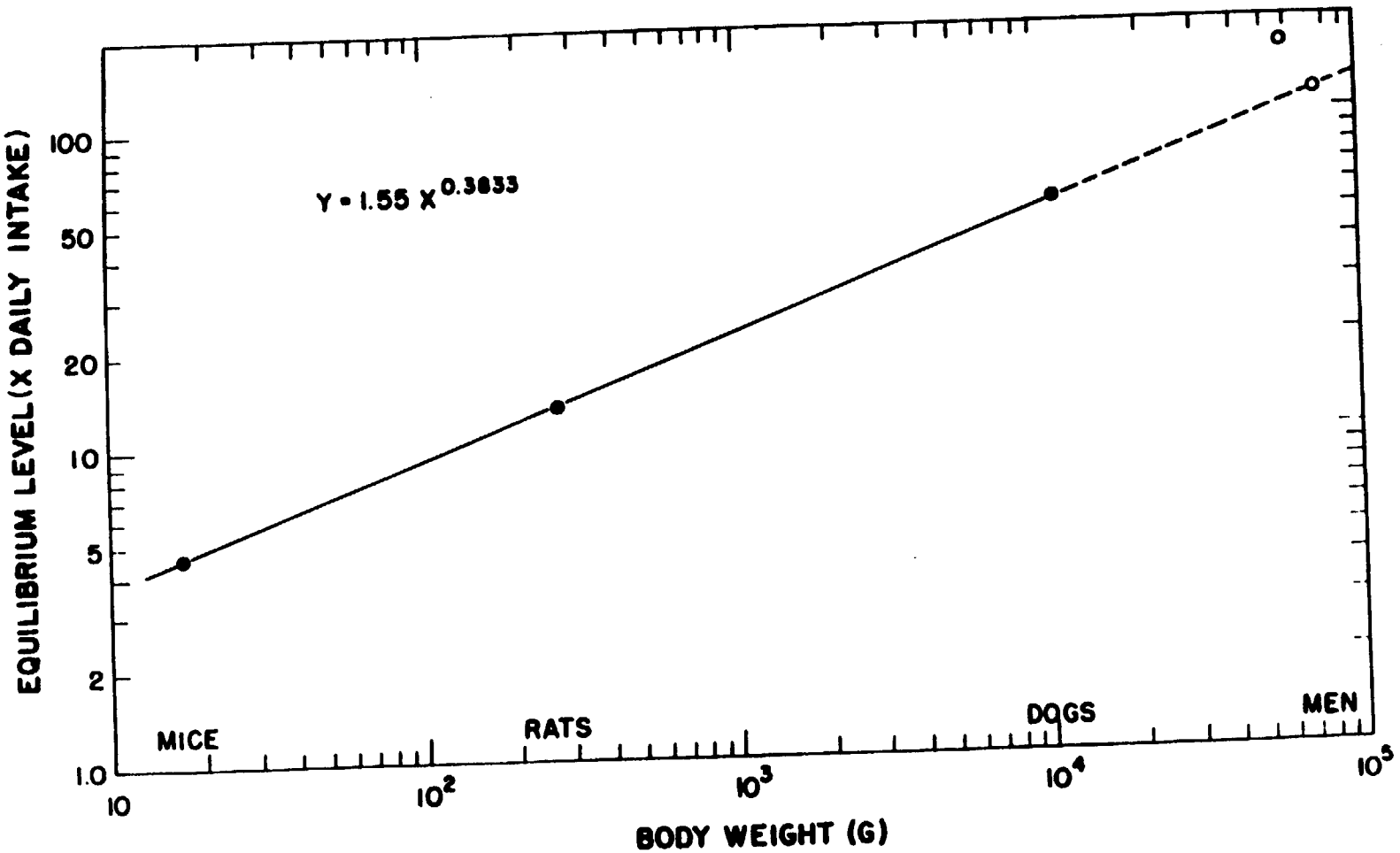

Fig. 1. Interspecies correlation between equilibrium retention level of Zn^{65} and species weight.

TABLE 1. MAXIMUM PERMISSIBLE CONCENTRATION OF $ZINC^{65}$ IN WATER $(MPC)_w$ FOR CONTINUOUS EXPOSURE

Source of Value	$(MPC)_w$ ($\mu c/ml$)
I. C. R. P. Recommendation (1960)	10^{-3}
Calculated from Human Data ([redacted])	2.4×10^{-4}
Calculated from Human Data ([redacted])	1.7×10^{-4}
Calculated from Interspecies Extrapolation*	2.4×10^{-4}

$$*(MPC)_w = \frac{q}{(A)\ (I)} = \frac{60}{\left[1.55\ (70{,}000)^{0.3833}\right]\left[2200\right]}$$

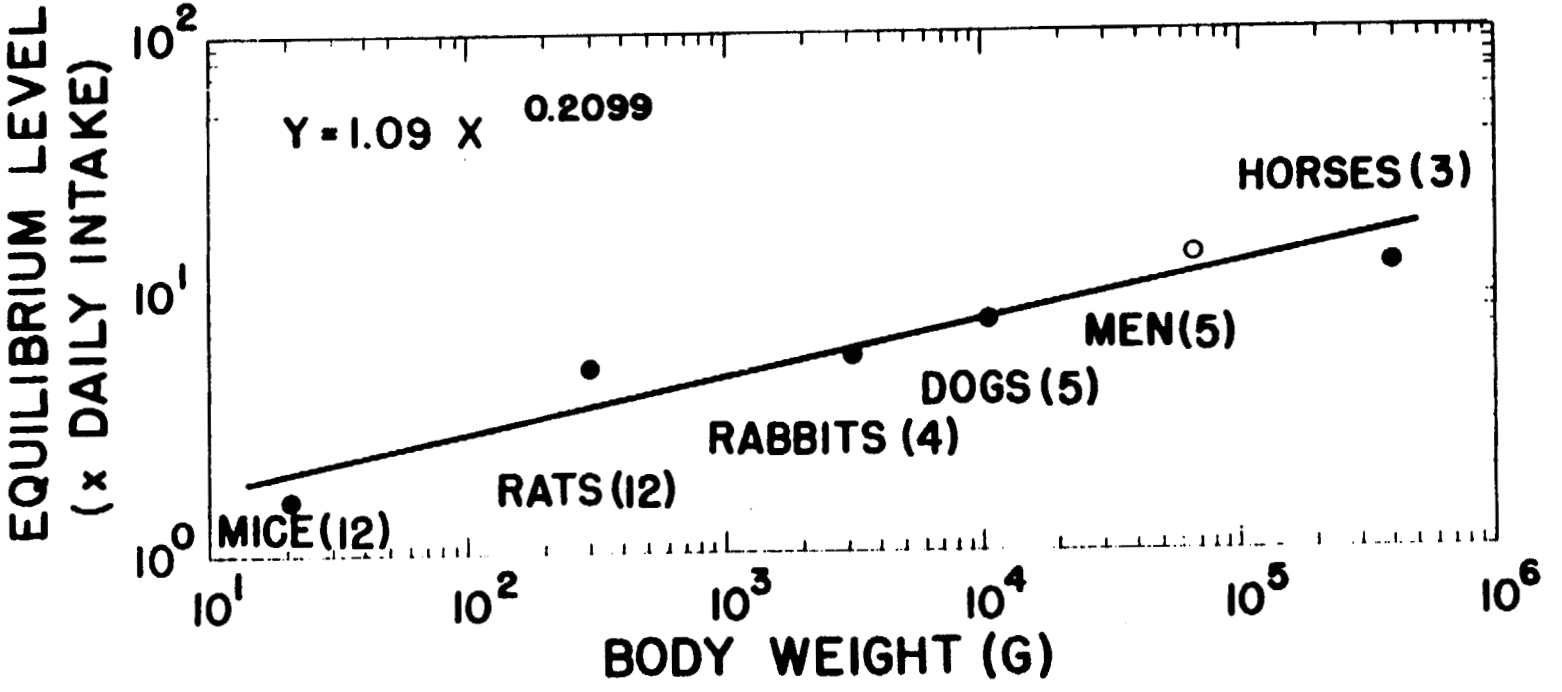

Fig. 2. Interspecies correlation between equilibrium retention level of tritium (as HTO) and species weight.

TABLE 2. MAXIMUM PERMISSIBLE CONCENTRATION OF TRITIUM IN WATER $(MPC)_w$ FOR CONTINUOUS EXPOSURE

Source of Value	$(MPC)_w$ ($\mu c/ml$)
I. C. R. P. Recommendation (1960)	5×10^{-2}
Calculated from Human Data	7×10^{-2}
Calculated from Interspecies Extrapolation	6×10^{-2}
Calculated from Interspecies Interpolation*	8×10^{-2}

$$*(MPC)_w = \frac{q}{(A)\ (I)} = \frac{2000}{\left[1.09\ (70{,}000)^{0.2099}\right]\left[2200\right]}$$

HTO and those obtained from this study. A single rate of elimination is assumed for all species. Admittedly, the organic binding of tritium in animals represents a small fraction of the total administered dose and would have a small effect on the equilibrium level. However, because organically bound tritium does not begin to show up until the retention function has dropped approximately 5 decades (4), its long-term retention is not considered significant in the present calculation.

Because horses were available for the HTO study, it was possible to interpolate an equilibrium value for man from Fig. 2 and to estimate an $(MPC)_w$ value. When the horses were not included in the calculation of the interspecies correlation, extrapolation to man was possible. The interspecies correlation, in this case, was:

$$Y = 0.90\ X^{0.2488}$$

The $(MPC)_w$ values resulting from both extrapolation and interpolation are given in Table 2, assuming daily water intake was 2200 ml and q 2000 μc (3). The values are in good agreement with each other and with that presently recommended by the I. C. R. P.

DISCUSSION

Of necessity, most of the presently recommended $(MPC)_w$ values are determined from experiments on laboratory animals. Unfortunately, no rational basis is available for extrapolation to man and, in most cases, the data obtained from small animals are merely substituted.

This report gives a basis for such an extrapolation from small animals to man and presents human data to demonstrate the validity of the extrapolation. Without additional refinements, the method presented here is restricted to cases in which the whole body is the critical tissue and the time required for equilibrium to be reached is less than the exposure time (i.e., assumed to be 50 yr). There is no assurance, however, that such relations exist for all radionuclides. When a tissue other than the whole body is the critical tissue, the equilibrium level for that tissue must be determined before this method can be used.

REFERENCES

(1) C. R. Richmond, J. E. Furchner, and G. A. Trafton, Los Alamos Scientific Laboratory Report LAMS-2445 (1960), p. 80.

(2) C. R. Richmond, T. T. Trujillo, and W. H. Langham, Los Alamos Scientific Laboratory Report LAMS-2445 (1960), p. 94.

(3) Report of the International Commission on Radiological Protection, Committee II, on Permissible Dose from Internal Radiation (1959), Health Phys. 3 (1960).

(4) E. A. Pinson and W. H. Langham, J. Appl. Physiol. 10, 108 (1957).

Retention and Excretion of Orally Administered Cesium^{137} by Mice. II. Prediction of Retention after Chronic Exposure

(J. E. Furchner, C. R. Richmond, and G. A. Trafton)

INTRODUCTION

In a previous report (1), a comparison was made between predicted and actual equilibrium levels in mice exposed to constant Cs^{137} levels in the drinking water. The predicted levels were derived from integration of the retention equation obtained from a single acute exposure. The change in retention levels after withdrawal from chronic exposure also should be predictable, and the following report gives the method and results of such a prediction.

METHODS AND RESULTS

Mice that had been exposed to a constant level of Cs^{137} (as the chloride) in drinking water for 100 days were measured at suitable intervals after cessation of the chronic exposure. The results are plotted in Fig. 1, where day zero is the first day of withdrawal from Cs^{137} and 100 per cent is the activity measured on that day. The points are derived from measurements made on the designated days.

Previous experiments at this Laboratory (2) showed that the retention parameters obtained from mice exposed to a single oral dose of Cs^{137} varied as a function of age between

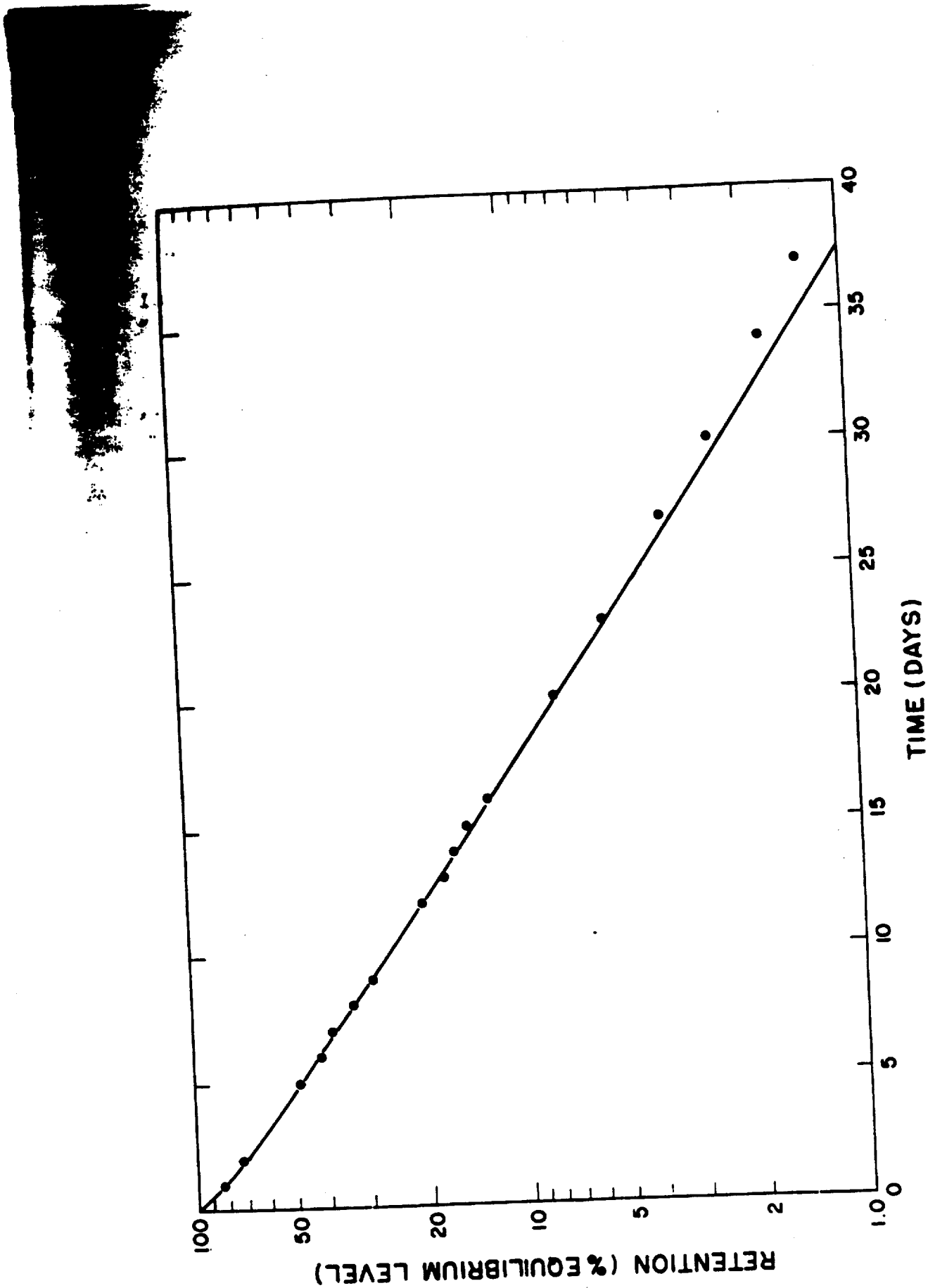

Fig. 1. Comparison of predicted and measured retention of Cs^{137} by mice following chronic oral administration.

4 and 51 weeks. Because the chronically exposed mice were 12 weeks old at the initiation of the exposure and because the chronic exposure was of 14 weeks duration, an acute oral dose of Cs^{137} was administered to a group of controls (12 weeks of age at the beginning of the study) coincident with the beginning and termination of the experiment involving chronic exposure. No residual activity from the first dose remained in the controls at the time of the second exposure. The parameters of the retention equation obtained from the first acute dose were used to predict equilibrium levels in the chronic exposure experiment. The parameters of the retention equation obtained from the second acute dose were used to predict the retention pattern after cessation of chronic exposure. While the parameters obtained from the first acute exposures were adequate for predicting equilibrium levels, they failed to describe retention after termination of chronic exposure. However, the predicted fall-off, shown by the solid line in Fig. 1, agrees reasonably well with the measured values represented by the points. The equation used for prediction was of the form

$$R_t = \sum_i^3 \left[\frac{a_i}{k_i} e^{-k_i t} \right]$$

where the a's and the k's are the intercept and rate constants of the control retention equation.

DISCUSSION

The use of the retention patterns of acute exposures for predicting equilibrium levels during chronic exposures is a common practice, which has rarely been subjected to experimental verification. The present experiment provides additional justification for such practice. However, chronic exposures of much greater duration would give more information about changes in equilibrium levels due to age differences. In addition, isotopes whose retention patterns are described by power functions might also be tested by chronic exposures.

REFERENCES

(1) J. E. Furchner, C. R. Richmond, and G. A. Trafton, Los Alamos Scientific Laboratory Report LAMS-2455 (1960), p. 9.

(2) J. E. Furchner, C. R. Richmond, and G. A. Trafton, Los Alamos Scientific Laboratory Report LAMS-2455 (1960), p. 14.

Enhancement of Cesium^{137} Excretion by Rats Fed Potassium-Supplemented Diets (C. R. Richmond, J. E. Furchner, B. E. Cummins, and G. A. Trafton)

INTRODUCTION

Possible enhancement of Cs^{137} excretion is of importance as it is a high yield product of uranium and plutonium fission and ranks high on the list of the potentially hazardous by-products of peaceful applications of nuclear energy.

Published studies regarding enhancement of Cs^{137} excretion by laboratory animals through increased potassium intake are still somewhat inconclusive. Many of the results are questionable, as potassium-deficient semisynthetic diets were used for the control animals. It is known that the feeding of diets deficient in a specific element causes pronounced perturbations from the normal metabolic pattern obtained for that element. In addition, potassium-deficient diets are also deficient in other elements (i.e., magnesium) and cause renal damage (1,2).

METHODS

Thirty male Sprague-Dawley rats, 84 days old (average weight 317.5 g), were divided into 5 equal groups. One group was fed ground Purina Lab Chow (basal diet), another was fed a commercially supplied potassium-deficient diet, and the

remaining 3 groups were fed the basal diet supplement with varying amounts of potassium added as the chloride. The potassium concentration was ~ 1 per cent for the basal diet (3), and 5, 8, and 11 per cent for the supplemented diets. A Patterson-Kelley twin-shell laboratory blender was used to facilitate mixture of the basal diet and the potassium supplements. All animals were fed the basal diet for several days in order to acclimate themselves to the pulverized food and special feeders.

Immediately after intraperitoneal injection of 0.65 μc carrier-free Cs^{137} per animal, each group was placed on its specific dietary regimen. Animals were counted individually at 30 min following injection and at suitable intervals thereafter in a whole-body liquid scintillation counter (4). Whole-body retention at each time of measurement was calculated by a standardized procedure given elsewhere in this report (5).

Approximately 80 days after injection, 3 of the animals fed the potassium-deficient diet had died, and the survivors were placed on basal diet for the remainder of the experiment.

RESULTS AND DISCUSSION

Data showing the mean whole-body retention values for each group as a function of time are given in Fig. 1. The time-course of Cs^{137} retention for the control animals is

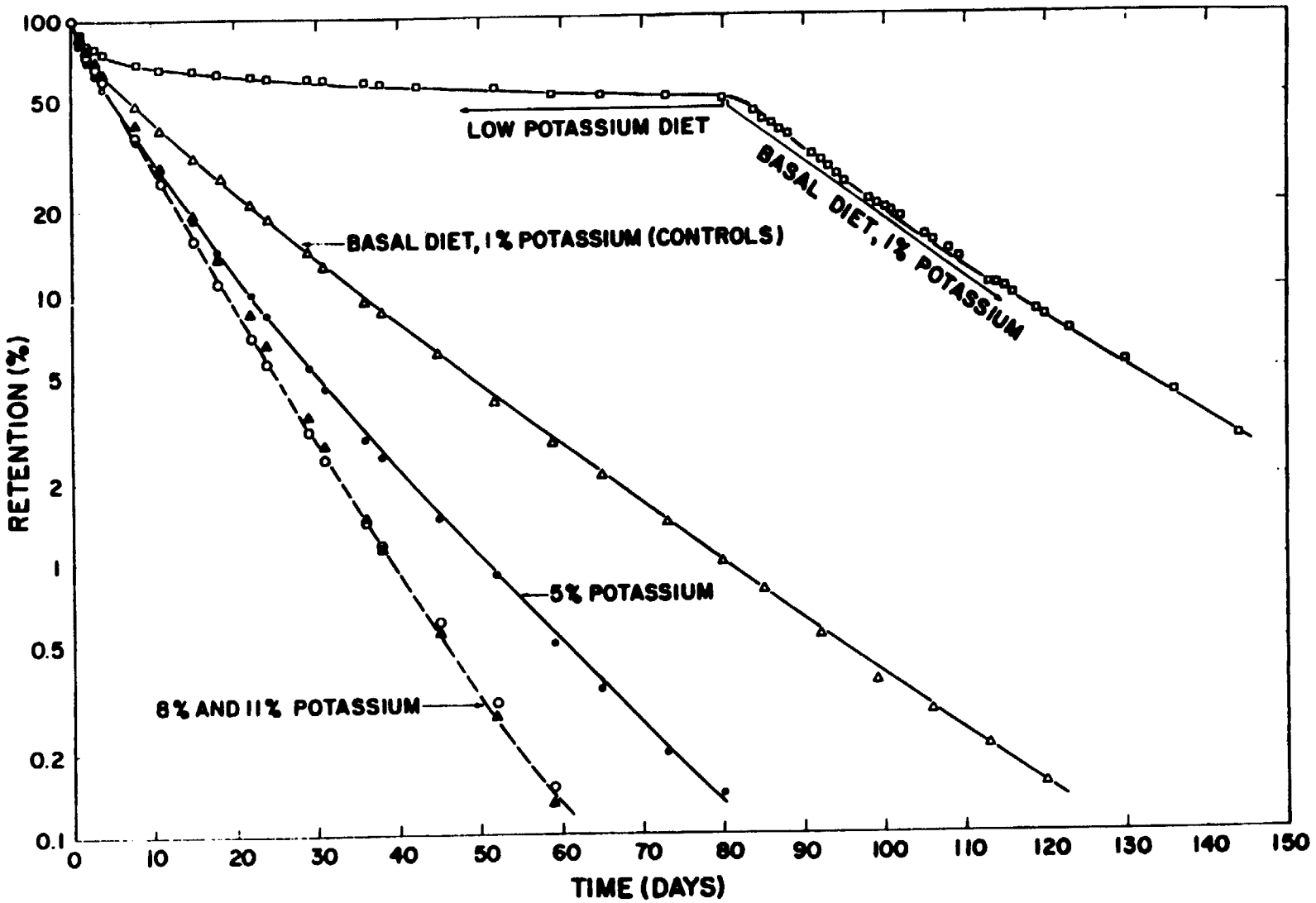

Fig. 1. Effect of dietary potassium on the retention of Cs^{137} administered intraperitoneally to rats (curves eye-fitted).

[redacted]ilar to that previously observed in normal rats at this [redacted]boratory (6).

It is apparent from Fig. 1 that the potassium-deficient diet caused increased retention of Cs^{137} and, therefore, does not serve as an adequate base line or control for studies designed to assess the effect of dietary potassium on Cs^{137} excretion. It is also apparent that when these animals were returned to the basal diet, the retention pattern approximated that of the control animals on an adequate potassium diet.

All groups receiving supplementary dietary potassium lost Cs^{137} more rapidly than the control group. Increased Cs^{137} excretion, however, did not appear to be linearly related to the potassium content of the diet, as no further increase was observed when the dietary potassium was increased above 8 per cent.

Even without a statistical analysis of the retention data, it can be seen in Fig. 1 that the initial Cs^{137} burden of animals on a 5 per cent potassium diet decreased by a factor of 100 in 50 days, whereas the time required for a similar reduction in the initial body burden of animals fed the basal diet containing 1 per cent potassium was 80 days. At 20 days after injection, the Cs^{137} burden of the animals maintained on the diet containing 5 per cent potassium was half that of the animals fed the basal diet.

This experiment simulates conditions of accidental Cs^{137} contamination and suggests the order of effect that may be expected from immediate therapeutic measures based on increased dietary potassium. In view of the possible practical applications of such therapy, similar experiments should be repeated on a larger mammalian species.

REFERENCES

(1) G. C. Kennedy and R. A. Parker, Quart. J. Exptl. Physiol. 45, 77 (1960).

(2) G. C. Kennedy, C. T. G. Flear, and R. A. Parker, Quart. J. Exptl. Physiol. 45, 82 (1960).

(3) Ralston-Purina Company, Laboratory Manual.

(4) R. L. Schuch, Los Alamos Scientific Laboratory Report LAMS-2455 (1960), p. 105.

(5) C. R. Richmond, J. E. Furchner, B. E. Cummins, and G. A. Trafton, This report, p. 34.

(6) C. R. Richmond, Los Alamos Scientific Laboratory Report LA-2207 (1958), p. 132.

ffect of Stable Cesium on the Retention of Cesium^{137} by Rats

. E. Furchner, C. R. Richmond, B. E. Cummins, and G. A. rafton)

INTRODUCTION

There have been many attempts to find methods of increasing excretion of Cs^{137} from animals, as this radioisotope is among the potentially more hazardous products of nuclear fission. The list of materials which have been tested includes stable sodium, stable potassium, combinations of stable sodium and potassium, diuretics, enzyme inhibitors, cortisone, parathyroid extract, dinestrol diacetate, ion exchange resins, alfalfa, and vermiculite.

One might hopefully expect to increase Cs^{137} excretion by administering stable cesium, as the isotope dilution effect has been used successfully to enhance the excretion of certain elements (i.e., sodium, potassium, hydrogen, and iodine). Increasing the dietary level of zinc (1) and magnesium (2) also appears to have a beneficial effect on reducing the body burden of acutely administered Zn^{65} and Mg^{28}, respectively. This effect is one of reduced gastrointestinal absorption, however, and might not be advantageous for materials such as cesium, which are thought to be absorbed completely from the gut.

METHODS

Twenty-four male Sprague-Dawley rats, 84 days old (initial weight about 318 g), were divided into 4 equal groups. The groups were maintained on ground Purina Lab Chow and water ad libitum. Spectrographic analysis of the food showed the cesium content to be $\sim 6.5 \times 10^{-5}$ per cent. Stable cesium (as the chloride) was added to the basal diet of 3 of the groups to make the cesium concentration 6.5×10^{-4}, 6.5×10^{-3}, and 6.5×10^{-2} per cent, respectively. These levels approximated 10, 100, and 1000 fold increases over the cesium level of the basal diet. A Patterson-Kelley twin-shell laboratory blender was used to facilitate mixture of the ground Purina Lab Chow and the supplemental cesium chloride.

The groups were placed on their respective dietary regimens immediately after each animal was injected intraperitoneally with 0.65 μc carrier-free $Cs^{137}Cl$. At 30 min following injection and at suitable intervals thereafter, the individual animals were counted in a whole-body liquid scintillation counter (3). Whole-body retention was calculated by a standardized procedure given elsewhere in this report (4).

RESULTS AND DISCUSSION

Figure 1 shows the mean whole-body retention values as a function of time for all 4 groups. These data show that retention of Cs^{137} by rats was not decreased by the dietary levels of cesium used. It is apparent that Cs^{137} retention was increased by the highest cesium intake level. Periodic weighings showed that the 2 lowest cesium intake levels had no deleterious effects on the growth pattern of the animals, but after 50 days there was no increase in body weights of animals on the highest cesium intake. At equilibrium, the concentration of cesium in these rats would be approximately half the LD_{50} (5) for a single intraperitoneal injection of cesium chloride. Presumably, the increase in retention and the disruption of the growth pattern are responses to cesium toxicity.

The results of this study are negative from the standpoint of increasing excretion of a Cs^{137} body burden by increasing dietary cesium. It should be kept in mind that the Cs^{137} was administered via intraperitoneal injection and that the observed effects of increased cesium level in the diet were strictly on retention and not on absorption plus retention, as would have been the case had the Cs^{137} been administered orally.

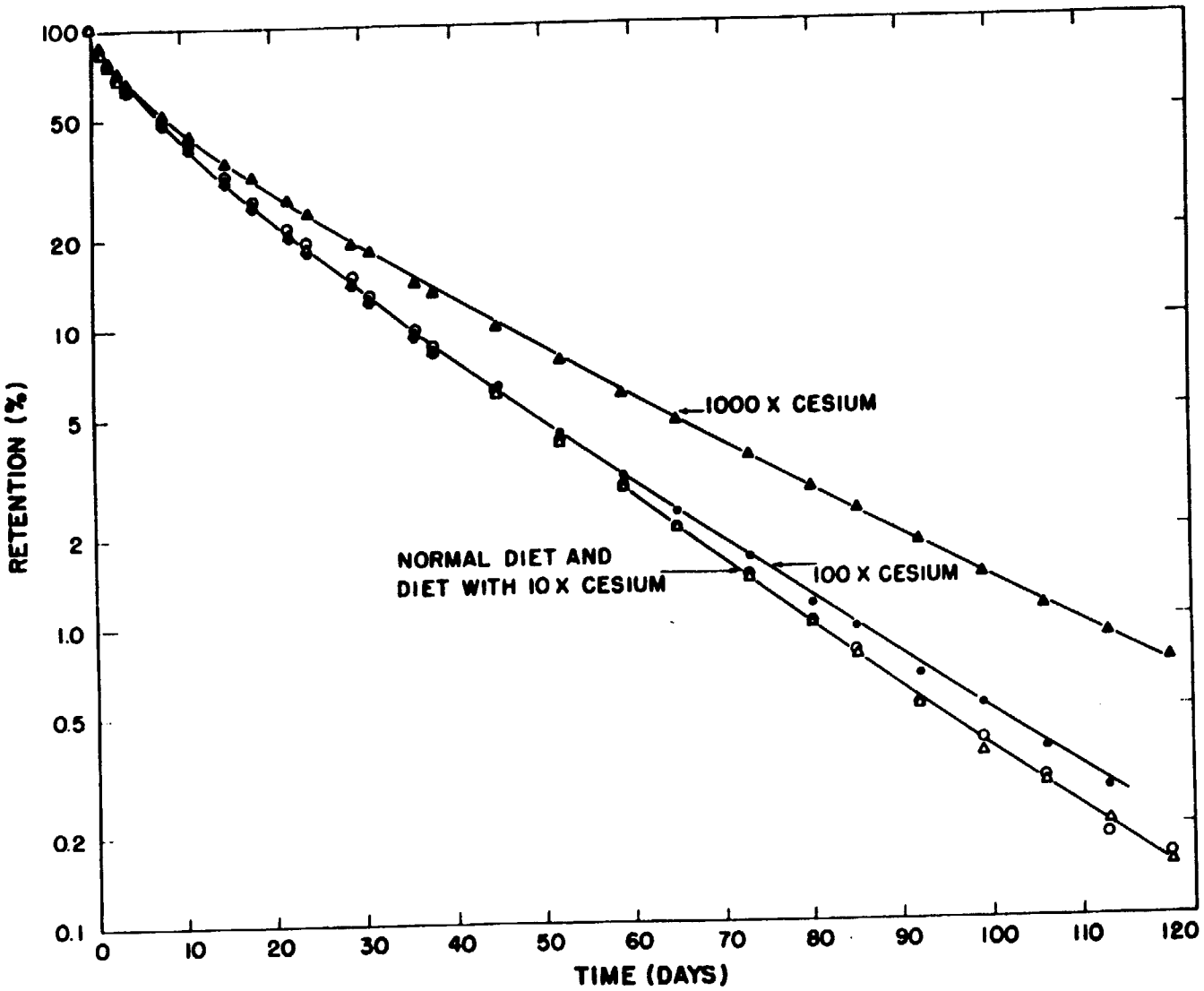

Fig. 1. Effect of dietary cesium on the retention of Cs^{137} administered intraperitoneally to rats (curves eye-fitted).

REFERENCES

(1) J. E. Furchner, C. R. Richmond, and G. A. Trafton, This report, p. 15.

(2) L. A. Graham, J. J. Caesar, and A. S. V. Burgen, Metabolism 9, 646 (1960).

(3) R. L. Schuch, Los Alamos Scientific Laboratory Report LAMS-2455 (1960), p. 105.

(4) C. R. Richmond, J. E. Furchner, and G. A. Trafton, This report, p. 48.

(5) K. W. Cochran, J. Doull, M. Mazur, and K. P. DuBois, Arch. Indust. Hyg. Occup. Med. 1, 637 (1950).

Effects of Age, Sodium Depletion, and Sodium Repletion on the Retention of Sodium^{22} by Rats (C. R. Richmond, J. E. Furchner, B. E. Cummins, and G. A. Trafton)

INTRODUCTION

A large body of information clearly indicates that about one-third of the total body sodium is in the skeleton. Results of previous experiments at this Laboratory showed the presence of a long retention component in the whole body retention pattern of Na^{22} given to 5 species of animals (1). The results suggested that human subjects retained less than 1 per cent of the administered dose with a biological half-time of approximately 460 days. Miller and associates (2) also detected the presence of this component in a human subject with the aid of the high pressure ionization chamber at Leeds and subsequently recommended the limited use of Na^{22} in clinical investigations. This component, which is thought to represent radiosodium bound in bone, has been detected only with whole-body counting systems. The contribution to the total integrated radiation dose from radiosodium deposited in the skeleton is by no means insignificant as at least 10 per cent of the total disintegrations which occur in the body after Na^{22} administration are associated with the long-lived component.

This experiment was designed to investigate the effects of age, sodium depletion, and subsequent sodium repletion on the long-term retention of radiosodium.

METHODS

Thirty-six male Sprague-Dawley rats of 2 different ages were used. Twelve animals 30 days of age (mean weight 106 g) and 12 animals 86 days of age (mean weight 292 g) were divided into groups of 6 animals each. Two groups (1 group of each age) were fed ground Purina Lab Chow, and the other 2 were fed a commercially supplied low sodium diet. An additional 12 animals (86 days old) were maintained on Purina Lab Chow and used for tissue distribution studies. Members of this group were given Na^{22} intraperitoneally and sacrificed at intervals during the experiment to determine Na^{22} content of bone as a function of time after injection. All animals were housed individually in metabolism cages and allowed free access to diet and water throughout the experimental period.

After a 3 week acclimatization period on the respective diets, each rat was given 0.4 μc Na^{22} as the chloride by intraperitoneal injection. Thirty minutes later, the gamma ray activity of each animal was determined by whole-body counting in a 4π liquid scintillation counter (3). A standard consisting of an aqueous solution of $Na^{22}Cl$ in a polyethylene bottle 5 in. in length and 2-1/4 in. in diameter was measured with each group of rats. Animals and standards were measured at appropriate intervals over a 163 day period. Forty days after injection of the Na^{22}, the 2 groups on the low sodium

diet were transferred to a diet of ground Purina Lab Chow and allowed to replete their body sodium for the remainder of the experiment. All animals were weighed periodically as a check for possible deleterious effects of the low sodium diet. The biological retention of Na^{22} was then calculated by the following expression:

$$\text{Biological Retention} = \left(\frac{\text{Animal Count Rate}}{\text{Std. Count Rate}}\right)_t \Big/ \left(\frac{\text{Animal Count Rate}}{\text{Std. Count Rate}}\right)_o$$

in which the subscripts t and o refer to the times after Na^{22} administration. This expression eliminates the effect of radioactive decay and corrects for minor day-to-day fluctuations in the counting system.

RESULTS AND DISCUSSION

Figure 1 shows the whole-body retention data for all 4 experimental groups. Of the animals kept on Purina Lab Chow throughout the entire experimental period (lower curves), the younger group lost radiosodium at a faster rate initially and retained more of the administered dose at later times than did the older group.

Data represented by the upper curves in Fig. 1 show that both age groups retained Na^{22} tenaciously during the 40 day period on a low sodium diet. During this period, younger rats

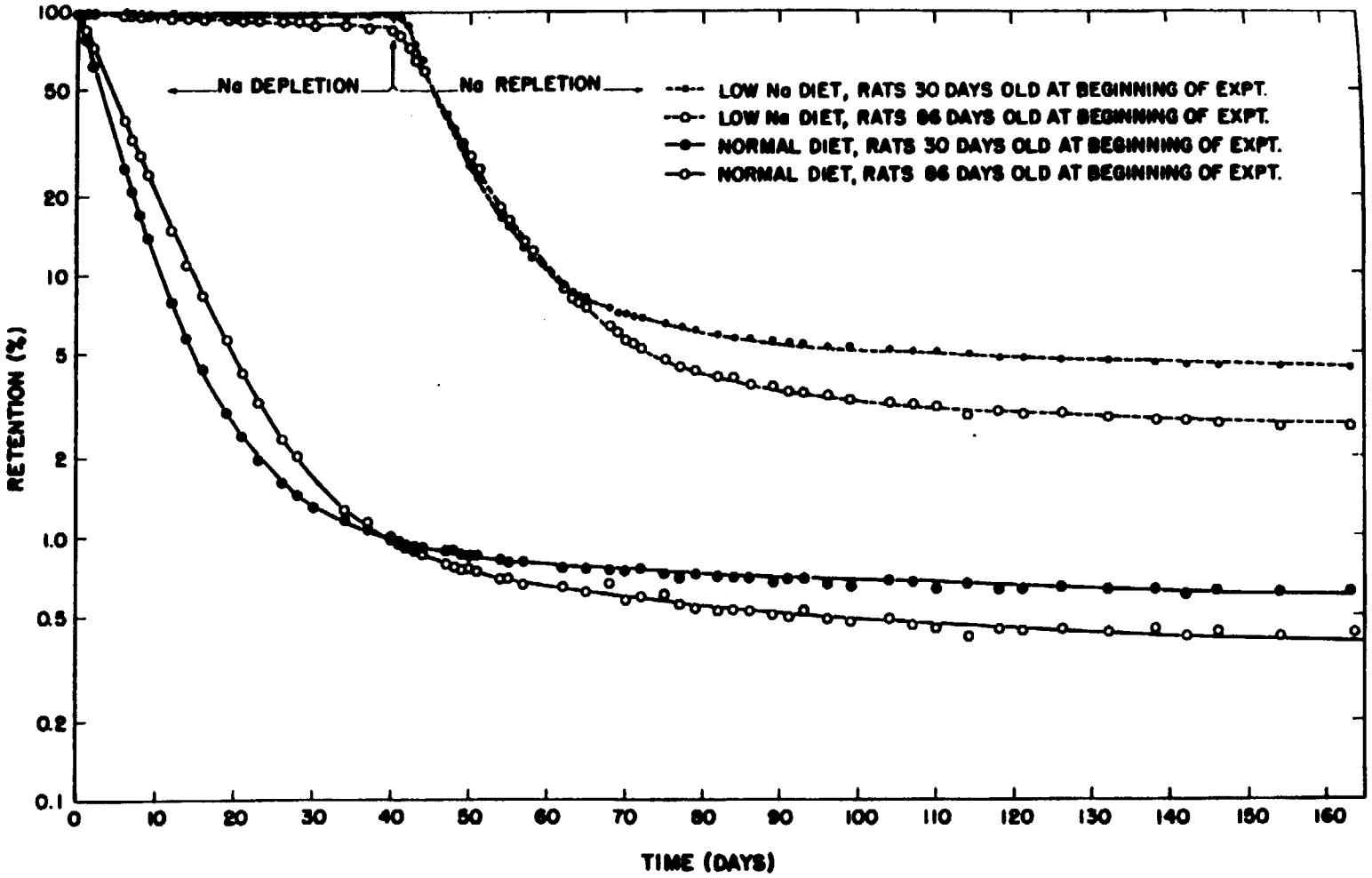

Fig. 1. Effect of age, sodium depletion, and sodium repletion on the retention of Na^{22} by rats (dashed lines eye-fitted).

appeared to retain more of the radiosodium than the older animals. After the change to Purina Lab Chow on day 40, however, sodium repletion began and both groups lost Na^{22} at an accelerated rate. The younger animals appeared to lose Na^{22} more rapidly during the initial phase of the repletion period than did older animals. Ultimately, however, the younger group incorporated more radiosodium in the slowest changing component.

The most striking feature of Fig. 1 is the large difference between the amounts of Na^{22} retained by the normal and repleted groups at long times following administration. Younger rats in both normal and repleted groups retained more of the initial Na^{22} burden than older rats. One might expect relatively larger amounts of Na^{22} to deposit in the skeleton during sodium repletion. It might be expected also that younger animals may deposit more Na^{22} in the skeleton than older ones. The above observations support these expectations.

The retention data for both the young and old age groups maintained on the normal sodium diet were reduced into exponential components by a 704 computer programmed to perform iterative least square calculations. Coding procedures require the retention values (Y) at each time (t) and estimates of the intercept and rate parameters of the function. Each

Y is weighted by a factor proportional to 1/Y. This procedure avoids the subjectivity inherent to eye-fitting a line to the experimental data and, by iteration, assures that best fit criteria are equally applicable to all components simultaneously. Preliminary results show the biological retention functions for animals in these groups to be of the form

$$R_t = \sum_i^3 \left[a_i e^{-k_i t} \right].$$

The values for the intercept (a) and rate constants (k), which best described the biological retention data out to 163 days, are:

$$R_t = 91.14\ e^{-0.24715\ t} + 7.52\ e^{-0.09196\ t} + 0.88\ e^{-0.00247\ t}$$

and

$$R_t = 98.60\ e^{-0.16341\ t} + 1.19\ e^{-0.03511\ t} + 0.59\ e^{-0.00257\ t}$$

for young and old groups, respectively. These equations are represented by the solid lines drawn in Fig. 1. The last term of each equation shows that 0.88 per cent of the injected dose (I. D.) was retained by the young animals with a biological half-life (T_b) of 281 days, whereas 0.59 per cent of the dose was retained with a T_b of 269 days in the older animals. These components should not be ignored when estimating total radiation dose, as they account for ~ 38 and ~ 22 per cent,

respectively, of the total area under the "effective retention function" (i.e., retention as the result of physical decay and biological loss of Na^{22}) from t_o to t_∞.

Figure 1 shows that the dose delivered to animals on a restricted sodium intake (by both young and older age groups) would indeed be considerably greater than that delivered to animals maintained on a normal diet. This is also true during the repletion phase, as much more of the administered Na^{22} is associated with the slow-changing component. Presumably, more Na^{22} is bound in this compartment during sodium repletion to replace the labile skeletal sodium which was mobilized during the period of restricted sodium intake.

The distribution studies showed about two-thirds of the activity related to the slow-changing component can be attributed to Na^{22} in the skeleton. This preliminary finding suggests that some of the administered radiosodium is retained in the soft tissues of the body with a relatively long half-time.

Future plans include continuation of the retention measurements on the 2 groups that received the low sodium diet, analyses for skeletal Na^{22} at the termination of the experiment, and estimation of the contribution of the long-lived component to the total radiation dose.

REFERENCES

(1) C. R. Richmond, Los Alamos Scientific Laboratory Report LA-2207 (1958), p. 136.

(2) H. Miller, D. S. Munro, and G. M. Wilson, Lancet 272, 734 (1957).

(3) R. L. Schuch, Los Alamos Scientific Laboratory Report LAMS-2455 (1960), p. 105.

Long-Term Retention of Ruthenium^{106} by Rats (J. E. Furchner, C. R. Richmond, and G. A. Trafton)

INTRODUCTION

Earlier reports from this Laboratory (1) showed that retention of Ru^{106} by rats, after intraperitoneal injection, could be described by a 3 component exponential function. The data from which the 3 component function was derived extended to 319 days. The present report describes the time-course of retention up to 400 days, at which time it was necessary to terminate the experiment because of mortalities in the experimental animals.

METHODS AND RESULTS

The methods of injection, assay, and data analysis have been reported previously (1). The retention data over the entire period of 400 days were submitted to analysis by a 704 computer with estimated values for 3 components, and the resulting equation is given as Eq. I in Table 1. Visual examination of a plot of the data points and the line generated by the equation initiated a second analysis with a 4 component estimate, and the resulting equation is given as Eq. II in Table 1. Equations III and IV in Table 1 give the results of computer analyses when the data to 319 days only are fitted to 3 and 4 components, respectively.

TABLE 1. BIOLOGICAL RETENTION FUNCTIONS AND HALF-TIMES FOR RATS INJECTED INTRAPERITONEALLY WITH RUTHENIUM^{106}

I*	$R_t = 29.22\ e^{-0.5979\ t} + 48.58\ e^{-0.0506\ t} + 20.19\ e^{-0.0016\ t}$					
	T_b (days)	1.16	13.7	445		
II*	$R_t = 18.38\ e^{-2.3860\ t} + 40.33\ e^{-0.1102\ t} + 22.84\ e^{-0.0271\ t} + 18.45\ e^{-0.0013\ t}$					
	T_b (days)	0.29	6.3	25.6	553	
III**	$R_t = 26.51\ e^{-0.8084\ t} + 51.03\ e^{-0.0574\ t} + 21.38\ e^{-0.0019\ t}$					
	T_b (days)	0.86	12.1	370		
IV**	$R_t = 17.42\ e^{-2.8033\ t} + 33.92\ e^{-0.1318\ t} + 28.96\ e^{-0.0350\ t} + 19.70\ e^{-0.0015\ t}$					
	T_b (days)	0.25	5.3	19.8	452	

*$t_o - t_{401}$.

**$t_o - t_{319}$.

In Table 2, it can be seen that when the "least square" criterion is used to select the "best fit" from a choice of equations, 4 component expressions provide a better fit than 3 component expressions over both time intervals. Although the retention function with 4 components derived from data covering 319 days only has a smaller summed squares of deviations, the additional deviations appearing after 319 days should be included for comparison with the corresponding function derived from data through 400 days.

The effect of the data collected between 319 and 401 days has been to decrease the retention constants (i.e., increase the biological half-time, T_b). As mentioned in the previous report (1), a value of 340 days for the biological half-time of Ru^{106} in bone has been reported by others (2). The most recently recommended value of the International Commission on Radiological Protection (3) is 16 days, based perhaps on short-term studies of retention in soft tissue. These values are considerably smaller than the 553 day T_b value obtained for the long component in this study. This component (Table 2) contains about 92 per cent of the total area under the retention function. The areas under the retention function are increased by the changes in the retention constant, and the estimate of the equilibrium level from the best fitting expression is 159 times the daily dose of stable ruthenium, rather than 123 times the daily dose as reported by us previously (1).

TABLE 2. AREAS UNDER THE RETENTION FUNCTIONS FOR RATS INJECTED INTRAPERITONEALLY WITH RUTHENIUM^{106} AND THE SUMMED SQUARES OF DEVIATIONS FROM THE RETENTION FUNCTIONS

Equation Number	Component	Area (per cent days)	Area (per cent of total)	Total Area (per cent days)	Sum of Squares of Deviations
I*	1	48.87	0.35		
	2	959.75	6.87		
	3	12,964.02	92.78	13,972	42.68
II*	1	7.70	0.05		
	2	365.95	2.30		
	3	842.30	5.29		
	4	14,715.81	92.37	15,932	4.03
III**	1	32.79	0.27		
	2	888.77	7.20		
	3	11,414.12	92.53	12,335	29.41
IV**	1	16.09	0.12		
	2	257.32	1.84		
	3	826.56	5.92		
	4	12,858.66	92.92	13,958	2.91

*$t_o - t_{401}$.

**$t_o - t_{319}$.

DISCUSSION

The best estimates of the number and values of the retention parameters are desired because they will be used for making interspecific correlations. The advantage of collecting retention data as long as possible is emphasized by the observed changes in the parameters of the retention functions resulting from extension of the data from 319 to 401 days.

Several other phases of the problem are under investigation. The whole-body activity of Ru^{106} in mice is at the limit of detection (405 days after administration) by in vivo counting. Similar studies on dogs, and possibly on monkeys, are planned. Studies of distribution of Ru^{106} in rats are in progress and will be utilized in assessing the biological significance of the retention functions. Lastly, the question of administering radioruthenium to human subjects is being considered.

REFERENCES

(1) C. R. Richmond, J. E. Furchner, and G. A. Trafton, Los Alamos Scientific Laboratory Report LAMS-2455 (1960), p. 32.

(2) R. C. Thompson, Hanford Atomic Operations Report HW-41422 (1956).

(3) Report of the International Commission on Radiological Protection, Committee II, on Permissible Dose for Radiation (1959), Health Phys. 3, 182 (1960).

[redacted]oactivity in Cervidae Antlers (H. Foreman, M. B. Roberts, [redacted]. H. Lilly)

INTRODUCTION

[redacted] Although the intense concern about "fallout" which ex-[redacted]ited a couple of years ago has largely subsided, there still remains considerable interest and need for information on levels of ambient radioactivity. The following report is an evaluation of the use of Cervidae antlers as a means for collecting such data (i.e., for sampling and estimating levels of radioactivity spread sparsely over large areas).

The idea of deer antlers as indicators of environmental radioactivity has occurred to a number of individuals over the years,* undoubtedly because of certain characteristics of this species. In its browsing, the deer takes in foliage and brush representative of a tremendous surface area for fallout deposition and metabolically concentrates the radioactivity in a compact structure which is relatively easy to obtain. Moreover, isotopes of special interest -- the bone

*Only 1 published report has appeared on radioactivity in deer antlers (1), but information, opinions, and indications of interest in the subject have come in the form of personal communications (i.e., from E. C. Anderson of this Laboratory, A. Schulert of the Lamont Geological Observatory, A. Kramish of the Rand Corporation, J. Lade of the New York State Department of Health, and V. Schultz of the AEC's Division of Biology and Medicine). Dr. Schultz has 3 preliminary reports on studies of radioactivity in deer antlers: 1 of his own, 1 by Lindberg et al. from UCLA on Nevada deer, and 1 from Y. Hiyma of the University of Tokyo.

seekers -- are involved. The time of activity accumulation can be readily determined, and the year-by-year accumulations can be compared in the same herd. The present project was undertaken more as a feasibility study in an attempt to ascertain the limitation and usefulness of deer antler radioactivity studies rather than to answer any specific question on environmental or biospheric contamination.

EXPERIMENTAL PROCEDURE

Specimen Sources

Specimens were sent to the Laboratory as a result of publicity in local news bulletins and articles in Time and Sports Illustrated magazines. No attempt was made to obtain specimens from any one particular geographic area or according to any special pattern. All antlers received, whose identity with respect to year and site of procurement was well established, were analyzed. By and large, specimens were obtained from animals killed during hunting season. A few specimens were taken from animals killed for other reasons, and these were received in the velvet stage rather than as mature antlers. No dropped antlers were used. A total of 72 specimens were obtained from the United States, Canada, and Alaska. These included not only deer antlers but also those from elk, caribou, and reindeer. At least 1 specimen

for each year from 1945 through 1958 inclusive was obtained, and in addition 1 from the year 1935.

Methods of Assay

Two types of measurements were made: Sr^{90} assays and total beta counts. Strontium^{90} assays were done by a procedure developed in this Laboratory and described in the last semiannual report (2). The samples were prepared for assay merely by cutting the antlers into small pieces and ashing 100 g samples in a muffle furnace for 4 hr at 700°. Replicates were done to the extent of the quantity of specimen available. Counting times were such that at levels of 10 d/m/g ash or higher the standard deviation due to counting procedure was less than 2 per cent. At less than 10 d/m/g ash, the standard deviation was less than 5 per cent. The standard deviation between replicate analyses is discussed in the procedural report (2). It was of the order of 10 per cent.

For total beta counting, ash was used without further treatment and since color in the ash sample affected the counter efficiency, care was taken to obtain as white a sample as possible. In the preparation of the ash, the antlers were first washed with cold running water to remove as much blood pigment from the bone marrow as possible, and

then thoroughly washed with hot soap and water to remove surface dirt and contamination. The samples were autoclaved for 2 to 3 hr and again washed with water and detergent and rinsed thoroughly with hot water. Rinsing resulted in the removal of the rest of extraneous debris, liberated marrow fat, and gelatin, and most if not all of the soluble mineral phase including sodium, potassium, and cesium. The sample was then ashed for 8 to 10 hr at 700°. After cooling, a fine powder was obtained by grinding in a mortar. Each counting sample consisted of 10 g of ash and enough scintillation solution to bring the volume to 30 cc. The scintillation solution was the standard terphenyl-POPOP-toluene mixture containing in addition 25 per cent by weight of powdered polystyrene plastic. The plastic dissolved to give a clear viscous solution, which kept the bone powder in suspension. The counting setup has been described in a previous publication (3). Each sample was counted for a total of 10,000 counts to give a standard deviation for counting of less than 5 per cent. When sufficient sample was available, 3 separate counting samples were prepared and counted. An internal standard of Y^{91} was used at the counting of each sample to determine counting efficiency. Yttrium^{91} was selected because it could be conveniently prepared as a standard and because it has an "average" beta spectrum.

RESULTS

The analytical results are presented in Table 1. Strontium^{90} data are expressed as d/m/g of ash rather than the customary μμc/g of calcium because calcium analyses were not done. However, a good average value for calcium in deer antler ash is generally considered to be 38.5 per cent (4,5), and by using this number the results in column 2 (Table 1) can be converted to μμc/g calcium merely by multiplying by the factor 1.18. Strontium^{90} assays are missing on a number of specimens because not enough sample was available. Column 3 in the table shows total beta count in c/m/g. This is the crude net count after background has been subtracted. In the next column, the results for beta counting are given after correction for counting efficiency has been made. In the last column are presented results of calculations illustrating the relative importance of Sr^{90} versus short-lived fission products with respect to radiation dose delivered to bone. The assumptions involved and the method of calculation are presented in the Discussion section below.

In Fig. 1, yearly Sr^{90} averages are shown for the various areas from which antlers were obtained. The data for deer, caribou, elk, and reindeer are all averaged together, since there appeared to be little difference among them. The overall U. S. averages listed do not include Alaska data, since

TABLE 1. RADIOACTIVITY IN CERVIDAE ANTLERS

Area and Year of Sample	Sr^{90} (d/m/g ash)*	Total Beta Counts (c/m/g ash)	Corrected Beta Counts (d/m/g ash)	Relative Dose Contribution of Sr^{90}/Y^{90} (per cent)
1958				
Alaska (R)	105.1	35.5	206.0	100
Alaska (R)	162.7	25.0	237.1	100
Alaska (C)	145.5	51.5	218.4	100
Alaska (C)	64.0	33.6	127.8	100
Arizona (D)	9.5	4.5	27.0	87.7
Br. Columbia (D)	--	17.9	67.9	--
Br. Columbia (D)	--	11.9	74.3	--
California (D)	10.2	2.5	19.7	100
California (D)	10.1	6.5	25.2	92.5
California (D)	--	8.8	26.5	--
Colorado (E)	30.5	9.1	68.7	96.1
Michigan (D)	--	4.3	40.6	--
Missouri (E)	21.4	8.4	79.8	77.5
Missouri (E)	21.1	7.0	73.3	80.3
Missouri (E)	28.8	7.6	62.9	97.1
Nevada (D)	18.9	5.9	61.8	82.7
New Hamp. (D)	15.6	11.1	39.4	92.4
New Mex. (D)	20.3	10.7	62.9	84.9
New Mex. (D)	15.5	5.2	41.6	89.8
New Mex. (D)	18.6	11.2	48.3	91.2
New Mex. (D)	10.0	2.1	25.1	92.4
New Mex. (D)	--	5.7	55.0	--
New Mex. (D)	--	9.4	61.1	--
New Mex. (D)	--	5.0	30.4	--
Oregon (D)	--	10.7	92.3	--
Oregon (D)	--	6.5	52.6	--
Oregon (D)	--	8.5	94.6	--

*Can be converted to approximate μμc/g Ca by multiplying by 1.18.

TABLE 1 (continued)

Area and Year of Sample	Sr^{90} (d/m/g ash)	Total Beta Counts (c/m/g ash)	Corrected Beta Counts (d/m/g ash)	Relative Dose Contribution of Sr^{90}/Y^{90} (per cent)
Pennsylvania (D)	--	5.3	44.8	--
Pennsylvania (D)	--	7.8	54.6	--
Quebec (D)	35.0	7.4	89.4	91.54
Quebec (D)	30.3	7.2	60.6	100
Quebec (D)	35.1	18.4	72.4	100
Texas (D)	--	2.6	31.0	--
Wyoming (D)	22.4	10.6	54.6	93.2
1957				
Alaska (C)	73.3	4.4	36.2	--
California (D)	7.6	2.0	32.0	--
California (D)	8.5	11.0	25.4	--
Colorado (E)	16.8	4.3	36.8	--
Michigan (D)	--	3.9	38.1	--
New Mex. (D)	14.7	1.5	30.3	--
New Mex. (D)	5.8	4.0	30.1	--
Oregon (D)	10.8	6.8	39.2	--
Pennsylvania (D)	--	4.5	35.9	--
1956				
California (D)	--	1.6	18.1	--
Nevada (D)	12.7	16.8	74.3	--
New Mex. (E)	11.1	4.4	39.0	--
Oregon (D)	12.4	4.0	31.5	--
Oregon (D)	11.9	3.0	19.6	--
Pennsylvania (D)	--	2.1	30.2	--
Wyoming (E)	20.3	3.0	53.4	--

TABLE 1 (continued)

Area and Year of Sample	Sr^{90} (d/m/g ash)	Total Beta Counts (c/m/g ash)	Corrected Beta Counts (d/m/g ash)	Relative Dose Contribution of Sr^{90}/Y^{90} (per cent)
1955				
California (D)	7.0	6.2	59.7	--
Michigan (D)	9.1	13.9	37.4	--
Nevada (D)	--	1.0	12.1	--
New Mex. (D)	8.5	2.7	19.8	--
1954				
California (D)	--	6.8	21.7	--
Michigan (D)	--	10.7	39.6	--
Pennsylvania (D)	--	3.6	53.6	--
Wyoming (D)	6.5	3.9	25.3	--
1953				
California (D)	--	6.5	24.0	--
Yukon (M)	3.2	3.9	15.9	--
Yukon (C)	6.9	1.3	27.8	--
1952				
California (D)	1.7	1.1	30.2	--
Wyoming (D)	0.5	10.3	9.7	--
1951				
California (D)	1.4	4.5	30.2	--
Michigan (D)	4.1	2.2	22.5	--
1950				
California (D)	--	3.0	14.1	--

BLE 1 (continued)

ea and ir of ample	Sr^{90} (d/m/g ash)	Total Beta Counts (c/m/g ash)	Corrected Beta Counts (d/m/g ash)	Relative Dose Contribution of Sr^{90}/Y^{90} (per cent)
1949				
California (D)	--	1.5	59.5	--
Oregon (D)	--	4.5	38.9	--
1948				
California (D)	1.02	1.8	14.7	--
1947				
California (D)	1.22	2.9	25.8	--
1946				
California (D)	0.6	4.6	32.0	--
1945				
California (D)	0.08	10.0	47.4	--

NOTES:

D = deer; C = caribou; R = reindeer; E = elk; M = moose.

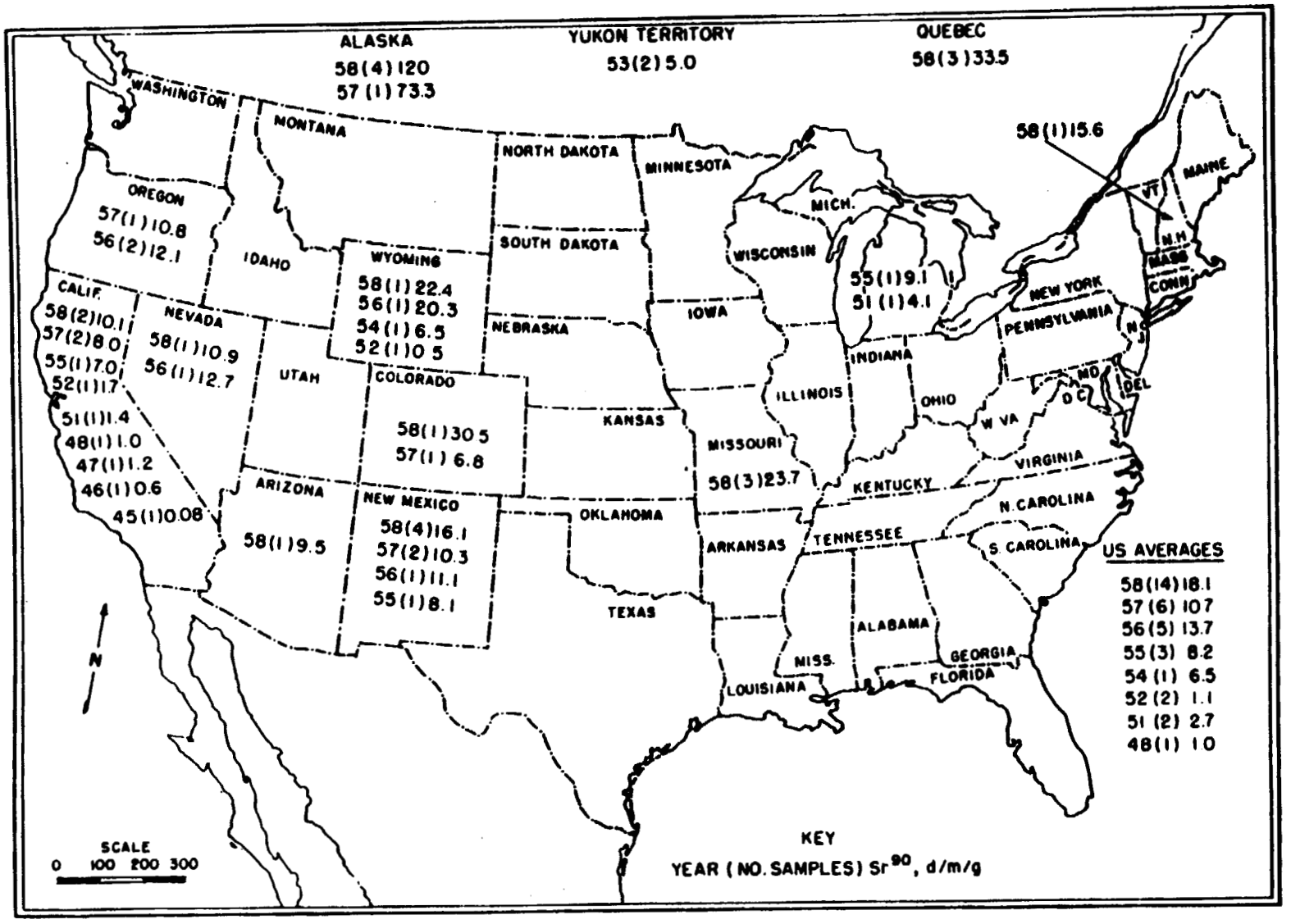

Fig. 1. Strontium^{90} in Cervidae antlers (location, year, Sr^{90} content, and number of samples).

these values are so much higher than any of the others and are available for only the last 2 years. The inclusion of these values would unduly weight the 1957 and 1958 averages upward.

DISCUSSION

As was anticipated, the introduction of Sr^{90} into the environment by bomb testing is readily manifested in antlers. It appears that this structure has a capacity to concentrate Sr^{90} to a greater extent than any other biological material which has been studied, except perhaps sheep bone. The very high concentration of Sr^{90} with respect to calcium most likely is due to the fact that deer, by nature of their feeding habits, consume a good deal of fallout that is not associated with calcium. It would be surprising if the metabolic discrimination factors which operate with respect to strontium and calcium in other mammals do not apply to the deer.

It is of interest that Sr^{90} in antlers increased year by year as more and more Sr^{90} was released into the environment with the exception of the 1956-1957 interval. Deer antlers grow in the spring and early summer, and it might be expected that the radioactivity accumulated in the antler would be the ambient fallout during that time, especially since the deer is a browsing animal and has access to fallout deposited

directly on vegetation. In other words, the Sr^{90} levels are probably indicative of relatively fresh fallout rather than integrated deposition levels in the soil. The extent to which this is true depends, of course, upon the degree to which the animal draws upon its skeleton to build its antlers. This is not known at the present time. If Sr^{90} in deer antlers is indeed representative of differential fallout, then this would explain the sharp rise in 1956, followed by the dip in 1957, since there was a high rate of large-scale bomb tests in early 1956, followed by a lull in late 1956 and early 1957.

Although there were too few samples from which to draw conclusions relating Sr^{90} levels to given areas, the values for the Alaska animals are so very much higher than those from other areas that one can be quite certain, even from this limited sampling, that this is a significant difference. These very high levels are puzzling. The specimens were obtained from a region of about 65°N latitude, a general region of relatively low fallout, at least as judged by reported soil levels.

In judging the usefulness of deer antlers as indicators of radioactivity, it is of value to consider the variation from animal to animal in the same area. The data in Table 2 give an indication of this, but again the paucity of samples limits the value of these comparisons.

TABLE 2. STRONTIUM^{90} VALUES IN HERD-RELATED ANIMALS

Area	Year	Sr^{90} (d/m/g ash)
California	1958	a. 10.2 b. 10.1
Quebec	1958	a. 29.5; 31.1 b. 35.1 c. 36.5; 32.5; 36.0
Missouri	1958	a. 21.4 b. 21.1 c. 28.9; 28.9; 27.6; 29.1; 29.2
California	1957	a. 7.6 b. 8.5
Oregon	1956	a. 13.6; 11.1; 12.2 b. 11.5; 12.3

NOTE: Each lower case letter represents a single animal. Horizontally arranged series of numbers are replicate analytical results.

Although it is customary to do gross beta counts in environmental studies, these numbers are often of relatively little value due to lack of information as to the isotopic composition of the radioactivity. This was certainly true in the present study. The raw beta counts exhibited so much uninterpretable variation that they were of value only in indicating the presence or absence of activity. When the numbers are corrected for counting efficiency, the variation was decreased and a certain amount of gross structure could be seen in the data. For instance, the 1958 Alaska values could be distinguished easily from the other numbers. In fact, the 1958 counts for all areas sampled were considerably higher than those of the previous years.

The total beta count, together with the Sr^{90} data, were used in an attempt to consider the repeatedly raised question of the relative importance of Sr^{90} versus short-lived bone seekers in delivering radiation dose to the bone. In doing this, the count due to Sr^{90}/Y^{90} was subtracted from the corrected total beta count. In many instances, as can be seen from Table 1, the Sr^{90}/Y^{90} count accounted for all the beta activity. In these cases, the radiation dose attributable to the Sr^{90}/Y^{90} equilibrium mixture was considered 100 per cent. In other specimens, there was a surplus of beta counts. These were arbitrarily attributed to Sr^{89}. By

correcting the count for decay between the time of counting and time of collection of the specimen, the number of microcuries of Sr^{89} as compared to microcuries of Sr^{90} present could be determined. From there it was possible to compare the dose contribution of the 2 isotopes, since 1 μc of Sr^{90} eventually delivers 100 times the radiation dose of 1 μc of Sr^{89}.

It can be seen even in the antler situation, which favors relatively high deposition of short-lived emitters, the radiation dose to bone was overwhelmingly associated with Sr^{90}. If the assumption that the surplus beta activity is due to Sr^{89} is wrong, then even more of the dose must come from Sr^{90}, since the other short-lived bone-seeking fission products deliver less radiation dose than does Sr^{89} microcurie for microcurie. Thus it can be seen, even from rough calculations as these, the dose from isotopes other than Sr^{90} in bone is relatively unimportant.

It is felt that Sr^{90} measurements on antlers are worthwhile and can provide interpretable and meaningful information. Strontium^{90} assays by the procedure indicated above are relatively simple and easy to do (as compared to other methods) and because of the propensity of deer for Sr^{90}, in areas where antlers are available their collection and assay are probably one of the most sensitive, convenient, and

inexpensive ways to log levels of radioactivity. The concomitant rise of Sr^{90} in antlers with Sr^{90} fallout over the years suggests that periodic assays of Sr^{90} in antlers from captive herds, such as the caribou herd in Alaska or the elk herd on the Federal Reservation in Missouri, could be used to measure the rate of stratospheric fallout. With the cessation of large-scale air bursts in late 1958, one could expect, on the basis of Libby's predictions (6), that Sr^{90} levels in antlers would peak in 1960, and show a decline in subsequent years at a pace indicative of the Sr^{90} fallout rate. It might be fruitful to do such a study to supplement the data on fallout rate being obtained by other methods.

There are, of course, situations other than those involving fallout from bomb tests in which it is necessary and desirable to know levels of environmental contamination (i.e., the environs of reactors or in areas in and about radioactive dumps). In such areas, it could be very useful to foster deer herds so that antlers could be added to the specimens that are usually collected to monitor biospheric contamination. Antlers and probably sheep skeletons could provide the most sensitive indicators of Sr^{90} contamination that are available.

Again from the experience of this study, it appears that total beta counts are of limited value and unless a very

large series of samples is to be tested merely for the presence or absence of radioactivity, they are probably not worthwhile.

REFERENCES

(1) J. Hawthern and R. B. Duckworth, Nature 182, 1294 (1958).

(2) H. Foreman and M. B. Roberts, Los Alamos Scientific Laboratory Report LAMS-2455 (1960), p. 61.

(3) F. N. Hayes, B. S. Rogers, and W. H. Langham, Nucleonics 14(3), 48 (1956).

(4) V. Schultz, unpublished results on deer bones.

(5) R. G. Lindberg and J. H. Olafson, unpublished results on deer bones.

(6) W. F. Libby, U. S. Atomic Energy Commission Report TID-5556 (May 1956).

Determination of Tritium Beta Activity in Microgram Amounts of Nucleic Acids from HeLa Cells Cultured in Agitated Fluid Medium

(D. F. Petersen, L. B. Cole, and P. C. Sanders)

INTRODUCTION

The use of tritiated thymidine as a precursor in the study of HeLa cell growth in agitated fluid medium necessitated the development of a counting technique which could be applied to large numbers of replicate samples on a routine basis. Main and Walwick (1) have recently described such a procedure for liquid scintillation counting of tritiated thymidine incorporated into deoxyribonucleic acid (DNA). The basis of their technique involves formate hydrolysis of DNA, resulting in final solution of labeled thymine in an alcoholic solvent compatible with a nonaqueous scintillator solution of high efficiency. In our experiments, specific activities were sufficiently high to permit less complicated chemical manipulations, and we have therefore developed a simplified procedure for routinely counting tritium beta activity, which can be applied to a variety of biological materials in studies employing both obligate (thymidine) and ambiguous (deoxycytidine) precursors involved in the synthesis of deoxyribonucleic acid. The procedure is based in principle on the classical differential isolation methods of Schmidt and Thannhauser (2) and Schneider (3) modified to yield aqueous solutions derived from DNA, RNA, and

the acid-soluble fraction. The fractions were counted in a scintillator compatible with aqueous solutions (4). Although lipid and protein fractions have been omitted from the present study, minor modifications of the procedure would permit their inclusion. The method is sensitive and reproducible and appears to preclude use of the more laborious hydrolytic procedures owing to the less rigorous conditions for hydrolysis and consequently greater stability of the relatively labile H^3 attachments of tritiated deoxycytidine.

METHODS

HeLa S3 cells grown in agitated fluid medium were sampled volumetrically at daily intervals following introduction of the labeled precursor. For these experiments, tritiated thymidine and deoxycytidine of high specific activity were used. Four-ml aliquots from the cultures containing from 1.2×10^4 to 1.2×10^5 cells/ml (determined with an electronic particle counter) were diluted with 5 volumes of Hanks' balanced salt solution. Cells were isolated by centrifugation in the cold, and washed twice with 5 volumes of the salt solution. Washings were discarded and the pellet containing a known number of cells was immediately frozen by immersion of the tube in an acetone-Dry Ice freezing mixture. The frozen pellets were stored in a freezing chest until all samples had been accumulated.

Details of the fractionation scheme are summarized in Fig. 1. In all steps involving the removal of perchloric acid, solutions of KOH and perchloric acid which had been previously titrated and precisely adjusted were used to ensure that the resultant solutions were between pH 6.5 and 6.6. Four cc of ice-cold 0.3 N perchloric acid (PCA) was added and the pellets extracted in the cold room at 4°C for 20 minutes. After centrifugation for 10 minutes at 2000 times gravity, 2.0 ml of the supernatant was removed and the PCA precipitated as the insoluble potassium salt by the addition of 0.6 ml of 1 N KOH and 2.4 ml of absolute ethanol. The remainder of the cold PCA supernatant and an equal volume of PCA wash were discarded and the centrifuged pellet containing DNA, RNA, and protein was hydrolyzed for 60 minutes at 37°C in 0.2 ml of 1 N KOH. Under these conditions, RNA was hydrolyzed but DNA was not (2), and the DNA was reprecipitated upon addition of 4.0 ml of 0.3 N PCA. After centrifugation of the precipitate at room temperature, a 2.1-ml aliquot was removed, 0.5 ml of 1 N KOH and 2.4 ml of absolute ethanol were added to remove the PCA, and the tube was chilled in an ice bath. Final dissolution of the DNA precipitate was achieved by addition of 4.0 cc of 0.3 N PCA and heating at 90°C for 20 minutes in a stoppered tube. The tube was chilled in an ice bath, and perchlorate removed from the DNA solution by addition of

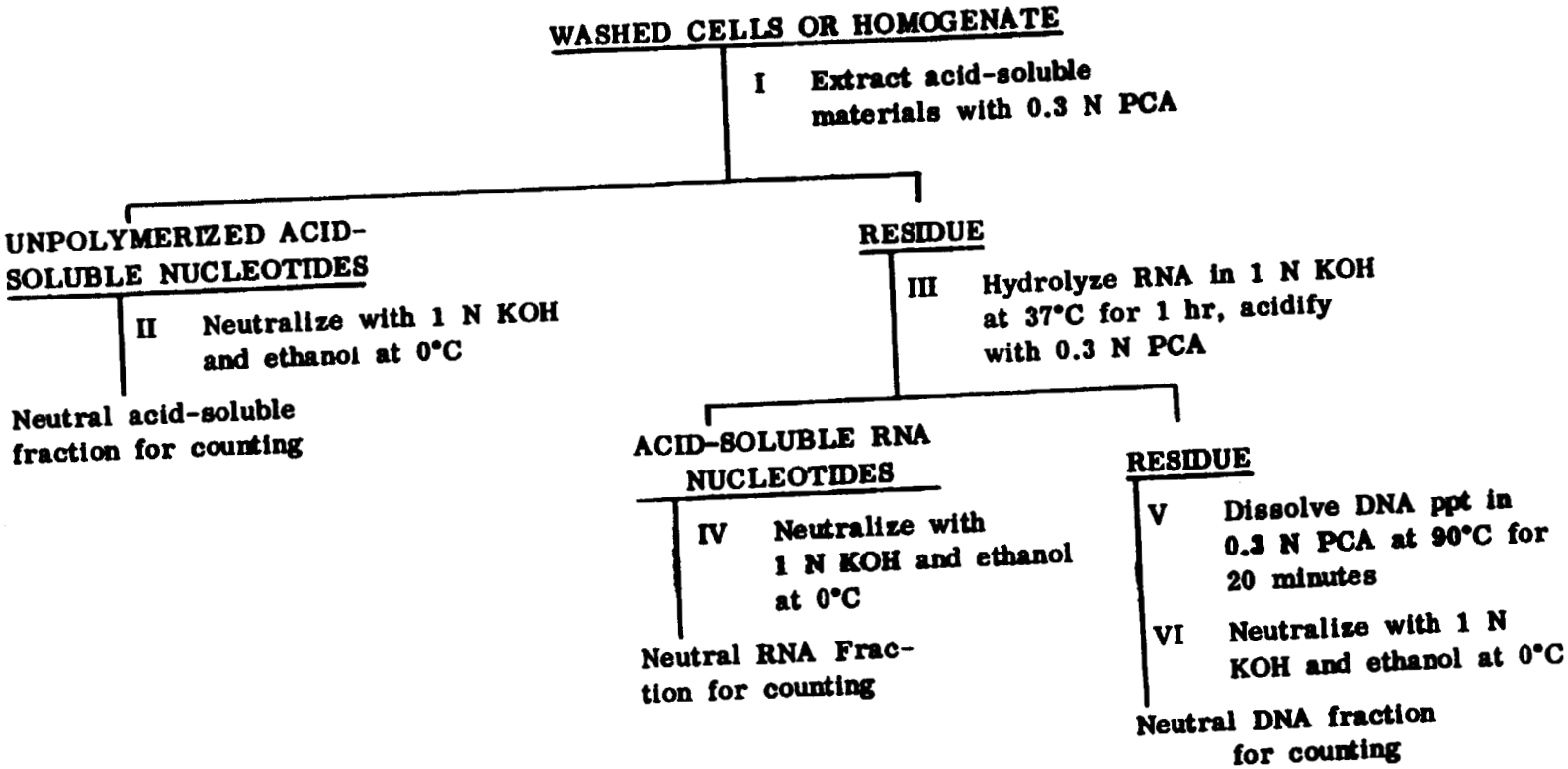

Fig. 1. Flow diagram for the separation and quantitative determination of radioactivity in tissue fractions containing tritium-labeled pyrimidine precursors.

1.2 ml of 1.0 N KOH, 4.8 ml absolute ethanol, and chilling in an ice bath. Contents of the chilled tubes from each fractionation step were centrifuged, and 1.0-ml aliquots of the supernatants were added to 15 ml of PPO-POPOP-naphthalene-dioxane scintillator (4). An automatic 2-channel liquid scintillation spectrometer was used to determine radioactivity in the various fractions.

RESULTS AND DISCUSSION

Because of the effect of pH on scintillation counting, it was necessary to determine its influence on efficiency of the scintillator system. Figure 2 demonstrates that final concentrations of perchloric acid ranging from 0.015 N to 0.120 N decreased efficiency of the counting system by a maximum of 30 per cent, necessitating removal of the excess acid from the system. Removal of perchloric acid was investigated both in the presence and absence of ethanol. Data shown in Table 1 indicate that counting efficiency was essentially the same in the aqueous system and in the alcoholic system. However, alcohol materially shortened the time necessary to complete the precipitation and was, therefore, incorporated in the standard procedure. Recoveries ranging from 94.8 to 96.8 per cent were obtained in the absence of alcohol and 96.1 to 97.1 per cent in the presence of alcohol.

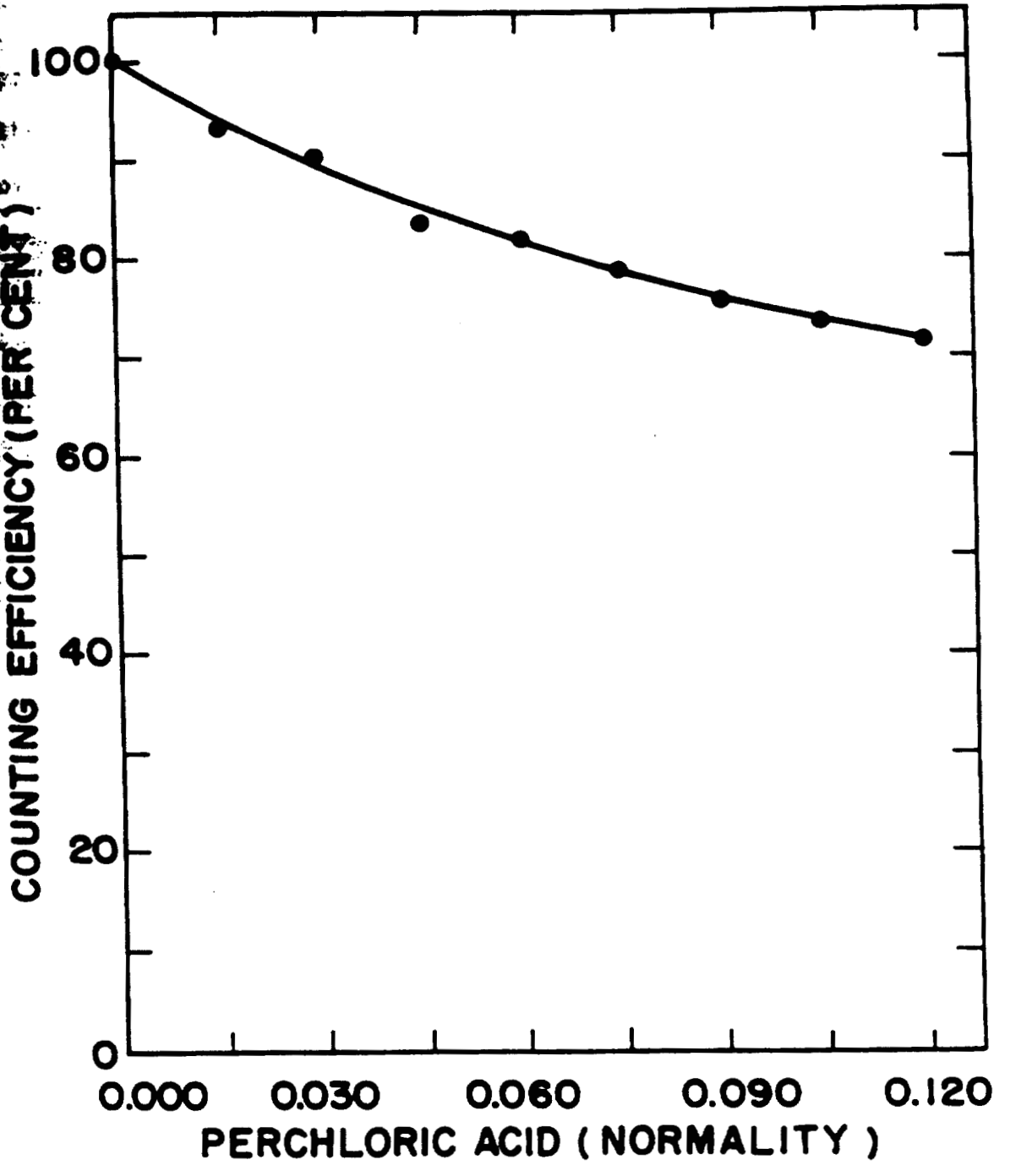

Fig. 2. The influence of perchloric acid concentration on counting efficiency.

TABLE 1. REPRODUCIBILITY OF COUNTING DATA OBTAINED FROM NEUTRALIZED PERCHLORIC ACID EXTRACTS CONTAINING TRITIATED THYMIDINE

Sample	PCA (ml 0.3 N)	KOH (ml 1 N)	H_2O (ml)	Ethanol (ml)	H^3TDR	c/m/ml	Recovery (per cent)
1	---*	---	---	---	0.10	2954	--
2	4.0	1.2	4.8	---	0.10	2828	95.9
3	4.0	1.2	4.8	---	0.10	2800	94.8
4	4.0	1.2	4.8	---	0.10	2859	96.8
5	4.0	1.2	4.8	---	0.10	2820	95.5
6	---*	---	---	---	0.10	3381	--
7	4.0	1.2	---	4.8	0.10	3284	97.1
8	4.0	1.2	---	4.8	0.10	3250	96.2
9	4.0	1.2	---	4.8	0.10	3248	96.1
10	4.0	1.2	---	4.8	0.10	3267	96.8

*Water and water/ethanol standards.

Additional examination of the method indicated that the procedure possessed considerable latitude with respect to the amount of material which could be analyzed. Total numbers of cells ranging from approximately 2×10^5 to 5×10^5 could be fractionated by the procedure outlined with essentially constant partitioning of activity when labeled thymidine was used as precursor. These data, shown in Table 2, demonstrate that HeLa cells during exponential growth accumulate thymidine largely in the deoxyribonucleic acid fraction with negligible amounts appearing in the RNA and acid-soluble fractions. Latitude in analytical capacity was of importance in maintaining a standard technique for analysis of cells in exponential growth where 2 to 4 fold increases in the concentration of cells per ml were expected during the course of an experiment. It would thus appear that the procedure outlined in this report is suitable for routine examination of the extent of tritiated thymidine incorporation.

Main and Walwick (1) have pointed out that high temperature formate hydrolysis tends to cleave the tritium attachments to ring carbons of deoxycytidine, while methyl attachments of thymidine are stable. In the present study, relative instability of the labeled compounds was investigated by two procedures. Extracts containing tritiated thymidine or deoxycytidine were counted directly, after charcoal adsorption

TABLE 2. THE INFLUENCE OF CELL CONCENTRATION ON DISTRIBUTION OF TRITIATED THYMIDINE RADIOACTIVITY IN TISSUE FRACTIONS

Cells per Sample	Acid-Soluble		RNA		DNA	
	(c/m)	(per cent)	(c/m)	(per cent)	(c/m)	(per cent)
2.3×10^5	3073	7.8	2806	7.1	33,705	85.2
3.9×10^5	840	1.2	6133	9.0	61,324	90.0
4.3×10^5	1622	2.2	3701	5.0	68,381	92.8
5.0×10^5	2216	2.6	4978	5.9	77,222	91.5
Average		3.5		6.8		89.8

and after hydrolysis and charcoal adsorption. The increase in the fraction not adsorbed by charcoal thus served as a measure of the extent of hydrolysis. Similar preparations were hydrolyzed and volatile material was trapped by low temperature vacuum distillation and counted. Results of these experiments, shown in Table 3, demonstrate that less than 2.0 per cent of the label was lost as judged by both procedures. However, since we have substituted a chemical precipitation step for the vacuum distillation recommended by Main and Walwick (1) for removal of excess acid, label cleaved from the tritiated pyrimidine precursors is largely retained and consistent recoveries of deoxycytidine label were obtained. Thus it is evident that the conditions of hydrolysis were not sufficiently rigorous to cause loss of labile tritium groups, and the absence of quenching materials suggests the procedure for a variety of quantitative biochemical investigations employing tritium-labeled precursors.

REFERENCES

(1) R. K. Main and E. R. Walwick, Naval Radiological Defense Laboratory Report NRDL-TR-452 (July 26, 1960).

(2) G. Schmidt and S. J. Thannhauser, J. Biol. Chem. 161, 83 (1945).

(3) W. C. Schneider, J. Biol. Chem. 161, 293 (1945).

(4) D. G. Ott, F. N. Hayes, and T. T. Trujillo, Los Alamos Scientific Laboratory Report LAMS-2445 (1960), p. 213.

TABLE 3. STABILITY OF TRITIUM-LABELED THYMIDINE AND DEOXYCYTIDINE DURING PERCHLORIC ACID HYDROLYSIS

Compound	Treatment	c/m Added	Net Increase (c/m)	Loss on Hydrolysis (per cent)
H^3-Thymidine	Charcoal adsorption	52,316	197	0.38
H^3-Thymidine	Vacuum distillation	54,104	670	1.23
H^3-Deoxycytidine	Charcoal adsorption	42,241	569	1.35
H^3-Deoxycytidine	Vacuum distillation	44,499	710	1.60

Deoxypolynucleotide Synthesis in Phosphorylating Rat Thymus Nuclei (D. F. Petersen, L. B. Cole, and V. E. Mitchell)

INTRODUCTION

Preliminary experiments employing phosphorylating rat thymus nuclei (1) suggested that small but consistent increases noted in deoxyribonucleic acid phosphorus were the result of a rearrangement of the total bound nucleotide and phosphorus complements of the nucleus in sucrose medium. This report deals with the results of labeling studies designed to examine this reaction in greater detail.

MATERIALS AND METHODS

Male Sprague-Dawley rats were used for these studies. Thymus nuclei were rapidly prepared in 0.25 M sucrose containing 0.0133 M $CaCl_2$ by the method described previously (1) and suspended in a final volume of 2 ml of sucrose-$CaCl_2$. Examination of the final suspensions by phase microscopy and by means of an electronic particle counter equipped with a 100-channel pulse height analyzer indicated that less than 5 per cent of the particles were either whole cells or fragments appreciably smaller than thymus nuclei. Nuclei suspensions were incubated aerobically for 20 minutes at 30°C in the presence of P^{32}, tritiated thymidine, or tritiated deoxycytidine. Aliquots were removed at 0, 5, 10, 15, and 20 minutes

and the distribution of the label in the organic acid-soluble, RNA, and DNA fractions was determined. In experiments employing P^{32} as the tracer, the fractions were selectively adsorbed on acid-washed Norit and counted. Tritiated pyrimidine distribution was determined by the liquid scintillation counting procedure described elsewhere in this report (2). Identification of deoxynucleotide polyphosphates on paper chromatograms was accomplished by the periodate oxidation method recently described by Saslaw and Waravdekar (3).

RESULTS AND DISCUSSION

Data shown in Fig. 1 indicate that tracer amounts of P^{32} orthophosphate are rapidly incorporated into the organic acid-soluble fraction and at a slower rate into the DNA fraction. The lag period before appreciable label appeared in the DNA was consistent with our preliminary observations based on chemical analysis for deoxyribose in perchloric acid-precipitable material. Virtually none of the P^{32} activity was incorporated into the RNA fraction.

Incorporation of labeled pyrimidines into the DNA fraction is shown in Fig. 2. These data demonstrate that thymidine was incorporated into DNA at approximately 4 times the rate of deoxycytidine, although the total amount of precursor introduced in the reaction mixtures was the same. Neither thymidine

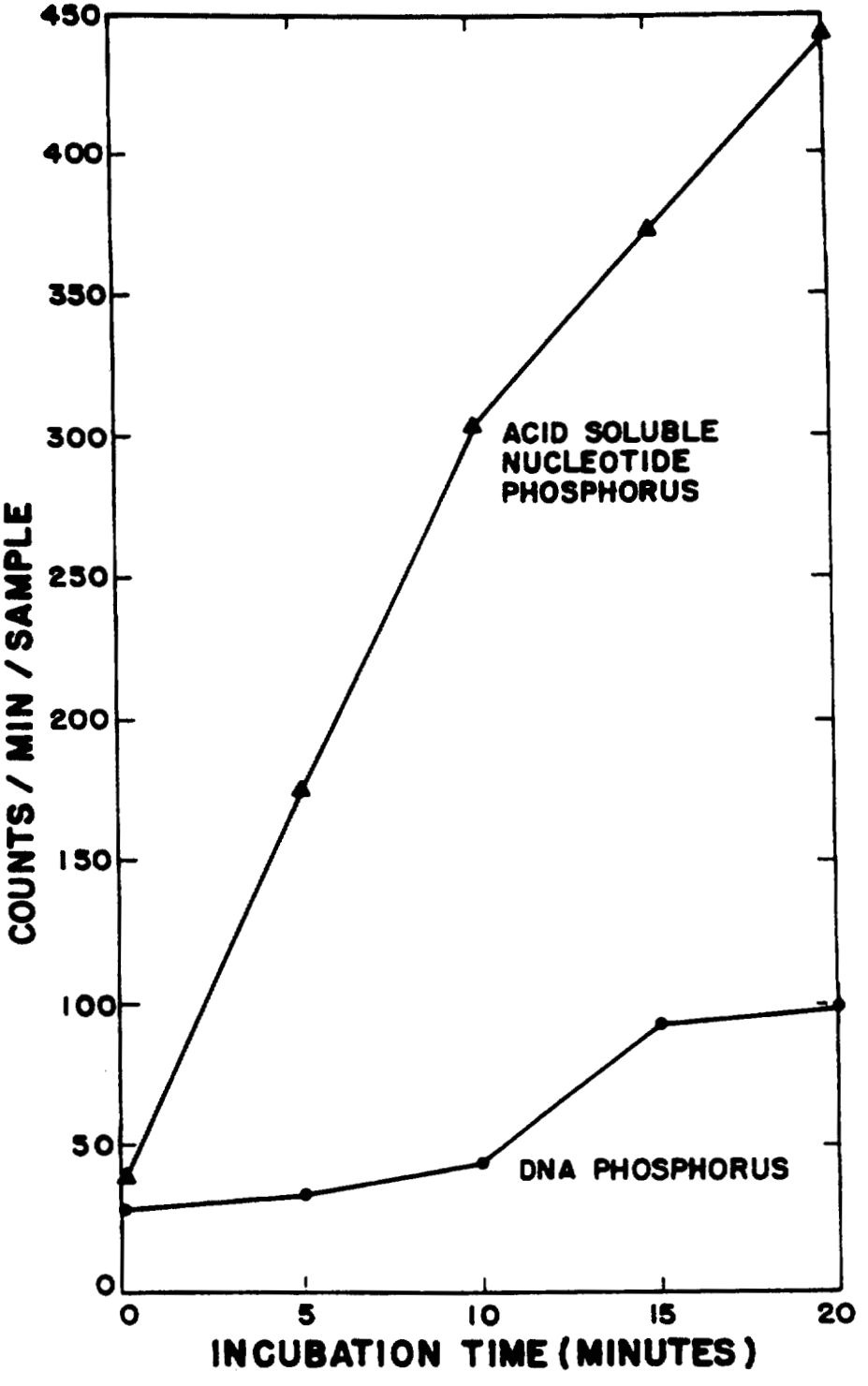

Fig. 1. Phosphorus^{32} incorporation by phosphorylating rat thymus nuclei.

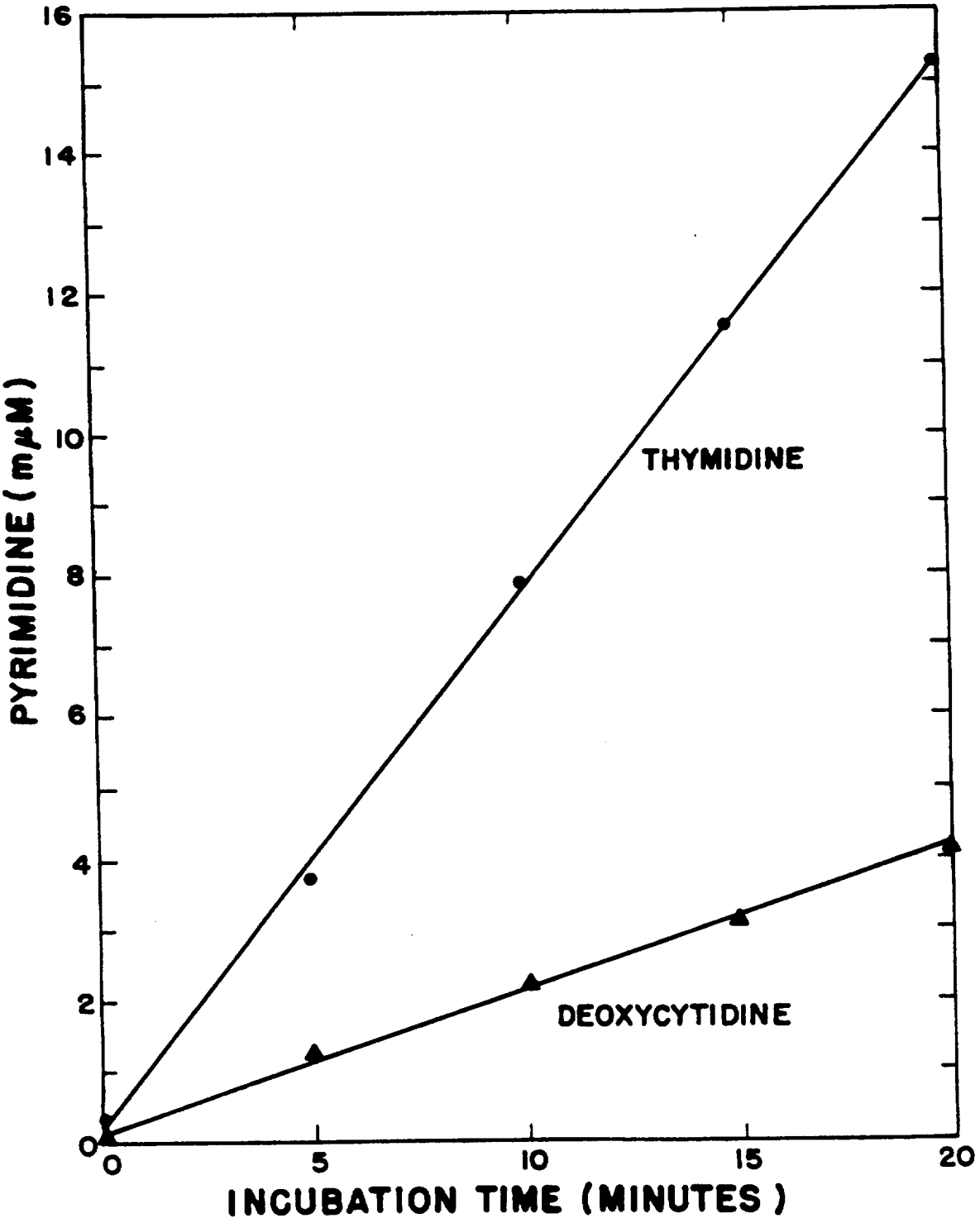

Fig. 2. Uptake of labeled pyrimidine precursors by phosphorylating rat thymus nuclei.

nor deoxycytidine was incorporated into RNA to an appreciable extent.

Paper chromatography of the nucleotides in the acid-soluble fraction indicated that the major ultraviolet absorbing spots contained demonstrable amounts of deoxyribose. Thus, although quantitative data are not as yet complete, both purine and pyrimidine deoxyriboside polyphosphates are present, and it is presumed that these compounds are the direct precursors of the labeled acid-precipitable material formed during the course of the reaction.

Mammalian systems capable of synthesizing DNA-like polymers have been described by several investigators (4-6). However, in the systems heretofore described, sufficient deoxynucleotide polyphosphate to account for the extent of synthesis has been added to the reaction mixture. The present studies describe a special case which, owing to the absence of precursors, raises the question of the origin of the building blocks for deoxypolynucleotide synthesis. The results imply that in addition to the capacity of thymus nuclei to synthesize ATP (1), kinases capable of forming deoxynucleoside polyphosphates as well as DNA polymerase must be present. At present it is not possible to state what the nature of the material formed is, and studies are now in progress to determine whether the labeled precursors are participating in a "limited reaction" or whether actual

synthesis utilizing native primer takes place. Preliminary experiments indicate breakdown of nucleolar RNA and suggest a possible source of bases. Other experiments have shown that the addition of 10 μM of thymidylic acid doubles the net increase in DNA phosphorus. Additional studies have also been initiated to ascertain whether sufficient reduced pyridine nucleotide is present in the preparations to permit reductive conversion of ribonucleotides to deoxyribonucleotides. Demonstration of reductive conversion would make this system an extremely valuable tool for further investigations on the pathways of purine and pyrimidine deoxyribonucleotide biosynthesis.

REFERENCES

(1) D. F. Petersen and L. B. Cole, Los Alamos Scientific Laboratory Report LAMS-2445 (1960), p. 27.

(2) D. F. Petersen, L. B. Cole, and V. E. Mitchell, this report (1961), p. 95.

(3) L. D. Saslaw and V. S. Waravdekar, Arch. Biochim. Biophys. 90, 245 (1960).

(4) F. J. Bollum and V. R. Potter, J. Biol. Chem. 233, 478 (1958).

(5) R. M. S. Smellie, H. M. Kier, and J. N. Davidson, Biochim. Biophys. Acta 35, 389 (1959).

(6) R. Mantsavinos and E. S. Canellakis, J. Biol. Chem. 234, 628 (1959).

per Chromatography of Nucleotides in Mildly Alkaline Aqueous Solvents (D. F. Petersen and M. Magee)

INTRODUCTION

Hems (1) has recently described a mildly alkaline aqueous solvent system consisting of 85 per cent saturated ammonium bicarbonate for the chromatographic separation of purine and pyrimidine analogs. This solvent system has proven extremely useful in this Laboratory and prompted the investigation of a variety of aqueous solvent systems consisting of various aliphatic amines adjusted to approximately pH 8. Several of these solvents appear to yield good resolution and as a class possess the advantage of rapid development in comparison with conventional alcohol-water systems.

MATERIALS AND METHODS

The aliphatic amines used in these experiments were either reagent-grade or were purified prior to use. CO_2 was bubbled through aqueous amine solutions until pH was 8, and final volume adjustments were made to attain 10 per cent solutions. Formic acid was added to yield a similar series of solvents at a final concentration of 10 per cent at pH 8. The purine and pyrimidine bases and their corresponding deoxyribonucleosides and deoxyribonucleotides* were spotted on

*Products of the California Corporation for Biochemical Research, Los Angeles, California.

Whatman No. 1 strips in amounts ranging from 10 to 30 μg. After equilibration for 2 hours, the chromatograms were developed in the ascending direction for 4 to 7 hours, dried in air at room temperature, and the location of the individual spots visualized in ultraviolet light (2). R_f values were determined and the separations evaluated with regard to trailing, paper background, and resolution.

RESULTS AND DISCUSSION

A systematic investigation of homologous series of primary, secondary, and tertiary amine carbonates and formates yielded results summarized in Tables 1 and 2. These data indicated that none of the solvents possessed the capacity to resolve completely complex mixtures of purine and pyrimidine bases, deoxynucleosides, and deoxynucleotides. However, satisfactory resolution could be obtained for any base and its corresponding deoxynucleoside and deoxynucleotide. In general, the formates appeared to be superior to the carbonates, and the best individual solvents of the series tested were judged to be the formates of ethyl and diethyl amine.

In addition, similar nucleotide series were separated in solvents containing trimethylamine, n-amylamine, 2-amino-2-methylpropanol, and ethylenediamine. Results shown in Table 3 indicate that in most cases good separation of members of a

TABLE 1. R_f VALUES OF PURINES AND PYRIMIDINES IN [redacted] SYSTEMS (pH 8)

Solvent System	Ethanolamine Carbonate	Diethanolamine Carbonate	Triethanolamine Carbonate	Ethylamine Carbonate	Diethylamine Carbonate	Triethylamine Carbonate
Purines						
Adenine	0.30	0.40	0.43	0.32	0.40	0.51
Deoxyadenosine	0.44	0.52	0.50	0.43	0.42	0.53
Deoxyadenylic acid	0.68	0.78	0.75	0.65	0.67	0.76
Guanine	0.04	P.A.*	0.05	0.57	0.44	0.17
Deoxyguanosine	0.57	0.62	0.56	0.54	0.54	0.72
Deoxyguanylic acid	0.77	0.84	0.79	0.72	0.72	0.87
Pyrimidines						
Cytosine	0.70	0.70	0.71	0.58	0.58	0.65
Deoxycytidine	0.74	0.77	0.71	0.68	0.66	0.74
Deoxycytidylic acid	0.95	0.90	0.86	0.79	0.82	0.86
Thymine	0.62	0.69	0.69	0.60	0.65	0.72
Thymidine	0.75	0.78	0.70	0.69	0.73	0.83
Thymidylic acid	0.90	0.91	0.84	0.79	0.81	0.90
Background	Dark	Dark	Dark	Dark	Fluorescent	Clear
Ultraviolet bands	Trailing	Trailing	Discrete	Trailing	Trailing	Trailing
Development time	4 hr	4 hr	4 hr	5 hr	5 hr	5 hr

*Point of application.

TABLE 2. R_f VALUES OF PURINES AND PYRIMIDINES IN ALIPHATIC AMINE FORMATE SOLVENT SYSTEMS (pH 8)

Solvent System	Ethanol-amine Formate	Diethanol-amine Formate	Triethanol-amine Formate	Ethyl-amine Formate	Diethyl-amine Formate	Triethyl-amine Formate
Purines						
Adenine	0.42	0.38	0.44	0.35	0.35	0.50
Deoxyadenosine	0.48	0.53	0.52	0.47	0.44	0.50
Deoxyadenylic acid	0.66	0.79	0.75	0.64	0.72	0.78
Guanine	0.02	0.05	P.A.*	0.26	0.37	0.54
Deoxyguanosine	0.55	0.66	0.58	0.52	0.59	0.66
Deoxyguanylic acid	0.69	0.81	0.75	0.68	--	0.86
Pyrimidines						
Cytosine	0.71	0.66	0.71	0.63	0.60	0.63
Deoxycytidine	0.71	0.79	0.72	0.74	0.70	0.67
Deoxycytidylic acid	0.85	0.93	0.87	0.83	0.87	0.78
Thymine	0.73	0.69	0.69	0.60	0.61	0.72
Thymidine	0.75	0.83	0.73	0.73	0.75	0.78
Deoxythymidylic acid	0.88	0.92	0.88	0.80	0.90	0.85
Background	Fluorescent	Fluorescent	Fluorescent	Clear	Clear	Clear
Ultraviolet bands	Discrete	Trailing	Trailing	Discrete	Discrete	Discrete
Development time	5 hr	7 hr	5 hr	4 hr	4 hr	8 hr

*Point of application.

TABLE 3. R_f VALUES OF PURINES AND PYRIMIDINES IN AMINE SOLVENT SYSTEMS

Solvent System	Trimethylamine Carbonate	n-Amylamine Carbonate	n-Amylamine Formate	2-Amino-2-methyl-1-propanol Carbonate	2-Amino-2-methyl-1-propanol Formate	Ethylenediamine Carbonate
Purines						
Adenine	0.48	0.42	0.46	0.40	0.39	0.32
Deoxyadenosine	0.58	0.58	0.57	0.51	0.48	0.48
Deoxyadenylic acid	0.78	0.78	0.79	0.75	0.74	0.69
Guanine	P.A.*	0.10	--	0.05	0.04	--
Deoxyguanosine	0.65	0.65	0.67	0.61	0.61	0.61
Deoxyguanylic acid	0.83	0.82	0.89	0.80	0.72	0.77
Pyrimidines						
Cytosine	0.64	0.69	0.69	0.66	0.66	0.67
Deoxycytidine	0.69	0.74	0.74	0.73	0.73	0.76
Deoxycytidylic acid	0.84	0.86	0.90	0.90	0.89	0.91
Thymine	0.70	0.62	0.71	0.65	0.69	0.62
Thymidine	0.75	0.78	0.81	0.75	0.78	0.77
Thymidylic acid	0.88	0.89	0.95	0.90	0.94	0.91
Background	Clear	Clear	Clear	Clear	Clear	Fluorescent
Ultraviolet bands	Discrete	Discrete	Discrete	Slight	Discrete	Discrete
Development time	5 hr	5 hr	5 hr	7 hr	7 hr	5 hr

*Point of application.

purine or pyrimidine series was achieved. However, complex mixtures could not be resolved adequately in one dimension.

It should be emphasized that these solvents are most useful for qualitative identification of small amounts of the various nucleotides, since in each case the residue of amine salts in the paper makes further manipulation difficult. However, the rapid development of these aqueous systems and their particularly good resolution of pyrimidine analogs suggest their application to a variety of biochemical problems necessitating rapid separation and identification of pyrimidine metabolites.

REFERENCES

(1) G. Hems, Arch. Biochim. Biophys. 82, 485 (1959).

(2) D. F. Petersen and A. Murray, Anal. Chem. 32, 443 (1960).

A Convenient Flash Drying Apparatus for Small Volumes (D. F. Petersen and M. Magee)

INTRODUCTION

Rotary film evaporation at room temperatures and under reduced pressure provides a convenient method for concentrating a variety of labile biological materials. Descriptions of several different types of apparatus have appeared in the literature (1-3). However, none of these could be readily adapted to small volumes and we have, therefore, constructed an all-glass device from standard laboratory equipment which is suitable for evaporation of volumes up to 5 ml.

MATERIALS AND METHODS

The drive mechanism was adapted from a cone drive laboratory stirrer simply by enlarging the diameter of the drive pulley from 1 to 2 in., as shown in Fig. 1. The rotating surface of the all-glass assembly was constructed from a 12/3 semiball joint. The female member was bent to clear the motor and held stationary while the rotating male member was held firmly in the collet chuck of the original stirring motor assembly. Silicone vacuum grease was used to lubricate the rotating joint, and the speed was varied by changing the location of the pulley on the drive cone. Since our application of the device necessitated the removal of an aqueous phase containing

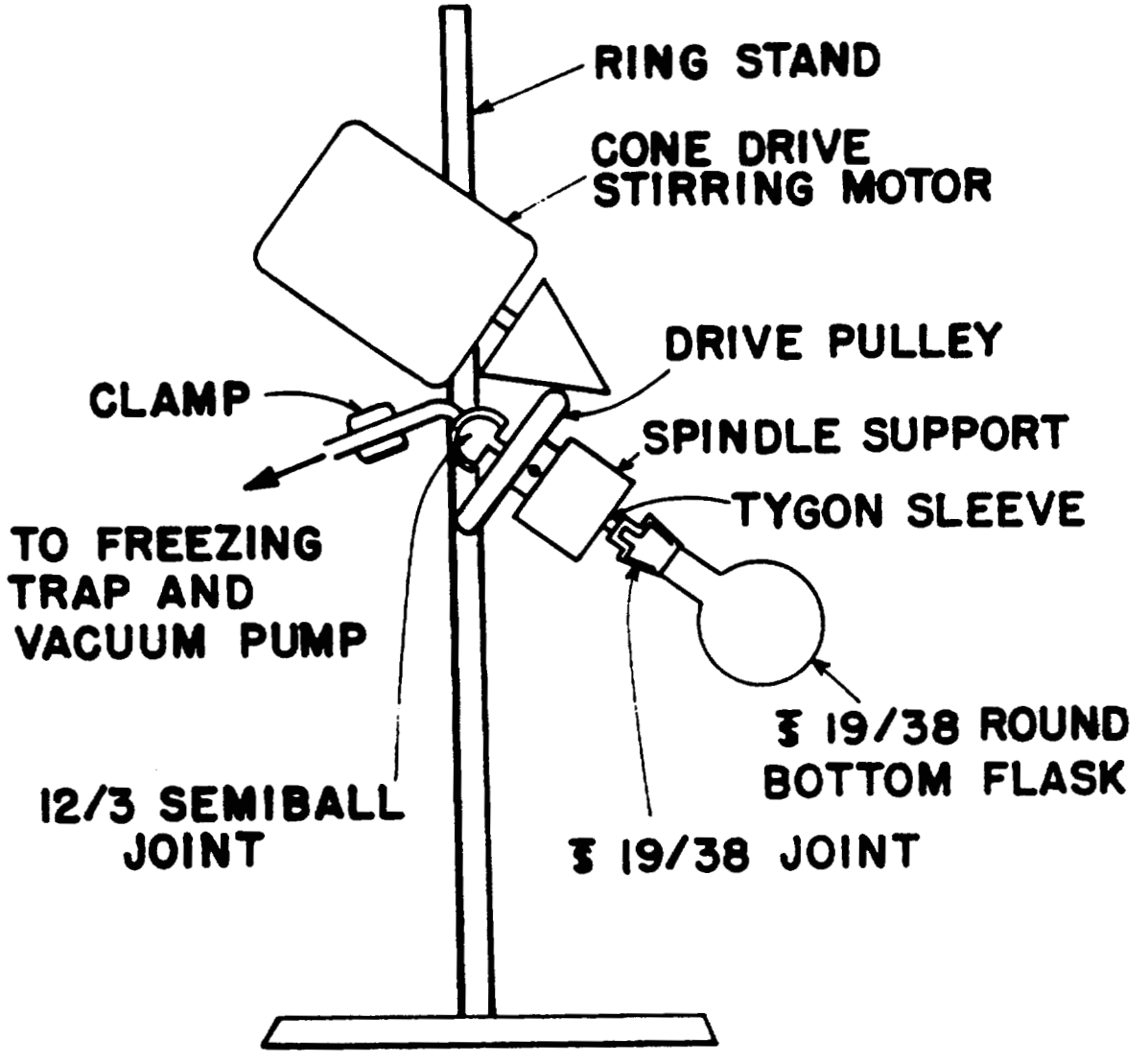

Fig. 1. Construction of small volume rotary evaporator.

volatile radioactivity, a freezing trap was also included and the distillate could thus be quantitatively recovered for further analysis or for controlled disposal. Since only minor modifications of the stirring apparatus are required, it is entirely feasible to construct several units without destroying the utility of the stirring motors for their conventional laboratory application.

REFERENCES

(1) G. Zweig, Anal. Chem. 31, 967 (1959).

(2) P. Kohn, Anal. Chem. 28, 1061 (1956).

(3) M. E. Volk, Anal. Chem. 27, 1207 (1955).

BIOCHEMISTRY SECTION PUBLICATIONS

(1) H. Foreman, The Pharmacology of Some Useful Chelating Agents, Metal-Binding in Medicine, Proceedings of a Symposium sponsored by the Hahnemann Medical College and Hospital, Philadelphia, Pa. (May 6-8, 1959). J. M. Seven and L. A. Johnson (eds.), J. B. Lippincott Company, Philadelphia (1960), pp. 82-94.

(2) H. Foreman, Application of Chelating Agents for Hastening Excretion of Radioelements, Metal-Binding in Medicine, Proceedings of a Symposium sponsored by the Hahnemann Medical College and Hospital, Philadelphia, Pa. (May 6-8, 1959). J. M. Seven and L. A. Johnson (eds.), J. B. Lippincott Company, Philadelphia (1960), pp. 160-168.

MANUSCRIPTS SUBMITTED

(1) H. Foreman, The Use of Chelating Agents in the Treatment of Metal Poisoning (With Special Emphasis on Lead), presented at the National Academy of Sciences-National Research Council Conference on Biological Aspects of Metal Binding, Pennsylvania State University, University Park, Pa. (September 6-9, 1960). To be published in Proceedings by J. B. Lippincott and Company, Philadelphia.

(2) D. F. Petersen, V. E. Mitchell, and W. H. Langham, Radiochemical Estimation of Fast Neutron Doses in Man, presented at Bioassay and Analytical Chemistry Meeting, Santa Fe, New Mexico (October 13-14, 1960). To be published in Proceedings as a TID- or Sandia-report.

(3) D. F. Petersen, V. E. Mitchell, and W. H. Langham, Estimation of Fast Neutron Doses in Man, submitted to Health Physics.

(4) C. R. Richmond and J. E. Furchner, Effect of a Carbonic Anhydrase Inhibitor (Diamox) on Cesium^{137} Excretion by Rats, submitted to Health Physics.

CHAPTER 3

LOW-LEVEL COUNTING SECTION

Cesium^{137} Levels in People (E. C. Anderson and B. E. Clinton)

INTRODUCTION

As previously reported (1,2), the frequency distribution curves for Cs^{137} in the U. S. population for the years 1956 and 1957 were normal with standard deviations of 36 per cent. Because of possible sampling errors introduced by averaging together subjects from areas of different fallout levels, a more accurate check of the normality of the distribution can be obtained by using only data from a single area. Sufficient data are available for New Mexico subjects for the past 5 years to permit this analysis.

METHODS AND RESULTS

Cesium^{137} was determined using Humco I, the LASL 4π liquid scintillation counter (3). Energy discrimination

[redacted]itted separation and simultaneous determination of both Cs^{137} and K^{40}, and the results are reported in terms of the Cs^{137}/K^{40} ratio which permits convenient comparison of widely [redacted]ferent types of samples.

[redacted]equency Distribution

Table 1 summarizes the frequency distribution of the [redacted]sults for New Mexico subjects for the years 1956 to 1960, [redacted]nclusive. "Adult" subjects only (arbitrarily defined as all subjects weighing more than 40 kg) are included to eliminate the possibility of any error due to a systematic variation of counter efficiency in a weight range where in vivo calibration has not been possible. (Actually, no difference was observed between the yearly averages for the 2 weight groups greater and less than 40 kg, respectively.) Reported in the table are the number of subjects observed to fall within successive increments of the Cs^{137} level, the cumulative number of subjects having less than a given Cs^{137} level, and the corresponding cumulative fraction of the population sample. The number of subjects varied from 215 (1958) to 81 (1959). (The 1960 summary was made in November and does not include all subjects for the entire year.) These data are plotted in Fig. 1 on linear probability paper. (On this paper, a normal frequency distribution curve plots as a straight line with

TABLE 1. DISTRIBUTION OF CESIUM^{137} LEVELS IN NEW MEXICO ADULTS

Cs^{137} (pc/g K)*	1956		1957		1958		1959		1960	
	Cumulative	Fraction	Cumulative	Fraction	Cumulative	Fraction	Cumulative	Fraction	Cumulative	Fraction
10	0	0	1	0.0099	0	0	0	0	0	0
20	1	0.0070	5	0.0495	1	0.0046	0	0	1	0.0079
30	15	0.106	19	0.188	4	0.0186	0	0	3	0.0238
40	49	0.345	41	0.406	14	0.0652	0	0	8	0.0634
50	79	0.548	70	0.693	70	0.325	4	0.0494	33	0.262
60	107	0.754	84	0.832	129	0.600	19	0.234	61	0.484
70	125	0.880	92	0.911	180	0.836	37	0.456	96	0.761
80	133	0.936	98	0.970	202	0.940	59	0.729	115	0.912
90	140	0.985	99	0.980	207	0.964	68	0.839	121	0.960
100	141	0.992	100	0.990	211	0.981	77	0.951	122	0.967
110	142	1.000	101	1.000	213	0.990	80	0.989	123	0.975
120					214	0.995	81	1.000	125	0.991
130					215	1.000			125	0.991
140									125	0.991
150									126	1.000
160										

*pc = picocurie = 10^{-12}curie.

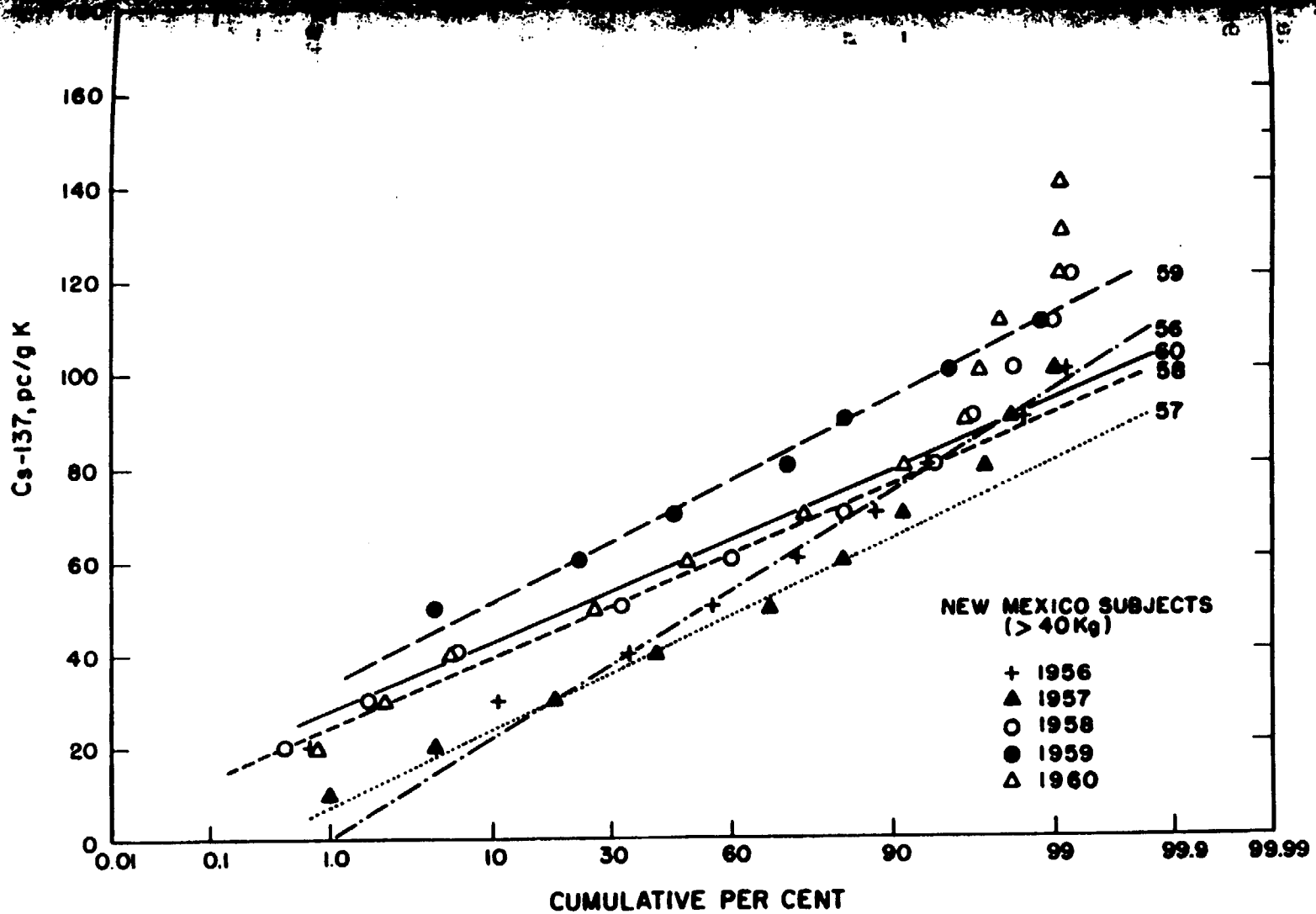

Fig. 1. Cumulative frequency distribution of Cs^{137} concentration in adult subjects (New Mexico), 1956-1960.

slope proportional to the standard deviation; the steeper the slope, the larger the standard deviation.) The curves for 1956 and 1959 are normal, and 1957 is not significantly abnormal. Both 1958 and 1960 appear to show a non-normal trend at high cesium level. The number of subjects whose Cs^{137} levels exceed 100 pc/g K were 5 and 4, respectively, compared with expectations of 0.4 and 0.25 from normal curves.

Table 2 and Fig. 2 give the same data for all adult subjects measured during this period. In this case, a deviation is detectable in all years except 1956, and is especially pronounced in 1959. The more pronounced abnormality may result from the inclusion of subjects from areas of higher fallout.

The latter data are replotted in Fig. 3 on logarithmic probability paper; here a log-normal distribution would give a straight line. The fit of the data to straight lines is only slightly better. The year 1959 still shows an upward deviation at high cesium levels, and all curves now show a significant drop at low cesium values (i.e., too many subjects show very low cesium values). Neither the normal nor the log-normal curve is, therefore, completely successful in describing the data.

For the purposes of predicting maximum probable radiation doses to individuals, the region of the frequency curve

TABLE 2. DISTRIBUTION OF CESIUM^{137} LEVELS IN ALL ADULT SUBJECTS

Cs^{137} (pc/g K)	1956		1957		1958		1959		1960	
	Cumulative	Fraction	Cumulative	Fraction	Cumulative	Fraction	Cumulative	Fraction	Cumulative	Fraction
0	1	0.0038	1	0.003	0	0	0	0	0	0
10	6	0.0229	8	0.027	1	0.0024	0	0	0	0
20	33	0.126	28	0.094	4	0.0092	1	0.0033	3	0.019
30	85	0.325	81	0.272	24	0.0551	6	0.0199	9	0.036
40	147	0.561	160	0.536	116	0.266	21	0.069	41	0.156
50	197	0.753	223	0.748	222	0.511	68	0.225	92	0.363
60	225	0.860	253	0.849	318	0.731	126	0.417	154	0.586
70	248	0.947	276	0.926	381	0.876	201	0.666	200	0.761
80	259	0.990	286	0.959	407	0.936	240	0.795	225	0.849
90	261	0.996	294	0.986	424	0.975	274	0.907	240	0.913
100	262	1.000	298	1.000	428	0.985	289	0.956	249	0.948
110					432	0.994	294	0.974	257	0.978
120					435	1.000	297	0.983	261	0.992
130							298	0.986	262	0.996
140							300	0.994	263	1.000
150							300	0.994		
160							301	0.997		
170							302	1.000		
180										

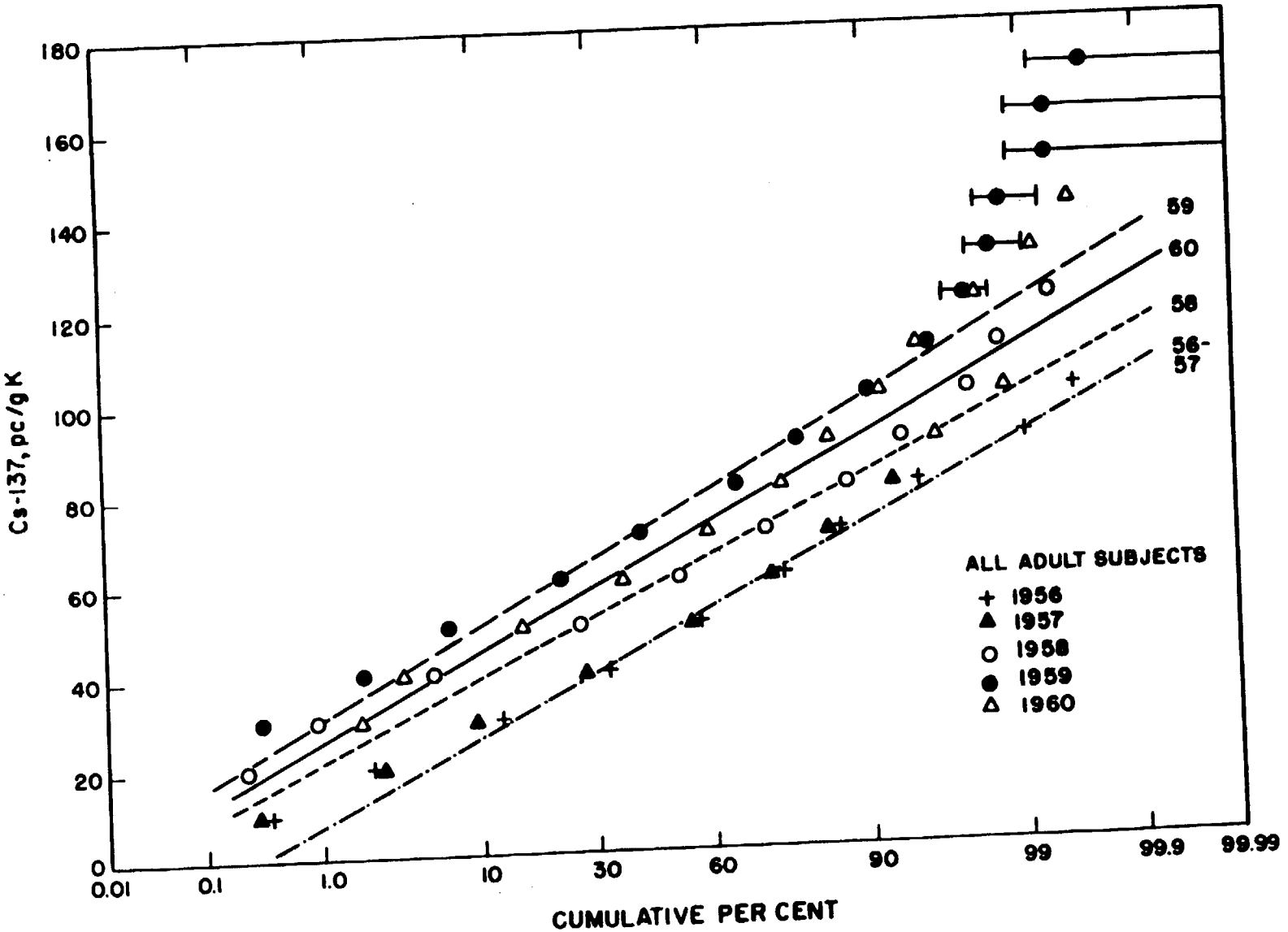

Fig. 2. Linear cumulative frequency distribution of Cs^{137} concentration in adult subjects (United States), 1956-1960.

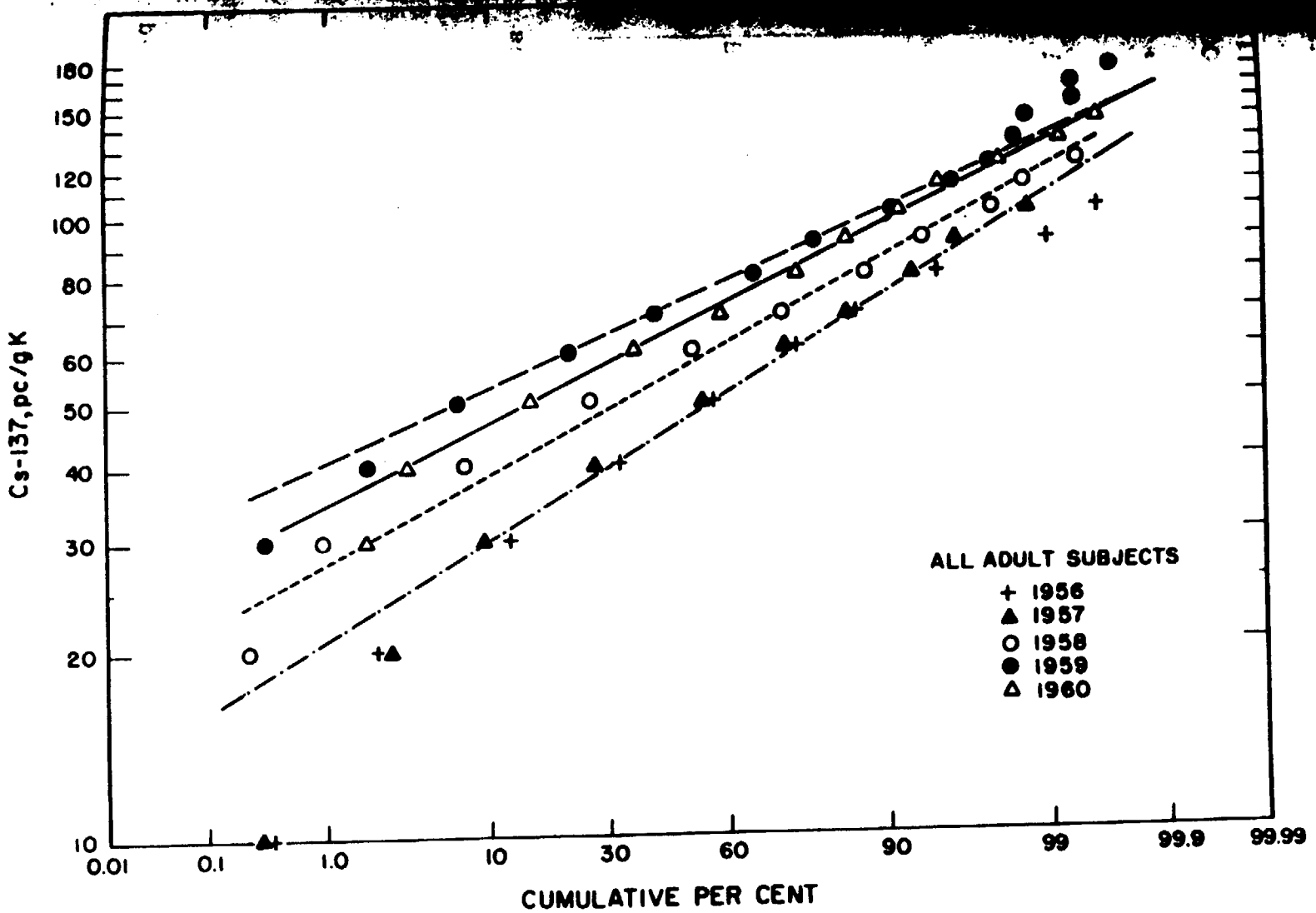

Fig. 3. Logarithmic cumulative frequency distribution of Cs^{137} concentration in adult subjects (United States), 1956-1960.

beyond 99.8 per cent may be of importance. However, since these persons are encountered at the rate of only 2 per 1000, a larger body of data is required. Pooling the Los Alamos, the Army Medical Research Unit Europe (4), and the Walter Reed Army Institute of Research (5) data would give a total approaching 10,000 subjects in which one might expect to find 20 examples.

Regional Averages

Sufficient data are now available to estimate the relative concentrations of Cs^{137} in various parts of the United States for the population sample represented. Since this sample is drawn from visitors to Los Alamos and hence represents an unusually mobile subgroup, these ratios may not correspond to the population-weighted average for the various regions. Because of possible variations of the source (geographic) and composition of diet with family income, the extent to which local fallout conditions are reflected in man may vary with economic status.

For purposes of this comparison, the U. S. was divided into 10 regions, as shown in Fig. 4. The method of division was determined by climatic and geographic uniformity, modified by number of subjects available. Certain states, such as New Mexico and Colorado, are so well represented that they can be

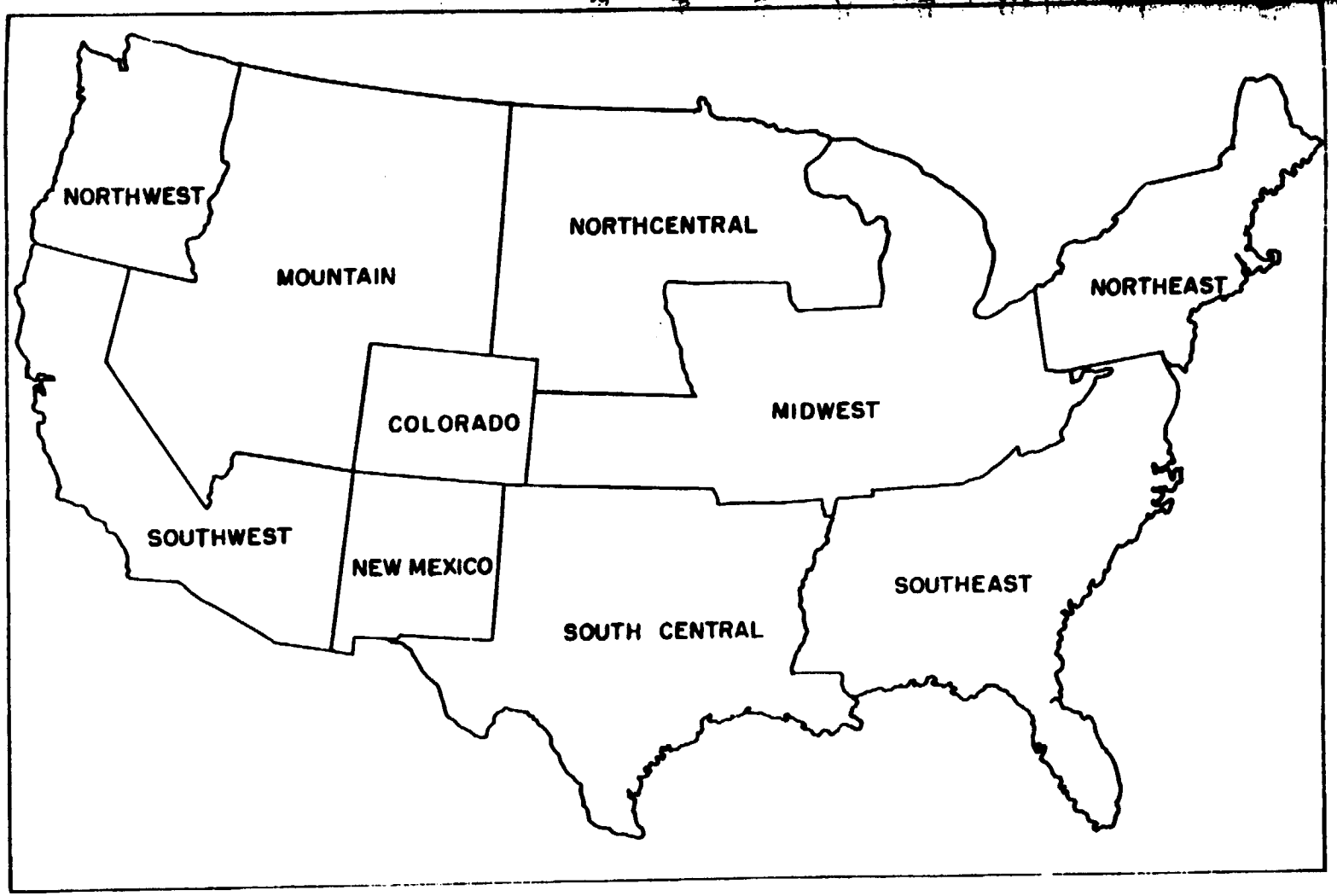

Fig. 4. Subdivision of United States population sample by areas.

treated as statistically significant units. The "Mountain" area is so poorly represented that no yearly average calculations are possible. The "Northwest" is of questionable homogeneity because of the extreme differences in rainfall on opposite sides of the Cascade Range. Similar objections apply to other areas, in some cases moderated by selectivity in the actual sources of subjects (e.g., the Californians are largely from the southern, dry part of the state). The data are presented with these reservations.

Table 3 summarizes the results for the past 5 years. To eliminate effects of a secular change, the New Mexico average (the best defined statistically) is taken as unity for each year and the averages for other regions referred to it. For reference, the actual New Mexico averages (in pc/g K) are given in the last line. The number of subjects is given in parentheses below each average.

The consistency of the ratios for a given area over the 5-year period adds confidence that the differences are real. In addition, the general agreement of the pattern of the ratios with that of rainfall and primary fallout is as expected. New Mexico is one of the lowest areas, but California-Arizona is the lowest. The highest areas are the Northeast and Northwest, in agreement with milk results. The narrow range of variation is noteworthy.

TABLE 3. COMPARISON OF CESIUM^{137} LEVELS IN SUBJECTS FROM VARIOUS PARTS OF THE UNITED STATES

Area	(Units Relative to New Mexico Averages*) 1956	1957	1958	1959	1960	Average
Southeast	1.10** (23)	1.05 (21)	1.10 (21)	1.18 (16)	1.46 (13)	1.18 (94)
Northeast	1.33 (19)	1.27 (31)	1.22 (40)	1.22 (21)	1.52 (13)	1.31 (124)
Southcentral	0.81 (14)	1.00 (11)	1.05 (35)	0.93 (33)	0.93 (13)	0.94 (106)
Midwest	1.01 (45)	1.16 (45)	1.17 (47)	1.10 (32)	1.14 (47)	1.12 (216)
Northcentral	1.49 (3)	1.13 (12)	1.37 (16)	1.19 (6)	1.19 (15)	1.25 (52)
Southwest	0.74 (17)	0.89 (20)	0.85 (39)	0.87 (20)	0.99 (16)	0.87 (112)
Colorado	0.81 (6)	1.30 (28)	1.00 (14)	1.07 (47)	1.05 (6)	1.12 (101)
Northwest	1.10 (5)	1.38 (15)	1.23 (12)	1.14 (9)	1.30 (9)	1.23 (50)
Mountain	Too few subjects					
New Mexico* in pc/g K	49.6 (143)	44.8 (103)	58.1 (223)	72.3 (81)	61.6 (143)	---- (693)

*New Mexico average = 1.00 for each year.

**Number of subjects given in parentheses below ratio.

Absolute values of the Cs^{137}/K level in pc/g can be compared with the averages recently reported by Rundo (6) for England. The best U. S. area for comparison is presumably the Midwest, on the basis of the good agreement reported between Rundo and the Argonne National Laboratory (7). Correcting our absolute numbers by the factor 0.915 based on standard recalibration (8), we obtain the results summarized in Table 4. The Los Alamos results appear to be consistently higher than the Harwell measurements by some 20 to 30 per cent. The secular pattern of the two sets of data is, however, in very good agreement as shown in Table 5 in which the 1959 level is taken as unity. The cause of the discrepancy on the absolute level is not known. A detailed recalibration of Humco I, which is planned at the time Humco II is calibrated, may shed more light on the problem.

TABLE 4. COMPARISON OF LASL AND HARWELL RESULTS - AVERAGE CESIUM^{137} IN PEOPLE (in pc/g K)

Source of Data	1956	1957	1958	1959	1960
Harwell, Berks. and Oxfs.	32	38	48	60	55
LASL, Midwest	46	47	62	73	64
Ratio, LASL/Harwell	1.44	1.24	1.29	1.22	1.16

TABLE 5. COMPARISON OF LASL AND HARWELL RESULTS - CESIUM^{137} LEVELS RELATIVE TO 1959

Source of Data	1956	1957	1958	1959	1960
Harwell, Berks. and Oxfs.	0.53	0.63	0.80	(1.00)	0.92
LASL, Midwest	0.63	0.64	0.85	(1.00)	0.88

REFERENCES

(1) E. C. Anderson, R. L. Schuch, W. R. Fisher, and W. Langham, Science 125, 1273 (1957).

(2) E. C. Anderson, Science 128, 882 (1958).

(3) E. C. Anderson, Brit. J. Radiol., Suppl. 7, 27 (1957).

(4) C. O. Onstead, E. Oberhausen, and F. V. Keary, Atompraxis 9, 337 (1960), and private communication.

(5) K. T. Woodward, H. A. Claypool, and J. B. Hartgering, Hearings before the Special Subcommittee on Radiation of the Joint Committee on Atomic Energy, Congress of the United States, Eighty-Sixth Congress, First Session on Fallout from Nuclear Weapons Tests (May 5-8, 1959), Vol. 2, 1349 (1959), and private communication.

(6) J. Rundo, Nature 188, 703 (1960).

(7) C. E. Miller and L. D. Marinelli, Argonne National Laboratory Report ANL-5919 (1958), p. 74, and ANL-6104 (1960), p. 78.

(8) E. C. Anderson and M. A. Van Dilla, Los Alamos Scientific Laboratory Report LAMS-2445 (1960), p. 136.

Variation of Human Potassium Concentration with Age (E. C. Anderson and B. E. Clinton)

INTRODUCTION

Previous studies of human potassium (1,2) have shown interesting correlations with sex and age, as well as with other physiological parameters including body water, lean body weight, and basal metabolic rate. The age effect has been confirmed by measurements on large population samples with liquid scintillation counters in Washington, D. C. (3) and in Landstuhl, Germany (4). Because the fine structure previously reported (1) in the age variation involves small changes in potassium concentration (as little as 5 per cent), it seemed worthwhile to check the reproducibility of the details using a completely new population sample.

METHODS AND RESULTS

During 1959-1960, an additional 1128 measurements were made (as of November 2, 1960) of the gamma activity (both K^{40} and Cs^{137}) of human subjects using Humco I, the large 4π liquid scintillation whole body counter (5). Of these, 802 were suitable for calculating the potassium concentration as a function of age. (The remainder of the measurements were on contaminated subjects or repeated determinations on a small group of controls.) Both this group and the

one previously reported consisted of visitors to the Health Research Laboratory, the first group covering the period 1956-1958 and the second group 1959-1960. Subjects were measured wearing surgeon's scrub suits previously monitored and shown to be free of radioactivity. Showers were not required.

The points plotted in Fig. 1 (circles for males, triangles for females) are the results of the new determinations. Each point is the average of a number of individuals in the appropriate age group, the number ranging from 11 to 60 except for the 2 oldest female groups, which contain 8 and 2 subjects, respectively. The indicated uncertainty is the standard error of the mean calculated from the observed standard deviation of the individual values within each group from the group mean and the number of determinations per group.

The curves drawn in the figure are identical with those representing the best fit to the previous determinations except that they have been displaced downward by 2 per cent to optimize the fit to the new data. The reproducibility of the measurements and of the 2 population samples is thus comparable with the standard errors of the means, which range from 1 to 3 per cent.

DISCUSSION

The principal discrepancy between the 2 sets of data is

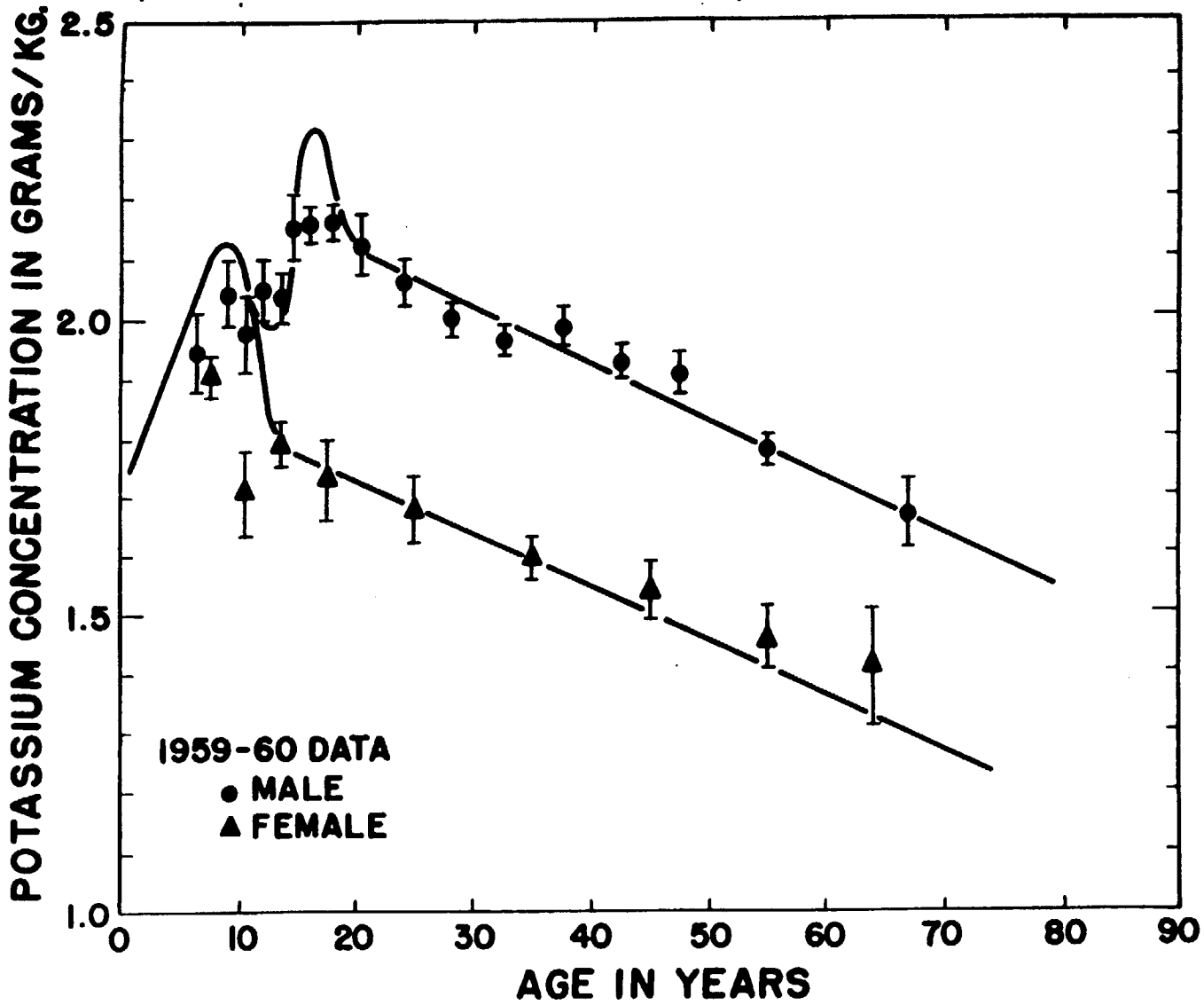

Fig. 1. Variation of human body potassium concentration with age and sex.

for the male subjects in the age range 15 through 18 years. Here the sharp peak previously observed did not appear. In the 1956-1958 data, 55 subjects in this age range gave an average of 2.303 $\pm$ 0.028 g K/kg, while in the 1959-1960 data, 66 subjects gave an average of 2.160 $\pm$ 0.022. Increasing the latter result by 2 per cent for the apparent systematic difference between the 2 periods gives 2.204 for the second group. The difference between the 2 is, therefore, 0.099 $\pm$ 0.036 so the difference is 2.8 times its standard deviation. Application of the t test (6) with 120° of freedom indicates that the probability is less than 0.01 that the 2 groups have the same average potassium content.

There is no internal evidence of a non-normal distribution in either group. Figure 2 is a graph of the cumulative frequency distribution of the potassium concentrations for subjects of ages 15 through 17 years inclusive. (The age range is narrowed here to concentrate on subjects falling in the peak region.) Normal curves give a straight line on this type of graph, the steeper the slope the larger the standard deviation of the distribution. The graphs indicate average potassium values of 2.30 and 2.15 g/kg for the 2 population groups with standard deviations of 0.20 and 0.17, respectively. There were 45 subjects in this age range in the earlier group and 52 subjects in the later group. The subjects of both

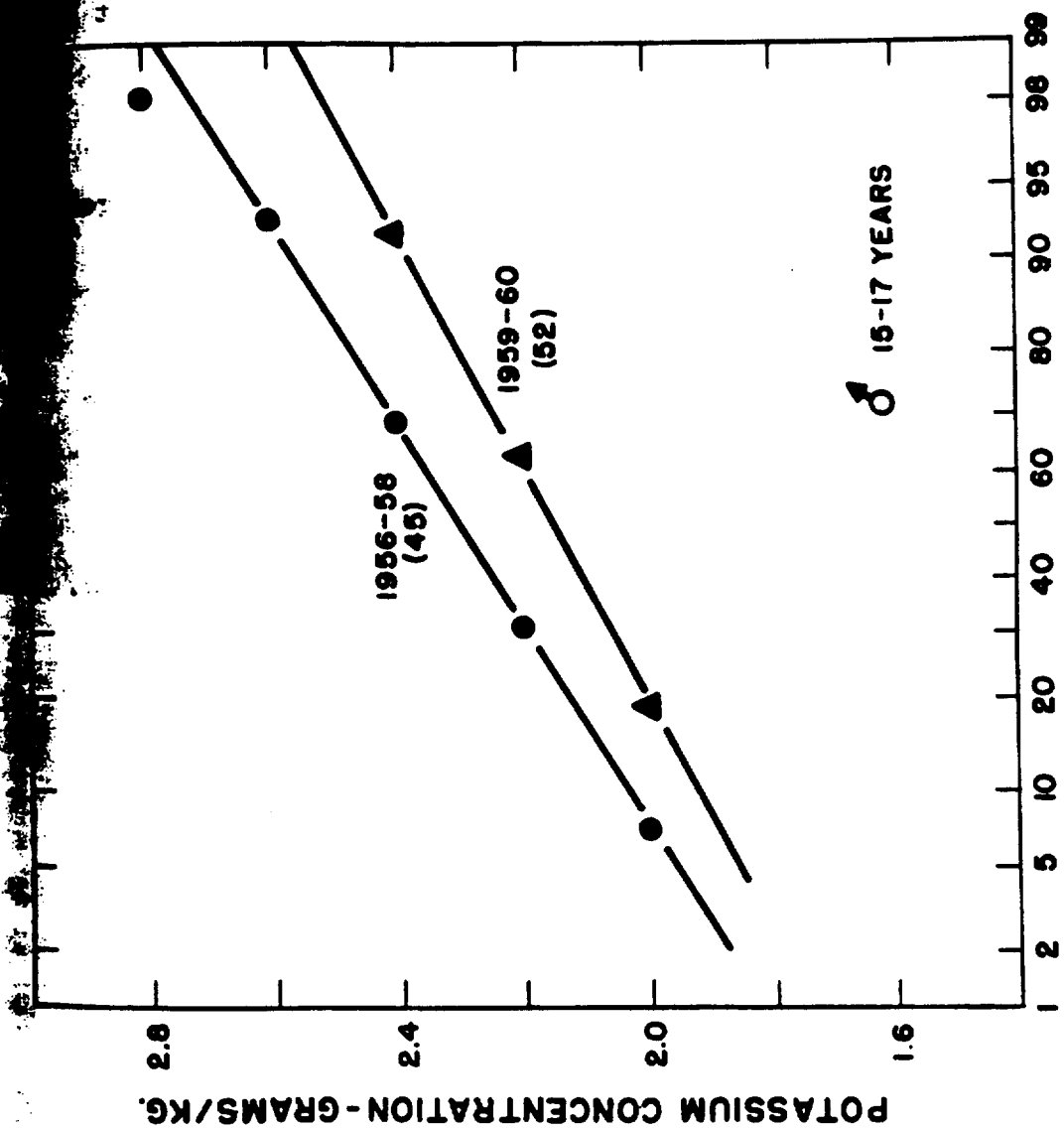

Fig. 2. Cumulative frequency distribution of potassium concentration in 15 to 17 year old male subjects.

groups were measured over considerable periods of time well interspersed among subjects of other ages, and no unusual conditions of background, calibration, or counter instability occurred during any of the measurements.

The disappearance of the peak may, therefore, represent a sampling variation. A slight excess of subjects who were more active physically than average could have produced the peak. A more detailed study of individuals in this age range with attention to their participation in athletics would be of interest. Variations of "physical" as opposed to "chronological" age could also produce significant variations during a period when potassium is changing rapidly with age.

The point for females of age 9 to 11 (14 subjects) is also aberrant, falling significantly below the expected value. This is apparently due to a sampling accident which led to the selection of a group of unusual gross weights. Figure 3 shows the observed gross weight in kilograms as a function of age for the population samples; the points are the 1959-1960 data and the lines represent the 1956-1958 data. The female group in question has an average gross body weight of 42 kg compared with 34 kg expected on the basis of the other age groups. Assuming the same total potassium, recalculation to "normal" weight gives a potassium concentration of 2.11 g/kg, which is very close to the expected value.

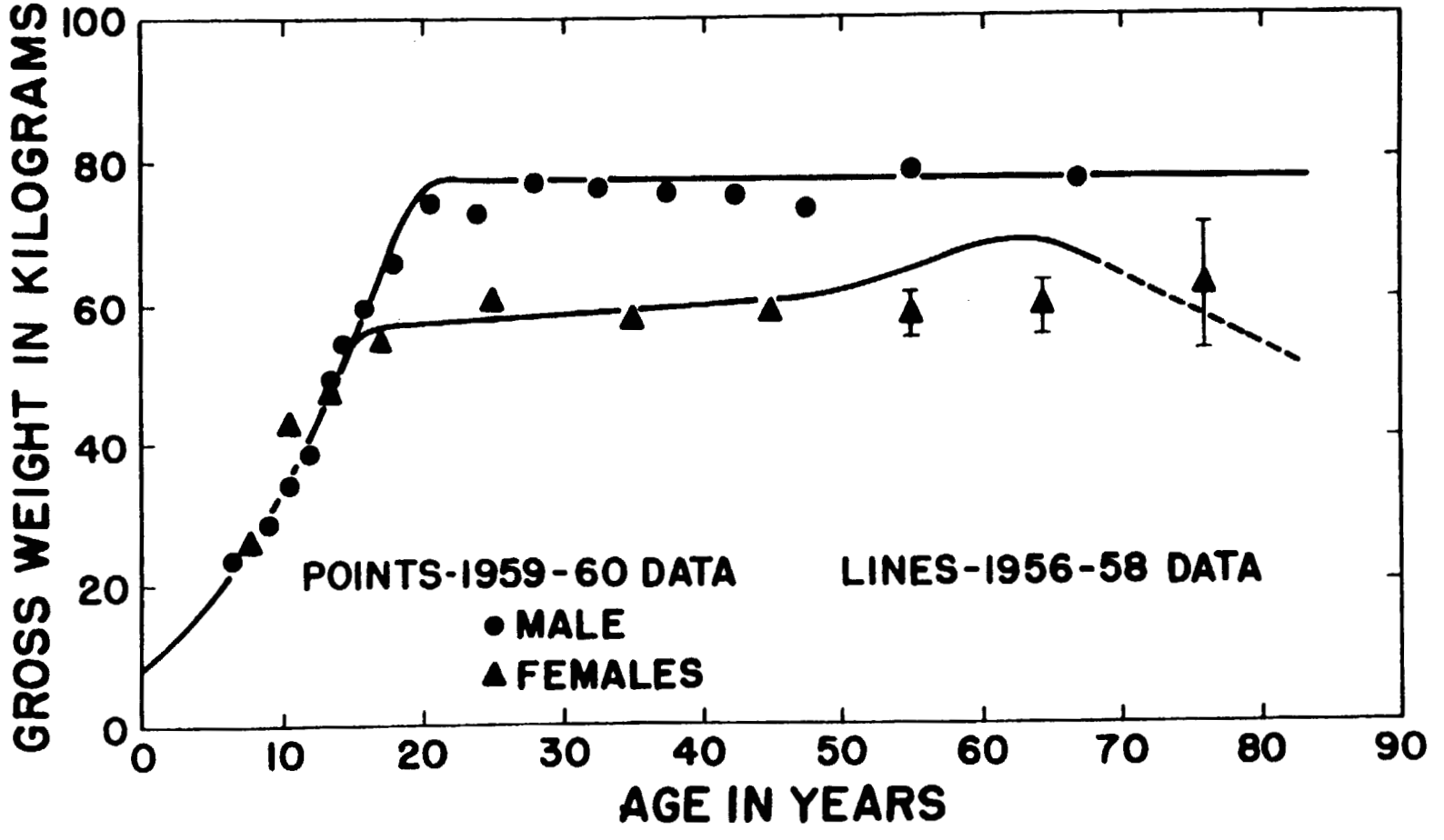

Fig. 3. Variation of average gross weights of male and female subjects with age.

These 2 areas of disagreement should not obscure the otherwise excellent agreement of ± 1 per cent between the 2 sets of data. This agreement confirms both the stability of the counter calibration and the reliability of the population sampling and averaging in general. Closer attention to sampling of subjects in or near puberty is indicated.

REFERENCES

(1) E. C. Anderson and W. H. Langham, Science 130, 713 (1959).

(2) T. H. Allen, E. C. Anderson, and W. H. Langham, J. Gerontol. 15, 348 (1960).

(3) K. T. Woodward, Walter Reed Army Institute of Research, unpublished results.

(4) C. O. Onstead, E. Oberhausen, and F. V. Keary, Atompraxis 9, 337 (1960).

(5) E. C. Anderson, IRE Trans. Nucl. Sci. NS-3, 96 (1956).

(6) G. W. Snedecor, Statistical Methods, The Iowa State College Press, Ames, Fourth Edition (1950), p. 77.

Survey of Local Conditions at Each Major Station in the LASL Milk Sampling Network (G. M. Ward*)

INTRODUCTION

Weekly samples of dried skim milk or dried buttermilk from plants in the United States and Canada have been analyzed for Cs^{137} and K^{40} since 1957 (1,2). This network reached a maximum of 55 sampling points in 1959 and was reduced to 16 on July 1, 1960. The mass of information collected provides a rather complete picture of this specific aspect of the fallout problem during the past 5 years. The principal deficiency in the data has been lack of information on local conditions at the individual production points. A survey of the remaining 16 stations was, therefore, undertaken.

METHODS AND RESULTS

Each of the plants shown in Fig. 1** will be visited in the course of the program. As of January 1, 1961, 12 of the visits have been completed. Information is obtained on the area of the milkshed and on the number of herds and number of cows supplying the plant. Feeding practices are noted with

---

*On leave of absence from Colorado State University, Fort Collins, Colorado.

**Turtle Lake, Wisconsin, has recently been substituted for Stillwater, Minnesota.

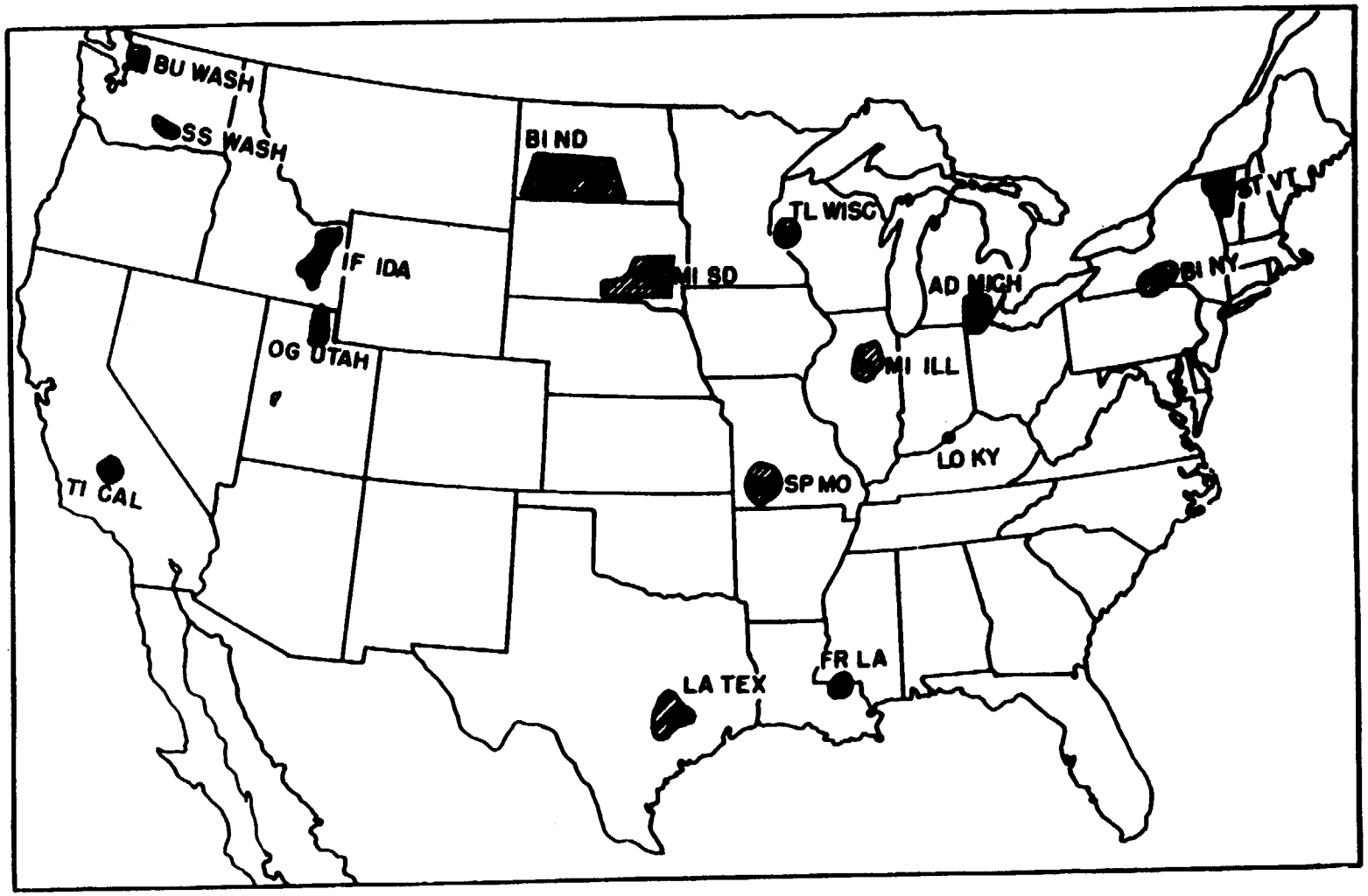

LASL MILK SAMPLING POINTS
JANUARY 1961

Fig. 1. Location of drying plants and approximate size of milksheds serving the LASL network.

particular attention to the date at which spring pasturing begins. The types and amounts of feed are determined, and an estimate is made of the number of acres required to produce forage for 1 cow. Soil types, soil acidity, and fertilizer and irrigation practices are also investigated. The above information is obtained from plant managers, dairy fieldmen, county extension agents, the dairy staffs of agricultural colleges, and from a few farmers in the areas.

DISCUSSION

Several interesting conclusions have already been drawn from the data so far obtained. One universal fact is that the high peaks for Cs^{137} in milk, which were found in 1959, coincide very closely (within 1 or 2 weeks) with the start of the pasture season. Furthermore, the decline in the cesium levels observed in the spring of 1960 also follow the beginning of pasture, presumably because the cows change from winter feed contaminated with 1959 fallout to pasture contaminated by the lower 1960 fallout rate.

Another general conclusion is that there is a close relation between the milk level of Cs^{137} and the number of acres used to provide a cow's forage. Thus one might propose that there will be an inverse relation between the price of land and the fallout concentration in milk. The idea is not

entirely facetious because the price of land will usually be directly related to the size of the herd it will support. The extremes in fallout (exemplified by Bismarck, North Dakota, and Tipton, California) almost certainly represent extremes in land values ($40 and $1,000 per acre, respectively). Bismarck, North Dakota, had an average 1959 level of 71 pc Cs^{137}/g K and 10 to 15 acres per cow, while Tipton had only 18 pc/g K and about 1 acre per cow. Average precipitation is 4 in. per year at Tipton and 12 in. per year at Bismarck. In 1958, however, precipitation was the same (12 in.) at the 2 points, but the difference in milk Cs^{137} was similar to the 1959 results.

REFERENCES

(1) B. Clinton, J. Allen, and E. C. Anderson, Los Alamos Scientific Laboratory Report LAMS-2445 (1960), p. 103.

(2) B. E. Clinton, J. Allen, and E. C. Anderson, Los Alamos Scientific Laboratory Report LAMS-2455 (1960), p. 83.

Progress Report on LASL Human Counter (Humco II) (E. C. Anderson, R. L. Schuch, and V. N. Kerr)

INTRODUCTION

With the replacement of toluene by a comparatively nonvolatile solvent and the improvement of the phototube complement, Humco II has reached its final state and it has been possible to begin intensive performance tests. As a guide for the design of future counters, an attempt is being made to gather basic information on the mechanism of energy deposition in the system with particular reference to multiple Compton scattering and "sum peaks." Because of the rapidly rising cost of the detector as size increases and because of the basic need for cheaper and simpler detectors for general use, it is important to establish optimum detector size, keeping in mind the requirements and limitations of possible applications. As the largest 4π gamma counter now extant, Humco II will provide valuable experimental data. Further extrapolation to larger sizes will be accomplished more economically through the use of IBM 704 computations rather than by additional construction.

Energy resolution is an important parameter, since mixtures of gamma-emitting nuclides are encountered in many applications. Humco I has adequate resolution to distinguish K^{40} and

Cs^{137}, permitting monitoring of foodstuffs and the general population. Humco II will be capable of much finer discrimination, such as the additional simultaneous determination of Co^{60}, Zn^{65}, I^{131}, and bremsstrahlung. Multiple low-level tracer studies will also be feasible with up to a maximum of 8 radioisotopes. Present investigations are directed toward quantification of the resolving power with particular reference to the very useful "sum peaks," which significantly enhance the capability of high efficiency systems.

METHODS AND RESULTS

New Solvent

Because of the serious fire hazard of toluene, a search was made by the Organic Chemistry Section for an economical, nonvolatile solvent with pulse height and transparency comparable to that of toluene. The hydrogenated naphthalenes (tetralin and decalin) were investigated but found to give inferior pulse heights (for decalin, 64 per cent of the standard 3 g/l. PPO in toluene scintillator). TS-28 (1), a paint solvent obtained from the Shell Oil Company, is the best practical material so far located. It consists of approximately 62 per cent aromatic hydrocarbons, 25 per cent naphthenes (derivatives of cyclopentane and cyclohexane), 12 per cent paraffin hydrocarbons, and 1 per cent olefins.

It is easily purified by passing through an activated alumina column and is as transparent optically as reagent-grade toluene down to 390 mμ. Flash point is 120°F (49°C); boiling range is 161 to 203°C.

Solutions of various scintillation solutes in TS-28 were prepared and tested both in small volumes and in the 450 gallon Humco II. Because of the high concentration of aliphatic and alicyclic hydrocarbons in TS-28, the solubility of terphenyl is limited to about 3 g/l. at room temperature. A solution of 3 g/l. terphenyl and 0.04 g/l. POPOP gave a pulse height of 0.53 relative to the PPO-toluene standard (2), compared with 1.16 for the best terphenyl-POPOP-toluene solution when tested air-saturated in small volumes. The ratio of the pulse height of the TS-28 solution to the best toluene solution was, therefore, 0.46 under these "small-volume" conditions. When this pair of solutions was compared in Humco II, an air-saturated pulse height ratio of 0.47 was observed, proving that the 2 solutions were equally transparent and that there was no differential loss of light on going to large volumes. The pulse height of this TS-28 solution rose by a factor of 1.50 on purging with argon, compared with a rise of 1.30 on deoxygenating the toluene solution, so that the oxygen-free pulse height ratio was 0.55 in large volumes. The comparatively low value is due to an inadequate amount of primary

solute even at saturation, evidenced by the fact that the pulse height was still rising with increasing terphenyl concentration. Addition of 3 g/l. PPO raised the air-saturated, small-volume pulse height of the TS-28 solution to 0.98 of PPO-toluene (equivalent to 0.85 of terphenyl-POPOP-toluene). In the large tank, the latter ratio was 0.80 (argon-saturated), in agreement with the small-volume, air-saturated result if equivalent oxygen quenching occurs in both solutions. Small-volume tests indicated that there is no significant gain from the addition of more PPO (although the solution is far below saturation). Since the PPO was added to the existing terphenyl solution, the final scintillator was 3 g/l. terphenyl, 3 g/l. PPO. and 0.04 g/l. POPOP. Small-volume tests indicated that the terphenyl was contributing little to the total pulse height and could probably be omitted without loss.

New Phototube Complement

The above comparison of solvents was carried out with a poor set of multiplier phototubes. One of the 24 tubes was missing completely and 4 tubes had noise levels of 100 kev or higher, the worst being 190 kev. The apparent energy of tube noise of the system was 120 kev with the toluene filling and 170 kev with TS-28. Replacing the poorer tubes with tubes of lower noise (see following report. page 151) resulted in significant improvement. The energy of noise dropped to 50 kev with

S-28 (calculated 40 kev with toluene) compared with 70 kev obtained with the Geneva Counter (3).

Energy Absorption Mechanism

Single Gamma Peaks. Using the TS-28 filling and the new phototube complement, the energy calibration of the system was determined. Contrary to our previously published observation (4), it now appears that there is definite evidence of multiple Compton scattering in Humco II. Figure 1 gives the results of careful energy calibration of Humco II (with the toluene filling) in which the observed pulse height of the gamma ray peak is plotted against 3 different energies: the full energy of the gamma ray (total absorption) and the maximum energies deposited in the solution by single and double Compton scatter, respectively. The slightly positive intercept of the extrapolated line of the "double" Compton approximation is in best agreement with expectation. A more rigorous examination of the energy deposition mechanism is underway using a Monte Carlo calculation for the absorption process based on a program written by Zerby and Moran (5). Spectra calculated from this program will be compared with experiments for liquid scintillation volumes ranging from a few cubic centimeters to "total absorption."

The determination of the average degree of multiplicity

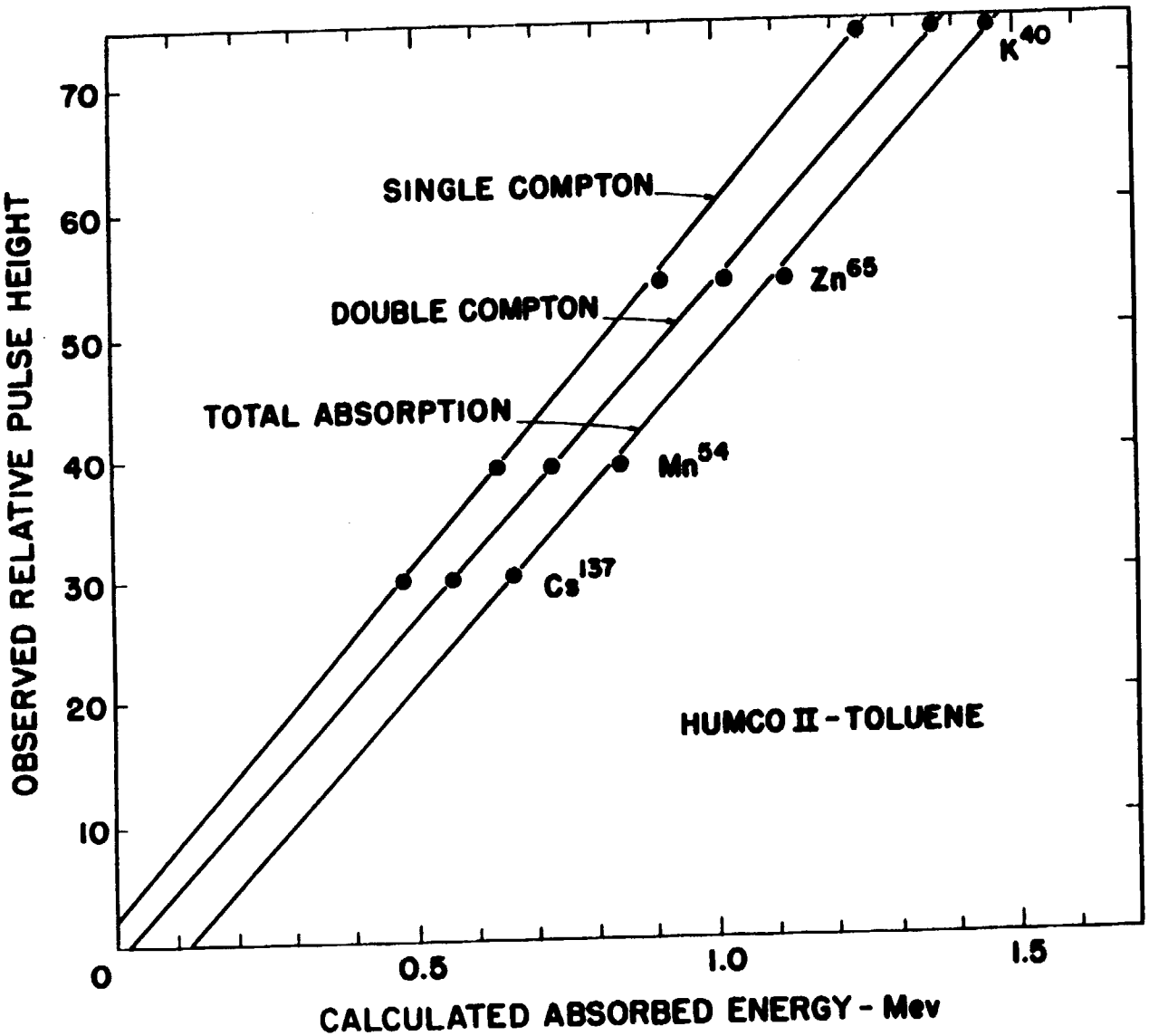

Fig. 1. Energy calibration of Humco II.

of Compton scattering is rather difficult on the basis of the energy calibration with individual gamma lines, since the effect of multiple scattering is merely to shift the calibration line more or less parallel to itself. The extent of the shift is of the order of 100 kev or less, and it must be judged on the basis of the extrapolated energy corresponding to zero pulse height. The expected value of this energy is uncertain, since the degree of nonlinearity of the scintillator is not well established. A more sensitive test is based on the observation of "sum peaks" from gamma rays emitted in cascade. It is easy to measure small deviations of the observed pulse height of these sum peaks from the energy calibration curve established with single gamma ray peaks, often by interpolation rather than by extrapolation.

Sum Peaks. Sum peaks result from the detection of 2 or more gamma rays emitted simultaneously to yield a single pulse whose energy depends on the total energy absorbed. The intensity of the sum peak will vary as the product of the individual detection efficiencies when these efficiencies are low, so that rather thick organic scintillators (20 cm or more) are required to make them important relative to the "singles" peaks. In addition, directional correlations often exist (e.g., for annihilation gammas which are always emitted in opposite directions), which greatly reduce or entirely eliminate these peaks when 2π geometry is used.

In Humco II, the sum peaks are comparable to the singles peaks. Figure 2 is the spectrum of Co^{60} showing the (unresolved) singles peak at 1.12 Mev and the sum peak at 2.25 Mev. The ratio of peak heights is 0.86. A more complicated case is shown in Fig. 3, which is the spectrum of Na^{22}. Here a 1.276 Mev gamma ray is emitted immediately following positron decay. The positron annihilates giving a pair of gamma rays of 0.51 Mev each. This pair of gamma rays will give a sum peak at 0.68 Mev if both undergo single Compton scatter, and at 0.80 Mev if both undergo double scattering. A peak is observed between these energies, perhaps closer to the double sum. If the 1.276 Mev gamma ray were detected alone, it would produce a peak at 1.05 or 1.16 Mev, depending on multiplicity of scattering. The latter is observed. A double sum of the 1.276 Mev gamma with only 1 of the annihilation gammas does not seem to occur, since there is no peak near 1.56 Mev. Triple sums would give peaks at between 1.73 and 1.96 Mev. The structure suggests multiple peaks in this region. Further analysis of intensity ratios may give more quantitative information on the average multiplicity of scattering.

Energy Resolution

Figures 4, 5, and 6 are spectra of interesting groups of nuclides determined with the TS-28 filling. The sources

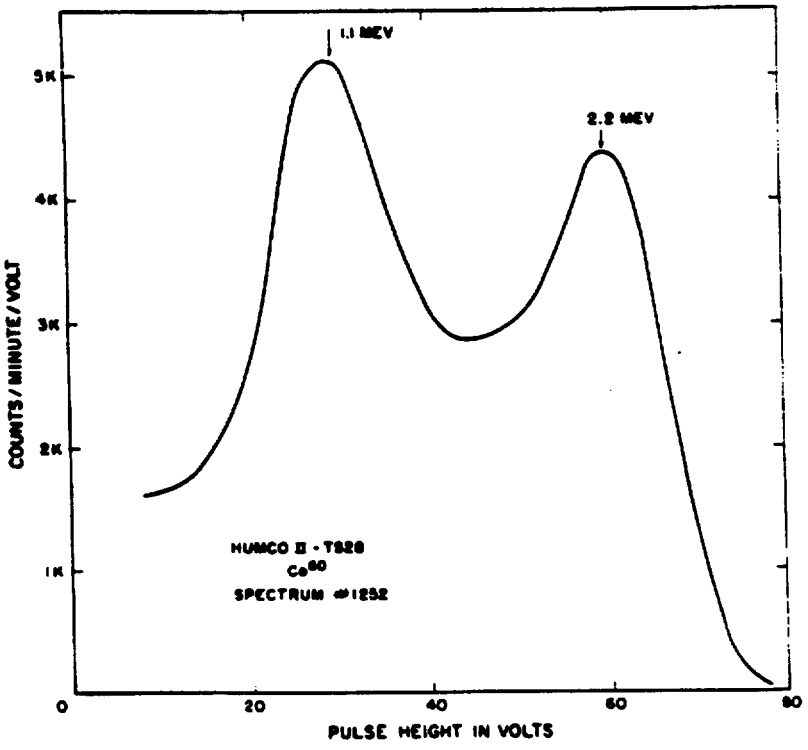

Fig. 2. Gamma ray spectrum of Co^{60} in Humco II.

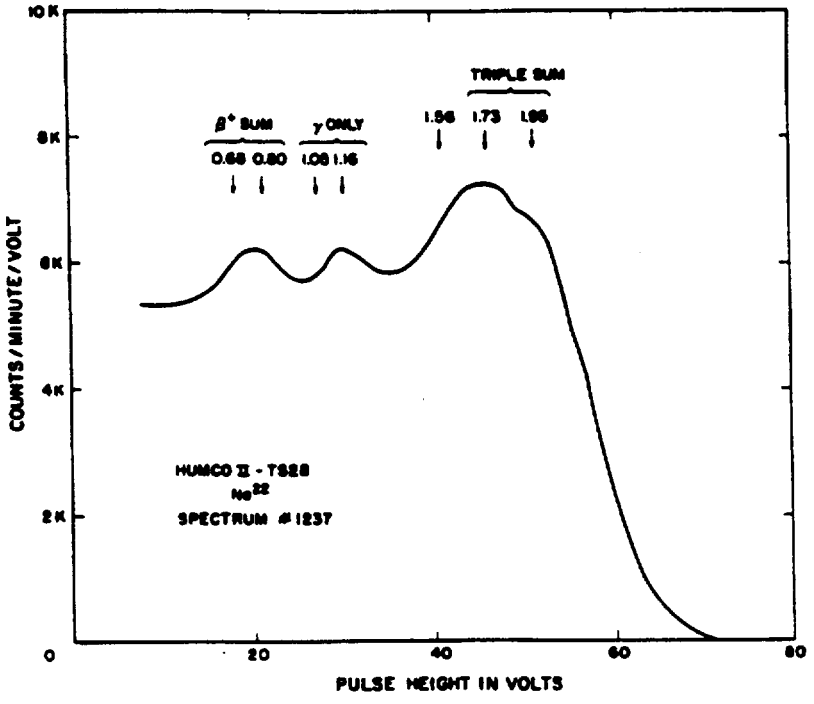

Fig. 3. Gamma ray spectrum of Na^{22} in Humco II.

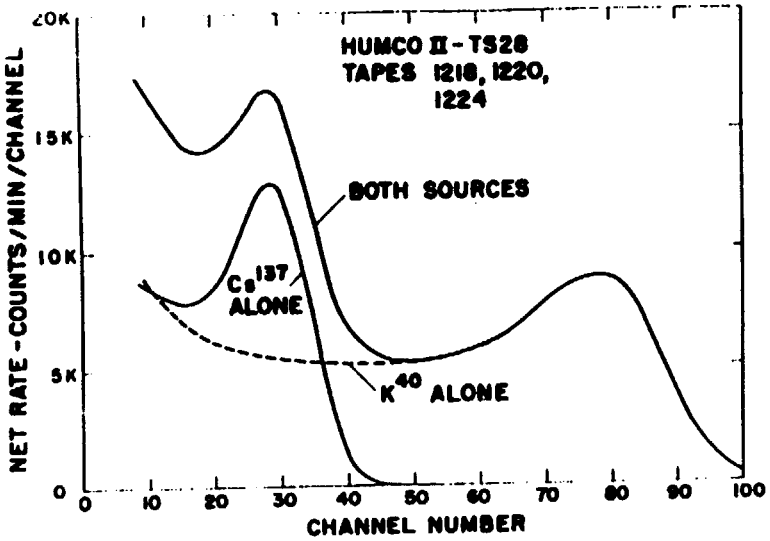

Fig. 4. K^{40} and Cs^{137}.

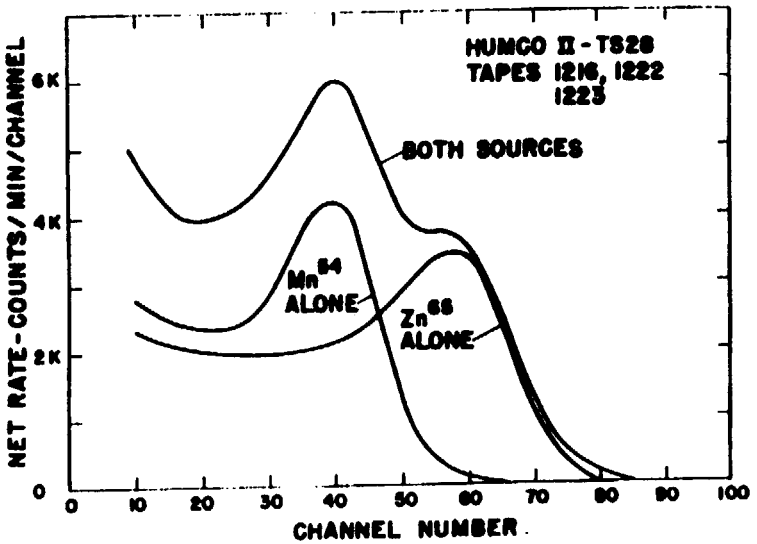

Fig. 5. Mn^{54} and Zn^{65}.

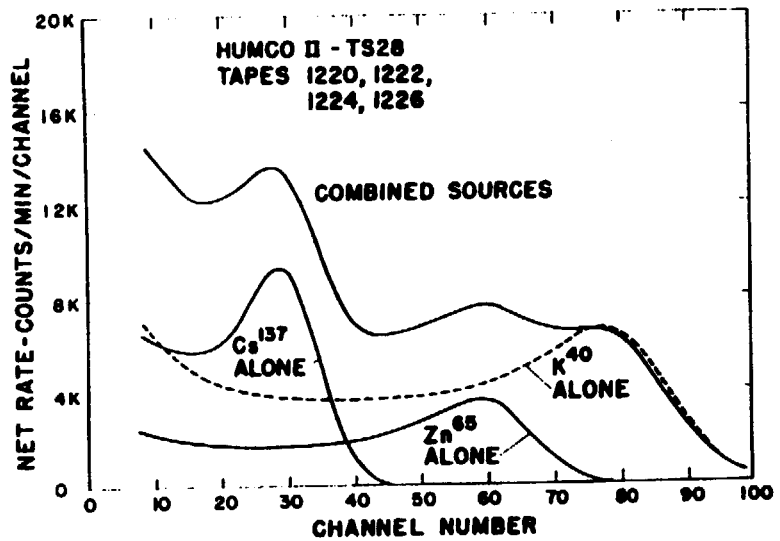

Fig. 6. K^{40}, Zn^{65}, and Cs^{137}.

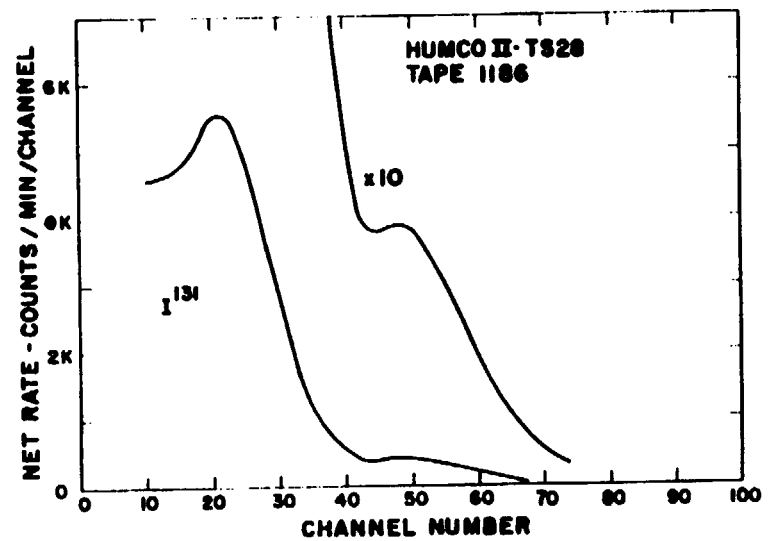

Fig. 7. I^{131}.

Gamma ray spectra from Humco II.

ere small standards with negligible self-absorption and cattering. Spectra were determined with single nuclides and hen with 2 or 3 sources in the detector simultaneously. Background has been subtracted in all cases.) Figure 4 hows the separation attainable with K^{40} and Cs^{137}. Because of the great energy difference (1.34 and 0.55 Mev double Compton, respectively), the separation is very clean. A closer pair, Mn^{54} and Zn^{65} (1.00 and 0.73 Mev, respectively), are shown in Fig. 5. The peaks are not completely resolved but the presence of 2 gamma rays is clear from the mixed spectrum. Quantitation of both components by solution of simultaneous equations for the counting rates in 2 channels would be feasible for this pair or other pairs of comparable energy separation (30 per cent energy difference). Figure 6 shows a ternary mixture: K^{40}, Zn^{65}, and Cs^{137}. Identification of the components, while possible, would be much more difficult than with a sodium iodide crystal spectrometer. Quantitation of a mixture of qualitatively known components would, however, be easy. The resolution obtained is comparable to that found in spectrophotometry of aqueous solutions. The spectrum of another nuclide of common interest, I^{131}, is given in Fig. 7, which shows the resolution of the small secondary peak given by the higher energy gamma ray of lower abundance.

Figure 8 shows the spectrum of a normal unexposed subject

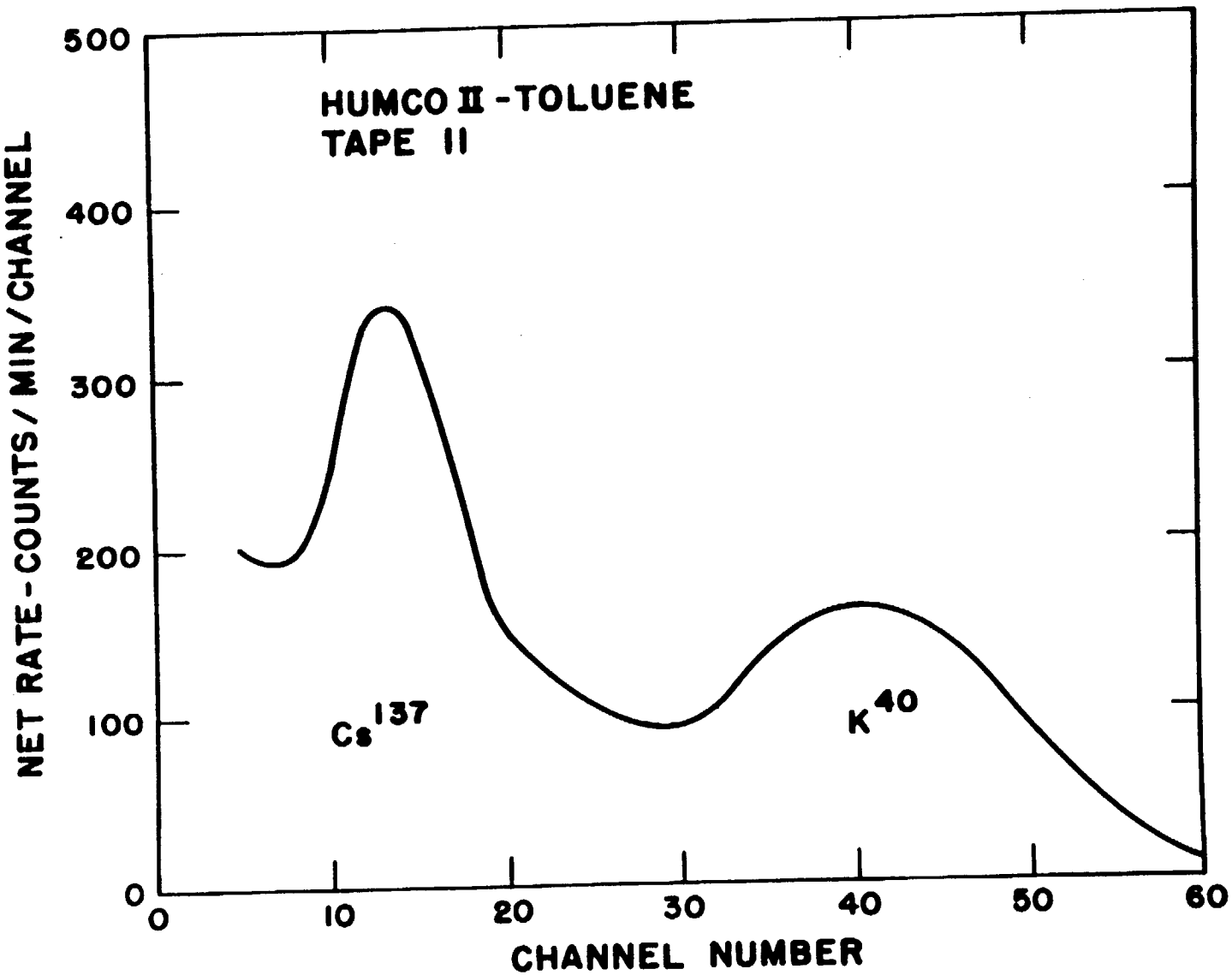

Fig. 8. Gamma ray spectrum of unexposed subject.

measured with Humco II. Natural K^{40} and fission product ^{137} are clearly resolved.

Some significant variations in peak-to-valley ratios have been noted which are apparently associated with pulse-shape variations as a function of preamplifier gain. Typical results are summarized in Table 1. The effect is almost entirely on the lower side of the peak; the upper half-resolution is not changed greatly. The spectra reported in Figs. 4 through 7 were taken with preamplifier gain 10 and are, therefore, subject to improvement. The effects may be due to a sensitivity to rate in the overload characteristic of the preamplifier. An attempt is being made by the Electronics Group of the Physics Division to eliminate this.

Sum peaks offer both advantages and disadvantages in terms of their effect on attainable energy resolution. The additional complexity they introduce into the spectra is, of course, undesirable. (A somewhat analogous situation exists in spectrometry with small sodium iodide crystals when Compton edges and "escape peaks" multiply single peaks. "Sum peaks" of the type under discussion are not observed in ordinary sodium iodide spectrometry of large samples because of the very low geometry.) However, the existence of sum peaks can sometimes be quite useful in improving the discrimination of a large organic scintillator. Table 2 summarizes the resolving power of Humco II for some nuclides of interest for medical

TABLE 1. EFFECT OF PREAMPLIFIER GAIN ON PEAK CHARACTERISTICS

Nuclide	Preamplifier Gain	P/V Ratio	Resolution	
			Upper Half-Width (per cent)	Lower Half-Width (per cent)
K^{40}	2	2.8	14	18
	10	1.9	15	--
Cs^{137}	2	2.9	20	28
	10	1.6	22	--

TABLE 2. SOME BIOLOGICALLY INTERESTING RADIONUCLIDE GROUPS CAPABLE OF RESOLUTION WITH HUMCO II

Group	Nuclide	Full Energy of Gamma Ray(s)	Double Compton Energy
1	Na-24	4.12 (S*)	3.93
2	Tl-208 (ThC'')	3.12 (S)	2.95
3	Co-60	2.50 (S)	2.25
4a	Na-22	2.30 (S)	1.76**
	Bi-214 (RaC)	1.76	1.64
4b	K-42	1.53	1.41
	K-40	1.46	1.34
5	Fe-59	1.20 (Ave. of 1.10 and	1.08
	Zn-65	1.12 1.29)	1.00
	Rb-86	1.08	0.96
	Cu-54	1.02 (β+ annihilation S)	0.80
6a	Mn-54	0.84	0.73
	Cs-137	0.66	0.55
	Sr-85	0.51	0.40
6b	Au-198	0.41	0.31
	I-131	0.36	0.27
7	Cr-51	0.32	0.23
	Hg-203	0.28	0.19
	Pb-214 (RaB)	0.24	0.16
8	P-32	bremsstrahlung (<0.15)	<0.08
	Sr-90		

*S indicates a sum peak.

**Observed center of a broad, complex peak including single and double Compton scatter, triple sum.

NOTE: Groups separated by a solid line can be determined simultaneously. Groups separated by a broken line are difficult to resolve.

tracer studies and for contamination monitoring. [A previous version of this table (6) applicable to organic scintillators in general, including thin detectors and 2π systems, did not include the effect of sum peaks.] A given nuclide can be determined simultaneously with any other nuclide listed in a group separated from the first by a solid line. Nuclides in adjacent groups separated by a broken line are difficult to resolve. The table suggests that, in theory at least, as many as 8 important tracers could be followed simultaneously.

Of more practical interest is the fact that many interesting pairs fall in different groups. Note that Fe^{59} and Co^{60}, a notoriously difficult pair to separate even with a sodium iodide spectrometer, are easily resolved. Although the gamma energies are nearly identical, 1.17 and 1.33 Mev for Co^{60} compared with 1.10 and 1.29 for Fe^{59}, the former pair is in cascade and gives a sum peak, whereas the latter pair is in parallel and does not. Another useful sum peak is that of Na^{24}, which is located well above possible interferences by its high energy (3.9 Mev). This fact should greatly increase the sensitivity of the sodium activation method of determining whole body neutron exposures (7) by reducing possible interference due to surface contamination of the subject with short-lived fission products such as La^{140} (2.52 Mev). Improved sensitivity will also increase the usefulness of the

method in diagnosing chronic neutron exposure. The short life of Na^{24} prevents determination of integrated dose by a single measurement. Routine measurements of personnel from a given area over a period of time could, if sufficiently sensitive, determine the integrated dose. Table 2 also suggests the possibility of a quadruple simultaneous tracer experiment with the 4 alkali metals: sodium, potassium, rubidium, and cesium.

Another interesting potential use of sum peaks is the possibility of determining the absolute counting efficiency (including self-absorption effects) from the ratios of the intensities of sum peaks to the intensities of the corresponding singles peaks, in a manner analogous to the well known beta/gamma coincidence method (8). This possibility will be investigated as an independent check on efficiency calibrations based on conventional phantom methods and as a "self-calibrating" technique for nuclides such as Co^{60}.

DISCUSSION

The prominence of sum peaks and their usefulness in separating important nuclide pairs probably constitute the principal advantages of the 4π over the 2π liquid scintillation counter. (The other advantage is the smaller variation of counting efficiency with sample size.) For simpler measurements not requiring the additional resolution, the 2π

system is probably the method of choice because of its lower cost.

Quantitative calculations of the amounts of the components of a mixture present in a subject will, of course, have to be based on the solution of the appropriate number of simultaneous equations, including subject weight as a parameter. A program for the IBM 704 computer is being written by H. Israel of Group H-6 for this purpose. Preparation and measurement of calibration phantoms will be a major problem occupying the counter during the coming year.

REFERENCES

(1) E. C. Anderson, R. L. Schuch, and V. N. Kerr, Los Alamos Scientific Laboratory Report LAMS-2455 (1960), p. 104.

(2) F. N. Hayes, B. S. Rogers, and P. C. Sanders, Nucleonics 13(1), 46 (1955).

(3) E. C. Anderson, F. N. Hayes, and R. D. Hiebert, Nucleonics 16(8), 106 (1958).

(4) R. L. Schuch, J. D. Perrings, and E. C. Anderson, Los Alamos Scientific Laboratory Report LAMS-2445 (1960), p. 176.

(5) C. D. Zerby and H. S. Moran, presented at the Total Absorption Gamma Ray Spectrometry Symposium, Gatlinburg, Tenn. (May 1960).

(6) E. C. Anderson, R. L. Schuch, V. N. Kerr, and M. A. Van Dilla, presented at the Vanderbilt University Symposium on Radioactivity in Man, Nashville, Tenn. (April 18-19, 1960), to be published in proceedings (in press).

(7) E. C. Anderson, R. L. Schuch, J. D. Perrings, and W. H. Langham, Nucleonics 14(1), 26 (1956).

(8) J. L. Putman, In: Beta and Gamma Ray Spectroscopy (K. Siegbahn, ed.), Interscience Publishers, Inc., New York (1955), p. 83.

Testing of Multiplier Phototubes for Humco II (E. C. Anderson)

INTRODUCTION

The utility of a large liquid scintillation counter can be greatly enhanced by extending downward the lower energy limit of efficient gamma ray detection. Of principal interest are the soft X rays or bremsstrahlung produced when beta rays are stopped in matter. Measurement of bremsstrahlung permits the in vivo counting of pure beta emitters such as Sr^{90} and P^{32}. Because the bremsstrahlung continuous spectrum rises rapidly with decreasing energy, the sensitivity of a counter depends strongly on the lower energy limit. The Geneva Counter (1) with a lower energy limit of 70 kev had a sensitivity of 0.03 μc Sr^{90} in a 70 kg subject with a 100 second counting time.

The limit of the useful energy range is set by the amplitude of the noise pulses from the multiplier phototubes. The apparent energy to be ascribed to the noise is determined by the average cathode photosensitivity, the light output of the scintillator, and the light collection efficiency of the system, in addition to the basic pulse height of the noise itself. The "noise level" of a given phototube, if expressed in apparent energy units, will therefore vary with the scintillator used for the energy calibration. The noise energy will be much lower (perhaps by a factor of 4) with a sodium iodide

crystal than with a large organic scintillator. Expressing the noise in terms of equivalent number of electrons emitted from the photocathode (2) would make the quantity independent of the scintillator. However, this conversion to absolute units is more difficult and, furthermore, it is desirable from the practical standpoint to include the effect of averaged cathode photosensitivity in the parameter.

METHODS AND RESULTS

In order to determine the equivalent noise energy of DuMont No. K-1328 phototubes for use in Humco II, individual tubes were mounted on a test tank of 40 l. volume, as shown in Fig. 1. The steel tank is 16 in. in diameter and 12 in. in depth and is filled with a solution of terphenyl and POPOP in toluene. Figure 2 is a view of the system with the multiplier phototube tipped back showing the reflecting liner of Teflon sheet (1/4 in. thick). Also visible is the method of mounting the phototube to provide a liquid-tight seal. The tube is clamped between 2 heavy aluminum rings, the seal between the rings and the tube envelope being made by a special molded silicone rubber gasket. The lower ring seals to the tank with a silicone rubber "O" ring and is held down by 16 studs. A torque wrench set at 20 inch-pounds is used to ensure uniform, minimum pressure. After the tube is in

Fig. 1. Test tank for 16 in. multiplier phototubes (K-1328).

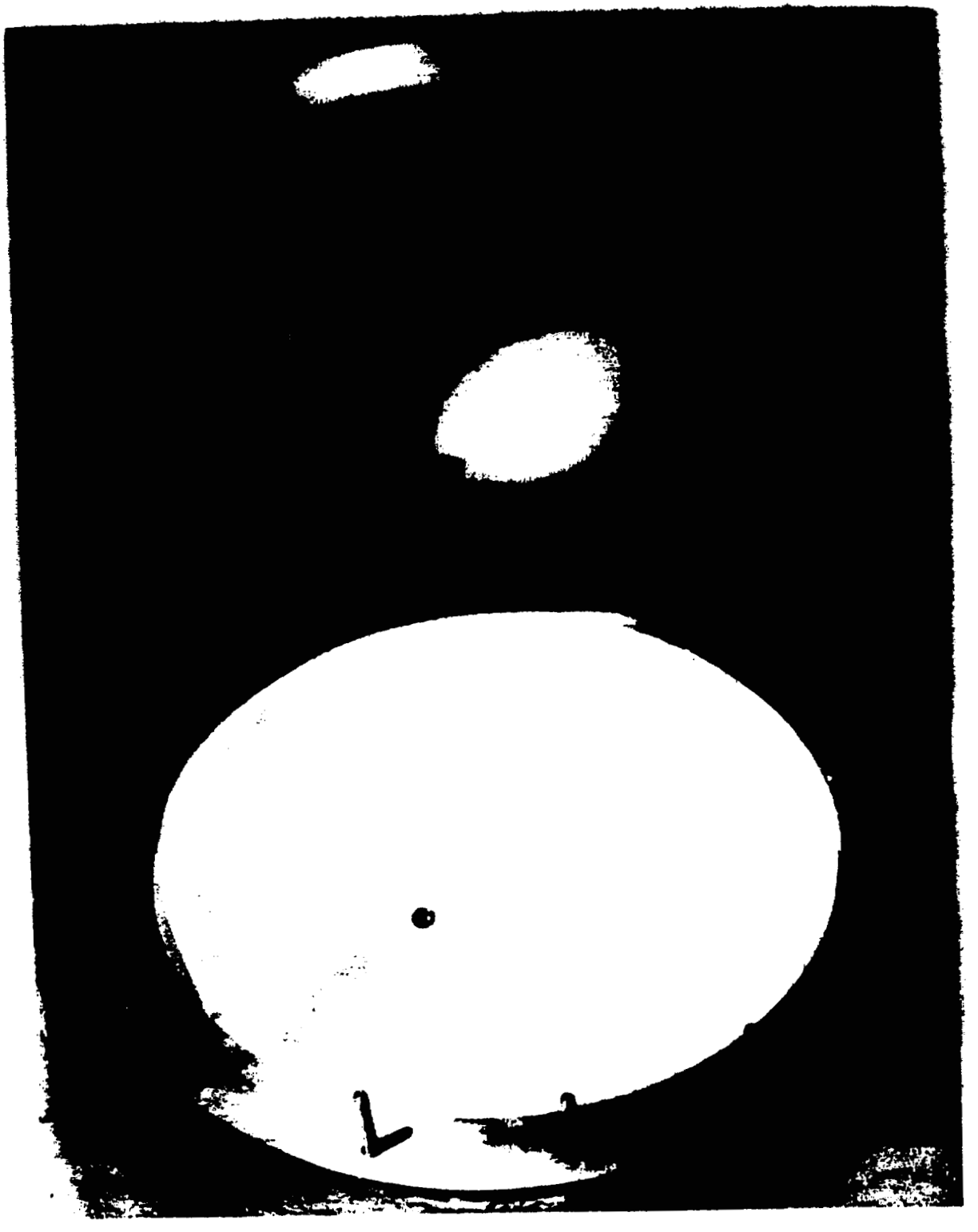

Fig. 2. Test tank open showing Teflon reflective liner.

place, the entire system is inverted about a pivot system not shown in the figure. This operation immerses the cathode window in the scintillator, providing optimum optical coupling and also providing a check on the liquid-tightness of the seal. Tubes which have been sealed to iron mounting rings with epoxide cement (the other mounting system tested for Genco and Humco II) can also be mounted on the test tank. The counter was shielded by 7 in. of steel during measurements.

Energy calibration can be accomplished by determining the pulse height of the Compton peak from a gamma ray of known energy. Figure 3 shows the spectrum (including background) obtained using 5 pounds of potassium chloride as a source.* One point is sufficient to establish the calibration accurately enough for present purposes. A complete energy calibration of this detector is given in Fig. 4. Here the measured relative pulse heights from 6 different gamma rays are plotted against full gamma energy and against maximum Compton energy. The latter quantity is related to the gamma energy by the equation (3):

$$T_{max} = E_o \left[1 + (1/2a)\right]$$

*This is a convenient standard, since it is readily available and of low enough specific activity to be comparatively harmless to man and to sensitive counters.

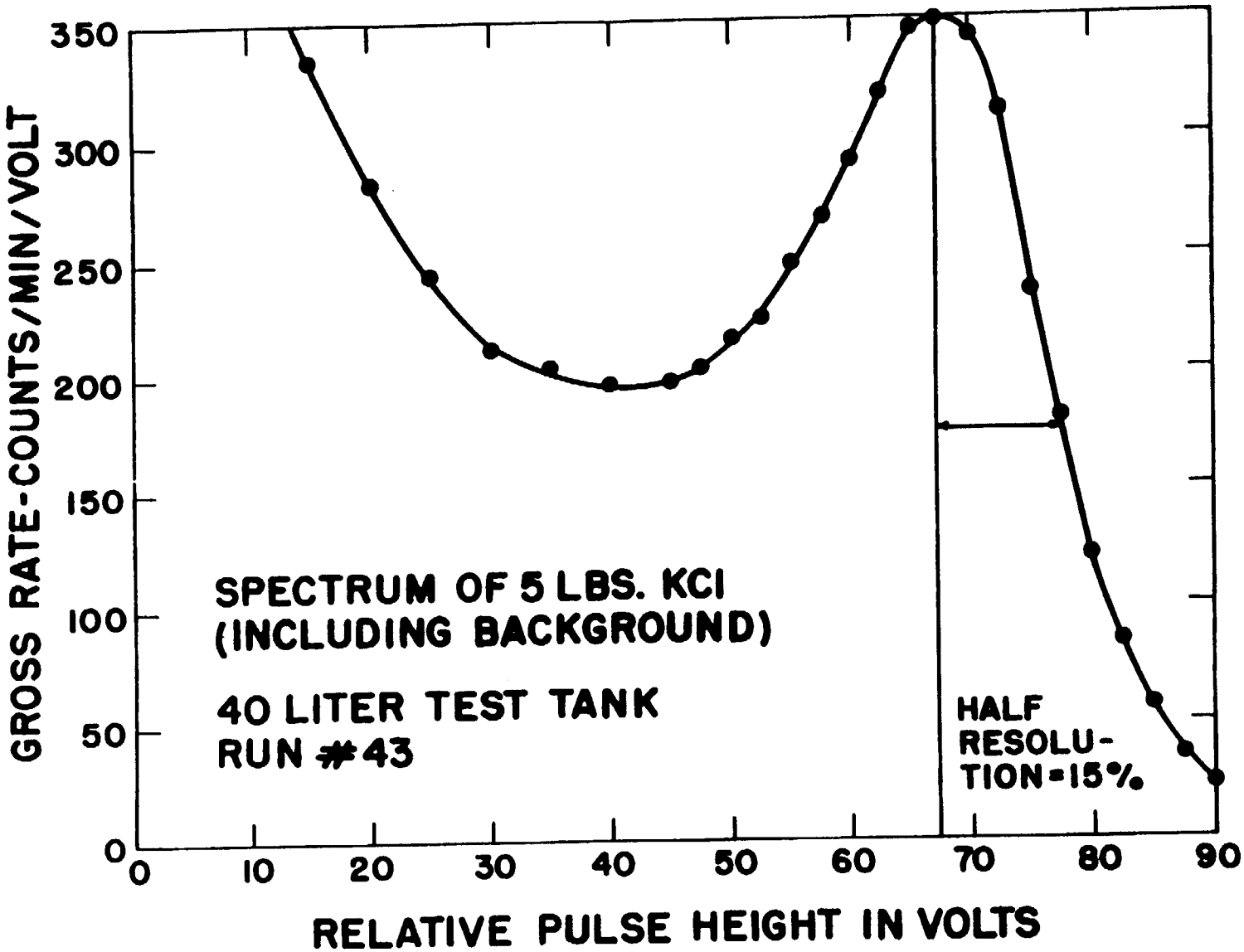

Fig. 3. Spectrum of K^{40} obtained with test tank.

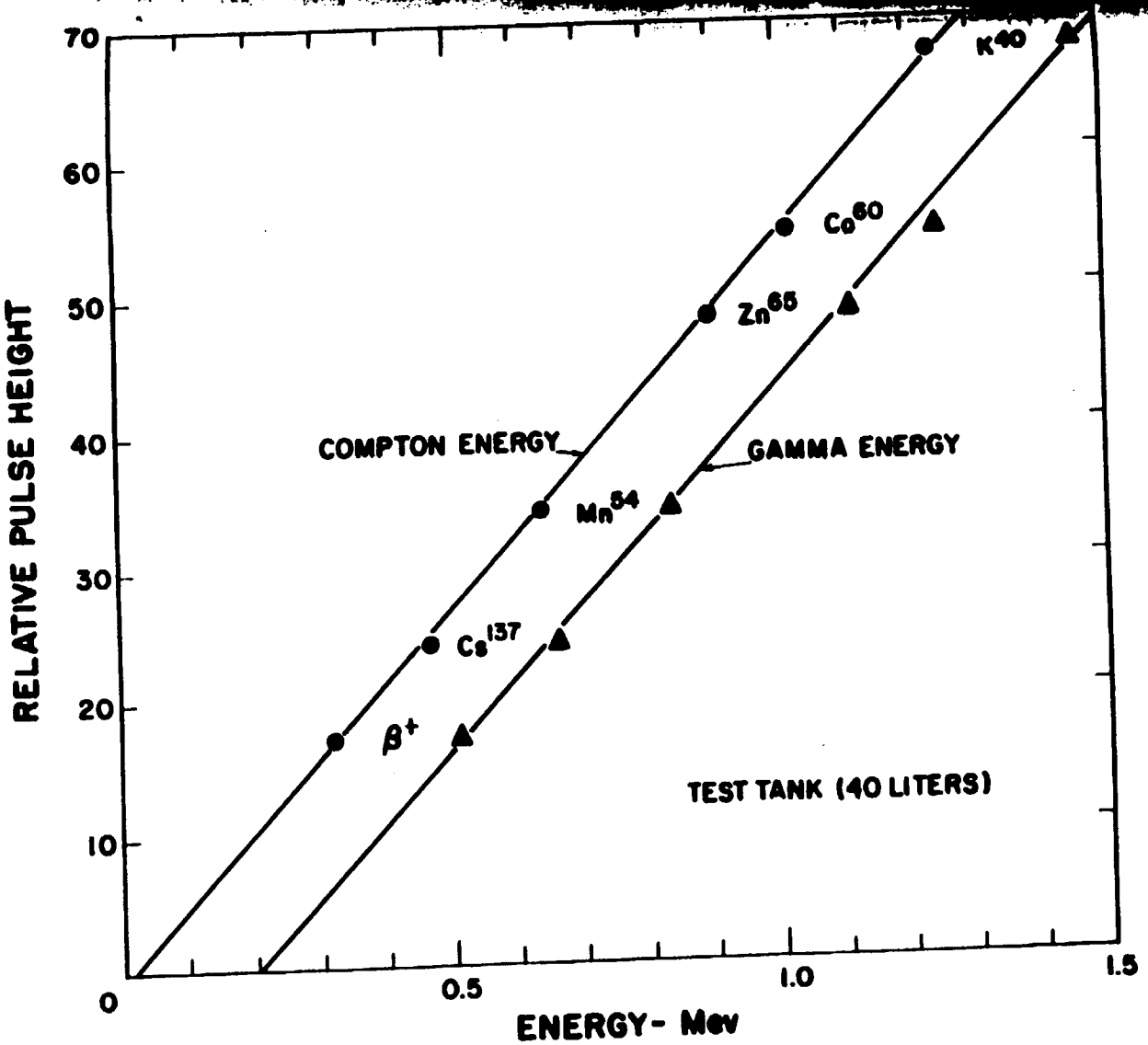

Fig. 4. Energy calibration of test tank.

where T_{max} is the maximum energy which can be transferred to a recoil electron by Compton scattering, E_o is the initial gamma ray energy, and a is the same gamma ray energy expressed in units of $m_o c^2$ (0.511 Mev). Because of the low atomic number of organic scintillators, Compton scattering is the only common process by which gamma energy is absorbed. Transfer of full gamma energy is, therefore, unlikely in such a small detector. This is evidenced by the fact that in Fig. 4 the plot against Compton energy extrapolates close to zero, while the plot against full gamma energy is widely divergent.

On the basis of the energy calibration, a resistance in series with the multiplier phototube bleeder string is adjusted so that all tubes have the same gain with a high voltage supply of 1500. This permits the tubes to be used interchangeably on Humco II without further balancing.

In order to quantify the energy of tube noise, use is made of the peculiar shape of the background spectrum of the system. When the logarithm of the differential counting rate (e.g., in counts per second per Mev) is plotted against the logarithm of the relative pulse height or of energy, the resulting spectrum has 3 linear sections with 2 well defined inflection points, as shown in Fig. 5. Above 1.1 Mev for the test tank, the rate drops sharply as one passes from the

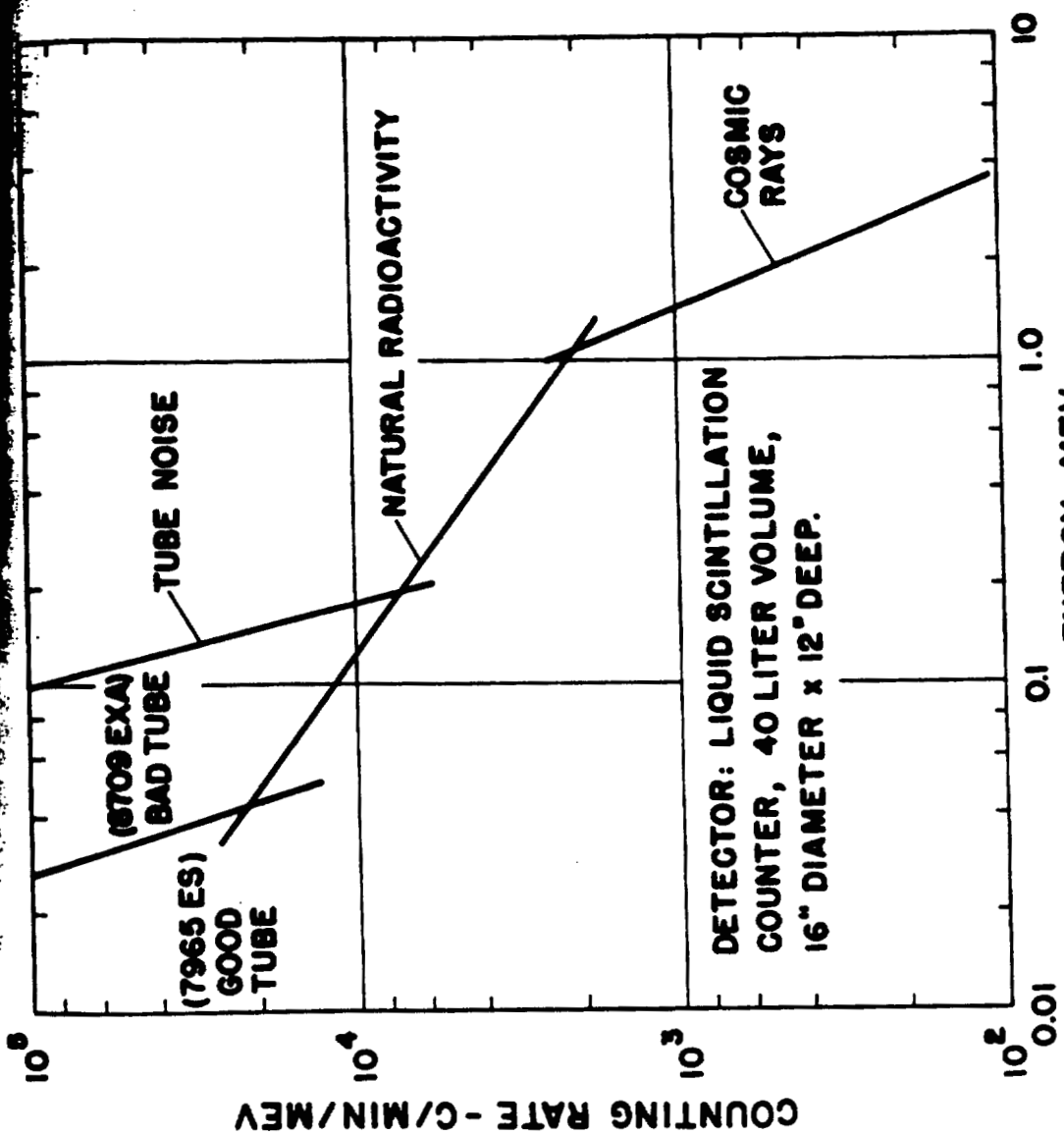

Fig. 5. Background spectra of the test tank.

region in which the background is due to more energetic cosmic ray secondaries. The energy of this point of inflection varies surprisingly little with counter size, being about 1.25 Mev in the 280 l. Geneva Counter and 1.40 Mev in the 1700 l. Humco II. (Once this energy is established, this point can be used for energy calibration, if desired.)

The second point of inflection represents the onset of tube noise. Below this point, the rate rises extremely rapidly. If a measurement is made with no scintillator present, only this portion of the spectrum is observed, indicating noise in the multiplier phototube to be the source. The energy of the intersection of the tube noise line with the natural radioactivity line is taken to represent the lowest gamma energy which can be efficiently measured. This noise can, of course, be eliminated through the use of a 2 channel coincidence system so that it is possible to work at lower energies. However, the much greater complexity of the electronics and the concurrent loss in energy resolution make it desirable to avoid this system except as a last resort.

The 2 tubes whose characteristics are shown in Fig. 5 represent extreme cases. The noise level of 40 kev is among the lowest encountered, and very few tubes run higher than 200 kev. The observed distribution of noise levels in a group of tubes is shown in the histogram of Fig. 6.

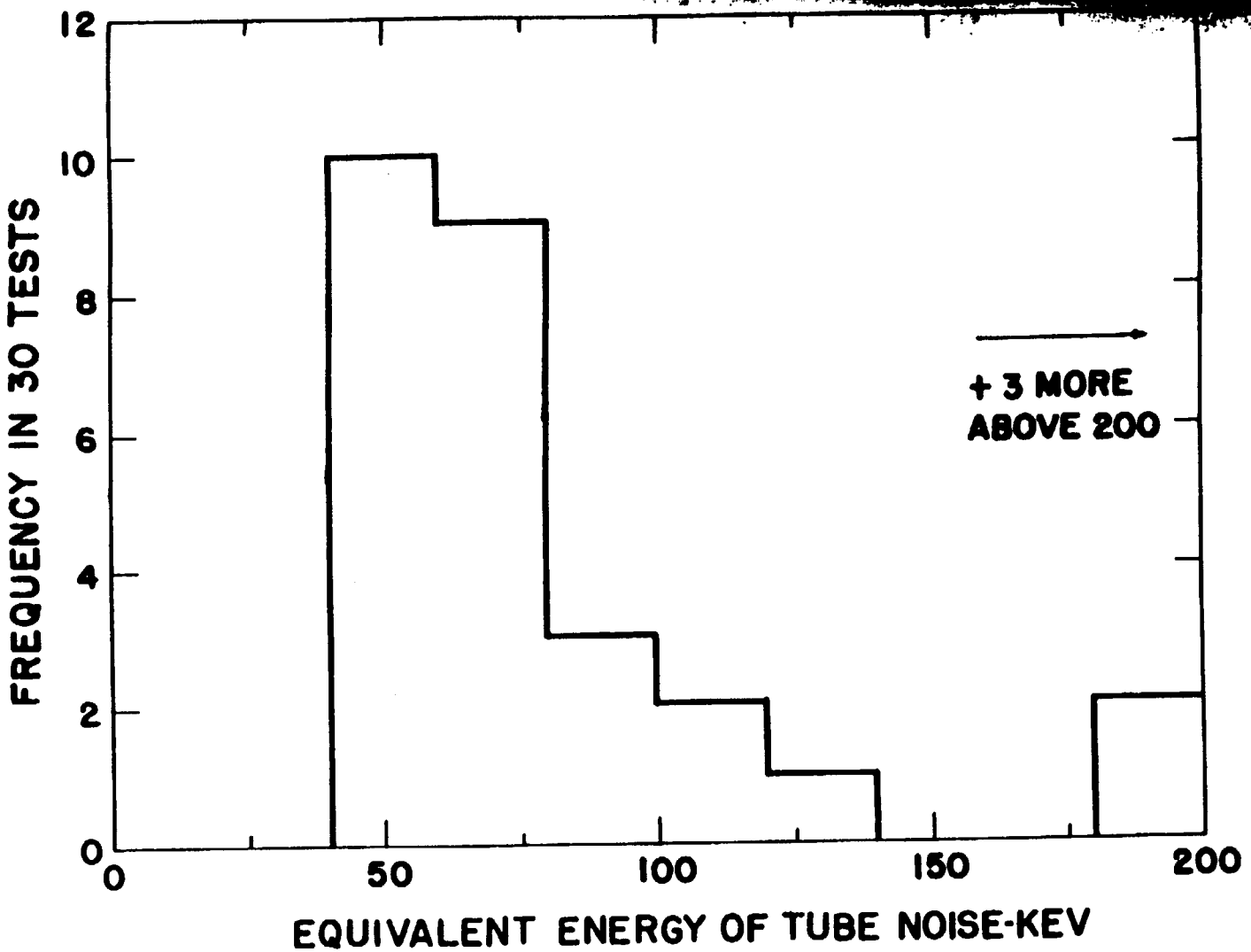

Fig. 6. Frequency distribution of noise levels in a group of DuMont No. K-1328 multiplier phototubes.

DISCUSSION

If a lower energy limit of less than 70 kev is desired, it appears that one can expect to reject about 1 tube in 3. The discontinuity in the distribution at 150 kev suggests that some uncontrolled factor in tube manufacture may be responsible for the poorest tubes. There is no obvious correlation of tube quality with serial number, and 2 batches of tubes purchased more than a year apart showed similar distribution patterns.

While their high noise level renders the rejected tubes unsuitable for low energy counting with liquid scintillators, there is no evidence that these tubes are inferior in other ways (e.g., cathode uniformity and energy resolution).

A complete set of 24 good tubes has now been selected for Humco II with noise levels ranging from 32 to 84 kev on the test tank. One of these has small cracks in the glass-metal seal of the faceplate, and probably has a limited life expectancy. Four spares are on hand with noise levels from 60 to 95 kev. Six more tubes are on order and will be tested with the hope of providing a set whose maximum individual noise level does not exceed 70 kev.

REFERENCES

(1) E. C. Anderson, F. N. Hayes, and R. D. Hiebert, Nucleonics 16(8), 106 (1958).

(2) G. A. Morton, RCA Rev. 10, 525 (1949).

(3) R. D. Evans, The Atomic Nucleus, McGraw-Hill Book Co., New York (1955), p. 676.

Cutaneous Absorption by Human Subjects. I. Studies with Sodium^{24} and Iodine^{131} (M. A. Van Dilla, C. R. Richmond, and J. E. Furchner)

INTRODUCTION

The feasibility of utilizing a whole-body gamma-ray spectrometer to study cutaneous absorption of radionuclides by human subjects was reported previously (1). Results obtained since then showed that absorption of Na^{24} through the palmar skin, if any, must be less than 0.1 per cent; definite absorption of I^{131} through the palmar skin was observed, the amount being 0.1 per cent of the applied dose.

METHODS

The technique used to apply the radionuclides was essentially the same as the patch technique used by Tas and Feige (2). A 5 x 7.5 cm rubber-backed Elastoplast bandage, containing 200 λ of the isotonic solution, was applied firmly to the palmar surface of the left hand. The 2.5 x 4.5 cm gauze portion of the bandage, containing the solution, was in direct contact with the intact skin. Two in. gauze bandage was then used to ensure proper positioning of the Elastoplast and to prevent the possible external contamination to other parts of the body. Prior to application of the Elastoplast, the subject was measured while his left hand, holding a

replicate preparation sealed in plastic, was inside the lead arm cave. Figure 1 shows a subject prior to measurement with her left hand in the arm cave. The 9 x 6 in. sodium iodide crystal is capable of detecting extremely small amounts of gamma emitters which traverse the skin barrier and enter the systemic circulation, but is very insensitive to the material failing to enter the circulation.

The experimental plan consisted of the following:

(a) Initial measurement on the subject holding the replicate preparation in his hand in the arm cave.

(b) Measurement immediately after preparation was applied to subject's hand.

(c) Several measurements during the next few hours.

(d) A measurement at 24 hours after application.

(e) Removal of the Elastoplast and immediate measurement of subject.

(f) Hand washed and subject remeasured.

(g) Measurement of subject at 48 hours post application. Duration of each measurement was 10 minutes.

About 10 μc Na^{24} as the chloride was applied to the palm of 1 subject, and 51 μc I^{131} as NaI was applied to the palm of another. At a subsequent time, each subject ingested a tracer dose of either 0.18 μc Na^{24} or 0.14 μc I^{131} so that proper calibration factors could be obtained for the efficiency of the detecting system.

Fig. 1. Subject in position under 9 x 6 in. NaI crystal with left hand in lead arm cave.

RESULTS AND DISCUSSION

Figure 2 shows spectra obtained for the subject given I^{131}. The effect of backscatter, due to gamma rays coming out the open end of the arm cave, is shown clearly as a backscatter peak at 0.15 Mev. The prominent 0.36 Mev peak between channels 27 and 40 shows the presence of I^{131} in the body. Results of these experiments indicated that little, if any, radiosodium was absorbed through the palmar skin, whereas I^{131} definitely traversed the skin barrier and entered the systemic circulation. Figure 3 shows the absorption of I^{131} as a function of time; about 0.1 per cent of the applied I^{131} was absorbed with the majority of the absorption occurring in the first 10 hours of the 48 hour experimental period. About 10 per cent of the applied dose of I^{131} remained in the superficial layers of the skin for a period of at least 48 hours, in spite of thorough hand washing.

Tas and Feige (2) showed that absorption of I^{131} from the palmar skin of 12 subjects ranged from 0.06 to 0.94 per cent of the administered dose when measured at 48 hours after application. The mean value was 0.4 per cent of the administered dose. Other workers were not able to demonstrate the cutaneous absorption of I^{131} (3,4).

The one experiment with Na^{24} failed to show positive

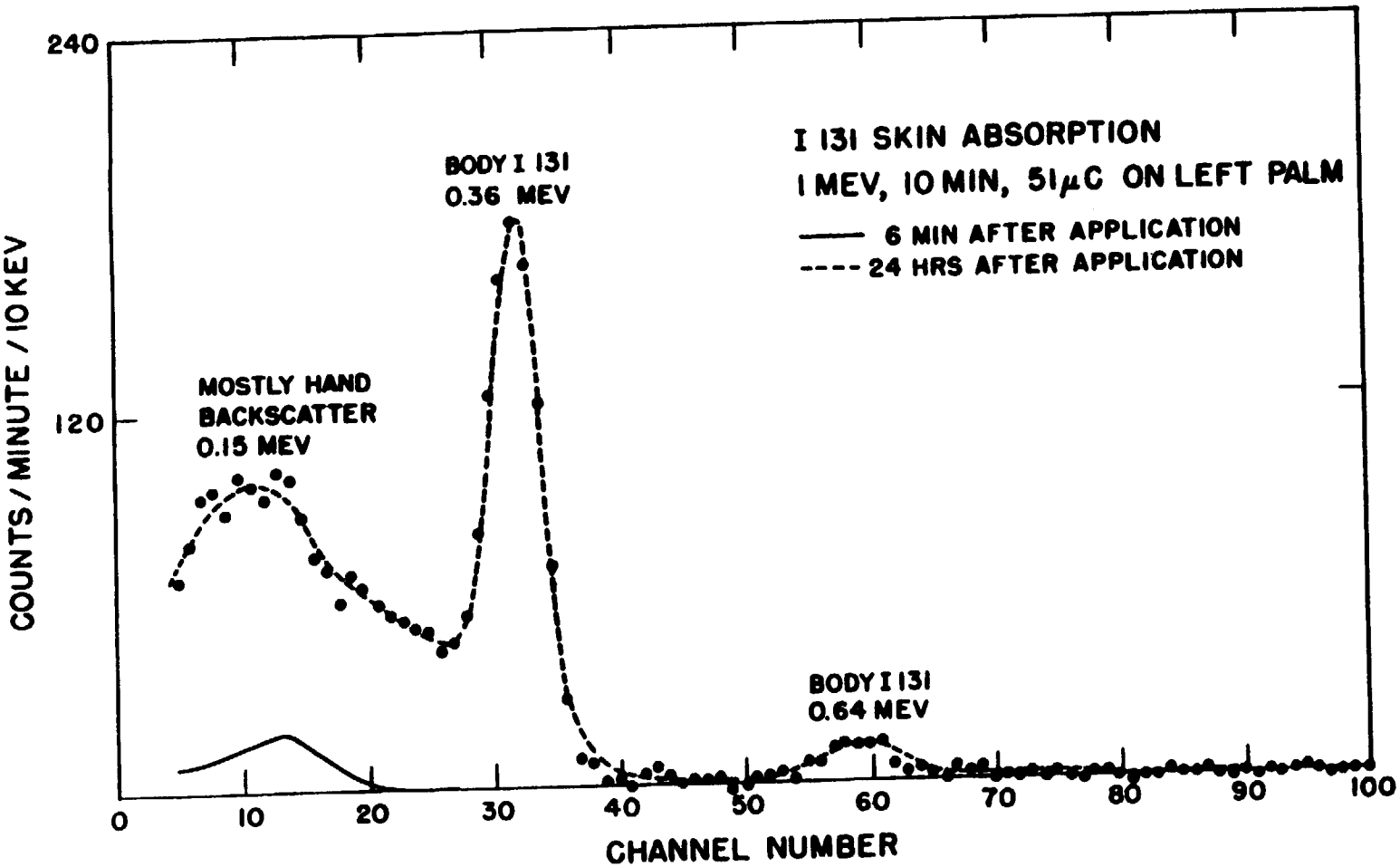

Fig. 2. Gamma ray spectra before (solid line) and after (dashed line) cutaneous absorption of I^{131}.

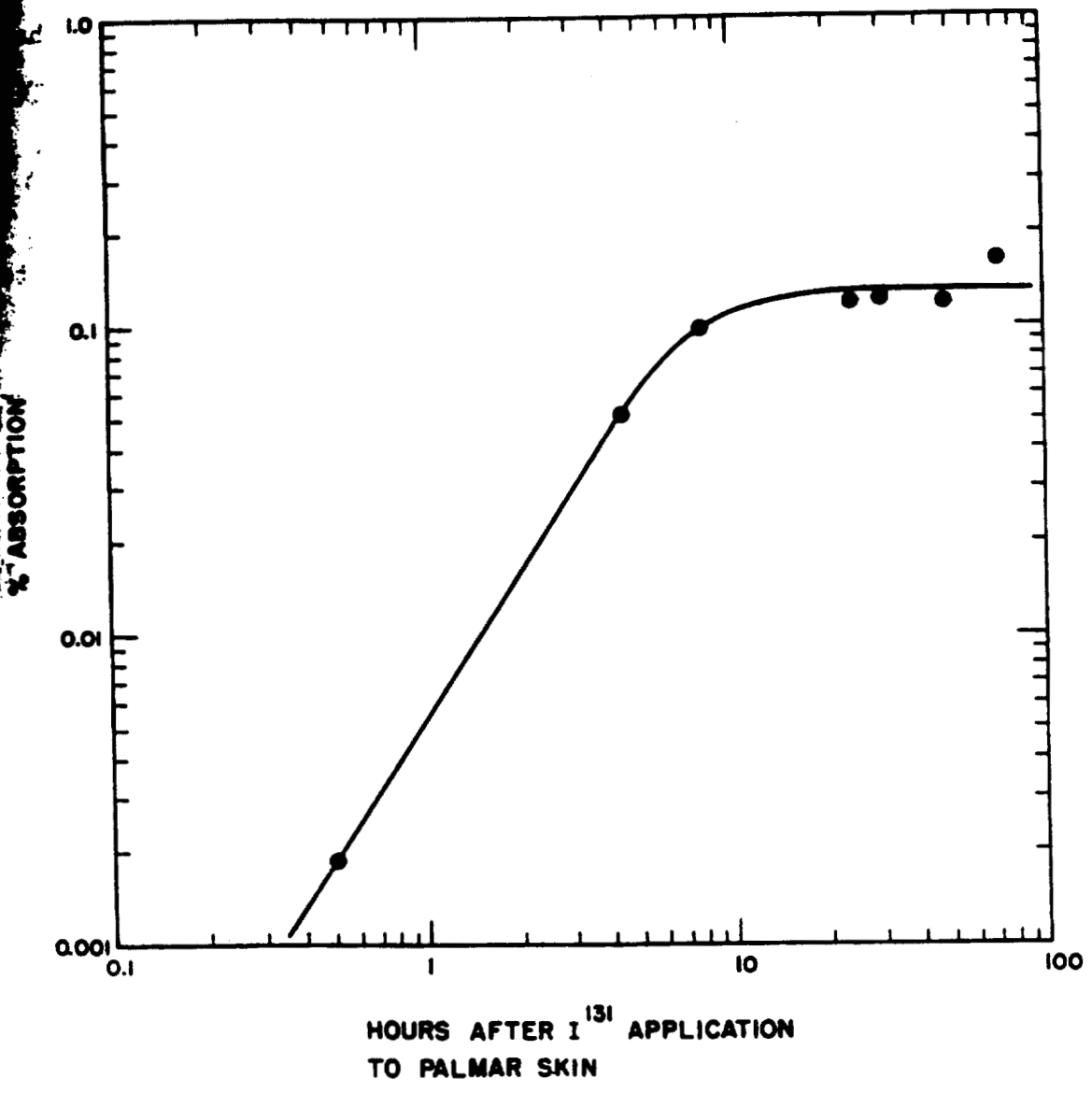

Fig. 3. Cutaneous absorption of I^{131} following palmar application.

skin absorption. The method was capable of detecting absorption of 0.1 per cent of the applied dose. It is possible, therefore, only to say that absorption, if any, was less than 0.1 per cent. In this case, 32 per cent of the radioactivity remained in the superficial layers of the skin for at least 48 hours despite thorough washing.

Johnston and Lee (5) reported that radiosodium penetrated the intact skin. Rothman (6), however, suggested that the mechanical effect of pressing ointments containing the radiosodium into the skin might have been responsible for the absorption.

Even though the above results represent single cases only, they do indicate the feasibility of the method of studying cutaneous absorption of radioisotopes by man. Longer-lived isotopes should be helpful in clarifying cutaneous absorption phenomena, and studies with Sr^{85}, Zn^{65}, and Cs^{134} are being planned.

REFERENCES

(1) M. A. Van Dilla and M. W. Rowe, Los Alamos Scientific Laboratory Report LAMS-2455 (1960), p. 113.

(2) J. Tas and Y. Feige, J. Invest. Dermat. 30, 193 (1958).

(3) O. B. Miller and W. A. Selle, J. Invest. Dermat. 12, 19 (1949).

(4) J. W. H. Mali and M. G. Woldring, Dermatologica 111, 45 (1957).

(5) G. W. Johnston and C. O. Lee, J. Am. Pharm. Assoc. 32, 278 (1943).

(6) S. Rothman, Physiology and Biochemistry of the Skin, University of Chicago Press, Chicago, Ill. (1954).

Radiation Dose Rates above the Atmosphere. III. Flight Results and New Design for a Tissue-Equivalent Ionization Chamber (M. A. Van Dilla, J. H. Larkins, R. D. Hiebert, and J. A. Sayeg)

INTRODUCTION

This report is a continuation of the work described in the previous two semiannual reports (1,2). The Lucite space ion chambers described therein have been flown in 4 high altitude balloons, in 2 Atlas ICBM's, and in the first rocket of the Blue Scout series. In addition, we have completed a new design which incorporates the ion chamber section, amplifier, high and low voltage power supplies in 1 self-contained unit; the ion chamber section is molded of tissue-equivalent plastic by Dr. Francis R. Shonka of St. Procopius College, Lisle, Illinois. Its response to gamma rays and neutrons has been measured and its ability to withstand mechanical vibration and shock demonstrated. This unit is now ready for use by the Air Force Special Weapons Center at Kirtland Air Force Base as a prototype for production by a commercial contractor.

METHODS AND RESULTS

The Lucite units have received rides to date in 4 high altitude balloon flights from Bemidji, Minnesota (summer 1960)

2 Atlas flights from Cape Canaveral down the Atlantic Missile Range (August 12 and November 9, 1960), and in Blue Scout 1, the largest solid-fuel rocket ever flown from Cape Canaveral and the first of a series of 12 research and development shots (January 7, 1961). Scheduled for 1961 are rides in an Atlas pod (the pod is a small, self-contained package which separates from the main vehicle after burnout) and in the 609A (Blue Scout) program to probe both Van Allen belts to very high altitudes. Two chambers have been delivered to Convair for the Atlas pod experiment, and a total of 7 chambers with wall thickness up to 4 in. are scheduled for Blue Scouts.

The status of flights made to date is given in Table 1. The news of the successful Blue Scout 1 arrived at the present writing. According to the AP release, all experiments aboard (including a Lucite ion chamber) radioed back clear signals; altitude reached was about 1800 km and the distance down the Atlantic Missile Range was about 1900 km. The data have not yet been received from Cape Canaveral.

The most significant data received and analyzed so far have come from the second Atlas flight; a preliminary reduction of the data on dose rate versus trajectory is plotted in Fig. 1. Cosmic rays will produce a dose rate of about 0.5 mr/hr above the atmosphere (3), so that the ion chamber readings are due entirely to the Van Allen radiation. The

TABLE 1. FLIGHT STATUS OF SPACE ION CHAMBERS MADE TO DATE

Vehicle	Date	Altitude	Results
4 Balloon flights (Bemidji, Minn.)	Summer 1960	to 142,000 ft	Data being analyzed; dose rates below 10 mr/hr. Solar flare activity extremely quiescent. Cosmic rays would produce about 0.5 mr/hr.
Atlas	August 12, 1960	1,200 km	Nose cone not recovered; data delayed but indications are that no radiation signals were received on ground from LASL SN4.
Atlas	November 9, 1960	1,200 km	Very successful flight; LASL SN5 ion chamber performed properly. Maximum dose rate was 340 mrads/hr in descending portion of flight shortly after apogee. Temperature almost constant at +20°C.
Blue Scout I	January 7, 1961	about 1,800 km	Successful first flight of a series to probe both Van Allen belts; data not available yet, but indications are that radiation signals were received on ground from LASL SN2.

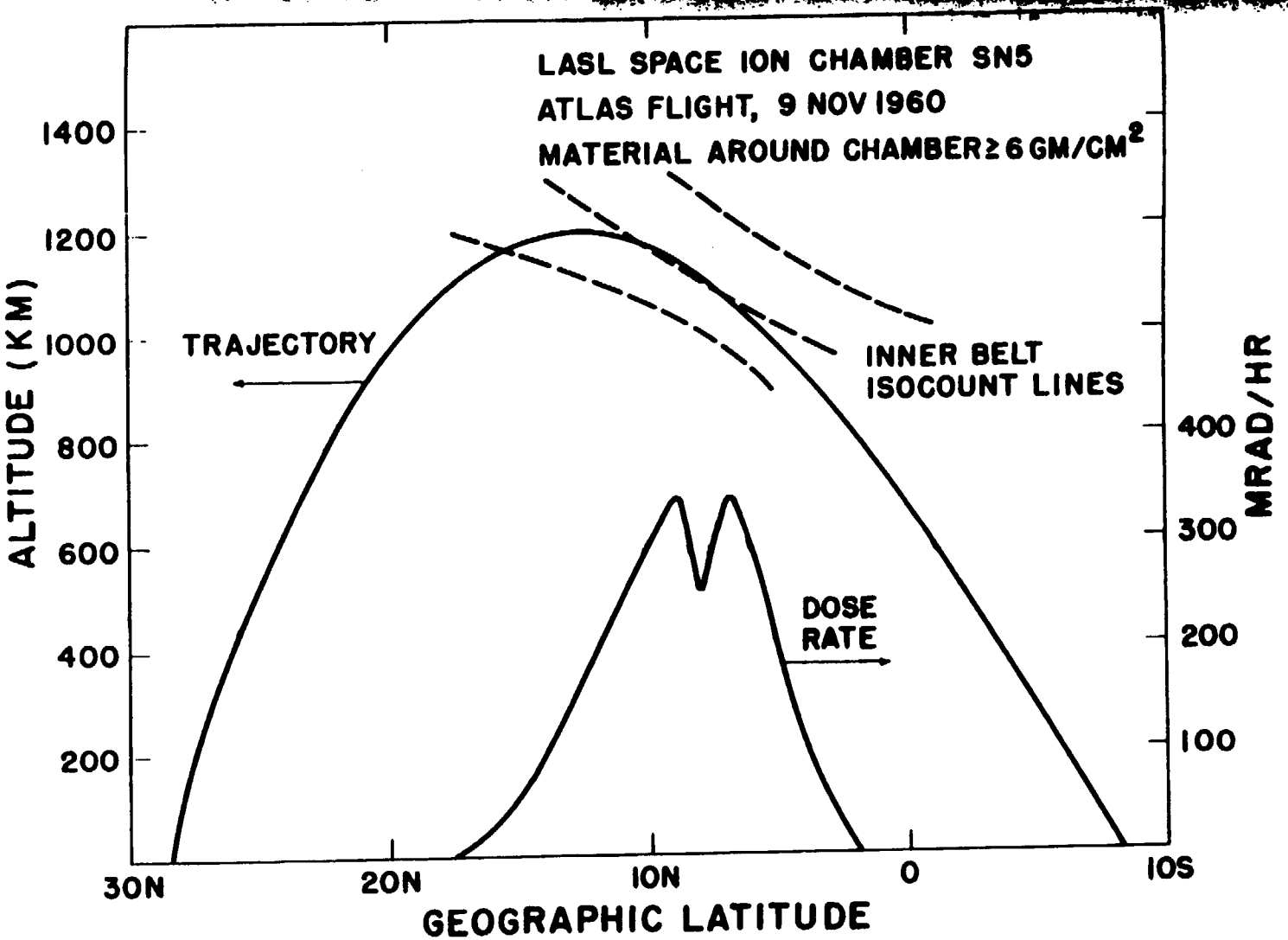

Fig. 1. Dose rate as a function of trajectory, LASL space ion chamber SN5 aboard Atlas flight (November 9, 1960).

fact that the dose rates are higher on the descending leg of the flight is due to the fact that Van Allen radiation is symmetrical about the geomagnetic equator, which dips about 15° below the geographic equator in the region of the Atlantic Missile Range. An interesting feature of the dose rate-latitude curve is a small but real valley shortly after apogee, apparently due to a slow rotation of the vehicle in the non-isotropic proton flux of the inner Van Allen belt. If the amount of material around the ion chamber were uniform in all directions, there would be no such effect. However, the actual shielding of the ion chamber by other nose cone equipment was not only considerable but also nonuniform, as shown in Table 2. This shielding will entirely eliminate the electrons and soft protons and allow only protons above 80 to 100 Mev (plus secondaries) to actuate the ion chamber. Calculations by S. W. Leeper and J. F. Tinney at Kirtland Air Force Base using the proton spectrum measured by Freden and White (4) in similar Atlas flights show that at a depth of 14 g/cm^2 the maximum expected dose rate should be about 500 to 700 mrads/hr; this is in surprisingly good agreement with the measured value of 340 mrads/hr.

The newly designed tissue-equivalent (TE) space ion chamber is shown in Figs. 2, 3, and 4. The new unit incorporates the following improvements: (a) unitized construction; the only power drain on the space vehicle is due to 2 relays

TABLE 2. MATERIAL AROUND ION CHAMBER IN ATLAS FLIGHT (NOVEMBER 9, 1960)

Per Cent of Total Solid Angle	g/cm^2
35	6
38	10
10	12
10	20
7	>20

Fig. 2. Photograph of LASL tissue-equivalent space ion chamber (prototype).

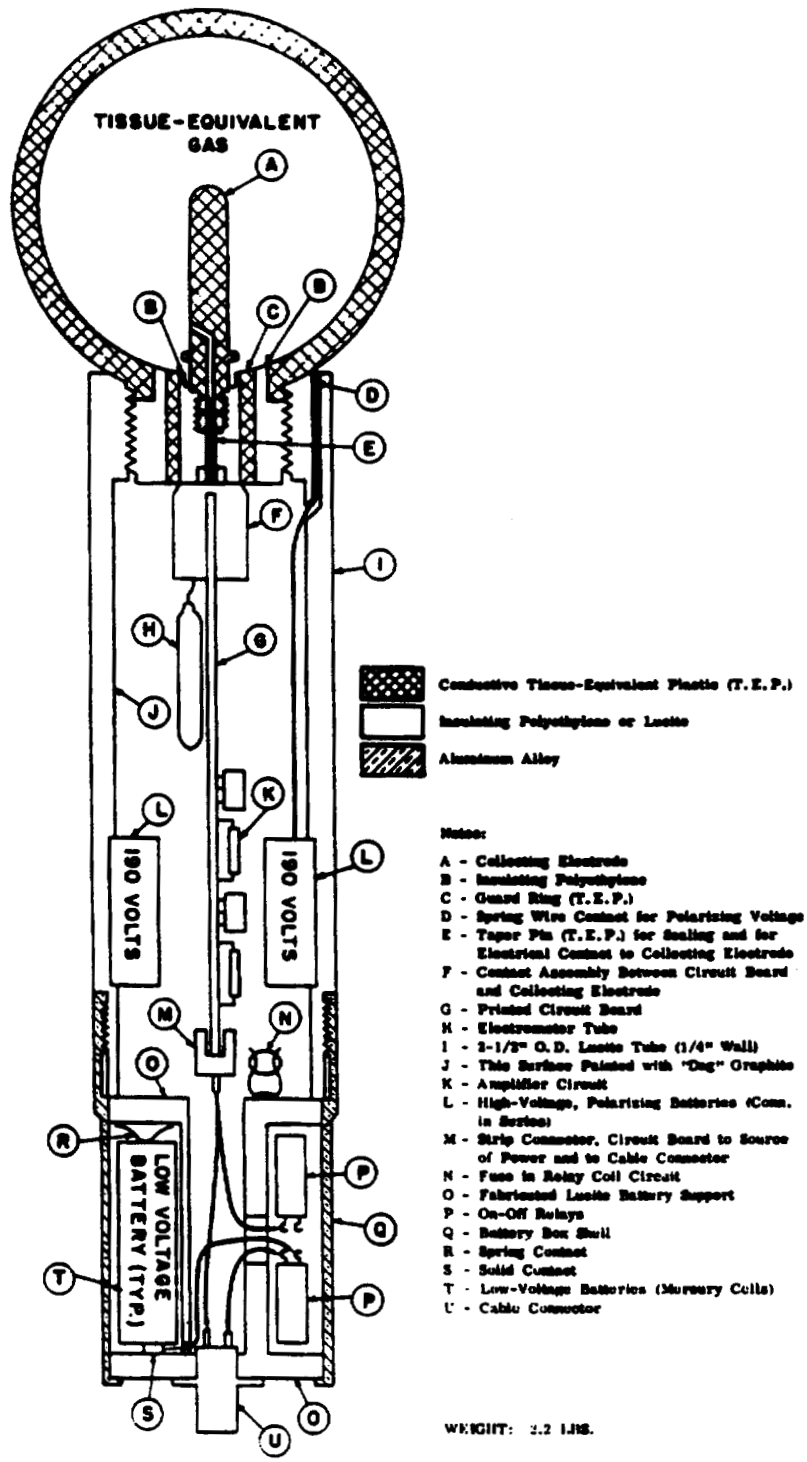

Fig. 3. Construction details, LASL tissue-equivalent space ion chamber (prototype).

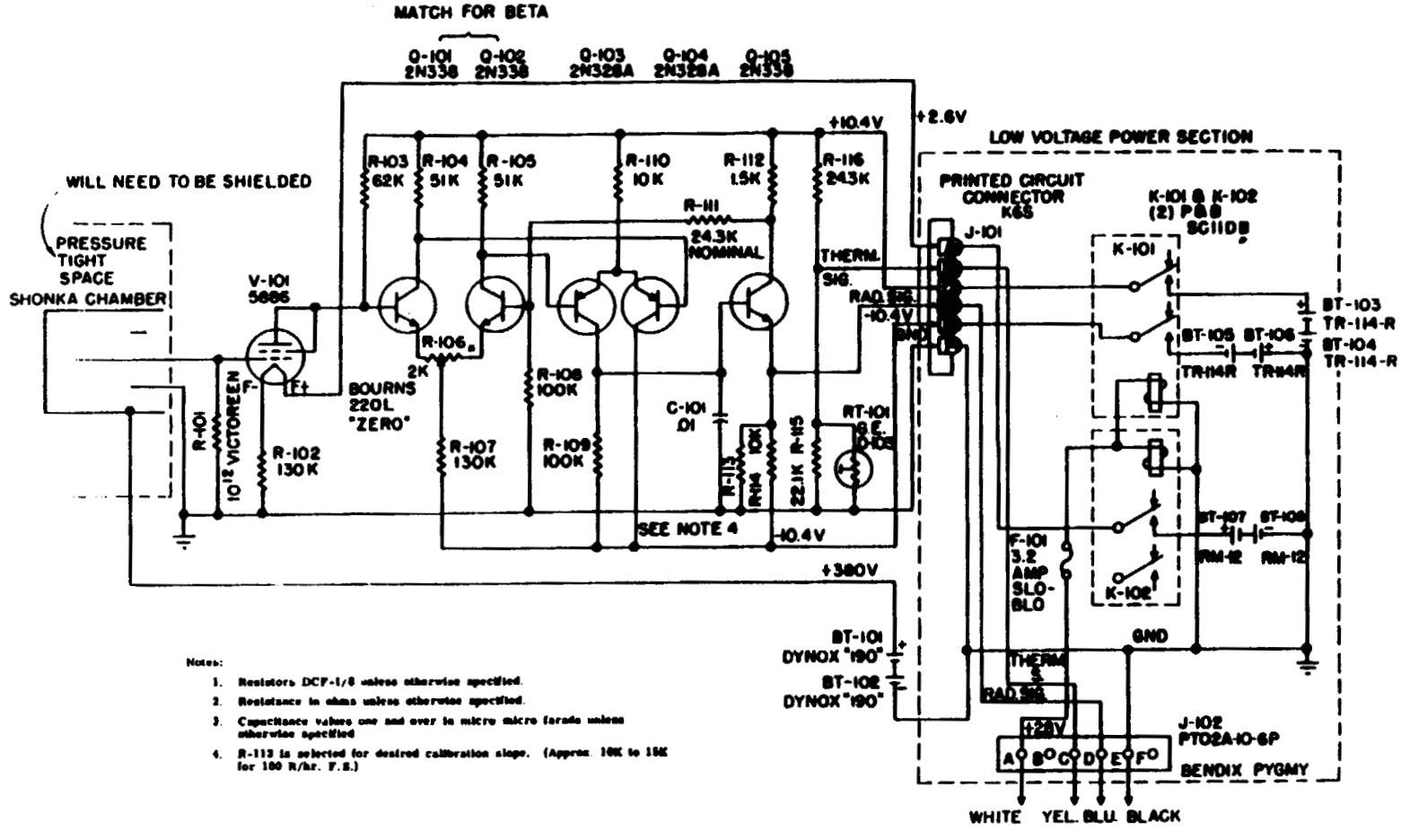

Fig. 4. Circuit diagram, LASL tissue-equivalent space ion chamber (prototype).

(24 V, 0.1 A), which turn on the amplifier when energized; (b) radiation-sensitive section (now spherical) made of tissue-equivalent (muscle) plastic; (c) radiation-sensitive section is removable and can be replaced by other designs with different wall thickness, sensitive volume, etc.; (d) polarizing voltage supplied by new, light-weight solid-state batteries (380 V, 1.67 oz.); (e) bulk of material dissimilar from tissue (metal, batteries, etc.) is about 10 in. from the center of the tissue-equivalent sphere so that the fractional solid angle subtended is only 0.04. Total weight is 1.0 kg (2.2 lb). The tissue-equivalent spherical section was subjected to acceleration (100 G) and vibration (1 G, 20 to 200 c/s, axial and transverse) at Kirtland Air Force Base with negligible effect. The neutron response was measured using 2, 8, and 20 Mev monoenergetic neutron beams at the vertical Van de Graaff generator; this was a repeat of similar measurements made previously with the Lucite ion chamber and reported earlier (2). The TE ion chamber produces the same output voltage (to $\pm$ 20 per cent) for equal dose rates from Co^{60} gamma rays and 2, 8, and 20 Mev neutrons. Thus, it is an improvement over the Lucite design which performed well at 8 and 20 Mev but read low by a factor of 3 at 2 Mev. The Co^{60} calibration curve of the TE ion chamber is given in Fig. 5.

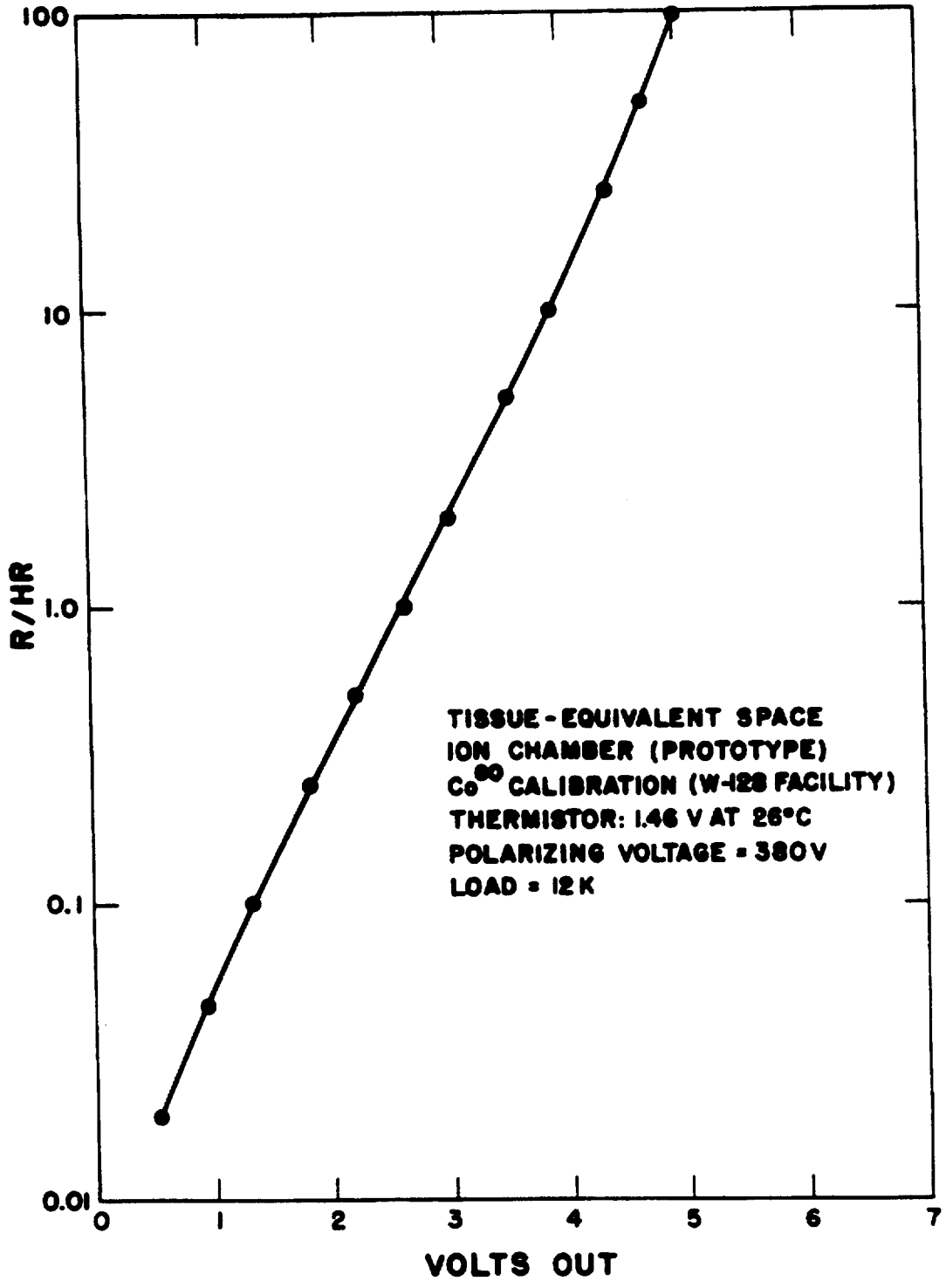

Fig. 5. Cobalt^{60} calibration, LASL tissue-equivalent space ion chamber (prototype).

DISCUSSION

The fact that reasonable data were received on the ground from the Atlas flights means that the ion chamber design is mechanically and electrically sound, and that its response to the high energy protons of the inner Van Allen belt is about as expected. Since the Atlas flights reach only into the lower fringes of the trapped radiation belts (mainly the inner belt) and are of short duration (about 30 min), the more revealing flights are those penetrating deeply into the Van Allen belts and orbital shots (which have the best chance of picking up solar flare radiation when it occurs). In these cases, we would be taking advantage of the wide range logarithmic response of the ion chamber electronics, which was designed with this in mind specifically. The initial flights in the Blue Scout series, which are scheduled to carry ion chambers, will improve the first situation considerably; expected altitudes are 1800 km (2 shots) and 3400 km (1 shot). The first of the 1800 km shots has just been made successfully (January 7, 1961); our hope is that success crowns the 3400 km shot, since this will penetrate into the heart of the inner belt. Satellites with extremely elliptical orbits (apogees about 20,000 km) to penetrate the outer belt and to be in a position to respond to solar flares would be most valuable vehicles for the ion chamber.

The new TE ion chamber represents an improvement in fundamental design and flexibility. Several ways in which this increased flexibility can be realized are: (a) if only low dose rates are expected, a linear amplifier circuit board can be designed and substituted for the present one, and a larger volume TE section fabricated and screwed on. This should make possible a much more sensitive scale (about 0 to 10 mr/hr). Probably only 1 (rather than 2 at present) high voltage battery would be needed. (b) If only high dose rates are expected, a smaller sensitive volume with closer electrode spacing would be preferable; this would again allow lower polarizing voltage to be used. (c) If it becomes desirable to isolate the TE ion chamber section from materials dissimilar to tissue, it would be feasible to remove the battery section, transistorized amplifier, and even the electrometer tube and 10^{12} ohm load resistor to a separate unit several feet away. This would be necessary if measurements relatively uninfluenced by the presence of the vehicle (at the end of a boom) were required.

There are several mechanical details which should be attended to in a production run by a contractor: (a) circuit board clamp and low voltage battery mount should be more rugged; (b) electrostatic shielding of TE and circuit board sections is necessary (it must be remembered that the TE

outer shell is 380 V aboveground); (c) TE section hub diameter should be increased to 2-1/8 in. to fit 2 in. inside diameter Lucite tubing which houses the circuit board); and (d) over-all length could be decreased 2 in. by relocating electrometer tube and 10^{12} ohm load resistor.

REFERENCES

(1) M. A. Van Dilla, J. H. Larkins, J. D. Perrings, and R. D. Hiebert, Los Alamos Scientific Laboratory Report LAMS-2445 (1960), p. 157-162.

(2) M. A. Van Dilla, M. W. Rowe, R. D. Hiebert, and J. A. Sayeg, Los Alamos Scientific Laboratory Report LAMS-2455 (1960), p. 118-122.

(3) J. A. Van Allen, In: Physics and Medicine of the Upper Atmosphere (C. S. White and O. O. Benson, eds.), The University of New Mexico Press, Albuquerque, N. M. (1952), Chapter 15, p. 254.

(4) S. C. Freden and R. S. White, Phys. Rev. Letters 3, 9 (1959).

Moonspec: Design of Detector for Measurement of Radioactivity of Lunar Surface (M. A. Van Dilla, R. L. Schuch, and E. C. Anderson)

INTRODUCTION

This project has now progressed from the initial stages described in the 2 previous semiannual reports (1,2) into the hardware phase. The major objectives have been the detailed design of the complete phoswich detector package and the fabrication of the proof test unit. These objectives have been met, and the proof test detector package will be delivered to the Jet Propulsion Laboratory, the NASA contracting agency in over-all charge, during the week of January 16, 1961.

METHODS AND RESULTS

After settling on the general design of the detector (2), the main problem involved the question of what components and fabrication technique to use so as to ensure that the final unit would withstand JPL environmental testing specifications and be biologically sterile. That is, the detector must be rugged enough to withstand launch, the long (about 66 hour) exposure to space conditions, and must not contaminate the lunar surface biologically after impact. This latter requirement has been established by international agreement; all

spacecraft which impact or land on the moon or planets must not interfere with later investigation of possible life on these astronomical bodies.

The JPL environmental specifications are set forth in JPL Spec. 30201A (May 28, 1959); the most drastic insult the detector must withstand is vibration (simulating launch). Hence, we have tested the critical components, mainly photomultiplier and cesium iodide-plastic scintillator phoswich, on the large GMX-Division shake table driven between 20 and 2000 cycles/sec at accelerations up to 15 G. Fortunately, operation of these components has been found satisfactory after these tests. This has allowed use of the CBS No. CL-1029 photomultiplier, a ruggedized version of the standard 3 in. CBS tube, the manufacturing procedure of which has been modified to ensure internal sterility.

The schedule established by JPL for the fabrication of the detector packages is shown in Table 1. R3, R4, and R5 refer to Rangers 3, 4, and 5, which are the third, fourth, and fifth spacecrafts in the Ranger series. They are to be launched with Atlas-Agena B rockets, the name Ranger referring to the spacecraft which separates from the launching rocket and goes into orbit. Rangers 1 and 2 are scheduled for 1961 for other purposes; Rangers 3, 4, and 5 are impact vehicles specifically for lunar research and are scheduled for 1962.

TABLE 1. SCHEDULE FOR FLIGHT DETECTOR PACKAGES

	SN1 (proof test) unsterile	SN2 (R3 flight) sterile	SN3 (R3 spare 1) sterile	SN4 (R3 spare 2) sterile	SN5 (R4 flight) sterile	SN6 (R4 spare) sterile	SN7 (R5 flight) sterile	SN8 (R5 spare) sterile
In hand at LASL	12-16-60	2-10-61	2-24-61	3-31-61	5-12-61	6-30-61	8-18-61	9-29-61
To JPL for environmental tests	1-13-61	3-10-61	3-24-61					
Delivery to spacecraft engineer	4-14-61	5-19-61	6-23-61	7-28-61	9-8-61	8-20-61	12-8-61	1-19-62

The first of the gamma ray detector packages is called the "proof test unit;" it will be subjected to more severe tests than the subsequent units. It will not fly but is expected to demonstrate the integrity of the design. The subsequent 7 units (flight and spare) will be sterile and must pass less stringent environmental testing. The design of the proof test unit is shown in Figs. 1, 2, and 3. The aluminum can contains the phoswich, photomultiplier, and circuitry necessary to develop signal and rejection (anti-coincidence) pulses.* Polyurethane foam is used to fix all parts firmly in place. The CsI (Tl) crystal surfaces are roughened to improve energy resolution. The crystal is sealed in 20 centistoke DC-200 silicone oil in the plastic scintillator cup; in the proof test unit, the lid is cemented on, but in subsequent units it will be heat-sealed with an induction heater by Group CMB-7. Teflon is used both as an optical reflector and to hold the phoswich-photomultiplier rigidly together. The aluminum can is hermetically sealed, so that the interior will remain at a pressure of about 1 atmosphere during flight to eliminate the possibility of corona discharge and arc-over in space.

*The other circuits necessary to make a complete spectrometer are the high voltage supply, now completed by JPL, and the RIDL pulse amplifier and 32 channel flight analyzer which are nearing completion.

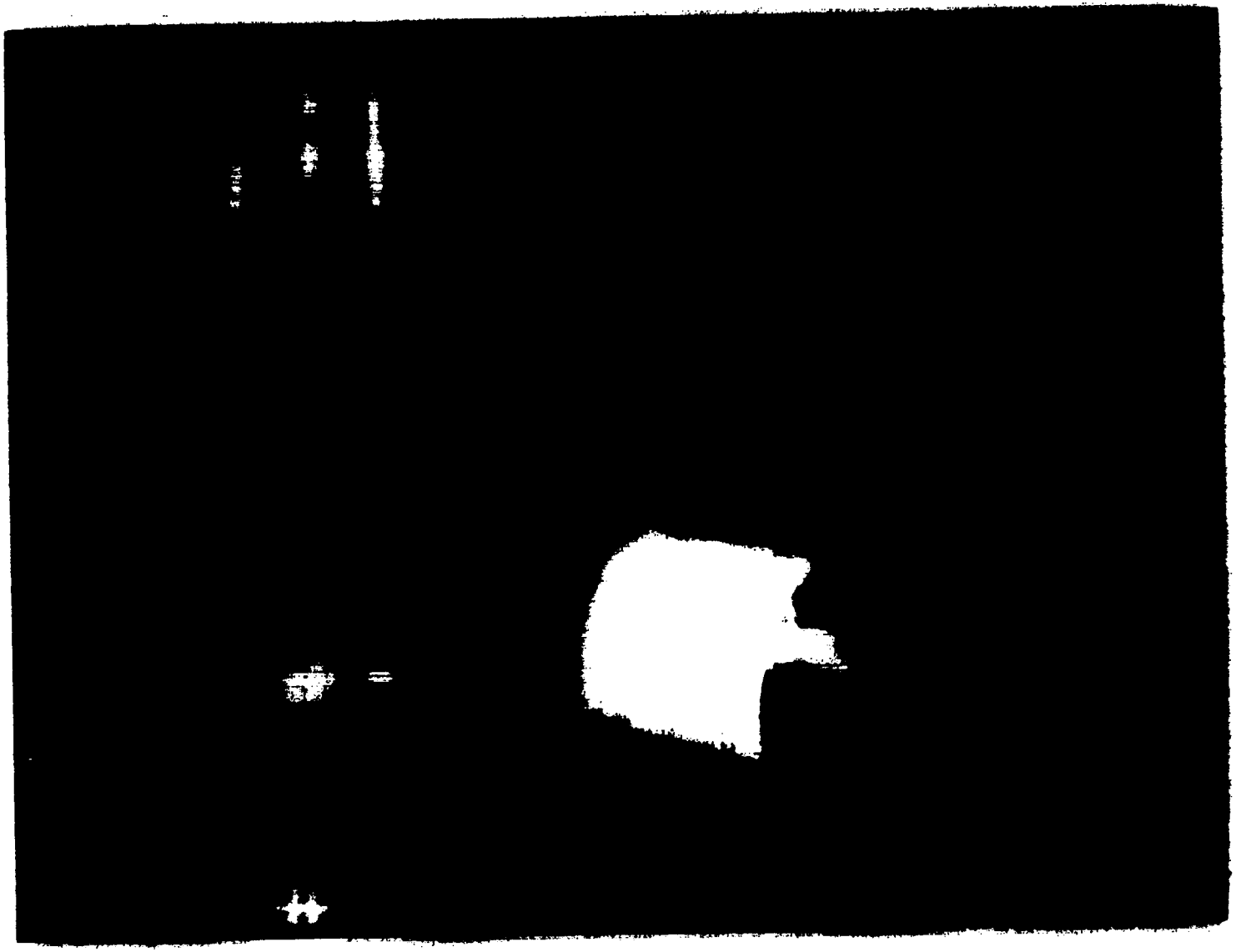

Fig. 1. Gamma ray detector for Moonspec before assembly.

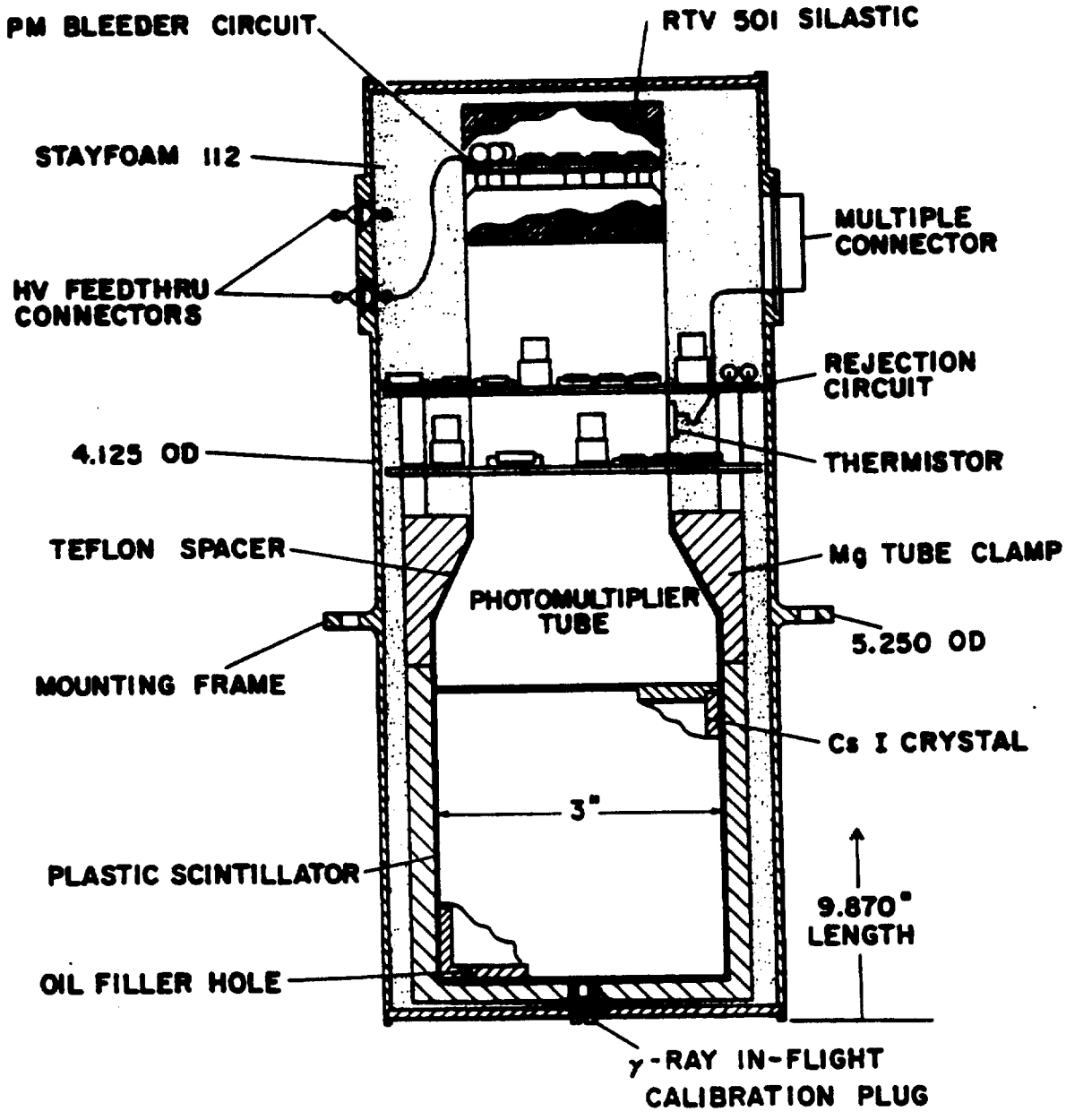

Fig. 2. Gamma ray detector for Moonspec showing construction details.

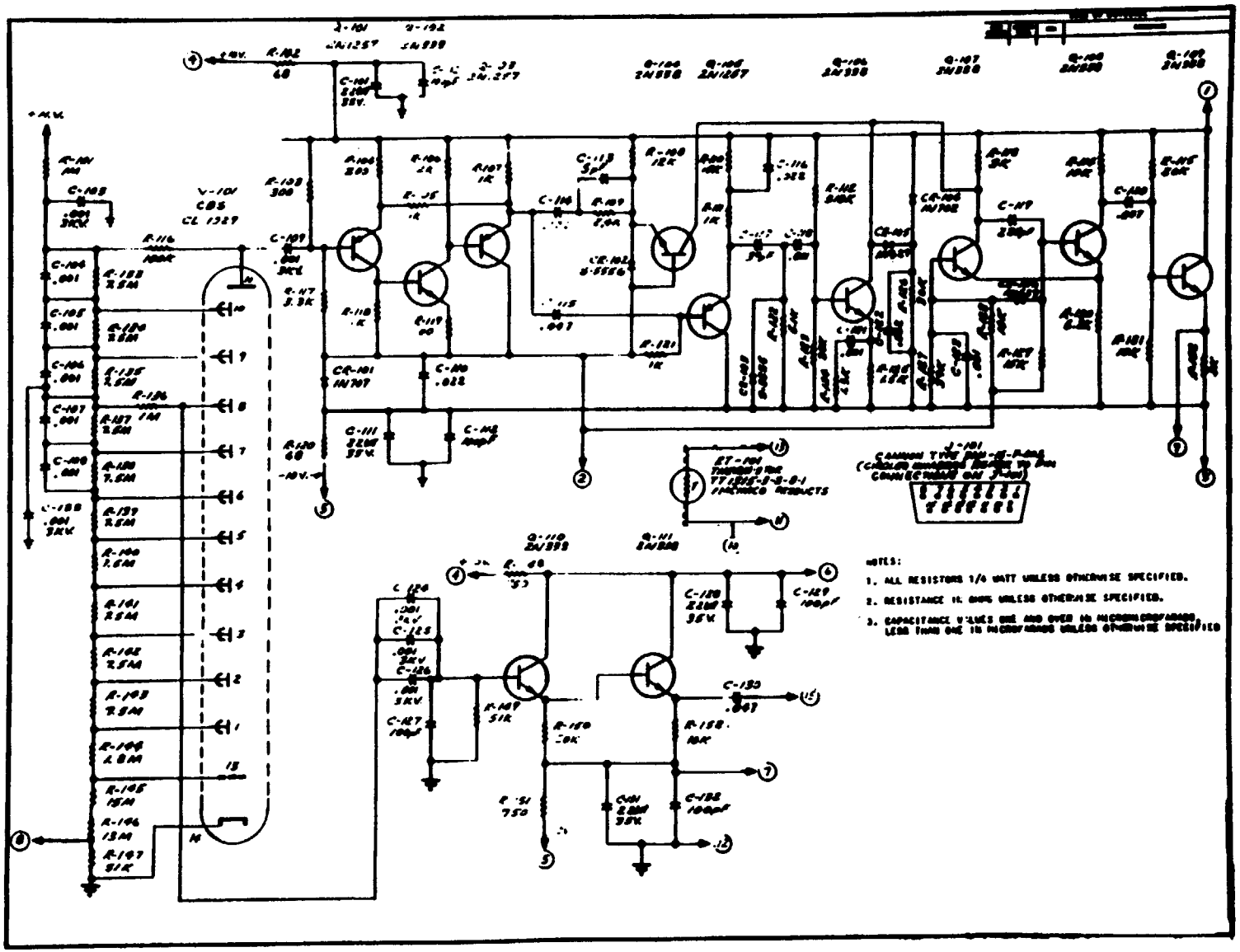

Fig. 3. Circuit diagram of phoswich rejection circuit.

The flat end of the can adjacent to the crystal is arranged so as to allow the rejection circuit to be tested before flight with a Sr^{90}/Y^{90} source, and to provide periodic in-flight gamma ray calibrations. Strontium^{90} and Y^{90} emit only beta rays, E_{max} = 2.2 Mev, and some bremsstrahlung; provision has been made to insert such a source very close to the plastic scintillator, where the beta rays will irradiate the plastic. If the rejection circuit is operating properly, anticoincidence pulses should be generated when light flashes in the plastic produce electrical pulses of energy equal to that due to the absorption of 300 kev gamma rays in the cesium iodide. In addition, the rejection circuit must not be tripped by large gamma ray pulses in the cesium iodide; this is checked using the 2.61 Mev gamma rays of ThC''. These checks of the rejection circuit are made on the ground.

Since the flight to the moon takes about 66 hours, there is the distinct possibility that drift of energy calibration will occur. We will be able to keep track of this by means of a small Ce^{141}/Hg^{203} gamma ray source cemented into the seal-off screw head near the crystal (see Fig. 2). This source remains fixed in flight, emitting gamma rays of energy 73, 142, and 279 kev. The pulse amplifier between the photomultiplier (dynode 8) and the analyzer has a gain switch allowing 2 energy ranges, 0 to 0.6 Mev and 0 to 3 Mev. The

first of these ranges is for energy calibration; the second range is designed so that the most important signal (K^{40}) falls at mid-range and the most energetic natural gamma rays (thorium, 2.61 Mev) fall at the upper end of the range. We anticipate a large amount of 0.51 Mev radiation ($\beta+$ annihilation) from the moon's surface, since cosmic ray spallation products are neutron-deficient and since high energy gamma ray interactions will also produce annihilation radiation. This makes the possibility of useful lunar signal at and below 0.51 Mev very slim, which is the reason for the choice of Ce^{141} and Hg^{203} as calibration sources. The central computer in the spacecraft is preprogrammed to flip the spectrometer from one range to the other by actuating the gain switch every 10 minutes, after which readout occurs and the data are telemetered back to earth. After terminal maneuver (about 1 hour before impact), the spectrometer is locked on the 3 Mev range to pick up the lunar signal. In this way, accurate energy calibration is achieved in flight.

DISCUSSION

The phoswich gamma ray detector described above has performed very well in laboratory tests to date. In the proof test unit (SN1), 12 per cent resolution for Cs^{137} gamma rays was attained; initial tests on SN2 yielded 10 per cent with

re careful tuning of the focusing electrode potential and gher dynode 1 potential. This is almost as good as NaI (Tl) d is a pleasant surprise. The large number of gamma rays nerated in the lunar surface by cosmic rays and natural adioactivity make good energy resolution important. A jor worry has been that the photomultiplier-crystal ssembly would fail under vibration; it turns out that these can be made more rugged than one might expect. All tests pplied so far to the rejection circuit indicate that it is performing as desired. We have planned for the future experiments using an alpha ray source or possibly a series of pure beta ray sources of $E_{max} < 2.2$ Mev in order to determine the rejection threshold more accurately.

ACKNOWLEDGMENT

We have had a large amount of invaluable support from the Physics Division in designing and fabricating the phoswich gamma ray detector. Especially helpful have been Jerry Gilland, John Northrup, Dick Hiebert, Jerry Conner, and Dick Crawford. The group in charge of the GMX-Division shake table (especially Norman Kernodle, Charles Anderson, Robert Hill, and Verdie Raper), Bob Sharp of the Shops Department, and Don Hull of Group CMB-7 have been unusually helpful.

REFERENCES

(1) M. A. Van Dilla and E. C. Anderson, Los Alamos Scientific Laboratory Report LAMS-2455 (1960), p. 163.

(2) M. A. Van Dilla and E. C. Anderson, Los Alamos Scientific Laboratory Report LAMS-2455 (1960), p. 123.

n the Radioactivity of Cesium Iodide (Thallium) Scintilla-tion Crystals (M. A. Van Dilla)

INTRODUCTION

In the course of testing the phoswich detectors to be used for the measurement of the radioactivity of the lunar surface (1-3), we noticed a peak in the background gamma ray spectrum of a cesium iodide-plastic scintillator-CBS No. CL-1003 photomultiplier combination that seemed to be due to Cs^{137}. Closer examination showed the presence of both Cs^{137} and Cs^{134} in a group of three 2-3/4 x 2-3/4 in. polished, uncanned Harshaw cesium iodide (thallium) crystals. The amount of this radioactivity was too small to affect the lunar experiment, but would certainly cause some difficulty in low level counting applications. The origin of the radioactivity is uncertain, but the Cs^{137} may be due to fallout and the Cs^{134} may be produced by capture of cosmic ray neutrons by cesium.

METHODS AND RESULTS

Three Harshaw CsI (Tl) crystals were placed in a group (as a radioactive sample) on an 8 x 4 in. NaI (Tl) spectrometer. Each crystal was cylindrical, 2-3/4 x 2-3/4 in., uncanned, and with all surfaces polished. The gamma ray spectrum is shown in Fig. 1. Note that peaks occur at 0.61,

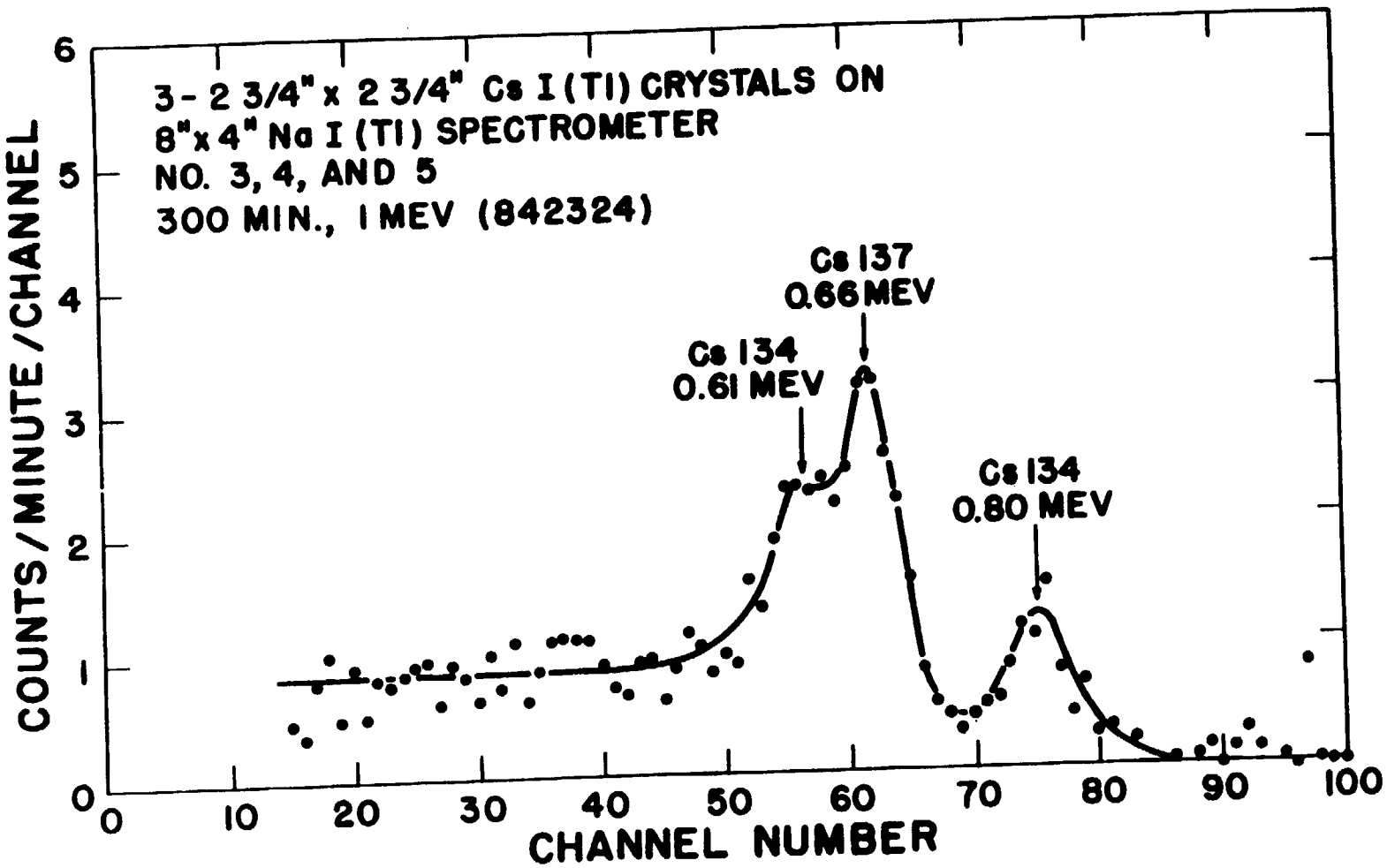

Fig. 1. Gamma ray spectra due to three 2-3/4 x 2-3/4 in. CsI (Tl) crystals as measured on a 8 x 4 in. NaI (Tl) spectrometer.

0.66, and 0.80 Mev, matching the energy of the gamma rays of 28-year Cs^{137} and 2.2-year Cs^{134}. A spectrum out to 2 Mev showed no detectable K^{40}.

DISCUSSION

While the identification of the observed radioactivity seems quite certain, we can only speculate about its origin. It seems likely that the Cs^{137} comes from radioactive fallout that has somehow gotten into the cesium compounds from which the crystals are grown. If capture by Cs^{133} of cosmic ray neutrons is responsible for the Cs^{134}, then one is prompted to ask about the possible activation of iodine and also sodium in NaI (Tl) crystals. Table 1 lists the pertinent properties of these elements for thermal neutron capture. From this it is clear that if thermal neutron capture predominates, then the gamma ray emission from Cs^{134} will be by far the most prominent at equilibrium, overshadowing I^{128} by a factor of 34 and Na^{24} by a factor of 60.

Unfortunately, the calculation of Cs^{134} production from cosmic ray-produced neutrons is difficult. It is known that the original source is mostly nuclear disruptions (stars) yielding high energy neutrons, which are slowed down by collisions with nitrogen and oxygen to low energies. Very few reach thermal energies (4) because of the n,p reaction in

TABLE 1. GAMMA RAY SPECTRUM OF THREE CsI (Tl) CRYSTALS AS MEASURED WITH 8 x 4 IN. NaI (Tl) SPECTROMETER

Element	Stable Isotopes	Abundance (per cent)	σ_{th} (barns)	Properties of Isotope Produced			
				Product	$T_{1/2}$	E_γ (Mev)	γ/dis
Cesium	Cs^{133}	100	30	Cs^{134}	2.2 yr	0.61 0.80	~1.0 ~1.0
Iodine	I^{127}	100	5.6	I^{128}	25 min	0.45	0.16
Sodium	Na^{23}	100	0.5	Na^{24}	15 hr	1.37 2.75	1.0 1.0

itrogen. The flux and energy spectrum of atmospheric neutrons near sea level are poorly known, as is the capture cross section of cesium as a function of energy.

REFERENCES

(1) M. A. Van Dilla and E. C. Anderson, Los Alamos Scientific Laboratory Report LAMS-2445 (1960), p. 163.

(2) M. A. Van Dilla and E. C. Anderson, Los Alamos Scientific Laboratory Report LAMS-2455 (1960), p. 123.

(3) M. A. Van Dilla, R. L. Schuch, and E. C. Anderson, this report, p. 186.

(4) W. O. Davis, Phys. Rev. 80, 150 (1950).

Radioactivity of Tektites (M. W. Rowe, M. A. Van Dilla, and E. C. Anderson)

INTRODUCTION

Tektites are rather strange looking silica glass objects (Fig. 1), which are found in extensive but limited areas of the earth. They are distinctly different from natural glasses of known origin (i.e., obsidian and other volcanic glasses). Some have very regular rotational forms (dumbbells, ellipsoidal shapes, etc.), some show interesting surface etching and marking, and many of the forms are the result of fragmentation. Their origin is controversial; some students of the subject favor a terrestrial and some a lunar, meteoritic, or cometary origin. This question of origin would be solved if cosmic ray-produced radionuclides (as Al^{26}) could be detected in them. Such radionuclides can only be produced by exposure to cosmic ray bombardment outside the earth's atmosphere. In the case of stone meteorites, Al^{26} concentrations have been found while previous reports of Al^{26} in tektites (1) are now questioned by one of the authors (2). Hence, three groups of tektites* from various parts of the world (philippinites from the Philippine Islands, bediasites from Texas, and australites

*Loaned by E. P. Henderson, Smithsonian Institution, U. S. National Museum, Washington, D. C.

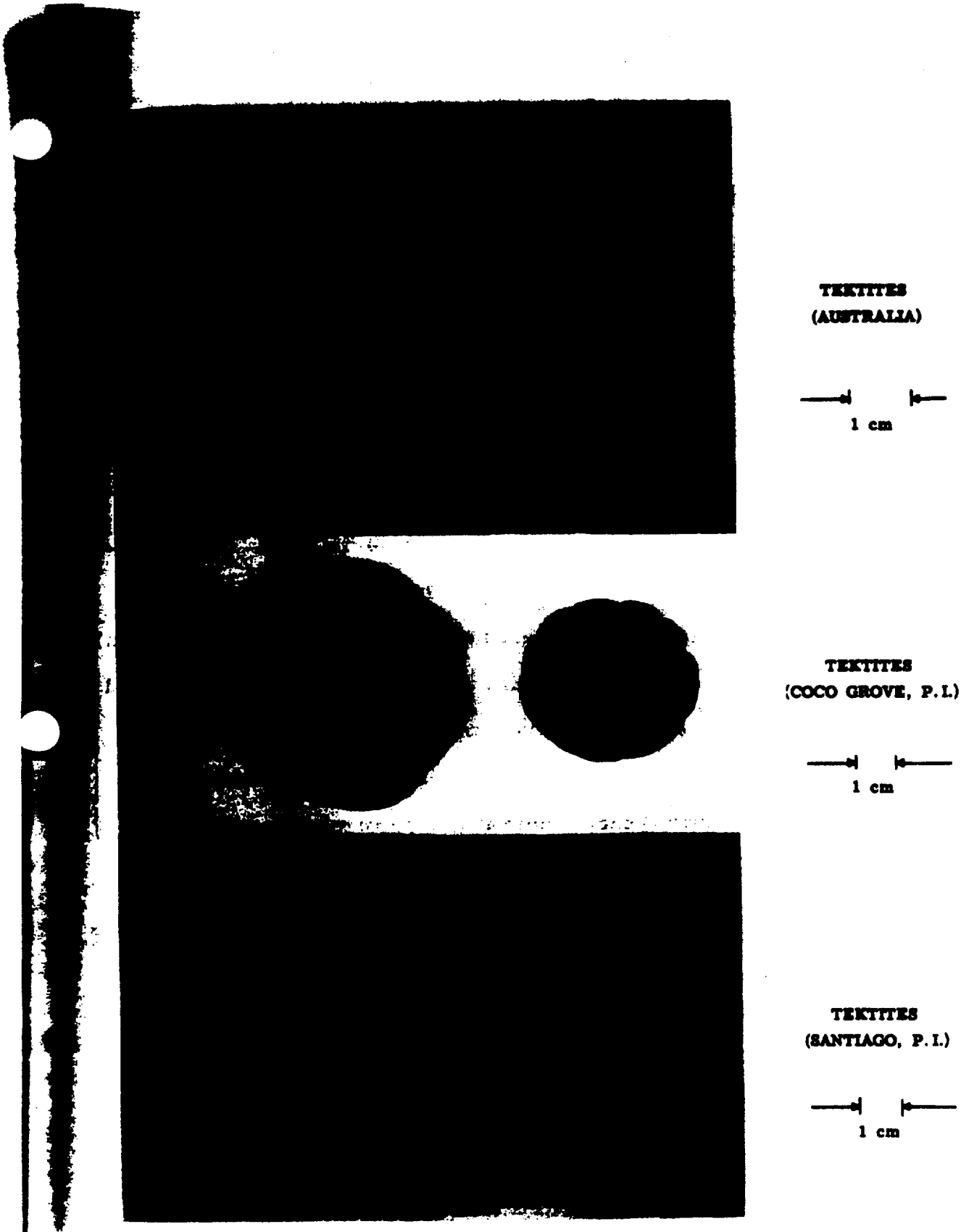

Fig. 1. Tektites from Australia (australites) and the Philippine Islands (philippinites).

from Australia) were measured for gamma radioactivity. It was found that the uranium, thorium, and potassium present swamped observation of any possible Al^{26} and suggests that the tektites resemble terrestrial rock much more than stone meteorites.

METHODS AND RESULTS

All samples were measured on an 8 x 4 in. NaI (Tl) spectrometer (3). Counting times were only a few hours, since the radioactivity levels are relatively high (like terrestrial rocks). The gamma ray spectrum of the australites is plotted in Fig. 2, along with the spectra of a stone meteorite and terrestrial rock sample. In order to make semiquantitative comparisons, the areas under characteristic photopeaks were measured; these corresponded to potassium (1.46 Mev), thorium (0.935 and 2.61 Mev), uranium (1.76 Mev), and thorium-uranium (0.58 Mev).

Table 1 shows the results, the numbers under the various energy bands being approximately proportional to the concentration of the nuclide present. It can be seen from this table that the tektites from Texas, Australia, and the Philippine Islands all have similar concentrations of gamma-emitting radionuclides and are quantitatively close to some terrestrial rocks.

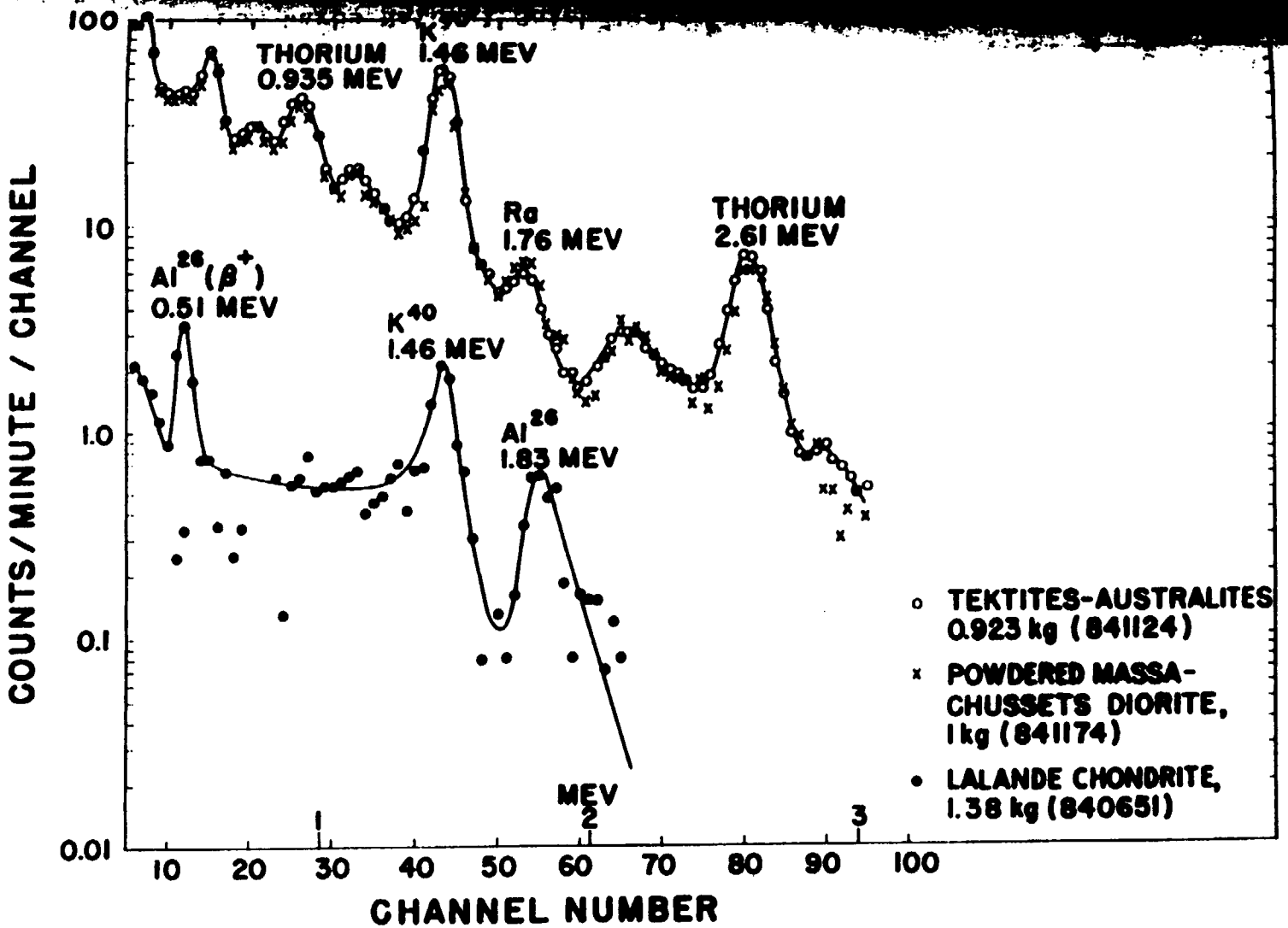

Fig. 2. Spectra of tektites (australites), stone meteorite (LaLande chondrite), and terrestrial rock (Massachusetts diorite).

TABLE 1. RADIOACTIVITY OF TEKTITES COMPARED TO TERRESTRIAL ROCKS AND METEORITES

Sample	Wt. (g)	Peak Area (c/m/g) 0.58 Mev	0.935 Mev	1.46 Mev	1.76 Mev	2.61 Mev
Philippinites						
Pugad Babuy	642	0.138	0.132	0.302	0.012	0.071
Coco Grove	716	0.112	0.117	0.299	0.013	0.067
Santiago	957	0.090	0.085	0.259	0.014	0.062
Santa Mesa	1160	0.090	0.092	0.196	0.008	0.040
Bediasites						
A	430	0.072	0.068	0.220	0.010	0.030
B	285	0.111	0.080	0.227	0.013	0.033
Australites	923	0.078	0.077	0.183	0.012	0.045
Rocks, Terrestrial*						
Diorite (Early Paleozoic, Salem, Massachusetts)	1000	0.079	0.116	0.134	0.011	0.034
Diorite (Triassic, Palisade, Jersey City, New Jersey)	810	0.025	0.066	0.123	0.006	0.016
Syenite Breccia (Boulder County, Colorado)	885	0.455	0.135	0.530	0.103	0.137
Biotite Granite (Westerly, Rhode Island)	820	0.200	0.450	0.540	<0.002	0.240
Glasses						
Libyan Desert	822	0.031	0.020	<0.002	0.005	0.012
Thailand Silica	680	0.080	0.077	0.200	0.054	0.044
Stone Meteorites						
Ladder Creek Chondrite	1010	<0.002	<0.002	0.011	<0.002	<0.002
Norton County Achondrite	1590	<0.002	<0.002	<0.002	<0.002	<0.002

*Purchased from Wards Natural Science Establishment.

Stone meteorites, on the other hand, are seen to contain to 2 orders of magnitude smaller amounts of uranium, thorium, d potassium than are present in tektites and terrestrial ocks. The tektites have about 20 to 30 times the potassium ound in chondrites. The chondrites have so little uranium nd thorium that it is not seen by the crystal spectrometer, hereas tektites and terrestrial rocks show easily measurable ranium and thorium.

DISCUSSION

The presence of Al^{26} or other cosmic ray-induced radioactivity would prove the extraterrestrial origin theory. Unfortunately, any possible Al^{26} is completely masked by uranium, thorium, and potassium in our measurements, and the results of others are conflicting. Ehmann and Kohman (1) reported Al^{26} in australites in amounts similar to that of the stone meteorites (i.e., ~ 50 d/m/kg meteorite). No activity was seen in the bediasites or another group, the moldavites,* that they investigated. However, Anders (4) reported no Al^{26} activity in the australites with a gamma/gamma coincidence spectrometer, which is more specific and requires less chemical processing of the sample than Ehmann and Kohman's Geiger counter. Kohman (2) has recently stated that he now feels

*Tektites are named after the region in which they are found (i.e., moldavites after the Moldau River in Czechoslovakia, bediasites after the Bedias Indian country in Texas, etc.).

that a check on his and Ehmann's Al^{26} work on the australites is highly desirable, and there are plans to do that at their laboratory at the Carnegie Institute of Technology.

The results of uranium, thorium, and potassium measurements in tektites by other workers are given in Table 2, along with results on terrestrial rocks, natural silica glasses, and a typical stone meteorite. Both these results and ours show that tektites are similar to terrestrial rocks in uranium, thorium, and potassium concentrations and that the stone meteorites have much lower concentrations. This evidence supports the terrestrial origin theory, but certainly does not prove it. In fact, recent analyses of tektites from Indo-China and the Philippines by Pinson and Schnetzler (13) show uniform trace element compositions; the specific gravities of these two groups were very uniform (2.43 to 2.46) for 35 samples. These results favor an extraterrestrial origin. If the theory of lunar origin of tektites (14) were upheld, the high potassium, uranium, and thorium levels would have important consequences for our lunar gamma ray experiment.

It may be concluded that tektites are still very much a mystery and that the question of their origin is still unanswered.

ABLE 2. URANIUM, THORIUM, AND POTASSIUM IN TEKTITES, ROCK, NATURAL GLASSES, AND A STONE METEORITE

Sample	Uranium (ppm)	Thorium (ppm)	Potassium (per cent)
Philippinites	2.3 (5)*	---	---
Bediasites	1-2 (5)	---	1.44 (7)
Australites	1.74 (6)	9.19 (6)	1.51 (7)
Terrestrial Rocks:			
Peridotite	1.6 (8)	3.3	0.8
Average igneous	4 (8)	~ 10	~ 3
Glasses:			
Libyan Desert	1.1 (5)	---	0.017 (12)
Thailand	3 (5)	---	---
Stone Meteorite:			
Richardton	0.0121 (9)	0.0380 (10)	0.085 (11)

*Numbers in parentheses refer to references in text.

REFERENCES

(1) W. D. Ehmann and T. D. Kohman, Geochim. Cosmochim. Acta. 14, 340 (1958).

(2) T. P. Kohman, private communication (1960).

(3) M. A. Van Dilla, J. R. Arnold, and E. C. Anderson, Geochim. Cosmochim. Acta 20, 115 (1960).

(4) E. Anders, Geochim. Cosmochim. Acta 19, 53 (1960).

(5) I. Friedman, Geochim. Cosmochim. Acta 14, 316 (1958).

(6) G. R. Tilton, Geochim. Cosmochim. Acta 14, 323 (1958).

(7) V. E. Barnes, University of Texas Publication 3945, pp. 477-656 (1939).

(8) Report of the United Nations Scientific Committee on the Effect of Atomic Radiation, p. 52, New York (1958).

(9) H. Hamaguchi, G. W. Reed, and A. Turkevich, Geochim. Cosmochim. Acta 12, 337 (1957).

(10) G. L. Bate, J. R. Huizenga, and H. A. Potratz, Geochim. Cosmochim. Acta 16, 88 (1959).

(11) G. Edwards and H. C. Urey, Geochim. Cosmochim. Acta 7, 154 (1955).

(12) L. J. Spencer, Min. Mag. 25, 425 (1939).

(13) W. H. Pinson and C. C. Schnetzler, Program Abstracts, 1959 Annual Meetings, Geol. Societies of America, p. 98A (1959).

(14) J. A. O'Keefe, Origin of Tektites, in Space Research, (H. Kallman, ed.), Interscience Publishers, New York (1960), p. 1080.

LOW-LEVEL COUNTING SECTION PUBLICATIONS

(1) T. H. Allen, E. C. Anderson, and W. H. Langham, Total Body Potassium and Gross Body Composition in Relation to Age, J. Gerontol. 15, 348 (1960).

(2) W. H. Langham, Some Radiation Problems of Space Conquest, Talk presented at the XIth International Astronautical Congress, Stockholm (August 15-20, 1960), Appendix A to Trip Report, compiled by E. B. Konecci (ed.), pp. 15-62; also published as a report sponsored by the University of Virginia, Air Force Contract 18(600)-1792, Air Research and Development Command Headquarters (August 1960); also published in Astronautical Sciences Review, 7th Annual Meeting Issue (October-December 1960), pp. 9-18.

(3) M. A. Van Dilla, J. R. Arnold, and E. C. Anderson, Spectrometric Measurement of Natural and Cosmic Ray-Induced Radioactivity in Meteorites, Geochim. Cosmochim. Acta 20, 115 (1960).

MANUSCRIPTS SUBMITTED

(1) E. C. Anderson, R. L. Schuch, V. N. Kerr, and M. A. Van Dilla, Humco II: A New 4π Liquid Scintillation Counter, presented at the Vanderbilt University Symposium on Radioactivity in Man, Nashville, Tennessee (April 18-19, 1960), to be published in Proceedings by C. C. Thomas, Springfield, Illinois (in press).

(2) E. C. Anderson, R. L. Schuch, and V. N. Kerr, The New Los Alamos Human Counter: Humco II, presented at the University of New Mexico Conference on Organic Scintillation Detectors, Albuquerque, New Mexico (August 15-16, 1960), to be published in Proceedings as a TID-report.

(3) G. R. Farmer, V. A. Bohman, and M. A. Van Dilla, Fallout Radioactivity in Cattle and Its Effects, submitted to Science.

(4) W. H. Langham, Some Considerations of Present Biospheric Contamination by Radioactive Fallout, presented at the American Chemical Society's Symposium on Radioactive Fallout in Relation to Foods, Cleveland, Ohio (April 7, 1960), to be published in J. Agr. and Food Chem. (in press).

(5) W. H. Langham, Applications of Whole Body Liquid Scintillation Counters, presented at the Vanderbilt University Symposium on Radioactivity in Man, Nashville, Tennessee (April 18-19, 1960), to be published in Proceedings by C. C. Thomas, Springfield, Illinois (in press).

(6) M. A. Van Dilla, Some Applications of the Los Alamos Human Spectrometer, presented at the Vanderbilt University Symposium on Radioactivity in Man, Nashville, Tennessee (April 18-19, 1960), to be published in Proceedings by C. C. Thomas, Springfield, Illinois (in press).

CHAPTER 4

ORGANIC CHEMISTRY SECTION

Radiation Dose Rate Measurements from the Kiwi-A Series of Nuclear Reactors (D. L. Williams)

INTRODUCTION

A part of the desirable information which has been obtained during test of the Kiwi-A series of prototype rocket propulsion nuclear power units has been concerned with the radiation environment of the reactors during and following operation. Included in the experiments performed by H-Division personnel were the measurements of gamma ray and fast neutron dose rates.

METHODS AND RESULTS

A system of "paired" liquid scintillator photodetectors has been developed (1-3), which is capable of measuring the dose rates of the gamma ray and fast neutron components in a mixed radiation field. These detectors have an extremely

wide dynamic range (10^{-5} to 10^{5} r/min) but are subject to one limitation which has been noted in an earlier report (3). Significant fast neutron dose rate measurements are not obtained when the ratio of gamma-to-fast neutron energy deposition rate is greater than about 4.

In conjunction with the Kiwi-A series of reactors, dose rate measurements were made at 3 locations relative to the centers of these devices. During Kiwi-A and Kiwi-A Prime test operations, pairs of high dose rate detectors were placed at distances of 12.5 feet (test cell front face) and 20.5 feet (free air); 1 pair of low dose rate detectors was placed at 17.5 feet inside the test cell. During the Kiwi-A Three test operation, the station at 12.5 feet was moved to a distance of 71.5 feet. Dose rate data were obtained during all the experimental runs of the 3 Kiwi-A reactors. Transmission of low current signals over approximately 2 miles of coaxial cable, without amplification, was quite successful.

Typical gamma ray dose rate data from the Kiwi-A Prime test operation have been reported (4). A similar presentation of Kiwi-A Three results is being prepared currently.

DISCUSSION

Good gamma dose rate measurements were realized during testing of the 3 Kiwi-A type reactors. Fast neutron dose

rate measurements were of marginal significance and reliability, since the fast neutron dose rate is obtained as a calculated difference value and the fast neutron sensitivity of the gamma-neutron detectors is lower than their gamma sensitivity. This result is also a function of the gamma-to-fast neutron dose rate ratio.

Because of the relatively low fast neutron sensitivity of the detection system used, it appears quite feasible to use the hydrocarbon liquid scintillator of the pair to measure gamma dose rates in the presence of fast neutrons when the gamma dose rate to be measured is known to be more than 4 to 5 times the fast neutron dose rate. The fast neutron contribution to the total response of the gamma-neutron detector would be less than the inherent error in the system, which may be 5 to 10 per cent depending upon environmental conditions. This possibility allows the use of easily obtained hydrocarbon liquid scintillator solvents instead of hexafluorobenzene solvent, which is rare and difficult to prepare.

REFERENCES

(1) D. L. Williams, F. N. Hayes, R. L. Schuch, R. L. Crawford, and R. D. Hiebert, Los Alamos Scientific Laboratory Report LA-2375 (1959).

(2) D. L. Williams, F. N. Hayes, and R. L. Schuch, Los Alamos Scientific Laboratory Report LAMS-2445 (1960), p. 219.

(3) D. L. Williams and F. N. Hayes, Los Alamos Scientific Laboratory Report LAMS-2455 (1960), p. 134.

(4) D. L. Williams, Los Alamos Scientific Laboratory Report LA-2466 (1960), (Classified).

Neutron Response of Trichloroethylene-Saturated Water and Tetrachloroethylene Chemical Dosimeters (D. G. Ott, J. A. Sayeg, and P. S. Harris)

INTRODUCTION

The chemical dosimeter offers a possibility for measurement of the individual contributions of different radiations in a mixed radiation field. Various dosimeter systems have been used in attempts to accomplish this purpose (1,2). Most such systems are made to respond to a greater or lesser extent to the components of the mixed radiation by adjusting the system for maximum or minimum sensitivity. A subtractive method may be used for the evaluation of individual radiations.

Ideally, one would like to have dosimeters which respond only to a single radiation in a mixed field and for which the response in terms of energy deposited would be equivalent to that of a tissue mass of the same volume. In these experiments, two systems have been compared in their response to fast neutrons.

METHODS AND RESULTS

The two systems used were chlorinated ethylenes, which contained varying amounts of water. The fast neutron response varied with the water content of the system because of the preponderant n,p reaction with hydrogen by fast neutrons. In

th cases, the thermal neutron response was minimized by ielding with Li^6 metal.

The response of both types of dosimeter to neutrons of rious energies was determined by exposures to known doses neutrons of 1, 2, 4, 6, 8, and 14 Mev. The neutron sensitivity, in terms of response per rad of neutrons divided by he response per rad of gamma rays, is shown in Fig. 1. It ill be noted that the one-phase or trichloroethylene saturated ater system showed a much wider response over this energy egion. Over this energy region, the response increased by a factor of about 3-1/2.

DISCUSSION

If one checked the single collision curves for fast neutrons and soft tissue, it was found that this result was similar to the tissue response. Thus a reasonable approximation of neutron dose, in terms of rads in soft tissue, can be made by the system in this energy region. The error was increased by the neutron response of the two-phase system, which must be subtracted from the one-phase result. Since this response is not flat at all energies and since the neutron spectrum is presumably unknown, the exact assignment of neutron response to the two-phase system is unknown, thus introducing this complication. The systems have not been pursued further,

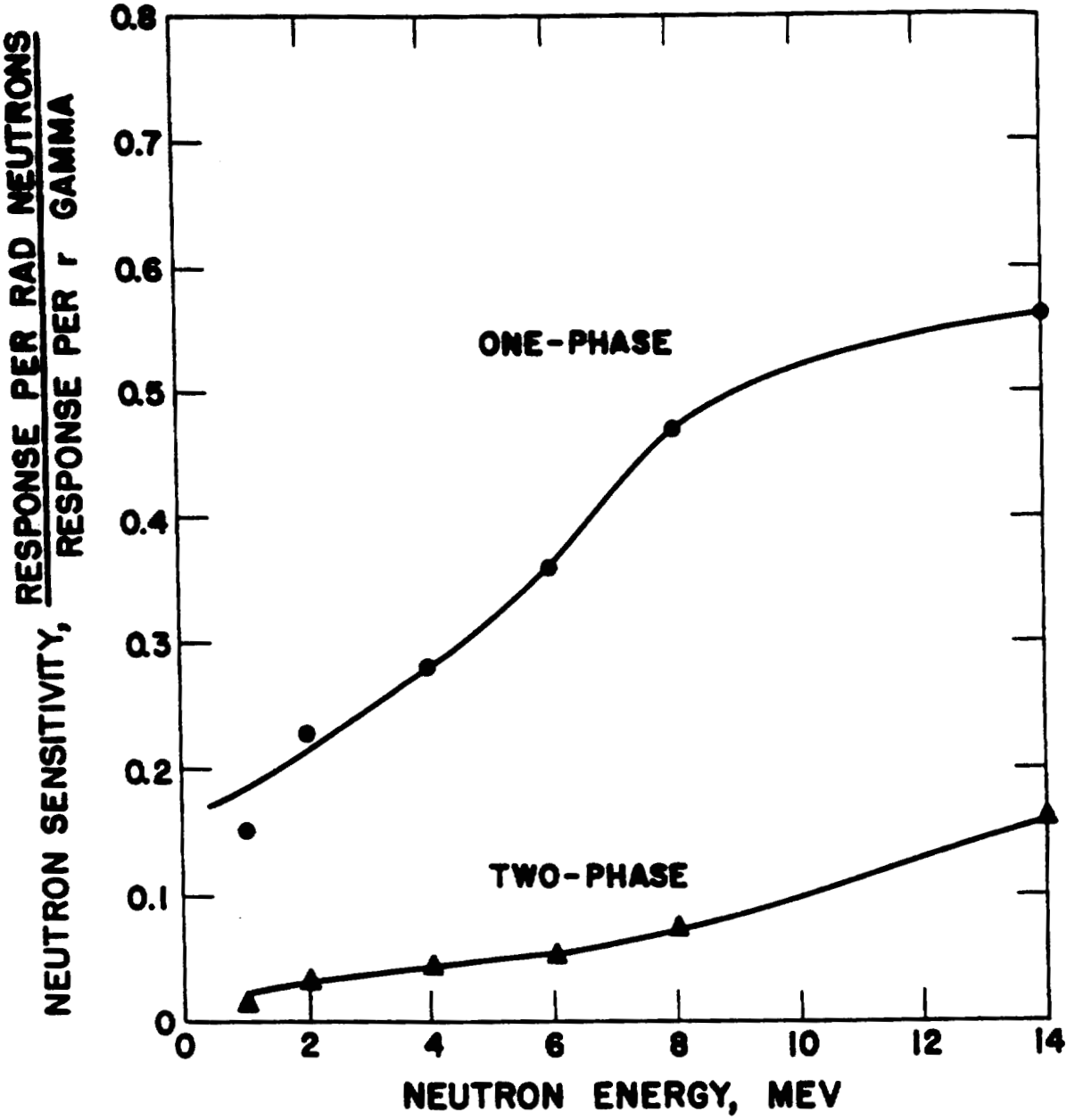

Fig. 1. Relative responses of chemical dosimeters to monoenergetic neutrons.

lthough it is felt that such investigations could be profit-

ble.

REFERENCES

(1) D. G. Ott, Los Alamos Scientific Laboratory Report LA-2249 (1959).

(2) D. L. Williams and F. N. Hayes, Los Alamos Scientific Laboratory Report LA-2375 (1960).

Contemporary Carbon^{14} in the Biosphere (E. Hansbury, V. N. Kerr, D. L. Williams, and F. N. Hayes)

INTRODUCTION

More than 2 years have elapsed since cessation of test explosions of megaton nuclear devices. Radioactive debris originally injected into the stratosphere has had ample time to become chemically fractionated and, within the small group having sufficient nuclide longevity to allow more than a few months of observation, biospheric measurements of Cs^{137} and Sr^{90} show decreasing levels of radioactivity, while C^{14} activity continues to rise. Whereas nuclear weapon tests gave rise to Cs^{137} and Sr^{90}, which were completely lacking before testing, the C^{14} produced has increased an already existent level of cosmic ray induced activity for this isotope. Up to the closing of the nineteenth century, there existed a constant atmospheric and biospheric level of C^{14} activity, the basis for radiocarbon dating. Since that time, the level of C^{14} has been changing: first, up until 1954, downward due to ever-increasing introduction (parallel to industrialization) of inactive C^{12} from fossil fuel combustion and second, since 1954, upward due to nuclear weapon testing.

The atmosphere and biosphere are such effective diluters

d the ocean is such an effective absorber of dynamic carbon
iz: that in the carbon dioxide cycle, in respiration, etc.)
at measurement of biospheric C^{14} is a low-level detection
roblem. Although chemical synthesis problems have inter-
ered with the general applicability of liquid scintillation
counting to the assay of low-level radiocarbon, special proce-
dures have been found and employed in this project to use
some plant-derived essential oils of commerce as sources of
liquid scintillator solvents to give very sensitive counting
systems.

Assays on plant chemicals bear importance in the relationship of plants to the atmosphere, via photosynthesis, and to animals and people through the ecological carbon chain. A fast growing promptly harvested plant may be an effective air carbon dioxide sampler, but different kinds of plant life may incorporate and metabolize carbon quite differently from each other. The rapidly changing radioactivity levels in atmospheric carbon dioxide during the last 6 years offer a tracer approach to plant physiology on a grandiose scale.

A variety of sampling and, therefore, of data and conclusions will be presented in this report.

METHODS

The essential oils, as received, are to a varying degree

crude and/or unsuitable for direct use as liquid scintillation solvents. Therefore, chemical processing is performed to convert these oils to p-cymene or a 2:1 mixture of p-cymene and p-menthane by procedures already described (1). The common scintillation solutes PPO and POPOP are then dissolved in the oil-derived solvents in concentrations of 5 and 0.2 g/l., respectively. The counting is done in triplicate, gathering sufficient statistics for 0.3 per cent standard deviation in the averaged result. Absolute activity levels are established by the use of an internal standard with each counting solution. Results are reported as A, d/min/g of carbon, corrected for all chemical fractionation of C^{14} from C^{12} from the time that the sample carbon was in the form of atmospheric carbon dioxide, to include photosynthesis, plant biosynthesis, and laboratory processing.

Small samples of p-cymene or the p-cymene and p-menthane mixture derived from a large number of all the essential oil types were quantitatively burned to carbon dioxide and the resulting gas samples were shipped to the Lamont Geological Observatory for determination of C^{13} fractionation relative to C^{12}. The results from these assays were converted into standard average fractionation corrections (f) to be applied to the counting data. The equation $f = 1 - 0.002\ (\delta C^{13} + 7)$ was used, where δC^{13} is in per mil relative to a Lamont

standard whose C^{13} fractionation is 7 per mil more negative than average atmospheric carbon dioxide. Carbon^{13} is considered to be an indicator for C^{14} fractionation with the C^{14} effect twice that of the C^{13}.

Values for f appear in Table 1. From the fact that all the values are greater than 1, it can be inferred that the net result of the sequence of reactions from photosynthesis through laboratory processing is to deplete the C^{14} content.

RESULTS AND DISCUSSION

Old Oils (pre-1954)

Twelve C^{14} assays for pre-1954 northern hemisphere essential oils and 2 southern hemisphere cases are listed in Table 2 and plotted in Fig. 1 as yearly averages at the middle of each year. The point, A = 14.00 at 1954, which is the activity at the beginning of the rise in lemongrass oil and turpentine, is included in the plot since it represents the transition point between the old era of dilution (2) and the new era of injection of C^{14} activity. The shape of the roughly fitted curve in Fig. 1 becomes flat at early years, corresponding to the end of the long era of constant C^{14} activity. The extrapolated constant value, A = 14.46, will be referred to in Section 3. The 2 southern hemisphere points are in good agreement with the northern hemisphere data.

TABLE 1. STANDARD AVERAGE CARBON^{14} FRACTIONATION VALUES FOR ESSENTIAL OILS

Essential Oil Source	f
Camphor	1.0376
Eucalyptus Oil	1.0372
Grapefruit Oil	1.0400
Lemon Oil	1.0370
Lemongrass Oil	1.0058
Lime Oil	1.0400
Orange Oil, sour	1.0400
Orange Oil, sweet	1.0370
Oil of Tarconanthus camphoratus	1.0334
Turpentine, gum and stump	1.0380
Turpentine, wood and sulfate	1.0400

TABLE 2. CARBON^{14} ASSAYS FOR OLD ESSENTIAL OILS

Year	A, d/min/g of carbon	Location	Essential Oil
Northern Hemisphere			
1953	14.04 ± 0.05	Formosa	Gum turpentine[a]
		Formosa	Gum turpentine[b]
		California, USA	Gum turpentine[c]
1951	14.11 ± 0.06	California, USA	Gum turpentine[c]
1950	14.12 ± 0.07	Burma	Gum turpentine[d]
		California, USA	Orange oil
		Idaho, USA	Gum turpentine[e]
1948	14.16 ± 0.06	North Carolina, USA	Gum turpentine[f]
		Texas, USA	Lemon oil
		Texas, USA	"Citrus oil"
1940	14.22 ± 0.07	India	Lemongrass oil
1914	14.41 ± 0.06	Georgia, USA	Stump turpentine[g]
Southern Hemisphere			
1947	14.17 ± 0.08	Australia	Gum turpentine[h]
1909	14.41 ± 0.05	Australia	Eucalyptus oil[i]

[a] P. armandi. [b] P. taiwanensis. [c] P. ponderosa. [d] P. khasya. [e] P. monticola. [f] P. echinata. [g] P. elliottii and P. palustris. [h] P. elliottii. [i] E. resinifera and E. leucoxylon.

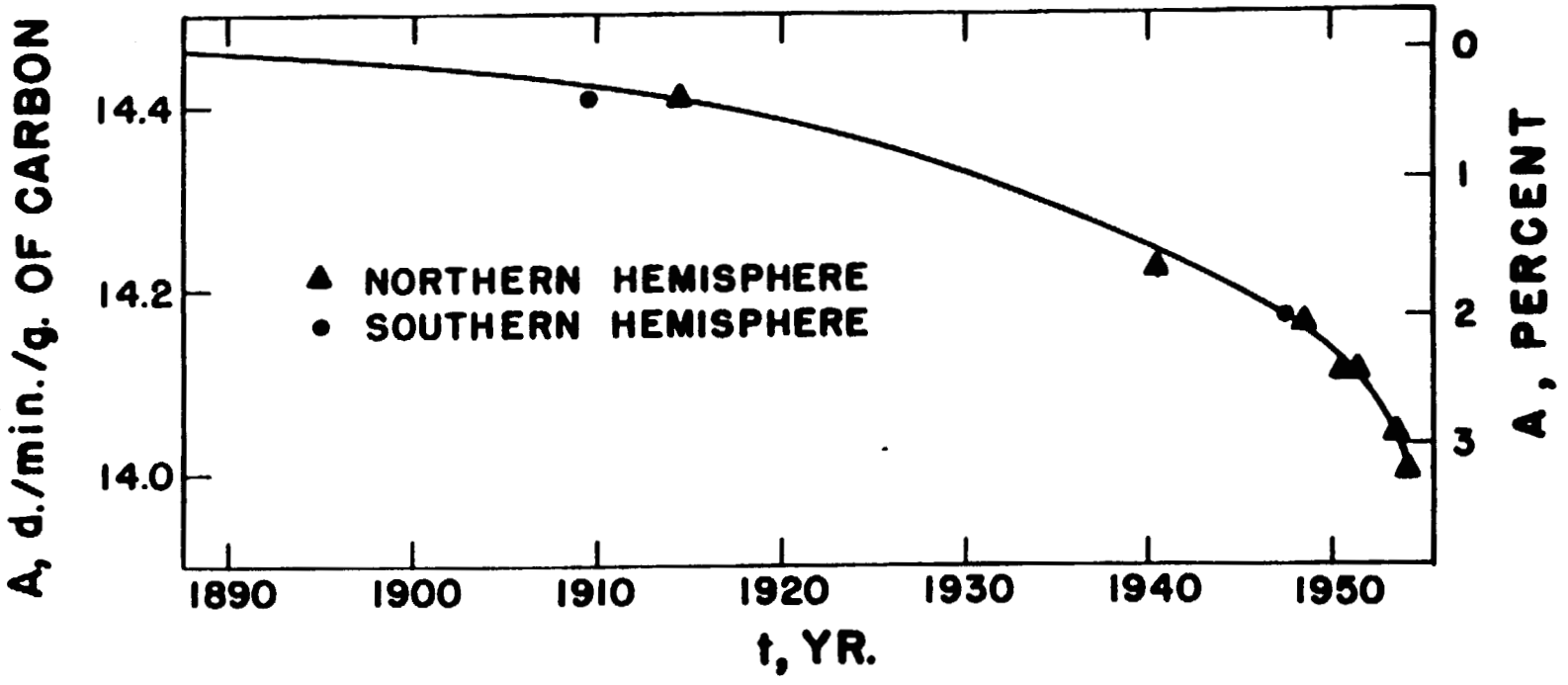

Fig. 1. Carbon^{14} assays for old essential oils.

A previous study (3) of C^{14} activity during this same span of years with dated wood samples analyzed by gas counting of combustion-derived carbon dioxide showed an over-all drop in activity of 2.03 $\pm$ 0.15 per cent. Another set of measurements (4) showed 4 per cent to be the drop. In this study, the corresponding value is 3.2 per cent.

Lemongrass Oil in the Northern Hemisphere

There are only 2 new northern hemisphere lemongrass oil C^{14} activity values to report. These are Guatemala, 15°N and 91°W, March 1960, A = 18.55 $\pm$ 0.10 and India, 8°N and 77°E, November 1959, A = 17.96 $\pm$ 0.04. These points are plotted on Fig. 2, which includes the previously published (5) 2 section linear fit to lemongrass data through June 1959. It was recognized that the linear fit in line 1 of Fig. 2 was a fortuitous occurrence as a result of discreet injections of C^{14} into the stratosphere followed by slow continuous transfer into the troposphere and the biosphere. An equation based on a simple model was presented (5) as an alternative to the linear fit shown in line 2 of Fig. 2. The curve 3 of Fig. 2 is a newly calculated fit to all the points after mid-1958. The new equation carries the previous assumptions that the mean residence times of a carbon dioxide molecule in the stratosphere and the troposphere are 5 and 7 years, respectively.

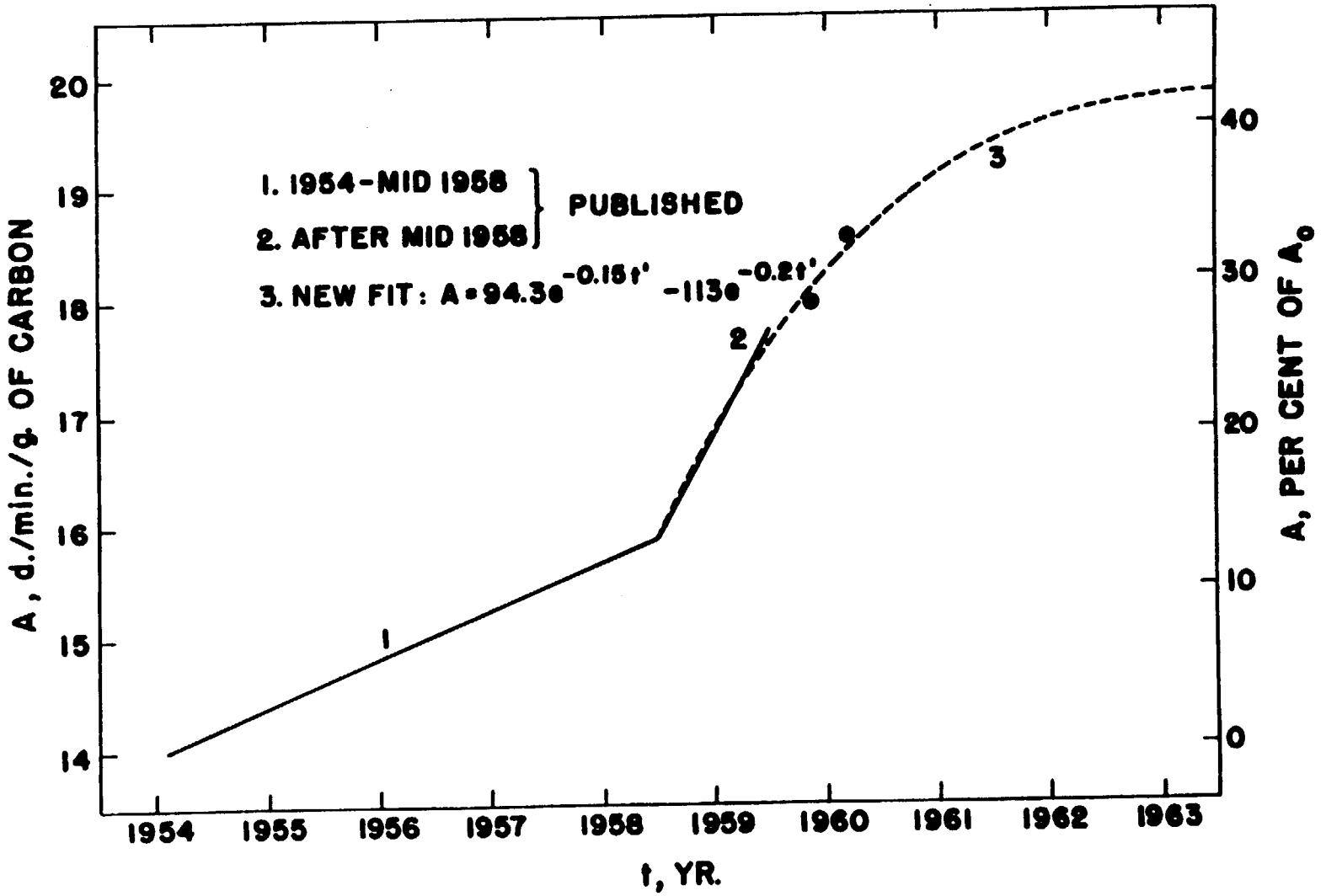

Fig. 2. The rise in C^{14} activity in northern hemispheric lemongrass oil.

The variables in the equation are A in activity above 14.00 d/min/g of carbon and t' in years beyond January 1954. The equation shows a peak at June 1963 and A = 19.78, which is 41.3 per cent greater than the C^{14} activity just before intensive testing of large-scale nuclear weapons.

The lemongrass phase of this essential oil program will be continued for a few years at the rate of only a few samples per year, just enough to evaluate the shape of the curve and recognize its peak. As time goes on, the validity of the 5-year mean stratospheric residence time assumption will be severely tested and re-evaluation of it will become possible.

Comparison of Air Sampling with Lemongrass Oil Assay

Essential oil analysis is by no means a self-justified means of estimating tropospheric C^{14} activity. Only when the organic carbon of the oil is very recently photosynthesized and virtually undiluted by older carbon of either stored or soil-derived origin can one be reasonably sure that the analysis of the oil will be the same as that of the carbon dioxide from which it was synthesized. Of the various essential oils used in this study, lemongrass oil would seem to be the best air sampler, since harvesting occurs (6) typically after 3 to 4 months of growth of the plant from the ground up. In the

following sections of this report, it can be seen that lemongrass oil has the highest activity of any essential oil for a given harvest time during the fast rising (since early 1954) portions of the C^{14} analyses.

As an attempt to correlate direct air carbon dioxide analyses with lemongrass oil analyses, northern hemisphere data by Broecker et al. (7,8) from June 1956 to March 1960 have been examined (Table 3) in conjunction with lemongrass A values at the air sampling time. If we had had an A value for the Lamont 1890 wood standard, then all the air values could have been converted directly into A values. Not having this, the correlation method chosen was, as shown in Table 3, to assume that lemongrass oil and air assays are interconvertible and to express the air assays as a factor directly related to the Lamont 1890 wood standard: $1+ (\Delta C^{14})10^{-3}$. The air units, ΔC^{14}, are expressed in per mil difference from the activity of the standard 1890 wood. When each lemongrass oil activity was divided by the corresponding factor, a set of values in d/min/g of carbon for A of 1890 wood was obtained. With the further assumption that the 5 numbers in this set with values either less than 14.00 or greater than 15.00 were unrepresentative, the remaining 9 were averaged to give A = 14.44, a value almost equal to that (A = 14.46) from the extrapolation of old oil assays in Section 1. Finally,

TABLE 3. A CORRELATION OF AIR AND LEMONGRASS OIL LEVELS OF CARBON^{14} ACTIVITY

Date	Air Activity, $1 + (\Delta C^{14})10^{-3}$	Lemongrass Oil Activity, A = d/min/g of carbon	1890 Wood Activity,[a] $A_{(\Delta C^{14} = 0)}$[b] d/min/g of carbon	Correlated Air Activity,[c] A = d/min/g of carbon
June 1956	1.031	15.00	14.55	14.89
July 1956	1.025	15.03	14.66	14.80
July 1956	1.054	15.03	14.26	15.22
November 1957	1.105	15.60	14.12	15.96
December 1957	1.075	15.64	14.55	15.52
August 1958	1.162	16.14	13.89[d]	16.78
August 1958	1.176	16.14	13.72[d]	16.98
October 1958	1.159	16.45	14.19	16.74
November 1958	1.159	16.61	14.33	16.74
May 1959	1.249	17.40	13.93[d]	18.04
May 1959	1.257	17.40	13.84[d]	18.15
October 1959	1.246	17.95	14.41	17.99
December 1959	1.221	18.16	14.87	17.63
March 1960	1.178	18.42	15.64[d]	17.01

[a] A of lemongrass oil divided by $\left[1 + (\Delta C^{14})10^{-3}\right]$.

[b] Average of unrejected 1890 wood values is A = 14.44.

[c] A of average 1890 wood multiplied by $\left[1 + (\Delta C^{14})10^{-3}\right]$.

[d] Rejected values.

multiplication of 14.44 by each of the air activity factors gave air values in A units. These were plotted versus time in Fig. 3, along with the lemongrass reference curve such that the fit arranged for above could be viewed. The unfilled circles represent the air assay values unused in deriving the C^{14} activity for pre-1900 wood.

A much more direct method than this to intercompare the A and ΔC^{14} units was attempted when a carefully assayed p-cymene sample of essential oil origin was sent to Broecker in New York and to Rafter in New Zealand for C^{14} analysis in their gas counting systems. As of this time, neither worker has yet had complete success to report.

Citrus Oils from the Northern Hemisphere

Northern hemisphere citrus oils (from the peels) harvested since early 1954, 34 of which are orange, 4 lime, and 1 grapefruit, have been analyzed for C^{14} activity and the results are listed in Table 4 and plotted in Fig. 4. For comparison, the lemongrass reference curve is given along with a portion of a mathematically derived curve representing a mean storage time, τ, of 0.2 year relative to the lemongrass curve. The method of derivation of expressions involving τ will be mentioned in Section 5.

The lime oil values agree with the lemongrass and

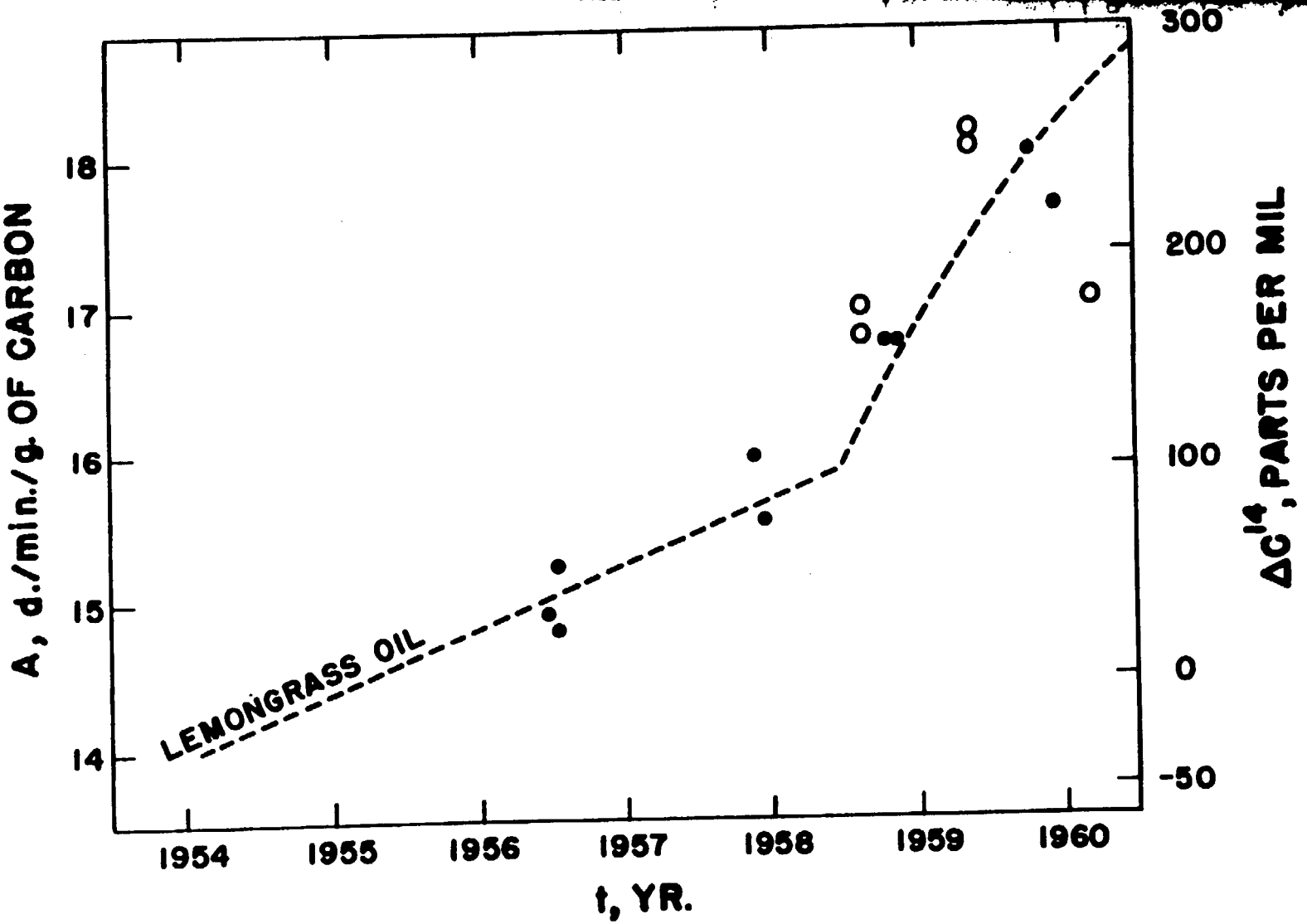

Fig. 3. Air assays fitted to the lemongrass oil reference curve.

TABLE 4. NORTHERN HEMISPHERE CITRUS OIL ASSAYS FOR CARBON[14] ACTIVITY

Location	Geographical Coordinates Lat.	Long.	Date of Harvest	A = d/min/g of carbon
British Honduras	17°N	88°W	January 1958	15.41 ± 0.04[a]
			January 1959	16.17 ± 0.07[a]
			January 1960	17.84 ± 0.05[a]
Guinea	11°N	12°W	January 1959	16.48 ± 0.07[a]
India	21°N	78°E	March 1959	16.63 ± 0.04[a]
Israel	32°N	35°E	March 1958	15.74 ± 0.08[a]
			March 1959	16.60 ± 0.04[a]
			March 1960	18.38 ± 0.04[a]
Italy	38°N	16°E	January 1958	15.72 ± 0.15[a]
			January 1959	16.37 ± 0.06[a]
Jamaica	18°N	77°W	January 1958	15.41 ± 0.08[a]
			January 1959	16.27 ± 0.12[a]
			January 1960	17.71 ± 0.17[a]
Japan	34°N	131°E	March 1958	15.56 ± 0.04[a]
	34°N	136°E	November 1958	16.54 ± 0.04[a]
Mexico	23°N	99°W	August 1954	14.30 ± 0.18[b]
			August 1957	15.42 ± 0.10[b]
			August 1958	16.00 ± 0.06[b]
			August 1959	18.10 ± 0.09[b]
Spain	39°N	0°	January 1958	15.75 ± 0.05[a]
			January 1959	16.59 ± 0.05[a]
USA, California	34°N	118°W	June 1957	14.62 ± 0.10[a]
			April 1958	15.42 ± 0.09[a]
			August 1958	15.29 ± 0.04[a]
			February 1959	15.59 ± 0.04[a]
			May 1959	16.24 ± 0.04[a]
			July 1959	16.19 ± 0.05[a]
			October 1959	16.47 ± 0.09[a]
			March 1960	17.67 ± 0.13[a]
	36°N	119°W	January 1958	15.74 ± 0.08[a]
			January 1959	16.37 ± 0.16[a]
			May 1959	17.38 ± 0.06[a]
			January 1960	18.14 ± 0.16[a]
USA, Florida	28°N	82°W	May 1958	15.73 ± 0.04[a]
			December 1958	16.14 ± 0.08[a]
			December 1958	16.26 ± 0.08[c]
			May 1959	16.33 ± 0.06[a]
			December 1959	17.53 ± 0.17[a]
			May 1960	17.69 ± 0.09[a]

[a]Orange oil. [b]Lime oil. [c]Grapefruit oil.

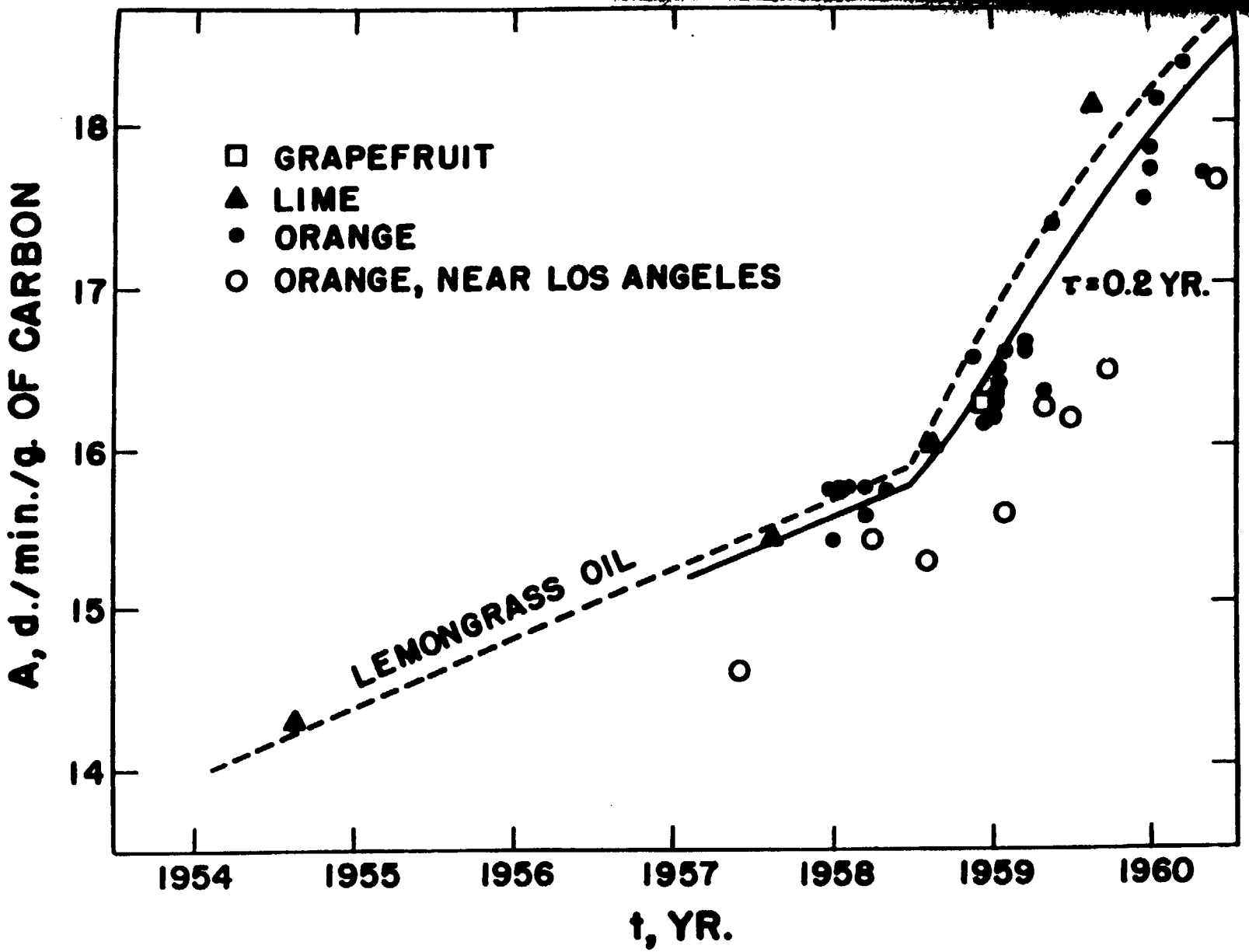

Fig. 4. Carbon^{14} activity increase in citrus oils from the northern hemisphere as a result of nuclear weapon testing.

suggest that lime oil at harvest is a material as freshly photosynthesized as lemongrass oil.

With the exception of the special set of near Los Angeles orange oil points, grapefruit and orange oil seem at most to be about 3 months later than the lemongrass in showing the same assay. One geographically related set of locations in this group of orange oils, which have consistently lower than average A values, are the Caribbean group: British Honduras, Florida, and Jamaica. The effect, although slight, seems real and begs for an explanation.

The 8 C^{14} analyses of orange oil from groves near Los Angeles, where appreciable man-made concentrations of non-radioactive carbon dioxide may be available during photosynthesis, show large depressions from the lemongrass curve, averaging 6.1 $\pm$ 0.8 per cent with no obvious internal trend about the average.

Having used citrus oils to show that they are at most only a few months physiologically older than lemongrass oil and that an industrial effect of C^{14} dilution is readily measurable with them, it is planned to discontinue citrus oil measurements.

Turpentine from the Northern Hemisphere

Most of the turpentine samples used in this study have

been obtained with the aid of Dr. N. T. Mirov, Pacific Southwest Forest and Range Experiment Station, U. S. Department of Agriculture, Berkeley, California. A few have been of commercial origin from Florida and Georgia.

On first examination of the counting results, it was evident that turpentines were acting not at all like lemongrass or citrus oils but were on the average lower in C^{14} activity and had a large scatter. In general, there may be 2 mechanisms for low activity during a time of increasing activity. One is activity dilution by old or dead carbon dioxide at the time of photosynthesis and the other, dilution after photosynthesis may be thought of as storage of photosynthetic products which, after some mean residence time, τ, become converted to the essential oil.

A mathematical model for the latter situation has been developed by Walter Goad of Group T-4, and his equations, which in part are derived from the lemongrass reference curve, have been evaluated for τ values of 0.2, 1, 2, and 4 years. The results of the 0.2 calculation were shown in Fig. 4 and the 1, 2, and 4 year curves appear in Figs. 5 and 6.

In Table 5 are presented turpentine C^{14} activity data for commercial samples containing bicyclic terpenes, for those with the monocyclic terpenes, l-limonene and l-β-phellandrene, and for 4 bicyclic terpenes harvested in 1954,

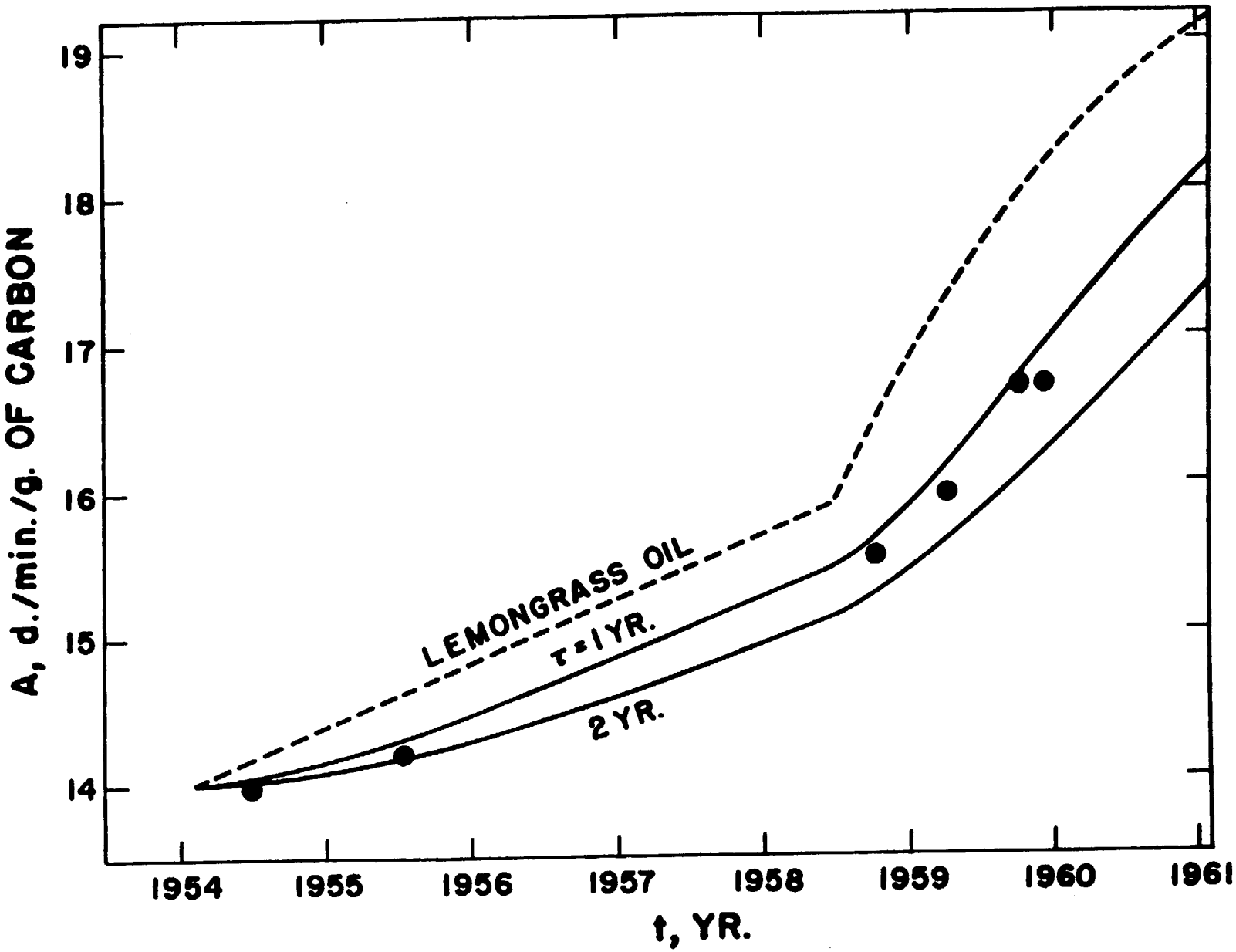

Fig. 5. Carbon^{14} activity increase in U. S. commercial turpentines.

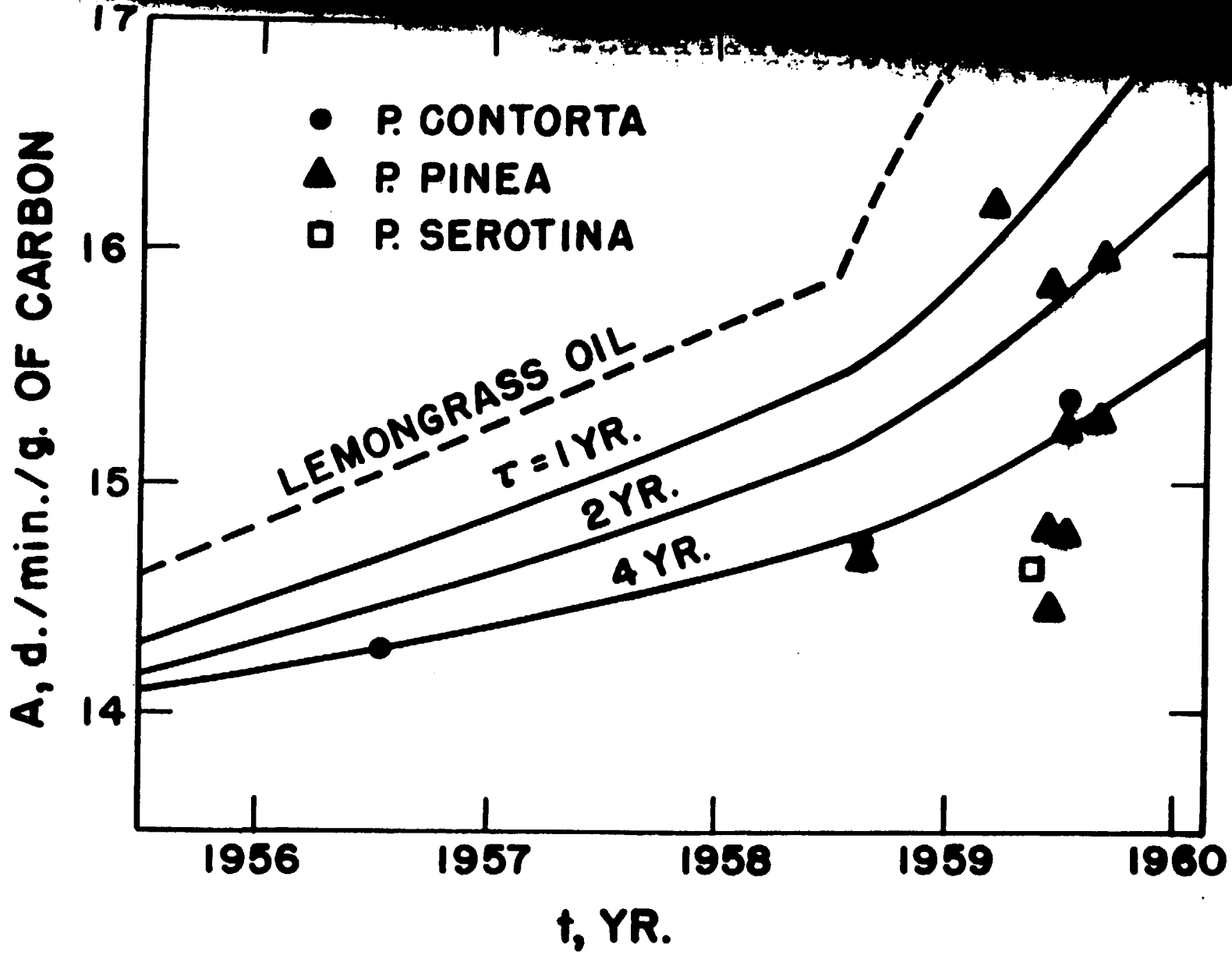

Fig. 6. Carbon^{14} activity increase in northern hemisphere monocyclic turpentines.

TABLE 5. NORTHERN HEMISPHERE TURPENTINE ASSAYS FOR CARBON[14] ACTIVITY

Location	Geographical Coordinates		Date of Harvest	A = d/min/g of carbon
	Lat.	Long.		
Cuba	23°N	82°W	1954	14.05 ± 0.04[a]
France	43°N	2°E	August 1959	15.28 ± 0.09[b]
Greece	41°N	23°E	August 1959	15.97 ± 0.08[b]
Israel	33°N	35°E	1954	14.01 ± 0.04[c]
			June 1959	15.85 ± 0.07[b]
Italy	43°N	11°E	June 1959	14.44 ± 0.04[b]
Mexico	19°N	102°W	1954	13.96 ± 0.06[d]
	28°N	108°W	1954	13.97 ± 0.04[e]
Portugal	38°N	9°W	July 1959	15.24 ± 0.17[b]
Spain	41°N	4°W	August 1958	14.71 ± 0.09[b]
Turkey	34°N	28°E	March 1959	16.19 ± 0.17[b]
USA, Alabama	31°N	88°W	July 1955	14.23 ± 0.06[h]
USA, California	38°N	122°W	June 1959	14.80 ± 0.11[b]
			July 1959	14.77 ± 0.08[b]
	39°N	120°W	July 1956	14.27 ± 0.13[f]
			July 1959	15.37 ± 0.06[f]
USA, Colorado	40°N	106°W	August 1958	14.72 ± 0.06[f]
USA, Florida	30°N	83°W	July 1955	14.32 ± 0.10[h]
			October 1958	15.51 ± 0.18[h]
			May 1959	14.63 ± 0.06[g]
			October 1959	16.67 ± 0.07[h]
	30°N	84°W	July 1955	14.13 ± 0.04[h]
USA, Georgia	31°N	83°W	July 1955	14.22 ± 0.10[h]
			April 1959	15.94 ± 0.08[h]
			December 1959	16.68 ± 0.10[h]
	32°N	82°W	July 1955	14.12 ± 0.05[h]
Mississippi	31°N	89°W	July 1955	14.18 ± 0.10[h]
Southeastern	--	--	July 1955	14.23 ± 0.10[h]

[a] P. tropicalis. [b] P. pinea. [c] P. halepensis. [d] P. pringlei. [e] P. arizonicus. [f] P. contorta. [g] P. serotina. [h] Of commercial origin.

at which time the storage mechanism could have had only a small effect on the measured activities.

The 1954 and commercial values are plotted in Fig. 5 along with the lemongrass reference curve and its related storage curves with τ = 1 and 2 years. It is evident that commercial bicyclic turpentine appears after a mean residence time of some precursor(s) in the tree of about 1.2 years. This is actually an upper limit, implying no prompt incorporation of old or dead carbon dioxide at photosynthesis. The latter mechanism becomes important to the extent that there may be nearby sources of dead carbon dioxide from petrochemical combustion or that dense forestation may be accompanied by significant concentration at photosynthetic sites of carbon dioxide of humic origin.

The assays on monocyclic terpene-containing turpentines are plotted in Fig. 6, along with the lemongrass reference curve and its related storage curves with τ = 1, 2, and 4 years. It may be impossible ever to explain this amazingly heterogeneous set of results, but for now a few generalizations will be stated.

The 3 U. S. assays for P. contorta, plus the France, Portugal, and Spain values for P. pinea, fall on the storage curve τ = 4 years. Three eastern Mediterranean values for P. pinea are considerably more radioactive, ranging from

τ = 0.8 to 1.9 years. An Italian and 2 U. S. assays for P. pinea and 1 Florida value for P. serotina correspond to $\tau > 4$ years. At present one cannot evaluate the geographical, biosynthetic, or sampling conditions which may be responsible for this $\pm$ 6 per cent spread in mid-1959 turpentine assays.

Many more bicyclic turpentines must be reported later, and it is now evident that their interpretation will be difficult. Further acquisition of turpentine samples is not contemplated.

REFERENCES

(1) F. N. Hayes, E. Hansbury, and V. N. Kerr, Anal. Chem. 32, 617 (1960).

(2) H. E. Suess, Science 122, 415 (1955).

(3) G. J. Fergusson, Proc. Roy. Soc. A243, 561 (1958).

(4) K. O. Münnich and J. C. Vogel, Naturwissenschaften 45, 327 (1958).

(5) F. N. Hayes, E. Hansbury, V. N. Kerr, and D. L. Williams, Z. Physik 158, 374 (1960).

(6) E. Guenther, The Essential Oils, Vol. IV, D. Van Nostrand Co., Inc., New York (1950).

(7) W. S. Broecker and A. Walton, Science 130, 309 (1959).

(8) W. S. Broecker and E. A. Olson, Science 132, 712 (1960).

[illegible]leic Acid Chromatography (A. Murray, E. H. Lilly, and L. B. [illegible])

INTRODUCTION

The implication of nucleic acids in basic research in radiobiology, genetics, carcinogenesis, and cell biology has stimulated interest in methods of separating specific macromolecular species of these complex polynucleotide mixtures. Although the application of column chromatography to these problems has evolved 7 different media of varying usefulness, the best of these, an anion exchanger (ECTEOLA), does not satisfy the need for greater fractionation resolution.

Since the electrostatic attraction between acidic phosphorus of nucleic acid and an anion exchange resin depends upon net charge of the polyelectrolyte (molecular size) and secondarily upon the distribution of that charge (molecular composition), it should be conceptually possible to fractionate species of different size and same composition, or of different composition and same size. The structure of the 2 exchangers DEAE and ECTEOLA differ fundamentally only in the presence of hydroxyl groups, yet give quite different elution profiles with calf thymus DNA.

The significant factor of selectivity in ion exchange makes it reasonable to expect that some difficulties attending fractionation of nucleic acids could be ameliorated by

developing special adsorbents. The objective of this study was to develop and characterize such new anion exchange media. For an earlier report, the reader is referred to Chapter 4 of the previous semiannual report (1).

METHODS AND RESULTS

Cellulose provides an insoluble cation-immobilizing matrix having several advantages, despite the fact that its reactivity, for purposes of synthesizing anion exchangers, is limited to the formation of an ether, ester, or replacement group. The ether is most generally satisfactory.

Amine base strength (pK_b) is a function of nitrogen electron density as governed by the character of the electron releasing groups attached to N. In order to place design of exchangers (weak base type) on a rational basis, a broad variety of amine substituted celluloses has been prepared, in homologous series wherever feasible. Every nitrogenous compound containing active hydrogen that is available in the Eastman Organic Chemicals catalogue has been submitted to reaction with alkali cellulose and epichlorohydrin after the method of Peterson and Sober (2).

Of a total of 143 preparations made and characterized by determination of (a) chloride ion exchange capacity, and (b) nitrogen (Kjeldahl) content, 55 are unsatisfactory as

anion exchangers and 41 are not fully evaluated. Aromatic amines have proved to be too weak to be satisfactory in this reaction, and indirect methods are required in such preparations.

DISCUSSION

The exchangers are being further characterized by determination of pK_b. It is quite possible that improvement in nucleic acid chromatography may be found in multiple column separations employing 2 or more specialized resins. These exchangers will be screened for selectivity with standard preparations of native DNA, RNA, and nucleoprotein, and with partially degraded preparations of each. If promisingly selective exchangers are found, further resolution may be sought by optimizing amine group density, altering the amine group distance from the matrix, and altering the matrix.

REFERENCES

(1) A. Murray, Los Alamos Scientific Laboratory Report LAMS-2455 (1960), p. 138.

(2) E. A. Peterson and H. A. Sober, J. Am. Chem. Soc. 78, 751 (1956).

Labeling of Biologically Important Compounds with Radioisotopes

(A. Murray)

The program of the Organic Chemistry Section has been supported by preparation of the following labeled compounds, the figures in parentheses being specific activity of the radiochemically pure compound in mc/g:

1. H^3-Thymine (5,000)
2. H^3-Thymidine (1,370)

A comparison of preparative-scale chromatograms, developed (descending) on Whatman No. 17 paper in the 2 solvent systems; (a) 86 per cent n-butanol-H_2O/NH_4OH (95/5 v/v) and (b) aqueous NH_4HCO_3 [16 g/100 ml (1)], showed a reversal of sequence and a 3 fold advantage in separating thymine and thymidine by the butanol system at maximum migration of the leading band.

As these preparations were achieved through catalytic exchange over 5 and 6 times recovered (degraded) HTO, which originally assayed 1300 curies/4 ml, the realized specific activity is low for some contemplated experiments with thymidine. Fresh HTO has been procured with an activity of 2700 curies/5 ml.

REFERENCE

(1) G. Hems, Arch. Biochem. Biophys. 82, 485 (1959).

ORGANIC CHEMISTRY SECTION PUBLICATIONS

(1) S. P. Birkeland, G. H. Daub, F. N. Hayes, and D. G. Ott, Liquid Scintillators. X. Some Aryl Substituted Phenanthrenes and Dihydrophenanthrenes, and Related p-Terphenyls and p-Quaterphenyls. Determination of Kallmann Parameters, Zeit. Physik 159, 516 (1960).

(2) D. L. Williams, Kiwi-A Prime Gamma Ray Dose Rate Measurements, Los Alamos Scientific Laboratory Report LA-2466 (September 1960), (Classified).

MANUSCRIPTS SUBMITTED

(1) S. P. Birkeland, G. H. Daub, F. N. Hayes, and D. G. Ott, Liquid Scintillators. IX. Synthesis of Some Aryl Substituted Phenanthrenes and Dihydrophenanthrenes, and Related p-Terphenyls and p-Quaterphenyls, submitted to J. Org. Chem.

(2) D. G. Ott, W. H. Schweitzer, J. A. Sayeg, and P. S. Harris, Trichloroethylene-Saturated Water and Tetrachloroethylene Chemical Dosimeter Systems. Neutron Response, submitted to Health Phys.

(3) D. L. Williams, Hexafluorobenzene Liquid Scintillators and Their Application to Gamma and Fast Neutron Dose Rate Measurements, presented at the University of New Mexico Conference on Organic Scintillation Detectors, Albuquerque, New Mexico (August 15-16, 1960), to be published in Proceedings as a TID-report.

(4) D. L. Williams, Kiwi-A Three Gamma Ray Dose Rate Measurements, Los Alamos Scientific Laboratory Report LA-2497 (in press).

CHAPTER 5

RADIOBIOLOGY SECTION

Lethality Studies with Fission Neutrons: Burst versus Steady State Exposures (J. F. Spalding, J. A. Sayeg, and T. T. Trujillo)

INTRODUCTION

The LD_{50}^{30} of mice exposed to degraded fission neutrons (average energy of 1.4 Mev) from the LASL Godiva critical assembly was reported to be 460 rads by earlier workers at this Laboratory (1). The above report also placed the relative biological effectiveness (RBE) of neutrons relative to X rays at 1.77 $\pm$ 0.28 and when normalized to a radium base line, the RBE was given as 2.3.

In establishing a base line for biological repair studies with fission neutrons, it was observed that the LD_{50}^{30} reported earlier was more than a factor of 2 higher than that obtained in this more recent study. As a result of this discrepancy, the RBE for fission neutrons relative to radium gamma rays (2.3)

was also nearly a factor of 2 lower. The earlier observation (1) was made with the Godiva assembly operated under burst conditions, while the more recent LD_{50}^{30} was observed with the assembly operating at a steady state over a period of several minutes. Because of the rather large disparity between the results of these 2 studies, it was felt that lethality observations should be compared on the same randomized population of mice under burst and steady state exposure conditions.

METHODS

One thousand and fifty-six RF strain female mice (4 months $\pm$ 10 days of age) were used. The mice were randomly divided into 33 groups with 32 mice in each group. Twelve groups were given whole body fission neutron exposures of from 183 to 475 rads with the Godiva critical assembly being operated under burst conditions. The 12 doses were delivered in 2 bursts with 6 dose groups per burst (Table 1). Twelve additional groups were given whole body fission neutron exposures of from 180 to 526 rads with Godiva operated under steady state conditions. These 12 doses were delivered in 2 steady state runs with 6 dose groups per run (Table 2). Six more groups were given whole body fission neutron exposures of from 158 to 242 rads with Godiva operated under steady state conditions as

TABLE 1. THIRTY DAY LETHALITY IN MICE EXPOSED TO FISSION NEUTRONS DELIVERED IN 70 μsec BURST (2 exposures with 6 dose groups per burst and dose rate varied with total dose delivered)*

Burst No.	No. of Mice	Source-to-Specimen Distance (cm)	Dose (rads) Neutron	Dose (rads) Gamma	30-day Lethality (per cent)
1	32	90	475	57.0	
	32	96	420	50.4	
	32	99	395	47.4	
	32	101	376	45.1	100 per cent in
	32	105	353	42.4	5 days
	32	110	325	39.0	
2	32	131	265	31.8	78
	32	137	238	28.6	69
	32	142	224	26.9	75
	32	147	209	25.1	56
	32	153	203	24.4	53
	32	160	183	22.0	44
	32 (controls)	---	---	----	0

*LD_{50}^{30} = 193 rads. Standard error (LD_{50}^{30}) = 9.7 rads; 95 per cent confidence limits = 157 to 207 rads.

TABLE 2. THIRTY DAY LETHALITY IN MICE EXPOSED TO FISSION NEUTRONS FROM STEADY STATE OPERATION (2 exposures with 6 dose groups per exposure and dose rate varied between 10 and 14 rads/min with total dose delivered)*

Run No.	No. of Mice	Source-to-Specimen Distance (cm)	Dose (rads) Neutron	Dose (rads) Gamma	30-Day Lethality (per cent)
1	32	90	526	63.1	
	32	96	465	55.8	
	32	99	437	52.4	100 per cent in 5 days
	32	101	416	49.9	
	32	105	391	46.9	
	32	110	360	43.2	
2	32	131	261	31.3	78
	32	137	235	28.2	81
	32	142	221	26.5	63
	32	147	206	24.7	44
	32	153	200	24.0	66
	32	160	180	21.6	25
	32 (controls)	---	---	----	0

*LD_{50}^{30} = 202 rads. Standard error (LD_{50}^{30}) = 5.5 rads; 95 per cent confidence limits = 188 to 212 rads.

fore; however, these 6 doses were delivered in 6 separate ns at the same source-to-specimen distance and at a constant se rate (Table 3). The 3 remaining groups were retained as exposed controls, 1 for each of the 3 types of exposure. ring exposure, the mice were housed in polystyrene tubes and rranged in arcs around the Godiva assembly as illustrated in ig. 1.

Neutron Dosimetry

Neutron exposures for this study were obtained from the Godiva III critical assembly. Dose measurements were made with the Hurst proportional counter (2), condenser-type beryllium-shelled tissue-equivalent and graphite-CO_2 ionization chambers (3), and threshold detectors Pu^{239}, Np^{237}, U^{238}, and S^{32} (4). Exposure doses were monitored by a fission counter mounted in the assembly housing approximately 20 in. below the critical mass. Neutron doses are presented to an accuracy of 15 per cent. A more detailed description of dosimetry for the Godiva critical assembly has been presented in earlier reports (5,6). The relative neutron doses and gamma ray contamination (12 per cent of neutron dose) are given in Tables 1, 2, and 3. The 50 per cent lethal dose determinations for 30-day observations were calculated by standard methods, according to Finney (7), and as programmed

TABLE 3. THIRTY DAY LETHALITY IN MICE EXPOSED TO FISSION NEUTRONS FROM STEADY STATE OPERATION (6 exposures with 1 dose group per exposure and dose rate constant at 12 rads/min)*

Run No.	No. of Mice	Source-to-Specimen Distance (cm)	Dose (rads) Neutron	Dose (rads) Gamma	30-Day Lethality (per cent)
1	32	140	242	29.0	75
2	32	140	221	26.5	75
3	32	140	211	25.3	63
4	32	140	200	24.0	47
5	32	140	179	21.5	16
6	32	140	158	19.0	3
-	32 (controls)	---	---	----	0

*LD_{50}^{30} = 206 rads. Standard error (LD_{50}^{30}) = 3.4 rads; 95 per cent confidence limits = 199 to 213 rads.

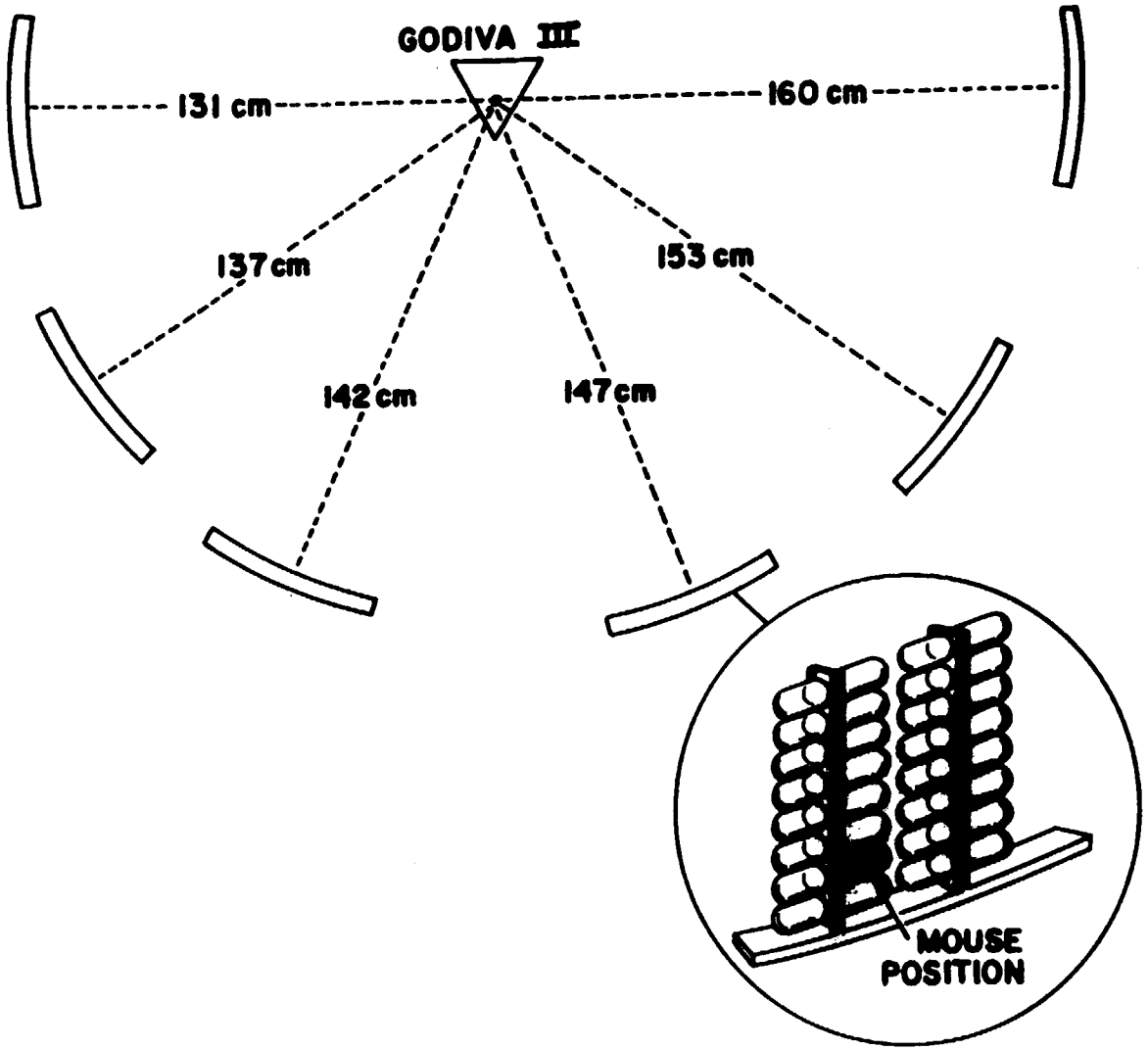

Fig. 1. Arrangement and retainment of mice around the Godiva critical assembly during burst and steady state neutron exposures.

by Group T-1 of the Theoretical Division on the IBM 704 computer.

RESULTS AND DISCUSSION

The LD_{50}^{30} for fission neutrons delivered at an average dose rate of approximately 2×10^8 rads/min (Godiva burst) was 193 rads (Table 1). In the first steady state exposure, dose rate varied from 10 to 14 rads/min with varying source-to-specimen distance. Under these conditions, the LD_{50}^{30} was 202 rads (Table 2). Six steady state exposures with a constant dose rate of 12 rads/min gave an LD_{50}^{30} of 206 rads (Table 3). All 3 LD_{50}^{30} observations, regardless of dose rate or method of exposure, were the same within the 95 per cent confidence limits. Therefore, the exposure data were pooled and the resultant LD_{50}^{30} was 204 rads with a standard error of 2.7 rads and 95 per cent confidence limits between 209 and 198 rads.

The LD_{50}^{30} for gamma rays with female mice of the same strain and age [presented in an earlier report (8)] was 782 rads, the standard error was 8.0 rads, and the 95 per cent confidence limits were from 767 to 799 rads.

From these most recent data, the RBE of fission neutrons with respect to Co^{60} gamma rays for production of lethality in mice was found to be 3.84 ± 0.06. This value is in good

agreement with the RBE of 3.6 reported by Henshaw (9) and that of 4.4 reported by Vogel (10). Vogel reported the LD_{50}^{30} for fission neutrons to be 197 rads, which is in excellent agreement with the 204 rads observed in this study. He also observed the LD_{50}^{30} for fission neutrons was independent of dose rate within a range of from approximately 0.09 to 2.00 rads/min (exposure delivered in 1-1/2 or 24 hours). This study shows the LD_{50}^{30} for fission neutrons was not dose rate dependent between dose rates of 12 and 2×10^8 rads/min.

The RBE (3.8) reported here is somewhat higher than that of 2.3 reported by Storer (1) and the value of 2.0 observed by Upton (11). There is no obvious explanation for the discrepancy between these results and those reported earlier from the same laboratory using essentially the same neutron source. The earlier work was done using commercially supplied CF_1 female mice. It is doubtful, however, that difference in mouse strain could provide completely an adequate explanation. Improvement in neutron and gamma ray dosimetry has been considerable during the 7 year period between the 2 sets of experiments. There is a good possibility that explanation of the discrepancy may be associated with the improvement in radiation dose measurements.

The relative biological effectiveness of fission neutrons relative to Co^{60} gamma rays for production of lethality in mice was 3.84 ± 0.06.

REFERENCES

(1) J. B. Storer, P. S. Harris, J. E. Furchner, and W. H. Langham, Rad. Res. 6, 188 (1957).

(2) G. S. Hurst, Brit. J. Radiol. 27, 353 (1954).

(3) J. A. Sayeg, J. H. Larkins, and P. S. Harris, Los Alamos Scientific Laboratory Report LA-2174 (1958).

(4) G. S. Hurst, J. A. Harter, P. N. Hensley, W. A. Mills, M. Slater, and P. W. Reinhardt, Rev. Sci. Instr. 27, 153 (1956).

(5) J. A. Sayeg, E. R. Ballinger, and P. S. Harris, Los Alamos Scientific Laboratory Report LA-2310 (1959).

(6) J. A. Sayeg, Los Alamos Scientific Laboratory Report LA-2432 (1960).

(7) D. J. Finney, Probit Analysis, Second edition, Cambridge University Press, London, England (1952).

(8) J. F. Spalding, T. T. Trujillo, and W. L. LeStourgeon, Rad. Res. (in press).

(9) P. S. Henshaw, E. F. Riley, and G. E. Stapleton, Radiol. 49, 349 (1947).

(10) H. H. Vogel, Jr., J. W. Clark, and D. L. Jordan, Rad. Res. 6, 460 (1957).

(11) A. C. Upton, F. P. Conte, G. S. Hurst, and W. A. Mills, Rad. Res. 4, 117 (1956).

Dependence of Recovery Half-Time on Magnitude of Gamma Ray Exposure (J. F. Spalding, T. T. Trujillo, and W. L. LeStourgeon)

INTRODUCTION

The recovery half-time (RT_{50}) from X and gamma ray exposures has been reported to be dependent on the size of the first or conditioning exposure dose (1-3). The extent of dependence of RT_{50} on the conditioning dose is a critical factor in the development of a workable biological repair formula. A study was designed to determine the RT_{50} for gamma ray exposures between 200 and 700 rads.

METHODS

Four thousand, six hundred and fifty-eight RF female mice 16 $\pm$ 2 weeks of age were used. The experiment was done in 3 parts using 2 approaches. In Part I, a fixed dose of 205 rads was given the mice, and at varied time intervals following the first exposure, groups of mice were subjected to gamma irradiation to determine the LD_{50}^{30}. The conditioning dose, time intervals to the LD_{50}^{30} exposure, and number of mice used are tabulated in Table 1.

Part II was carried out by the same methods as Part I. However, the first dose was increased to 600 rads. Conditioning dose, time intervals to LD_{50}^{30} determinations, and

TABLE 1. DATA FROM 205 RAD CONDITIONING DOSE WITH SAMPLE SIZE, LD_{50}^{30}'s SUBSEQUENT TO APPROPRIATE REPAIR INTERVALS, AND RESIDUAL DAMAGE

No. of[a] Mice	Repair Time (hr)	LD_{50}^{30} (rads)	S. E.[b] (rads)	95% Confidence Limits[c] (rads)	Residual Damage (rads)	Residual Damage (%)
360	24	559	8	574 542	206	100
177	52	580	27	660[d] 510	184	90
360	73	600	15	656 563	156	76
179	100	572	9	589 550	192	94
360	144	640	7	654 627	124	61
180	189	649	9	686 630	116	56
178	216	706	17	748 667	59	29
360 (controls)	---	764	6	776 753	---	--

[a]RF females, 16 ± 2 weeks of age.

[b]Standard error.

[c]Per Finney (Section 4.19, pp. 61-64). If b is not significantly different from zero, the limits are the antilogs of $m \pm t\, s_m$.

[d]The limits are the antilogs of $m \pm t\, s_m$.

1047107

number of mice used are tabulated in Table 2.

In Part III, the approach was reversed. The mice were divided into 7 groups and given conditioning exposures of from 0 to 692 rads. All groups were allowed a fixed repair interval of 144 hours and were then given LD_{50}^{30} exposures. This method is described in Table 3.

RESULTS AND DISCUSSION

The results of these studies are tabulated in Tables 1, 2, and 3. The time required for mice given a conditioning dose of 205 rads to repair 50 per cent of the effect was 181.3 $\pm$ 17.6 hours, and the recovery rate was fit best by a linear expression. The RT_{50} for mice conditioned with 600 rads of gamma rays was 168.0 $\pm$ 26.9 hours. and the recovery rate was fit best by an exponential plus a constant. The times required to repair the first 50 per cent of the damage were not significantly different for the 2 conditioning doses.

Six groups of mice given gamma ray exposures ranging from 205 to 692 rads showed an average residual damage of 48 per cent of their initial exposure after 144 hours of repair. There were no significant variances in the per cent residual damage regardless of the size of the conditioning dose. It was concluded that the time required for RF female mice to repair one-half of the radiation damage from acute

TABLE 2. DATA FROM 600 RAD CONDITIONING DOSE WITH SAMPLE SIZE, LD_{50}^{30}'s SUBSEQUENT TO APPROPRIATE REPAIR INTERVALS, AND RESIDUAL DAMAGE

No. of Mice	Repair Time (hr)	LD_{50}^{30} (rads)	S. E. (rads)	95% Confidence Limits (rads)	Residual Damage (rads)	Residual Damage (%)
192	21	201	22	308 142	565	94
173	69	364	20	414 330	402	67
179	172	411	14	437 381	355	59
178	237	525	11	548 504	240	40
179	312	670	24	733 631	96	16
174	547	722	32	818 671	44	7
171 (controls)	---	766	10	787 746	---	--

TABLE 3. DATA FROM VARIED CONDITIONING DOSES (205 TO 692 RADS) AND FIXED REPAIR INTERVAL (144 HOURS) WITH SAMPLE SIZE, LD_{50}^{30}'s, AND RESIDUAL DAMAGE

No. of Mice	Conditioning Dose (rads)	LD_{50}^{30} (rads)	S. E. (rads)	95% Confidence Limits (rads)	Residual Damage (rads)	Residual Damage (%)
180	205	676	13	709 655	105	51
182	302	692	18	743 662	90	30
180	408	586	9	605 569	195	48
181	512	520	8	537 504	262	51
177	603	475	18	555 420	307	51
177	692	382	35	494 296	399	58
180 (controls)	---	782	8	799 737	---	--

Co^{60} gamma ray exposure was 7.3 days and that the RT_{50} was not influenced by the magnitude of the conditioning dose between the dose levels of 205 and 692 rads.

REFERENCES

(1) R. H. Mole, Brit. J. Radiol. 29, 563 (1956).

(2) H. H. Vogel, Jr., J. W. Clark, and D. J. Jordan, Fed. Proc. 16, 132 (1957).

(3) J. A. Sproul, Jr., Rad. Res. 9, 187 (1958), abstract.

Inheritance of Radiation-Induced Decrement in Ability of Mice to Withstand Protracted Gamma Radiation Stress (J. F. Spalding and V. G. Strang)

INTRODUCTION

There is some evidence that irradiated male mice sustain genetic damage which is transmitted to subsequent generations as a decrement in the mean life span (1). From Selye's studies of "stress" phenomena (2), it may be postulated that the mean life span of a mouse population is an indication of the relationship between the population's inherited life potential or "adaptation energy" and the nonspecific intrinsic and extrinsic stress factors encountered during the life span. If, indeed, this broad generalization is blessed with an element of truth and a decrement in life span is inherited by the offspring of irradiated parents, it should be possible to demonstrate a similar decrement in the ability of such offspring to resist other stresses of a somewhat general or nonspecific nature. Among those "stressors" listed by Selye (2) as being somewhat general or nonspecific are trauma, hemorrhage, extremes of temperature, excessive muscular exercise, anoxia, and ionizing radiation.

The purpose of the present study was to determine whether unirradiated offspring from 10 generations of irradiated male mice showed a decrement in their ability to withstand protracted

Co^{60} gamma radiation used to similate a nonspecific chronic stress.

METHODS

Animals and Experimental Design

The mice used in this study originated from a single pair of the RFM strain, brother-sister mated for over 40 generations. Two males and 2 females (F_1) from a single litter of the parent generation were paired to begin the experimental and control lines. The male of the experimental line received 200 rads of whole body X irradiation at 28 days of age and at maturity mated to his unirradiated sister. The sires of each generation thereafter, through F_{10}, were given exactly the same exposure and subsequently sibmated also to their unexposed sisters. Progeny for continuing the irradiated line were sired as early as 25 days and as late as 120 days after exposure of the sire. The unirradiated control line was carried via sibmating in exactly the same manner and in the same environment as the experimental line. Irradiation of the experimental line was stopped after the F_{10} generation and F_{11} used to produce the observed population (F_{12}). Although not directly irradiated themselves, the observed animals were descendants of a germ line that had accumulated 2000 rads per sib pair (Fig. 1).

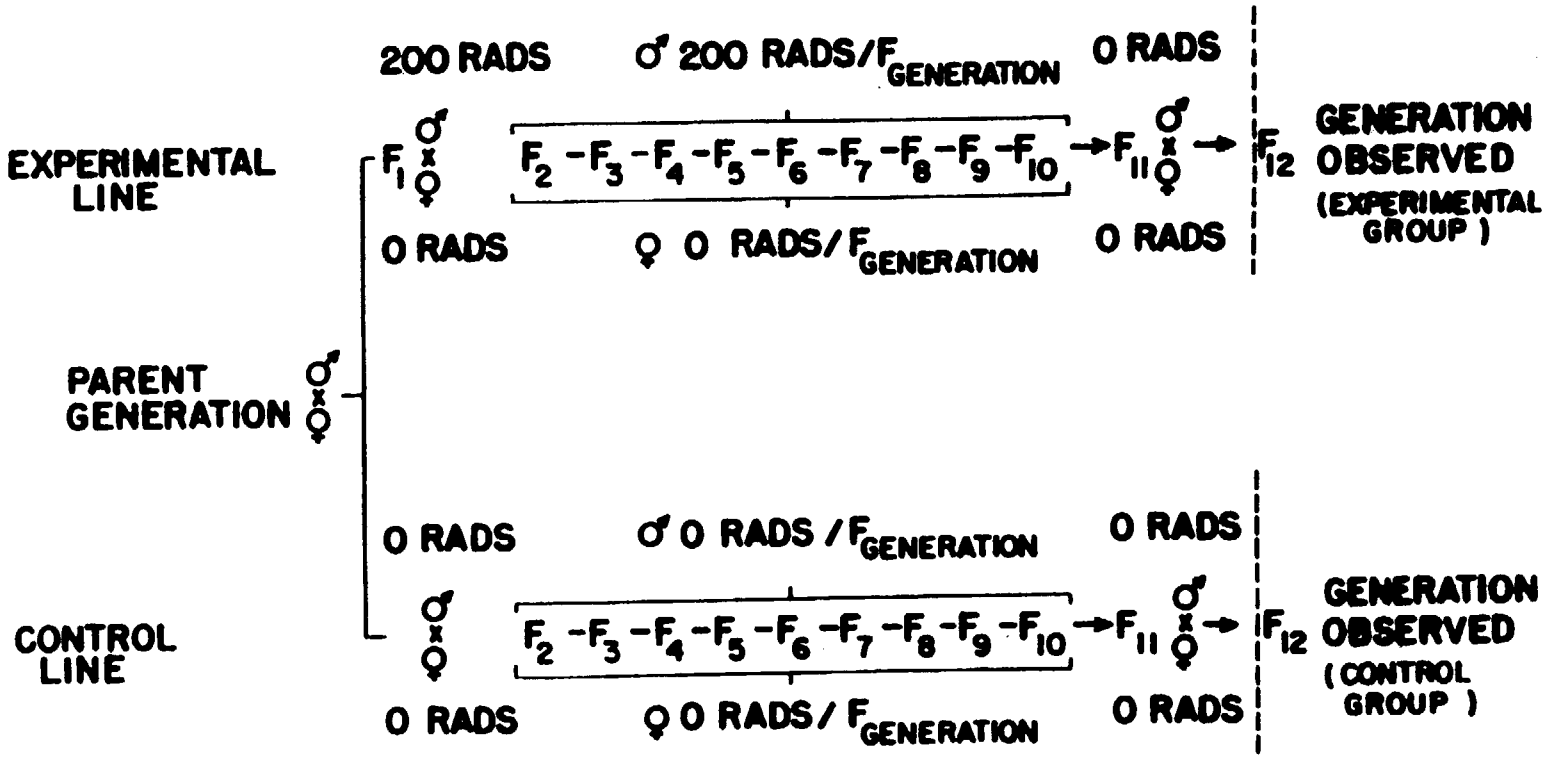

Fig. 1. Schematic design showing origin of experimental and control mice.

When 42 days of age, 85 mice (37 females and 48 males) from the F_{12} generation of the experimental line and 58 mice (23 females and 35 males) from the F_{12} generation of the control line were placed in a continuous Co^{60} gamma radiation field of 4.17 rads/hr, where they remained until death. The animals were exposed 24 hr/day (daily dose rate 100 rads) in Lucite cages with approximately 10 animals per cage. During exposure, they were allowed Purina laboratory chow and water ad libitum and given a supplement of oatmeal twice weekly. The gamma ray dose (up to the time of death) absorbed by each animal was recorded, the Mean Accumulated Dose (MAD) for each group determined, and the data subjected to an analysis of variance (3).

Radiation Exposures and Dosimetry

The sires of the experimental line were exposed to X rays from a Maxitron 250 with a beryllium window tube. Exposure conditions were as follows: voltage 250 KVP; filament current 30 ma; filtration Thoraeus II; HVL 2.6 mm Cu; target-to-specimen distance 60 cm; and dose rate 50 rads/min. The dose measurements were made with a Victoreen 100-r chamber at the midline of a Lucite mouse phantom. The chamber readings were corrected for barometric pressure and temperature and converted to tissue dose by the conversion factor 1 r = 0.96 rad.

RESULTS AND DISCUSSION

The Mean Accumulated Doses of protracted Co^{60} gamma irradiation sustained by males and females of the experimental and control lines are shown in Table 1. These data show that male and female descendants of a germ line that had accumulated genetically 2000 rads of X-ray exposure were able to sustain Mean Accumulated Doses of protracted gamma ray exposure that were respectively less by 908 and 1097 rads than those sustained by male and female controls.

Since there was no cage and sex interaction within either the control or experimental groups, the data from both sexes were pooled for analysis of variance. The results of the pooled analysis are tabulated in Table 2.* The F test showed that the Mean Accumulated Dose of the control line (3963 rads) was statistically greater than that of the experimental line (2994 rads) at the 0.01 level of significance. These results strongly suggest the presence of a genetic burden (nonspecific genetic damage) produced by an accumulation of recessive and/or sublethal mutants in the descendants of 10 generations of irradiated male mice. It may be presumptuous to interpret these data as conclusive; however, these

*The authors are grateful to W. L. LeStourgeon of Group T-1 of the Theoretical Division for analysis of the data.

TABLE 1. POOLED DATA: MEAN ACCUMULATED DOSE (TO DEATH) OF Co^{60} GAMMA RADIATION FOR CONTROL MICE AND MICE THAT WERE DESCENDANTS FROM 10 GENERATIONS OF IRRADIATED SIRES

Test \ Sex	Female	Male
Control	$\bar{X}_1^*$ = 3919	$\bar{X}_2^*$ = 3991
	SX = 90.1502 x 10^3	SX = 139.6856 x 10^3
	SX^2 = 402.42965 x 10^6	SX^2 = 598.63001 x 10^6
	n = 23	n = 35
Experimental	$\bar{X}_1^*$ = 2883	$\bar{X}_2^*$ = 3080
	SX = 106.6529 x 10^3	SX = 147.8570 x 10^3
	SX^2 = 326.76036 x 10^6	SX^2 = 475.70916 x 10^6
	n = 37	n = 48

*Mean Accumulated Dose in rads. SX = sum of X values; SX^2 = sum of squares of X values; n = number of mice.

TABLE 2. ANALYSIS OF VARIANCE OF POOLED DATA IN TABLE 1

Sources of Variation	Degrees of Freedom	Sum of Squares (10^6)	Mean Square (10^6)	F
Test	1	31.90687	31.90687	34.37*
Sex	1	0.77540	0.77540	< 1
Residual**	140	129.94439	0.92817	---

*$F_{0.01,1/140} \cong 6.83$.

**Residual includes interaction term, since value for F for interaction = 0.14.

preliminary observations appear worthy of further investigation. At present, this Laboratory is continuing these studies and extending them to include other forms of non-specific stress.

REFERENCES

(1) W. L. Russell, Proc. Nat. Acad. Sci. 43, 324 (1957).

(2) H. Selye, Stress: A Treatise Based on the Concepts of the General-Adaptation-Syndrome and the Diseases of Adaptation. Acta, Inc., Montreal, Canada (1950).

(3) G. W. Snedecor, Statistical Methods, The Iowa State College Press, Fourth Edition (1946), p. 284-293.

Protection of CFW Swiss Mice from Post Irradiation Transplantable AK Leukemia by Preirradiation Immunization (I. U. Boone, L. M. Conklin, and L. T. Rivera)

INTRODUCTION

CFW Swiss mice are normally resistant to transplantable AKR mouse leukemia but are made susceptible by whole body irradiation (1). Werder et al.(2) supplied indirect evidence that an immune response is involved in resistance to transplantable leukemia, since they were able to render X-irradiated and cortisone-treated mice resistant to Line I_b leukemia by previously immunizing the mice with leukemic cells. Preliminary experiments in this Laboratory have shown that C57Bl, Strong A, and CFW Swiss mice may be protected from post irradiation transplantable AK leukemia by preirradiation immunization with AK leukemic spleen homogenates. Whether this preirradiation immunization is a specific immunity to the leukemic cells or a nonspecific one with a general increase in circulating antibodies is unknown. A series of experiments has been designed to determine if the protection is due to a specific or nonspecific immunity.

METHODS

The CFW Swiss female mice used were ~16 weeks of age. One group of mice was immunized with leukemic AKR spleen

homogenate, while another group was immunized with normal AKR spleen homogenate. The immunization schedule consisted of 1 intraperitoneal injection of 5 to 10 x 10^6 spleen homogenate cells per week for 3 weeks. One week after the last injection, the animals were exposed to whole body acute radiation doses of 250 kv X rays ranging from 200 to 550 rads. Twenty-four hours after irradiation, the animals were challenged with AK leukemia. Control groups consisted of nonimmunized irradiated mice, some of which were and some of which were not challenged with leukemia.

RESULTS AND DISCUSSION

Table 1 indicates the various immunization and exposure groups and the number of animals per group. It also summarizes the lethality data at 12 and 30 days after irradiation. The nonimmunized irradiated group challenged with leukemia (Group III) had the highest percentage of deaths. Preirradiation immunization with AK leukemia protected the majority of mice from post irradiation transplantable leukemia. Immunization with nonleukemia spleens protected irradiated mice from transplantable leukemia at all dose levels except 550 rads. Since the AK leukemia which occurs spontaneously in AKR mice has been attributed to a virus (3), it is conceivable that the normal AKR spleens may possess a latent virus which may be responsible for the immunity seen here. Therefore, another study is in progress

TABLE 1. PROTECTION OF CFW SWISS MICE FROM POST IRRADIATION TRANSPLANTABLE AK LEUKEMIA BY PREIRRADIATION IMMUNIZATION

Experimental Conditions	Dose (rads)	Animals (No.)	12-Day Lethality (per cent)	30-Day Lethality (per cent)
Group I - Immunized with AK Leukemic Spleen, Irradiated, and Challenged with Leukemia				
	550	19	15.7	26.3
	500	20	0	0
	450	20	5.0	10.0
	400	20	0	0
	350	20	0	0
	300	19	0	0
	200	20	0	0
	Control	10	0	0
Group II - Immunized with Normal AK Spleen, Irradiated, and Challenged with Leukemia				
	550	19	68.4	79.0
	500	19	0	5.0
	450	20	0	0
	400	20	5.0	15.0
	350	20	5.0	5.0
	300	20	0	0
	200	20	0	0
	Control	10	0	0
Group III - Irradiated and Challenged with Leukemia				
	550	24	70.3	87.5
	500	19	84.2	89.5
	450	23	39.1	58.0
	400	19	21.0	26.3
	350	20	5.0	5.0
	300	20	0	5.0
	200	20	0	5.0
	Control	10	0	0
Group IV - Irradiated only				
	500	20	20.0	30.0
	450	20	0	5.0
	400	20	0	0

which includes, in addition to the groups as immunized in this study, groups of mice which are being nonspecifically immunized with spleens from an unrelated strain of mice (RF) and with killed Proteus vulgaris (OX-19) vaccine. This additional information should help clarify the degree of immunological specificity afforded by the AK leukemic spleen homogenates.

REFERENCES

(1) I. U. Boone, Rad. Res. 5, 450 (1956).

(2) A. A. Werder, J. Friedman, E. C. MacDowell, and J. T. Syverton, Cancer Res. 13, 158 (1953).

(3) L. Gross, Acta Haematologica, Separatum 13, 13 (1955).

Effect of Chronic Gamma Irradiation on Life Span of RF Mice

(I. U. Boone, L. T. Rivera, and T. T. Trujillo)

INTRODUCTION

Over the past few years, an effort has been made in this Laboratory to accumulate data on the delayed effects of irradiation in various strains of mice under various radiation conditions. This study reports life span data obtained from 2 separate groups of RF female mice exposed to chronic whole body gamma irradiation.

METHODS

Two different exposure conditions were used in this study, one involving fractionated acute doses and the other continuous low level exposure.

In the first experiment, 57 RF female mice (12 weeks of age) were exposed to 400 rads of Co^{60} gamma radiation at a dose rate of 13 rads/min. They were given 2 additional exposures of 200 rads each at ages 16 and 20 weeks, making a total exposure of 800 rads in 3 divided doses. Thirty-two animals from the same random population were kept as controls.

In the second experiment, RF female mice (16 weeks of age) were randomly divided into 3 exposure groups of approximately 100 animals each and 215 were retained as controls. The 3 experimental groups were exposed continuously (22 hr/day) to Co^{60}

gamma radiation at a dose rate of 70.5 rads/day until they had accumulated total doses of 494, 987, and 1480 rads. All animals were placed in holding cages, given Purina laboratory chow and water ad libitum, and followed for life span. Autopsies were performed at death and tissues taken for the determination of tumor incidence.

RESULTS AND DISCUSSION

The mean survival and life shortening data collected in both experiments are given in Table 1. An accumulated dose of 800 rads delivered in 3 acute divided doses had approximately the same life shortening effect as a total dose of 1480 rads delivered continuously at 70.5 rads/day. In the second experiment, a significant life shortening was produced at all dose levels. Further analyses of the data (now in progress) may indicate whether life shortening was linearly related to dose. Age-specific log rates of mortality will be calculated, and the incidence of tumors will be reported.

TABLE 1. MEAN LIFE SPAN AND LIFE SHORTENING OF RF MICE EXPOSED TO CHRONIC GAMMA IRRADIATION

Exposure Conditions	Total Dose (rads)	Animals (No.)	Mean Life Span (days)	Life Shortening (per cent)	p-Values*
Acute Divided Doses					
	800	57	466	31.3	<0.01
	Control	32	679	--	--
Continuous Low Level Exposure					
	494	93	513	15.6	<0.01
	987	82	443	27.1	<0.01
	1480	86	395	35.0	<0.01
	Control	215	608	--	--

*p-Values ≤ 0.05, as determined by "t" testing, were considered to indicate a significant difference from the control animals.

Effect of Single Doses of Whole Body X Irradiation on the Life Span and Tumor Incidence of C57Black Mice (I. U. Boone, L. M. Conklin, and L. T. Rivera)

INTRODUCTION

In previous semiannual reports (1,2) data on the delayed effects of single sublethal doses of whole body irradiation have been reported for CF_1 and CFW Swiss mice. This report deals with similar effects on C57Black mice. The mean survival data, per cent life shortening, and tumor incidence (particularly leukemia) will be reported.

METHODS

Prior to radiation exposure, a population of C57Black female mice (approximately 12 weeks of age) was randomized, divided into 4 groups of 100 animals each, and earmarked for group identification. The groups were given acute whole body exposure doses of 0, 100, 200, and 400 rads delivered by a 250 KVP Maxitron X-ray machine. The air dose rate was 52 r/min with a tissue dose rate of about 50 rads/min. After irradiation, the mice were again rerandomized, housed 10 animals per cage, and observed throughout their life span. Approximately 40 per cent of the animals were autopsied at death, and tissue samples were taken for histological observation.

RESULTS AND DISCUSSION

The mean survival time and per cent life shortening as compared to nonirradiated control animals are summarized in Table 1. The 24 per cent life shortening in C57Black mice following 400 rads of single whole body exposure was intermediate between that obtained for CF_1 and CFW Swiss female mice, for which the life shortening effect was 30 to 40 and 14 per cent, respectively (1,3,4).

There was a surprising lack of tumors in this strain of mouse. No lung tumors were seen in either irradiated or control animals, and only a few ovarian tumors were observed. The majority of deaths appeared to be due to pneumonia. Single whole body exposures produced some increase in the leukemia incidence as indicated in Table 2. This incidence was lower than that reported with fractionated exposures (5) in this strain of mouse.

Age-specific log rates of mortality (Gompertz function) will be calculated for all groups of animals.

TABLE 1. MEAN SURVIVAL TIME AND LIFE SHORTENING OF WHOLE BODY X IRRADIATED C57BLACK FEMALE MICE

Dose (rads)	Animals[a] (No.)	Mean Life Span[b] (days)	Life Shortening (per cent)	p-Values[c]
100	98	614	5.5	0.1
200	96	572	11.9	< 0.01
400	102	493	24.3	< 0.01
Controls	90	649	--	--

[a]Mice that died in the first 30 days after exposure were not included in the data.

[b]The standard error from the mean ranged from ± 15 to ± 19.

[c]p-Values ≤ 0.05, as determined by "t" testing, were considered to indicate a significant difference from the control animals.

TABLE 2. LEUKEMIA AND LYMPHOMA INCIDENCE IN WHOLE BODY X IRRADIATED C57BLACK FEMALE MICE

Dose (rads)	Animals (No.)	Leukemia and Lymphoma (per cent)
100	42	19.1
200	40	22.5
400	42	31.0
Control	39	15.4

REFERENCES

(1) I. U. Boone, G. Trafton, L. Conklin, and D. C. White, Los Alamos Scientific Laboratory Report LAMS-2445 (1960), p. 265.

(2) I. U. Boone, G. Trafton, and L. Conklin, Los Alamos Scientific Laboratory Report LAMS-2455 (1960), p. 163.

(3) I. U. Boone, Rad. Res. 11, 434 (1959).

(4) I. U. Boone, Rad. Res. 11, 424 (1959).

(5) H. Kaplan, J. Nat. Cancer Inst. 8, 191 (1948).

Correlation of Viability Plate Counts and Optical Density Measurements with Bacterial (Hemophilus) Cell Counts Using the Coulter Counter (I. U. Boone, L. T. Rivera, and C. C. Lushbaugh)

INTRODUCTION

This experiment was designed to determine the feasibility of counting Hemophilus influenzae organisms with the Coulter counter in order to facilitate certain procedures to be used in genetic transformation studies. A preliminary attempt has been made to correlate Coulter counter bacterial counts with the plate dilution method and optical density measurements during the growth of competent cells.

METHODS

Fifty ml of Elev broth (1 part Eugon and 1 part Levinthal broth), to which diphosphopyridine nucleotide (DPN) had been added, was inoculated with Hemophilus influenzae (Rd) to give a final cell concentration of 1×10^7 cells/ml of medium. The cell mixture was shaken continuously during growth at 37°C. Since the cell generation time is ~ 20 to 30 minutes during the logarithmic growth phase, the optical density, viability cell plate counts, and Coulter counter cell counts were measured every 30 minutes.

The viability counts were made by the standard dilution

method. Optical density measurements were made aseptically using the Model 14 Coleman spectrophotometer. Coulter counter cell counts were made with both the 50 and 100 μ orifice tubes. Cells were diluted in Eugon broth for the plate counts and in saline for the Coulter counter determinations. The 100 μ orifice was calibrated with puff balls (spores of 2 μ size). The machine aperture was on setting 8 with a threshold of 2.

RESULTS AND DISCUSSION

A summary of the type of results obtained is shown in Table 1. The Coulter counter results are given for the counts obtained only with the 100 μ orifice tube. The 50 μ orifice tube gave results which were not reproducible due to electronic noise level interference. Although the results obtained with the 100 μ orifice tube were in the proper orders of magnitude as the viability measurements, accuracy was lacking. The Coulter counter also counts dead cells as well as viable cells, which may account for the higher values near the end of the logarithmic growth phase.

Accuracy of the bacterial counts by the Coulter counter method could probably be improved by using a small orifice tube, filtering the saline used for dilutions through a fine sintered glass filter to decrease the background "debris," and calibrating the counter using polystyrene balls that have a maximum diameter of 1.17 μ which is more nearly the size of H. influenzae.

TABLE 1. OPTICAL DENSITY, VIABILITY PLATE COUNTS, AND COULTER COUNTER CELL MEASUREMENTS OF HEMOPHILUS INFLUENZAE DURING THE LOGARITHMIC GROWTH PHASE

Time after Inoculation (hours)	Plate Count (cells/ml)	Optical Density	Coulter Counter Cell Count (cells/ml)
0	6×10^6	0.005	1.0×10^7
1.0	1.9×10^7	0.01	2.6×10^7
1.5	5.0×10^7	0.01	2.5×10^7
2.0	6.0×10^7	0.014	2.8×10^7
2.5	1.4×10^8	0.026	7.1×10^8
3.0	3.2×10^8	0.055	1.2×10^9
3.5	4.0×10^8	0.089	---
3.7	7.7×10^8	0.109	1.4×10^9

Bacterial spores and larger virus particles have been counted and measured successfully using the Coulter counter (1). It is felt that perfecting the Coulter counting techniques in bacterial cell counting will facilitate and replace some of the tedious methods of cell counting involved in bacterial transformation studies.

REFERENCE

(1) H. E. Kubitschek, Research 13, 128 (1960).

Metabolism of Tritium-Labeled Pyridoxine in Rats (I. U. Boone, S. Cox, and A. Murray III)

INTRODUCTION

In vitro and in vivo studies (1-3) have indicated a possible antimetabolic relationship between isoniazid and pyridoxine (Vitamin B_6). Some of the principal side effects of isoniazid have been prevented by simultaneous administration of pyridoxine (2). The metabolism of C^{14}-isoniazid in tubercular and nontubercular patients was the subject of a previous study (4). No significant change in the pattern of urinary metabolites could be induced by the oral administration of nonlabeled pyridoxine. The possibility of using the alternate approach and of studying the influence of nonlabeled isoniazid on the metabolism of labeled pyridoxine is immediately apparent.

Technical difficulties have prevented labeling of pyridoxine with C^{14}, but recent techniques with tritium, using the exchange method over platinum catalyst, have provided pyridoxine labeled with tritium. A preliminary study of the blood turnover times and urinary excretion of H^3-pyridoxine in rats was undertaken to explore the feasibility of using it in more specific metabolic investigations.

METHODS AND RESULTS

The specific activity of the H^3-pyridoxine hydrochloride (H^3-B_6) was 308 μc/mg. The solution used for injection contained 2 mg (616 μc) of H^3-B_6 and 18 mg of unlabeled pyridoxine hydrochloride per ml. All injections were intravenous via the jugular sinus route. The rats weighed between 250 and 350 g. Rat A received 184.8 μc H^3-B_6. Rats B and C received 369.6 μc, while rats D to G received 616 μc H^3-B_6. Following injection of the drug, the rats were placed individually in standard metabolic cages. Rats A to C had blood and urine samples taken at various time intervals post injection. Urine samples were collected from rats D to G for detailed urinary excretion and chromatographic studies.

Blood and urine specimens were measured for tritium using the liquid scintillation-dioxane system as described previously in this Laboratory by Richmond et al. (5) and by Trujillo (6). Concentrations of H^3 activity in blood as a function of time after administration of labeled pyridoxine are shown in Fig. 1. The log of the per cent injected dose is plotted against time in hours. Excluding the early component of the blood clearance curve (i.e., the first 15 minutes after injection), the turnover half-time of the activity in the blood was approximately 45 minutes during the first 3 hours after drug injection. Activity in the red blood cells was less than 1 per cent of the total activity in the blood.

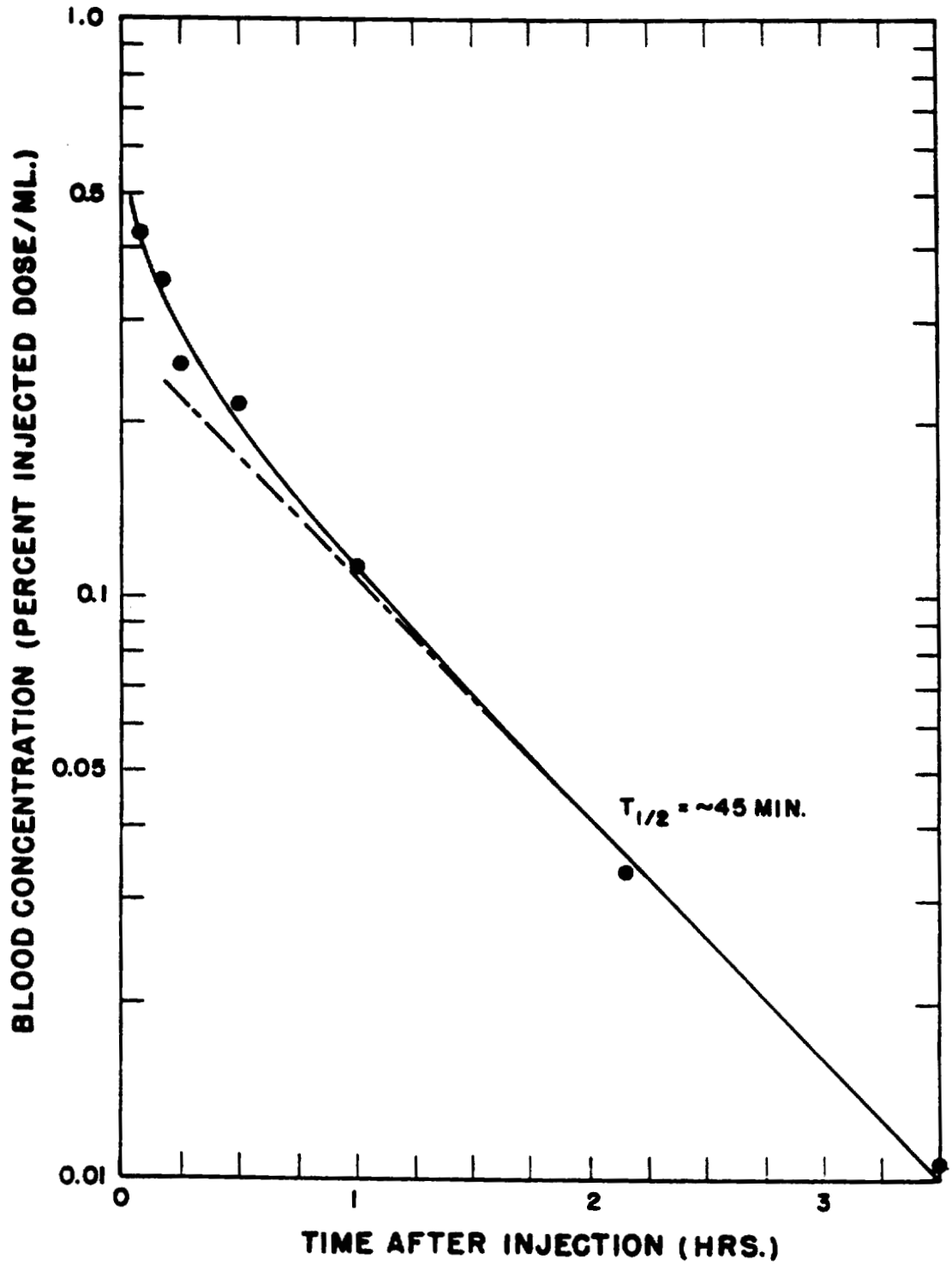

Fig. 1. Tritium activity in blood following intravenous administration of H^3-pyridoxine hydrochloride in rats.

The data in Table 1 show the accumulated urinary excretion of 4 rats. Seventy-five to 80 per cent of the activity was excreted in the first 24 hours. Figure 2 shows the average retention of pyridoxine as a function of time after injection, assuming excretion was essentially all via the urine. The retention curve was fit by the following 2 component rate equation:

$$R_t = 28.2\ e^{-0.0017\ t} + 71.8\ e^{-0.876\ t}$$

in which R_t is retention in per cent of injected dose, and t is time after injection in hours. Approximately 28 per cent was retained with a half-time of 17 days and 72 per cent with a half-time of only 47 minutes, corresponding to the blood clearance half-time of 45 minutes shown in Fig. 1.

All urine specimens obtained up to 5-1/2 hours after injection were chromatographed. One-tenth ml of urine was placed directly on No. 1 Whatman filter paper strips. In all instances. this was at least 5×10^6 d/m of H^3 activity. Eighty per cent propanol was the solvent system used. It was necessary to expose the chromatogram strips to X-ray film for ~ 4 weeks to get satisfactory exposure of the film. One predominant band with R_f value of 0.65 ± 0.03 was always present. This R_f value corresponded to that of unchanged pyridoxine. These results are in agreement with an earlier study (7) in which it was

TABLE 1. CUMULATIVE URINARY EXCRETION OF TRITIUM ACTIVITY FOLLOWING INTRAVENOUS ADMINISTRATION OF H^3-PYRIDOXINE HCl IN RATS

Time after Injection (hours)	Rat Number and Cumulative Excretion (per cent)				
	D	E	F	G	Average
1.5	64.3	54.5	58.0	57.2	58.5
2.5	69.3	62.4	65.1	62.3	64.8
3.5	--	68.1	--	67.5	67.8
4.5	--	--	68.4	--	--
5.5	71.9	--	--	--	--
12	73.3	73.5	69.7	69.1	71.4
24	75.6	75.7	71.5	70.5	73.3
31	76.3	76.2	71.7	70.8	73.7
96	79.8	78.1	78.3	73.8	77.5
122	80.2	78.1	78.4	73.9	77.7
144	80.4	78.2	78.4	75.0	78.0

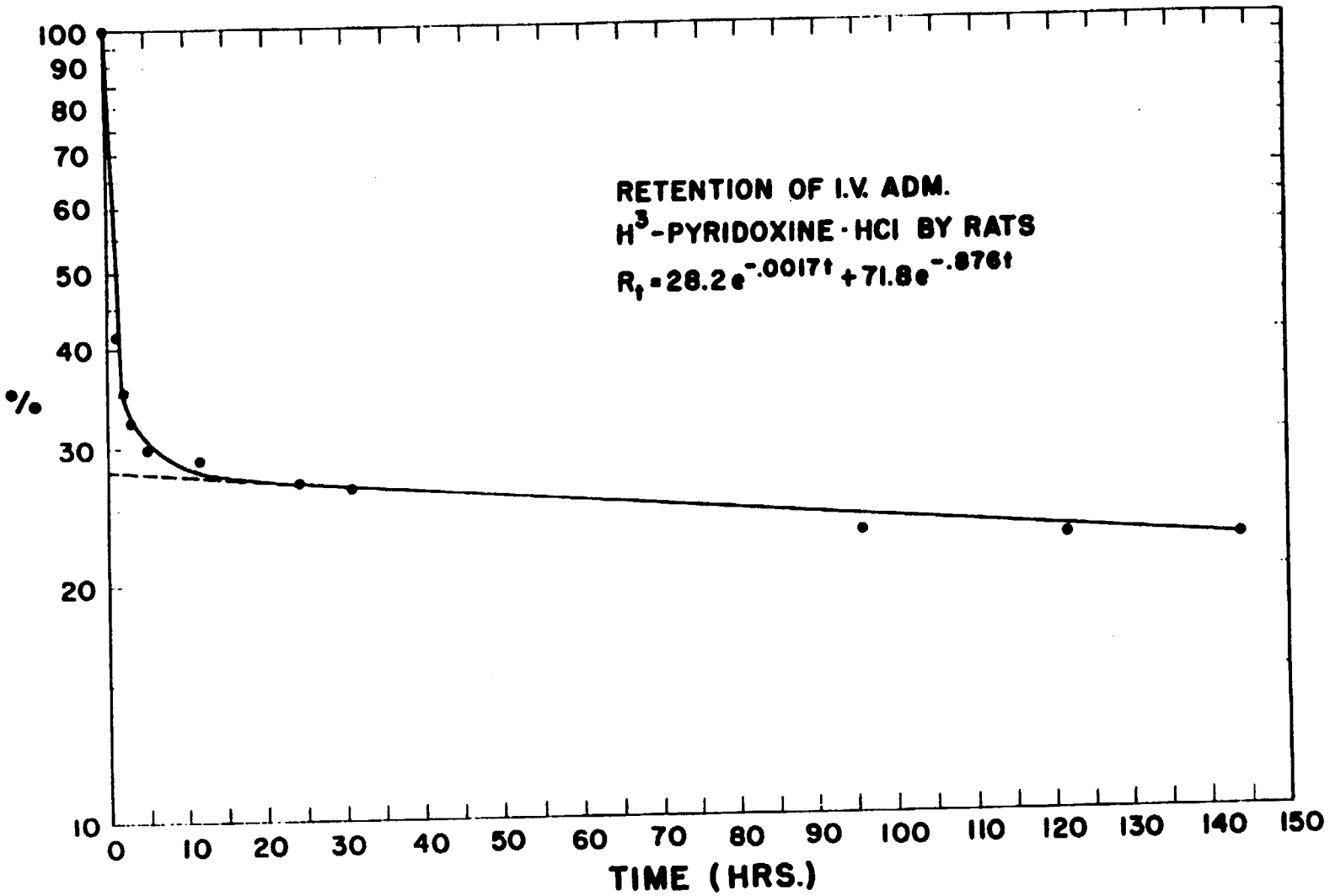

Fig. 2. Retention of intravenously administered H^3-pyridoxine HCl by rats.

reported that 50 to 70 per cent of pyridoxine was excreted unchanged by rats.

A very faint trace of 1 other band was present on all strips. The R_f value of this unidentified band was 0.53 ± 0.03. The only degradation product of Vitamin B_6 so far found in animals is 4-pyridoxic acid. This band may represent this product.

Although the use of H^3-B_6 may be applicable to more detailed studies of the metabolism of Vitamin B_6 in the rat, some of the technical problems encountered may limit its use in human subjects. No further studies are planned at this time.

REFERENCES

(1) H. Pope, Am. Rev. Tuberc. 68, 938 (1953).

(2) J. P. Biehl and R. W. Vilter, J. A. M. A. 156, 1549 (1954).

(3) I. U. Boone, D. F. Turney, and W. H. Langham, J. Lab. Clin. Med. 46, 549 (1955).

(4) I. U. Boone, A. Murray, and R. Des Prez, Los Alamos Scientific Laboratory Report LA-2420 (1960).

(5) C. R. Richmond, T. T. Trujillo, and D. W. Martin, Proc. Soc. Exptl. Biol. Med. 104, 9 (1960).

(6) T. T. Trujillo, Personal communication.

(7) E. E. Snell, Proc. of the 4th International Congress of Biochemistry XI, 250 (1958).

Establishment and Maintenance of Cells Grown in Agitated Fluid Medium (P. C. Sanders and D. C. White)

INTRODUCTION

In anticipation of increased emphasis on cellular radiobiology, a method whereby cells can be grown in large volumes of agitated culture media is being studied in considerable detail. The advantages of such a method involve the large number of cells that can be produced and the possibility of replicate sampling without the necessity of terminating the culture. A modified technique involving a combination of several methods (1,2) has been tried and found to give promising results.

METHODS AND MATERIALS

HeLa cells that have been grown attached to glass in T-60 flasks for approximately 1 year were used to initiate the spinner culture technique. To start the spinner culture, several T-60's were observed using an inverted phase-contrast microscope to ascertain which flasks contained healthy cultures in an active mitotic state. Those chosen were treated in the following manner: media were removed by aspirations, 3 ml of 0.035 per cent trypsin was added to each flask and these incubated at 37°C until the cells were freed from the glass surface. The action of the trypsin was stopped by the

addition of 5 ml of Eagle's basic medium containing 10 per cent inactivated horse serum, 0.25 μg/ml penicillin, and 0.25 μg/ml of streptomycin. The contents of the flasks were combined by pipetting the cell clumps broken up. An aliquot was taken at this point for determination of total cell population. A 1 ml aliquot was diluted 1:50 and the total cell count determined by using a Coulter cell counter. The cell suspension was diluted and a total of 3.5×10^4 cells/ml added to spinner flasks containing Eagle's culture medium plus 10 per cent horse serum and antibiotics. Each spinner flask contained a final volume of 300 ml of cell suspension. The flasks were placed on magnetic stirrers with sufficient agitation to create a small vortex in the liquid. Each flask was gassed for 5 minutes with 5 per cent CO_2 in air, sealed with silicone stoppers, and the entire stirrer apparatus placed in an incubator set at 37°C.

Aliquots were taken daily for total cell population determinations and cell viability tests. Total cell populations were determined as described above. Cell viability tests were performed by the method of McLimans et al. (1) using 0.5 per cent trypan blue water solution.

Media were routinely changed 48 hours after the original inoculation and every 4 to 5 days thereafter, as indicated by pH changes, total cell population numbers, or viability determinations. New spinners were started by removing an

aliquot from the stock spinners and adding it to fresh medium.

Media changes were made by placing a sterile cotton-plugged airway stopper in one side-arm and attaching the transfer apparatus to the other side-arm, the transfer apparatus being connected to a vacuum line and a 200 ml centrifuge bottle. The cell suspension was removed by gentle vacuum, the bottles capped with sterile aluminum foil, and centrifuged at 1000 RPM for 10 minutes. The old medium was removed by aspiration, being careful not to disturb the cells, and 20 ml of fresh medium was added to each bottle. The cell suspension was pipetted several times to assure a homogenous mixture and transferred by pipette to a spinner flask containing 260 ml of new medium. The cell suspension was gassed as described above and placed in an incubator.

DISCUSSION

The above method of establishing and maintaining stock cultures of cells growing in agitated fluid medium has been in use in this Laboratory during the past year and is proving to be most satisfactory. As a method of maintaining cells for experimental use, it is superior to glass-grown cells for several reasons. One of these is the ease of

replicate sampling from the same cell population without the necessity of resorting to chemical or mechanical means of freeing the cells from glass, thereby destroying the complete cell culture. Another advantage is the fact that each cell is separate and completely surrounded by medium; thus these cells are less susceptible to local concentrations of metabolites which limit growth in glass-grown cultures. Experiments are underway to determine the maximum and minimum number of cells and other important conditions necessary to initiate a healthy, actively growing culture.

REFERENCES

(1) W. F. McLimans, E. V. Davis, F. L. Glover, and G. W. Rake, J. Immunol. 79, 428 (1957).

(2) R. Wallace, A. Cox, and H. R. Cox, Proc. Soc. Exptl. Biol. Med. 101, 553 (1959).

Determination of the Hydrolysis Rate of Hafnium Tritide

(T. T. Trujillo and W. H. Langham)

INTRODUCTION

The potential hazards of handling tritium in the form of gas and water have been investigated in considerable detail. Relatively insoluble solid compounds of tritium have not been investigated at all. Such compounds would offer two obvious potential hazards: irradiation of the respiratory system (including pulmonary lymph nodes) by inhaled dust, and irradiation of the total body by tritium water produced from hydrolysis. Diagnosis of exposure via the convenient measurement of urinary tritium activity may be possible for readily hydrolyzed compounds.

Hafnium tritide was selected because it offers a relatively high concentration of tritium in a relatively refractory material.

METHODS AND RESULTS

A minute amount (1 to 2 mg) of HfT_2 was supplied by the Health Physics Group. The weight and tritium activity it represented were unknown; therefore, it could not be manipulated in a quantitative manner in the absolute sense. Consequently, the specimen as supplied was placed without

weighing or any previous measurement of specific activity into 2 ml of physiological saline and incubated at 37°C. One hundred lambda (0.1 ml) aliquots of the saline solution were withdrawn at 1, 5-1/2, 8, 24, 72, and 144 hours and these diluted to 10 ml with distilled water. A 0.5 ml aliquot of the diluted sample was vacuum distilled at room temperature and counted for tritium activity in the liquid scintillation counter. Since the sample was distilled prior to counting, any activity observed could be assumed to be due to tritium water formed by hydrolysis of the HfT_2 at body temperature. The counts observed were corrected for counting efficiency and background and converted to total microcuries of tritium activity per 2 ml of the original saline solution. Data showing the relative rate of hydrolysis are given in Table 1 and are shown graphically in Fig. 1.

TABLE 1. RATE OF HYDROLYSIS OF HfT_2 IN NORMAL SALINE AT 37°C

Sample No.	Time (hours)	Tritium Activity as HTO (μc/2 ml)
1	1	0.522
2	5-1/2	1.154
3	8	1.266
4	24	2.100
5	48	3.200
6	72	4.540
7	144	7.450

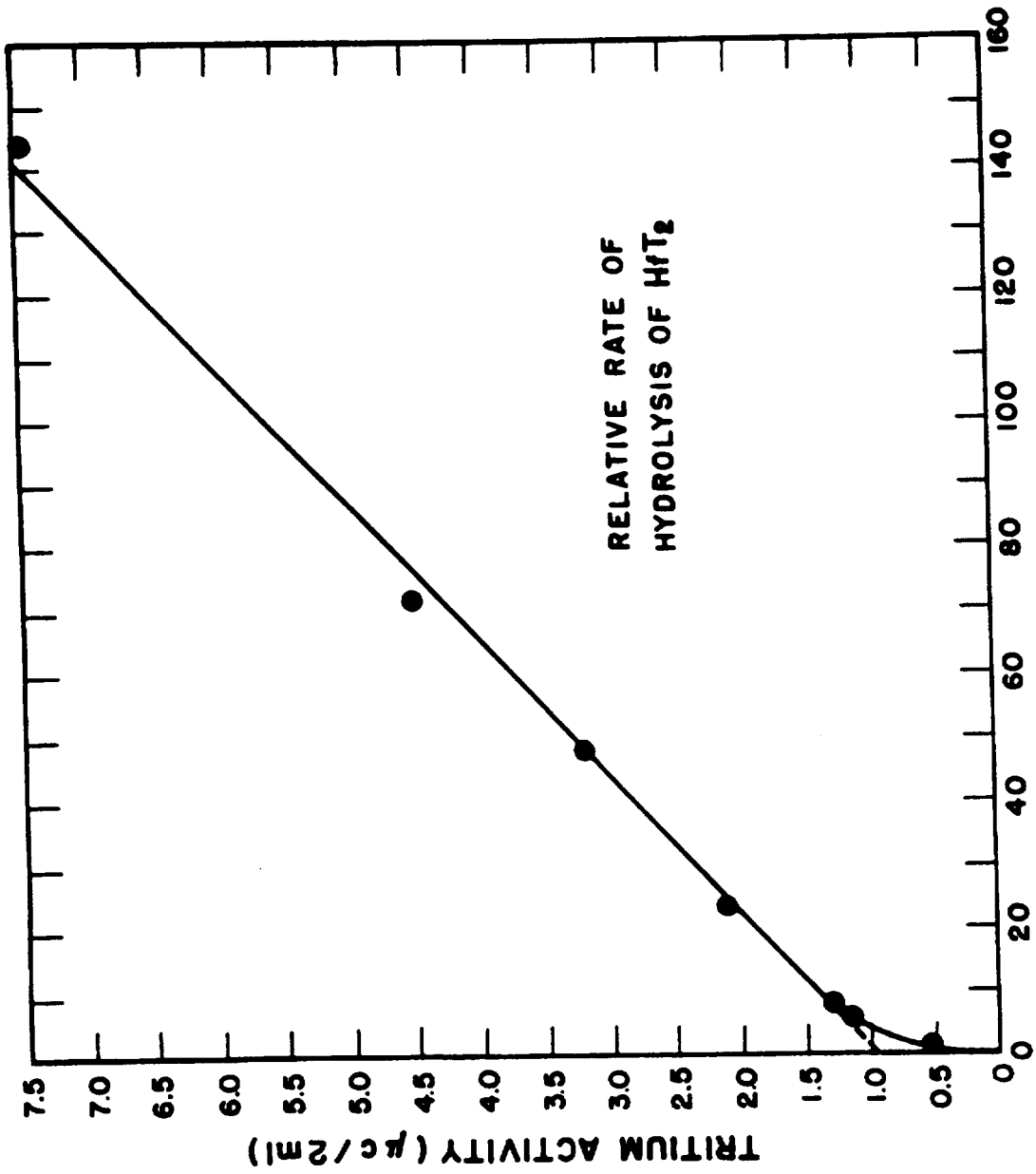

Fig. 1. Relative rate of hydrolysis of HfT_2.

Since the original specific activity and the quantity of material placed in the 2 ml of saline were not known, the absolute rate of hydrolysis could not be determined and the values are relative only. Qualitatively, however, it is apparent that the rate is slow. Even after 6 days, only 7.45 μc of tritium had been converted to tritium water, which undoubtedly represented a very small fraction of the tritium activity present in the original sample. As shown in Fig. 1, hydrolysis appeared to be linear with time. Failure of the extrapolated line to pass through the origin can be explained by atmospheric hydrolysis of the sample prior to being placed in the saline or by the presence of adsorbed tritium water formed during production of the HfT_2.

Influence of Extraterrestrial Gravitational Fields upon Plant Growth (E. R. Ballinger and E. F. Montoya)

INTRODUCTION

To the extent that we have been involved with biological problems of man in space, certain highly interesting but non-radiobiological considerations have received casual attention from time to time by members of this Group. One of these considerations, which received attention during the past reporting period, involved the question of edible plant growth to support man's existence under such gravitational fields as would be encountered in space and on planets other than the planet earth.

It is a matter of experience that the shoot of a seedling grows all over the world in an outward direction from the earth and that the root grows downward in a direction toward the earth's center. Until Knight's experiments in 1806 (1), light, heat, moisture, gravity, and mechanical influences were both individually and jointly assumed responsible for this observation of positive and negative geotropism. By growing plants on a rotating wheel with a horizontal axis, Knight excluded the one-sided action of gravity and replaced it by a centrifugal field. The resultant force, which the plant was unable to distinguish from gravitational, caused the root system to grow radially away from and the shoots radially toward the center of the wheel.

In 1874 Sachs (2), using a slowly rotating horizontal axis wheel, eliminated the one-sided action of gravity without imparting a significant centrifugal force. The result was that the roots and shoots were indifferent to orientation and grew in whatever direction they had at the beginning of the experiment. Thus we can say that plants exhibit directional dependence in a gravitational field and are unable to distinguish between gravitational and centrifugal forces in this regard. Carrying this conclusion one step further, one might question whether the influence of gravitation extends not only to plant stem orientation but also to stem development or strength exhibited perhaps as a change in diameter, stem length, or growing or maturation time.

If such an influence existed, one might anticipate certain difficulties to be experienced in attempting to grow certain vegetables or plants in gravitational fields significantly different from that of the earth. On the other hand, should stem growth be independent of gravity, it is possible that certain relatively heavy or long-stemmed or climbing plants might not be the best candidates for growth, whether the technique be hydroponic or otherwise on planets with gravitational fields in excess of that on earth.

Sachs (3), the famous German botanist, in the latter part of the 19th century postulated a theory of organ-forming

substances whose specific action and localized distribution were affected by gravity. Present day observers have given the name of phytohormones to these organ-forming substances and have isolated several causing extension of cellular growth and inhibition of budding and maturation. Plant hormones of this type are called auxins and are believed to be chemically related to beta-indoleacetic acid. Auxin precursor is, according to Audus (4), formed in the root and through gravitational influences passes upward to the apical tip of the plant, where in the presence of sunlight auxin is formed. Auxin, apparently being a heavier material than its precursor, descends the stem causing cellular extension and inhibition of budding and maturation. In a similar manner at a later time in the growth of the plant, an anti-auxin precursor formed by the roots travels to the apical tip and in the presence of light becomes an auxin-destroying substance, which also under the influence of gravity passes downward in the stem. Fisher (5), by weighting the apical tip of soybean plants, was able to cause apparent pooling of auxin in the dependent portion with early flowering at the basal nodes. However, because a casual review of botanical literature available to this Laboratory failed to turn up any positive answer to the question of gravitational relation to stem development, a 3 foot diameter centrifuge (Fig. 1) was designed and assembled to operate in such a manner that plant

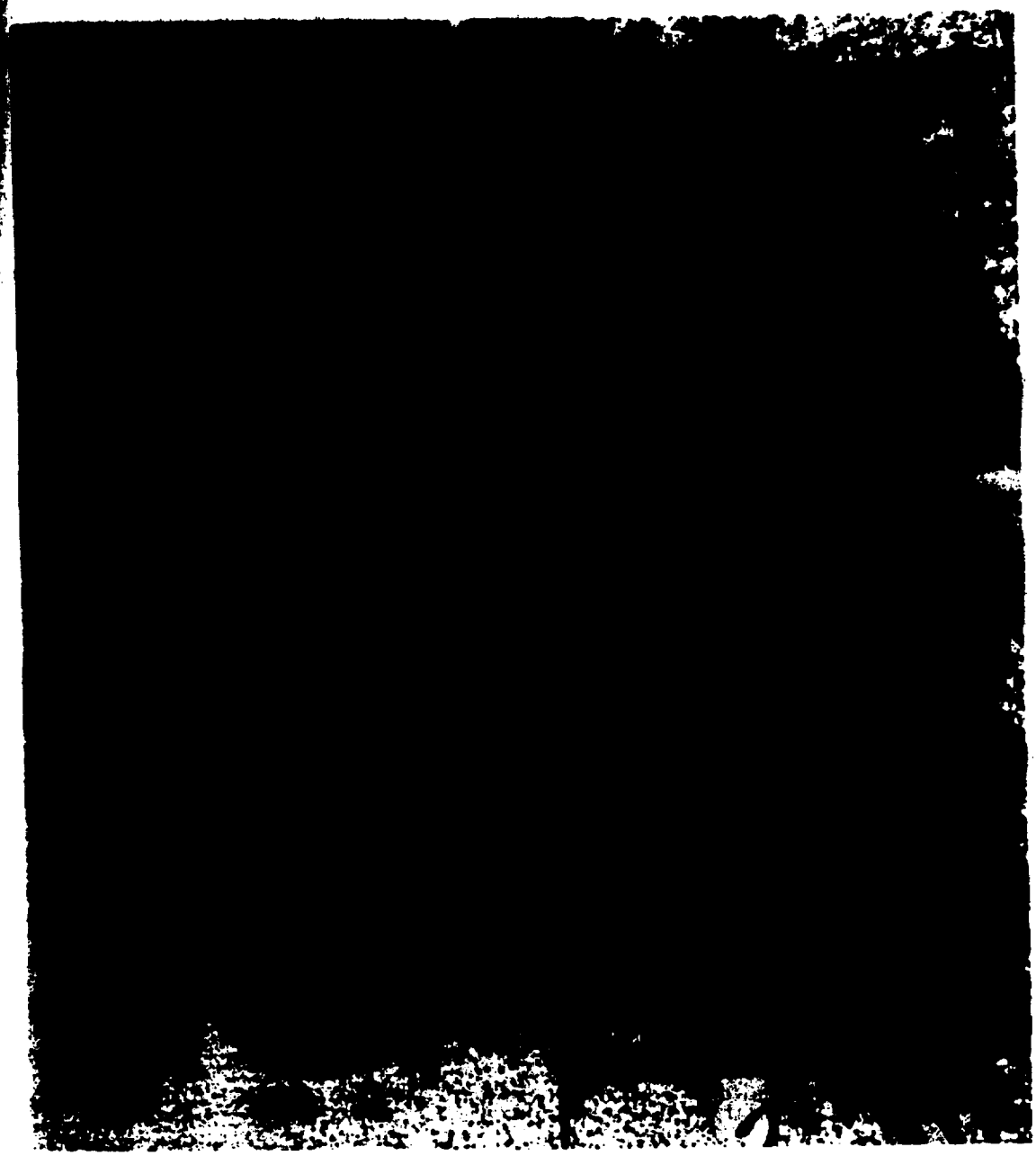

Fig. 1. Plant centrifuge.

growth at 2, 4, and 6 G could be observed photographically or under a strobe light geared to the wheel revolutions during continuous rotation.

METHODS AND MATERIALS

The centrifuge frame was constructed of angle iron as shown in Fig. 1. A 1/12 hp electric motor, through appropriate pulley belt reduction, turned the 3 foot diameter Plexiglas wheel at ~ 115 RPM. The wheel containing an inner, a middle, and an outer ring with Plexiglas dividers was filled to ~ 3 in. with a mixture of sand, loam, and plant nutrient. The inner, middle, and outer rings were located so that the seeds or bulbs in each ring would be exposed to 2, 4, and 6 centrifugal "G," respectively. The tangential effect of the 1 G earth gravity was not taken into account in the calculations of the desired ring diameter due to the relatively crude initial assembly and the rough approximation of the radii of the seed-to-wheel center measurement after packing and shifting of the dirt had taken place during the first few days of rotation.

The top of the Plexiglas drum or wheel was centrally supported and held in place by peripheral pins into the ribs of the outer ring. Water and nutrient were supplied to each ring by means of 3 flexible perforated tubes passing around

the rings to the center pole and upward through the top, ending in glass funnels which could be filled during rotation. Seeds of corn and marigold and bulbs of onion and gladiolus were planted in each ring, covered with ~1 in. of dirt, watered, and allowed to stand overnight before beginning rotation.

RESULTS AND CONCLUSIONS

Results were many and largely unexpected and unrelated to the purpose of the experiment. Water leakage between the inner and middle ring divider caused pooling in the outer ring and rotting of the seeds and bulbs placed in this ring. The "hot house" effect created moisture to collect on the otherwise transparent Plexiglas top, thus effectively precluding photographic observations except at night, when clearing occurred. Because of the short summer season, runs were concluded in the early fall with only meager but possibly pilotage observations made on one 3-week growth of corn.

Observation of corn grown for a period of ~3 weeks at 2, 4, and 6 G revealed no macroscopic morphologic difference in stem diameter, stalk length, strength, or growing time as a function of centrifugal gravity. All plants, with the exception of a few flattened out corn stems in the 6 G ring, were growing toward the center of the wheel in a tangential manner

as one would expect as a result of the 90° angle between the 1 G earth gravity and the 2, 4, and 6 G centrifugally obtained (Fig. 2).

The authors feel this experiment should be refined and repeated by a competent research organization using a larger centrifuge so that the variation in gravity field versus radii will permit long-stemmed plants to remain for more of their length in a reasonably high gravity field. Although gravity fields as high as 6 G would probably pose more serious problems than that of plant growth, it was felt that any change observed between 6 and 4 or 2 G, for instance, might indicate the possible manner or direction of change to be expected under fields of less than 1 G, which are not readily obtained by such simple techniques as a centrifuge.

REFERENCES

(1) Ostwald's Klassiker, Vol. 62 (1806).

(2) Maximov's Textbook of Plant Physiology (1930).

(3) E. Strasburger, Textbook of Botany (1930).

(4) L. J. Audus, Plant Growth Substances (1953).

(5) J. E. Fisher, Science 125, 396 (1957).

Fig. 2. Corn growth at 6 centrifugal "G."

Silver Phosphate and Cobalt Glass Systems for Gamma Dosimetry in Mixed Radiation Fields

(E. R. Ballinger, D. G. Ott, and J. W. Enders)

INTRODUCTION

Four major problems are inherent in gamma ray dosimetry in a mixed radiation field of unknown energy and spectra. These problems are enumerated below and have been considered criteria to be satisfied in the design and development of an adequate gamma dosimetry system for measurements at Kiwi nuclear reactor field tests.

1. The effect of neutrons upon a gamma dosimeter. Most gamma dosimeters respond in some degree to neutrons and hence require either that the degree of response and neutron flux and spectra be known, or that the dosimeter be shielded in some manner from effective neutrons.

2. The effect of the dosimeter upon the sample. Where the size of the dosimeter is large in terms of the sample, the two cannot be simultaneously exposed at the same position.

3. The effect of the container upon the dosimeter. If the dosimeter need be contained for neutron shielding or other purposes, the container may contribute to or detract from the gamma flux as seen by the contained dosimeter.

4. The effect of one dosimeter upon another. Where depth dose studies are attempted or in other exposure situations

where several dosimeters are placed in close proximity, the mass and composition of one may significantly alter the flux to which another is exposed.

In the past reporting period, this group has completed the design, development, and testing of a gamma dosimetry system covering the range from 10 to 10^7 rads in gamma-neutron fields of unknown energy and spectra. In most respects, this system represents a significant improvement in each of the previously listed criteria over other systems used by this group in the past.

MATERIALS AND METHODS

The components making up the gamma dosimetry system are as follows:

1. Bausch and Lomb $AgPO_3$ glass rods measuring 1 mm in diameter by 6 mm in length (Fig. 1).

2. Bausch and Lomb microphotofluorometer, as modified by this group (Fig. 2).

3. Cobalt glass plates as supplied by Bausch and Lomb, reduced in size to 1 x 4 x 6 mm (Fig. 1).

4. LASL Model II chemical dosimeter reader, modified (Fig. 3).

5. LASL Li^6 lead cylindrical dosimeter container, measuring 8 mm in diameter by 11 mm in height (Fig. 1).

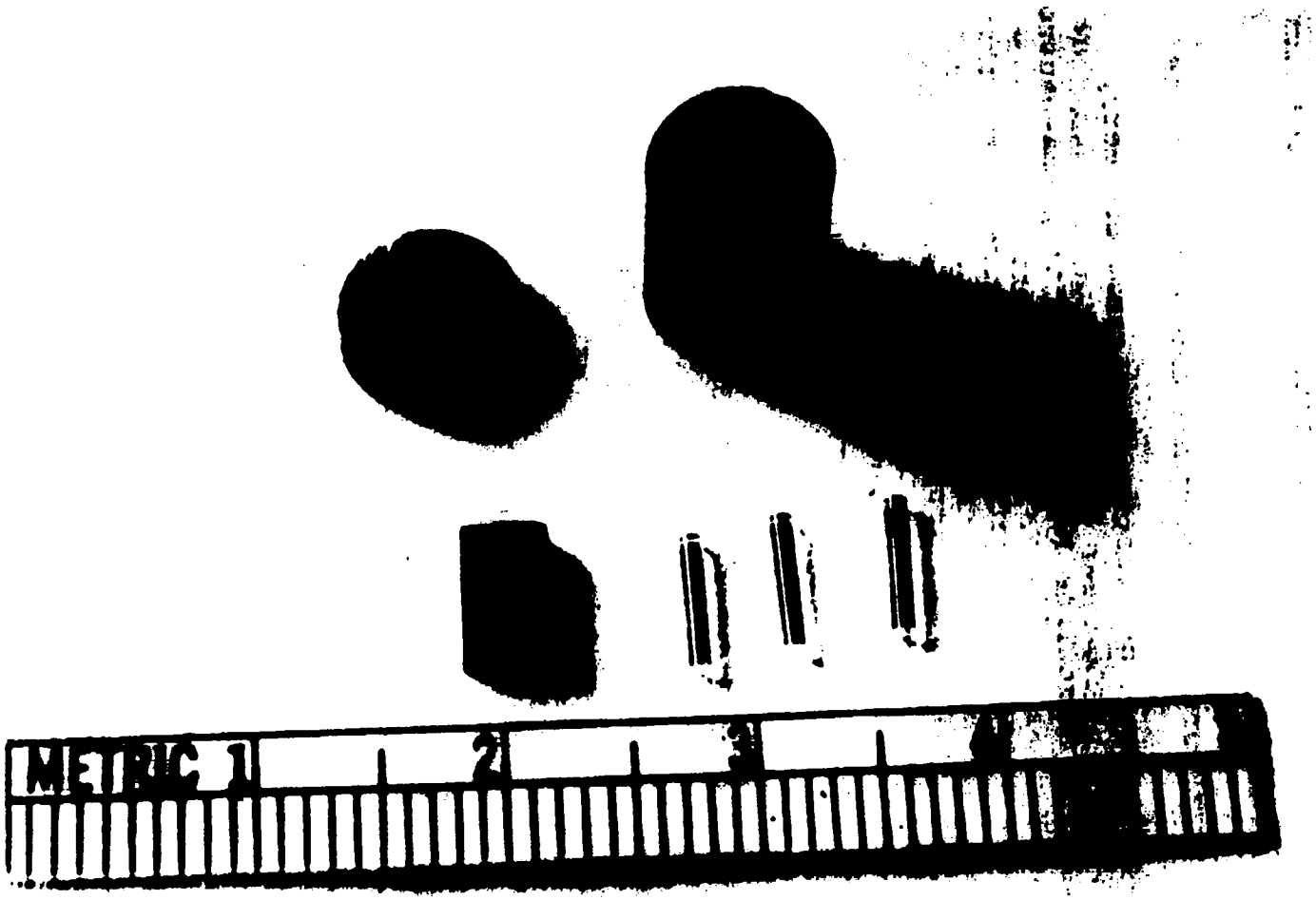

Fig. 1. Bausch and Lomb $AgPO_3$ rod modified cobalt glass plate with Li^6F-Pb container.

Fig. 2. Bausch and Lomb reader, modified.

Fig. 3. LASL Model II chemical dosimeter reader.

Because of the inherent neutron response of all gamma dosimeter systems covering a wide range, we have become resigned to the use of a neutron shielding container. Figure 4 illustrates the chronological developments in shielding containers for dosimeters used in the past 5 years at this Laboratory. The advent of the Bausch and Lomb microdosimeter ($AgPO_3$ and cobalt glass) and the LASL powdered metallurgy techniques made possible the latest millimeter sized container shown at the left. The total range of 10 to 10^7 rads is covered in 2 steps by the $AgPO_3$ rod range of 10 to 10^4 rads and the cobalt glass range of 10^4 to 10^7 rads.

The advantages of the millimeter sized glass rods (10 to 10^4 rad range) are to a certain extent depreciated by gamma energy dependence below several kilovolts and by thermal neutron sensitivity whether incident, reflected, or degraded in type. These undesirable features have been previously observed by this group in the field examination of the military version of the $AgPO_3$ dosimeter. The energy dependence observed is believed to be related to photoelectric effect at lower energies. The thermal neutron response is believed to be due to activation and subsequent gamma decay of the glass-contained silver phosphate, creating an internal source of the type

$$n + Ag^{107}\ (51\%) \longrightarrow Ag^{108} \xrightarrow{t_{1/2}\ 2.3\ min} Cd^{108} + \gamma$$

and

$$n + Ag^{109}\ (49\%) \longrightarrow Ag^{110} \xrightarrow{t_{1/2}\ 24\ sec} Cd^{110} + \gamma$$

Fig. 4. Thermal neutron shielding containers for gamma dosimeters.

The problem of combining heavy metal shielding to reduce low energy gamma dependence with high cross section thermal neutron shielding that would not involve gamma decay was resolved through the mixture of Li^6F with lead in powdered metallurgy combination to produce the 8 x 11 mm container (Fig. 1). The combination of 1 mm equivalent of Li^6 metal plus 0.75 mm of lead was experimentally determined adequate by exposure to thermal neutrons in the Los Alamos Water Boiler measuring internal flux by gold activation and by comparison of the response of the rods to the known gamma dose. The result was a 1.75 mm wall thickness container consisting of 21 per cent Li^6F and 79 per cent lead by weight. The Bausch and Lomb $AgPO_3$ microdosimeter reader as delivered needed adjustments for our purpose. Elimination of light leaks, substitution for null meter, and relocation of dials as shown in Fig. 2 resulted in satisfactory operation.

The cobalt glass plates supplied by Bausch and Lomb (10^4 to 10^7 rad range) respond to radiation by change in light absorption. Studies of the absorption spectra using the Beckman DK-1 Spectrophotometer indicated that a 2 band filter photometer measuring light transmittance at 430 and 570 mμ would be suitable. The transmission of the 2 bands was electronically set equal for unexposed plates such that $R = T_{570}/T_{430} = 1$. Calibration curves were prepared by plotting

$R_f - R_o$ versus dose (log-log). These glass plates as received from Bausch and Lomb measuring 6 x 15 x 1.5 mm were cut to 3 x 7.5 x 1.5 mm in order to fit the Li^6F-Pb container. The reader (LASL Model II chemical dosimetry reader, slightly modified to the transmission spectra above) proved adequate except for mechanical and optical alignment problems which are now being resolved.

Curves of the response of the $AgPO_3$ and cobalt glass dosimeters appear in Fig. 5. It will be noted that the $AgPO_3$ response above 4×10^3 rads begins to lose linearity with dose. Flattening of the curve occurs at $\sim 2 \times 10^4$ rads with a negative slope beginning at $\sim 4 \times 10^4$ rads. It is believed that the curve characteristic beyond 4×10^3 rads is due to radiation darkening of the glass competing with the fluorescence effect which itself may be linear considerably beyond. Although the cobalt glass plates show a beginning response at 10^4 rads, the reproducibility between plates and between readings is not completely satisfactory below 5×10^4 rads. Above 2×10^6 rads. the cobalt glass response loses its linearity; however, it does not approach a zero slope until doses in excess of 2×10^7 rads are delivered.

DISCUSSION

This new dosimeter system has proved satisfactory and is

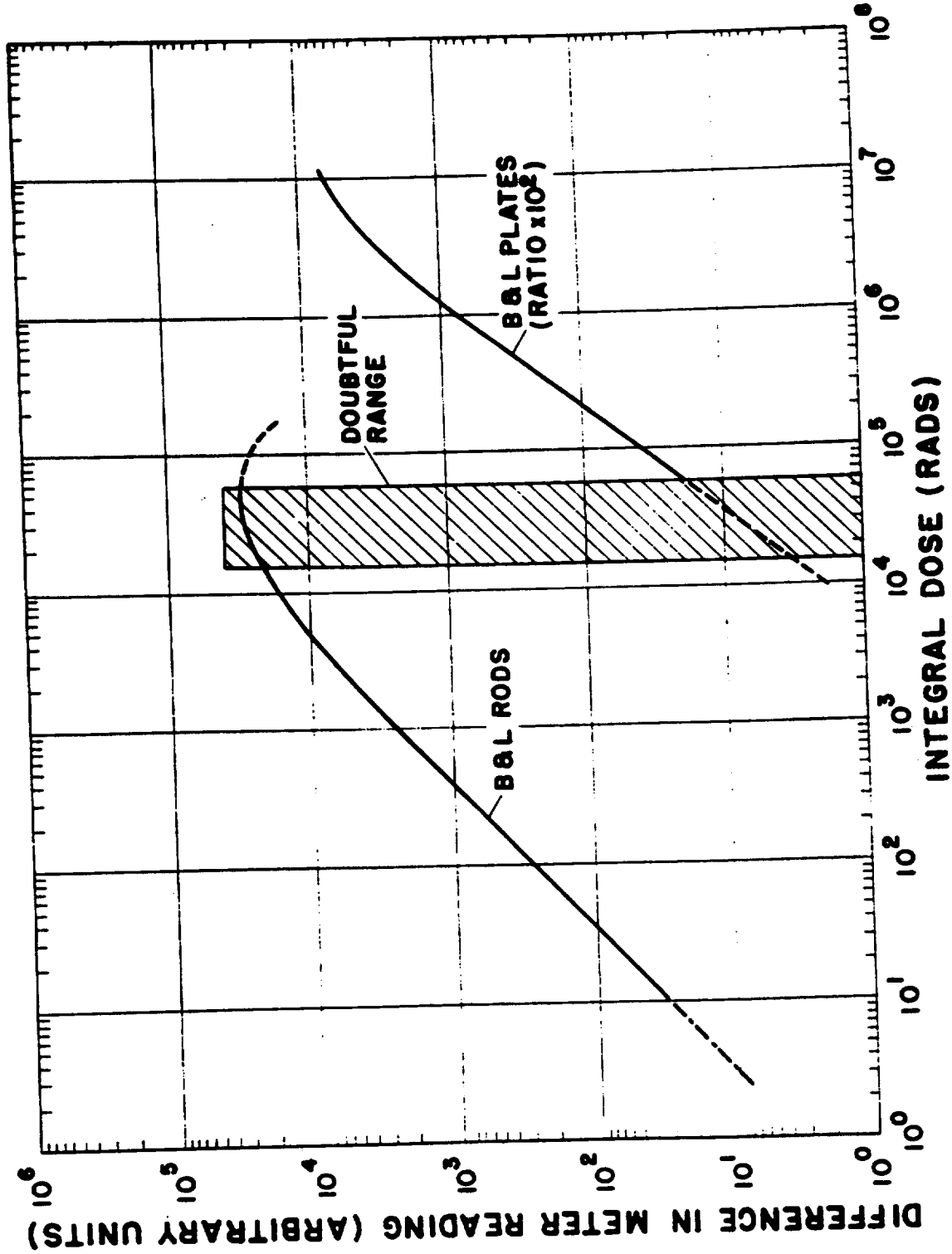

Fig. 5. Relative dose versus response for $AgPO_3$ and cobalt glass dosimeters.

now in routine use in both laboratory and field measurements of gamma dose. It has replaced the tetrachloroethylene chemical dosimeter owing to its greater stability, smaller size, ready availability, less cost, greater precision, lower response to fast neutrons, and increased convenience. Using 4 rods and 1 plate per container, reproducibility over the range of 10 to 10^7 rads is approximately $\pm$ 5 per cent except in the region of 1×10^4 to 5×10^4 rads. The fast neutron response of the system is less than 1 per cent on a per rad basis, while the thermal neutron transmission through the container wall is $\sim$ 5 per cent. The $AgPO_3$ rods require $\sim$ 48 hours to reach stability and if readings are required at earlier times, standards must be exposed simultaneously to a known gamma source. The Bausch and Lomb reader is a precision device optically. The LASL Model II chemical dosimeter reader was not designed particularly for the purpose of reading cobalt glass and thus could be improved in its mechanical and optical design; however, it has proven stable and usable provided the operator is experienced and mechanically inclined. A new design for the cobalt glass reader is presently under consideration.

Body Sodium^{24} Measurement for Personnel Monitoring and Casualty Assessment (E. R. Ballinger and P. S. Harris)

INTRODUCTION

This is a continuing study to investigate the feasibility and techniques of using neutron-induced body Na^{24} activity as a measure of personnel neutron dose for casualty assessment purposes. The technique presupposes that personnel to be monitored can receive surface decontamination and are ambulatory or can otherwise be removed to a relatively uncontaminated area for gamma measurements of body Na^{24} activity. Work accomplished and previously reported (1) consisted of the design, construction, and calibration of the Model I, 110 volt sodium activity meter and preliminary work on a Model II, battery operated, portable hand-carried meter and probe. The probe, a sodium iodide scintillator-photomultiplier tube assembly, when held over the lumbar area of the back, will cause the meter to read in rads of 1.5×10^6 ev neutrons at $t = 0$, which would be required to produce the body Na^{24} activity observed at $t \pm n$ days and hours.

Work accomplished during the present reporting period involved (a) measurements of Na^{24} activity produced in plastic phantoms under varied incident neutron spectra using

laboratory and field sources; (b) comparison and evaluation of body Na^{24} activity per neutron versus average neutron energy with theoretical predictions; (c) investigation of the ratio of body Na^{24} activity to the neutron-induced activity of an externally worn foil as a means of estimating the average incident neutron energy; and (d) attempts at construction of a curve of average neutron energy versus correction value to be applied to the meter reading when the average incident energy significantly differed from the 1.5×10^6 ev energy at which the meter calibration was made.

In theory, if one can measure the amount of body Na^{24} activity produced by neutrons of known energy, one can determine the neutron density and thus, with values for energy and density, calculate the dose in rads. If such a sodium activity meter, for the purpose of functional utility, is calibrated to read directly in rads of incident neutrons of a specific or average energy which would be required to produce the amount of Na^{24} gamma activity observed, then the meter will not necessarily correctly measure the dose from neutrons of another specific or average energy. If a relatively simple means of estimating average neutron energy could be devised, correction values could be developed and applied to the meter reading to approximate more closely the actual neutron dose received. An attempt to design such a method is the present basis of our study.

METHODS AND MATERIALS

The Sodium Activity Meter (SAM) is made up of 2 units: a lead-enclosed sodium iodide scintillator-photomultiplier tube probe connected by shielded cable to a power supply, amplifier, and rate meter unit with controls (Fig. 1). The power supply and amplifier use mercury cell batteries and transistorized circuitry. The meter is scaled in rads of 1.5 Mev neutrons required to produce the Na^{24} activity observed when the probe is applied to the lumbar area of the back of the individual being monitored. The controls permit a 2-scale range (1 to 100 rads and 1 to 1000 rads), a zero adjust to compensate for background activity up to ~ 5 mr/hr, and a decay correction in days and hours post exposure to obtain t = 0 readings. The meter will read directly and correctly in rads of incident neutrons of 1.5 Mev average energy and was so calibrated from exposures of plastic phantoms to the LASL Godiva II critical assembly. From theoretical curves adjusted to experimentally determined points, it has been shown that when the average neutron energy is greater than 1.5 Mev, the meter reading will tend to be low (i.e., the Na^{24} activity produced per neutron does not increase as the rads per neutron at these energies) and that when the average neutron energy is less than 1.5 Mev, the meter reading will tend to be high (i.e., the Na^{24} activity

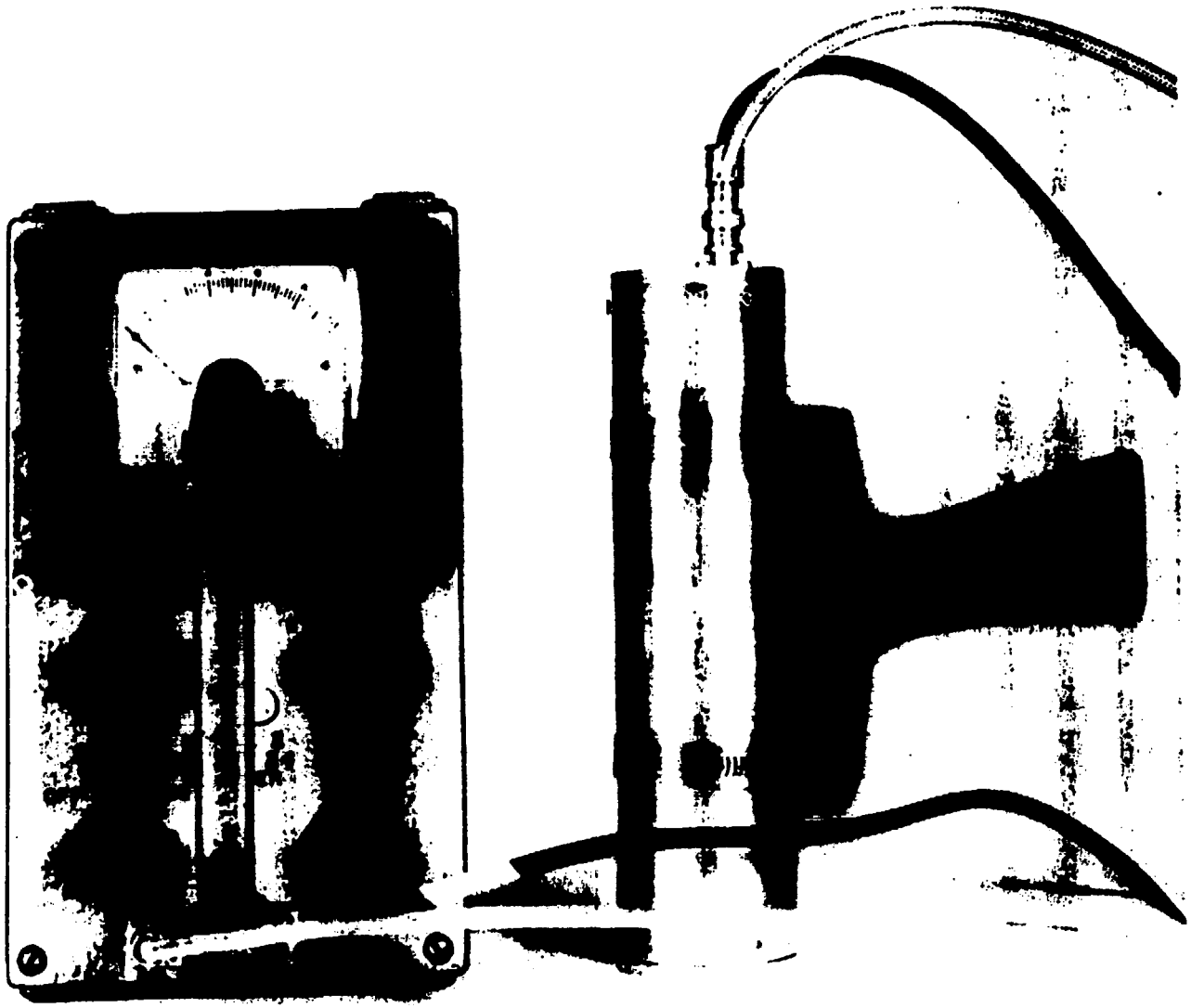

Fig. 1. Battery operated, portable sodium activity meter.

per neutron does not decrease as rapidly as the rads per neutron at these energies).

Although the $Na^{23} + n \longrightarrow Na^{24}$ reaction is higher for neutrons of thermal energy, the reverse is seen when plastic phantoms containing 1.5 g Na^{23} per kilo of water are exposed. In this case, the high albedo of thermal neutrons incident upon the body and the high degree of moderation of fast neutrons to thermal levels within the body results in an apparent high cross section of Na^{23} in the body for fast neutrons. Thus, since the body Na^{24} activity was found to increase roughly with increased neutron energy on a per neutron basis and since many materials capable of induced neutron activation vary inversely with neutron energy, it was considered that perhaps the ratio of the above might be related to and used to give a rough indication of the average neutron energy of unknown spectra (Fig. 2). If the average energy could be thus obtained, a curve of E_n versus meter correction value could be constructed. Because the electronic decay corrections were set for the 15 hour half-life of Na^{24}, copper (a material of similar half-life) was chosen as the counterpart in the ratio referred to above.

The metal copper is ~70 per cent Cu^{63} with a 4.4 barn cross section for thermal neutrons and a 12.8 hour half-life involving a 1.34 Mev gamma decay. The ~ 30 per cent Cu^{65}

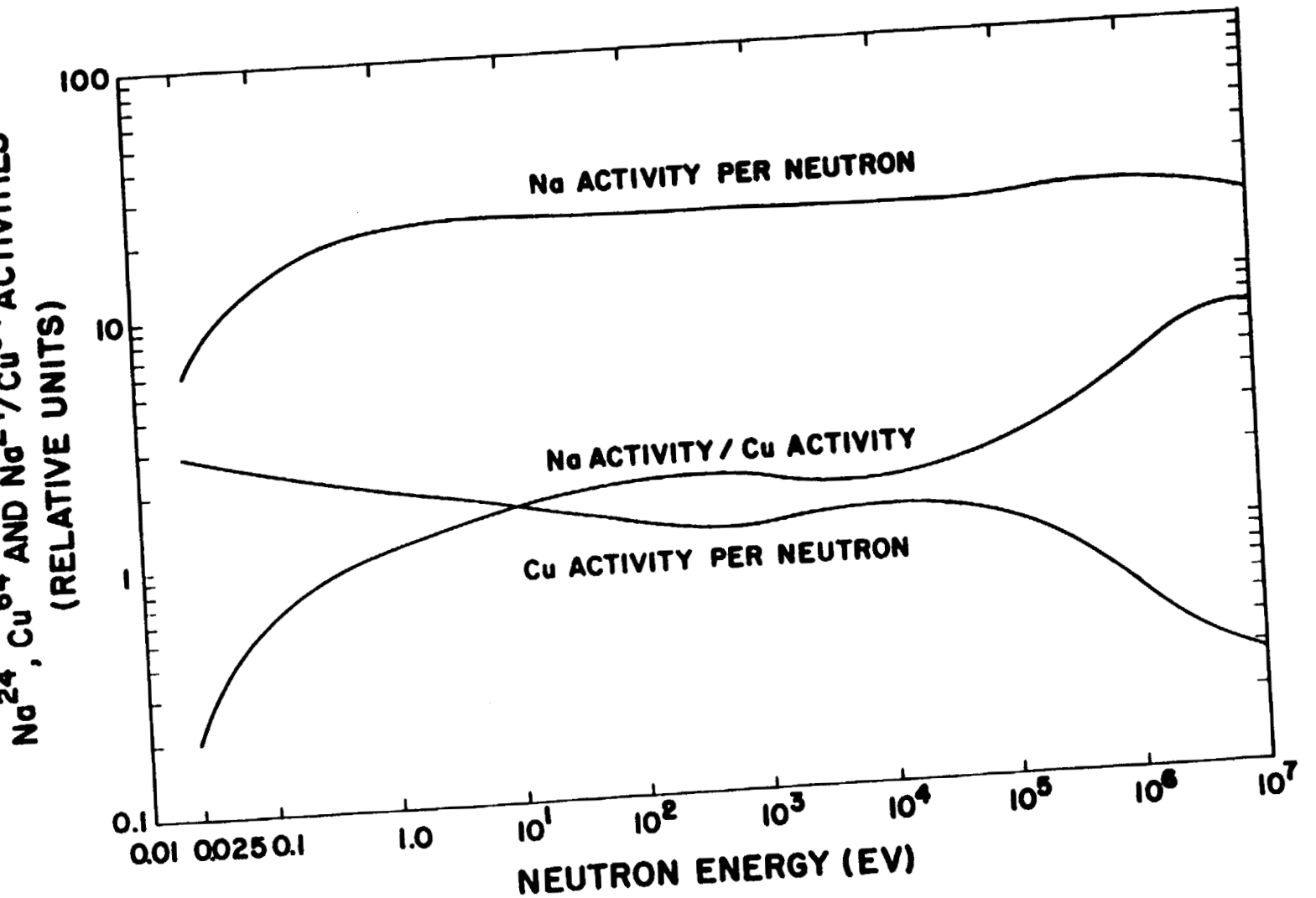

Fig. 2. Relative values of Na^{24}, Cu^{64}, and ratio of Na/Cu activities as a function of neutron energy.

with smaller cross section and 5 minute half-life can be disregarded. The cross section of Cu^{63} is 1/v in type and appears to have no significant capture resonances above thermal energies.

The presently proposed manner of operation of this system, which admittedly has not yet reached the desired degree of refinement, is tied in with the $AgPO_3$ gamma dosimeter when considered for use in casualty assessment procedure. The exposed personnel are removed to a relatively uncontaminated area after showering. An ideal location would be the lead shielded X-ray room of a local hospital. The $AgPO_3$ dosimeters are first read for gamma dose. In the event that the gamma dose is insignificant in casualty terminology, it can be assumed that any associated neutron exposure is also inconsequential and in the event large numbers of persons are involved, the procedure of screening can end at this point. In the event that the gamma dose is in excess of 10 to 25 rads, the individual is then probed over the lumbar area of the back with the SAM for induced Na^{24} activity. If the meter reading is in excess of ~50 to 100 rads, it would become desirable to correct this reading for the average incident neutron energy. This is accomplished by placing his copper foil (3/4 x 3/4 in.) on the probe and obtaining the ratio of body Na^{24} to copper foil activity. By entering the

graph (Fig. 3) at the Na^{24}/Cu^{64} value, one comes out with a correction value or multiplier which, when applied to the body sodium reading, will more closely approximate the actual neutron dose received.

DISCUSSION

It should be stated at the outset that this type of body sodium measurement can probably more correctly be termed monitoring than dosimetry. The accuracy involved in the case of unknown spectra cannot be expected to be much better than $\pm$ 50 per cent using the admittedly unrefined correction value curve, which is now based upon ~4 different spectral points, with theoretical guestimates as to the curve configuration between these points. However, despite the present state of development, the authors believe that it has considerable merit in terms of future potentiality. As it stands at present, the SAM can scan for the presence of induced body sodium activity for doses above 10 r out to several days post exposure at a rate of 2 to 3 persons per minute and requires only minimal training and a relatively low background area with shower facilities. To correct the readings by use of the copper foil could probably be done at the rate of 1 person per minute with an accuracy of ~$\pm$ 50 per cent. Future plans involve continuing plastic phantom and copper foil exposures to different neutron spectra to obtain as many additional

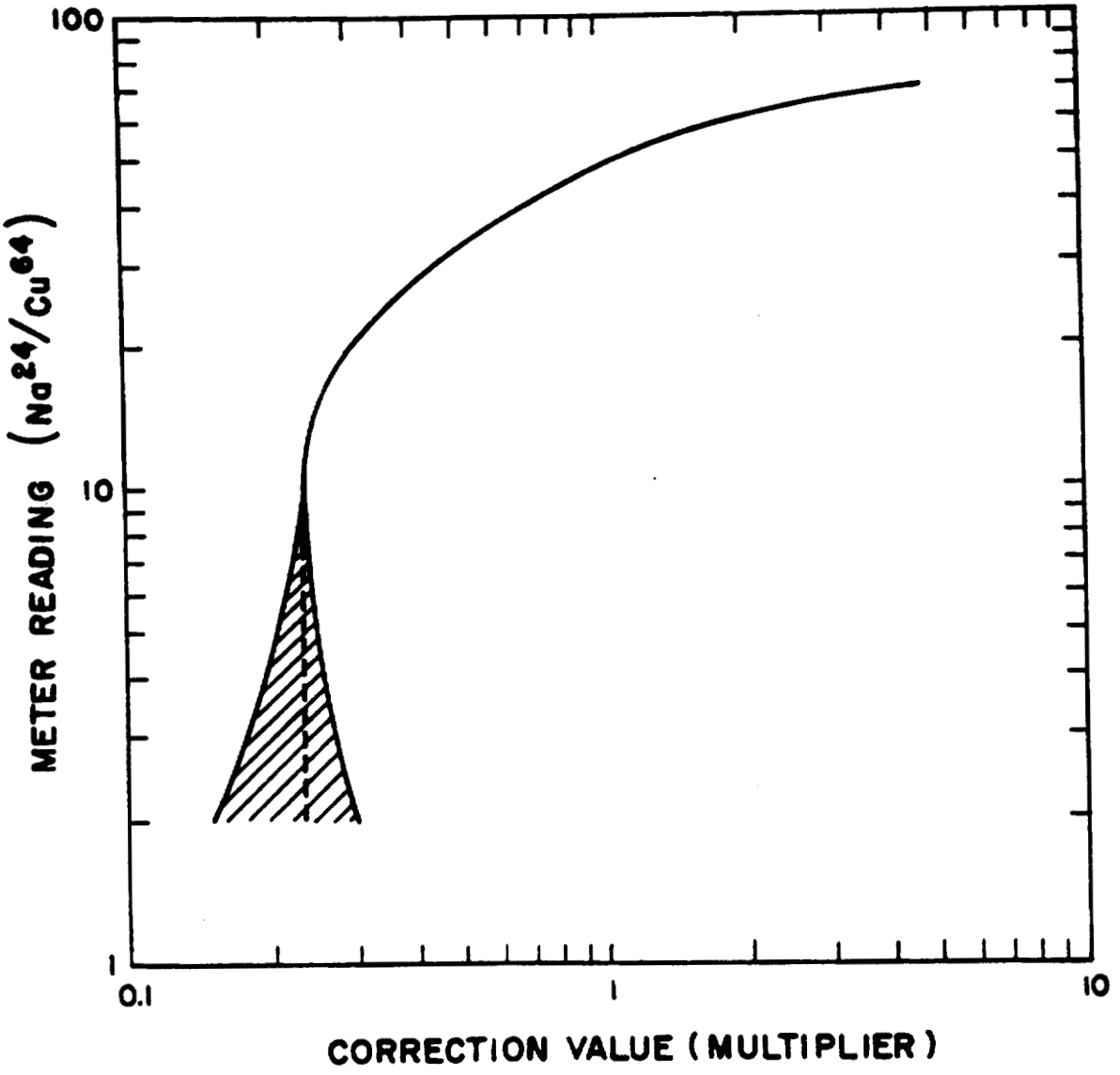

Fig. 3. Meter correction factors as a function of the ratio of body Na^{24}/Cu^{64} determined from meter reading.

experimental points as possible in order to refine the correction value curve, to modify the circuitry in such a way as to introduce a lower gate at ~ 1.5 Mev and in so doing enable Na^{24} gamma readings to be made in relatively high background areas, and to investigate the use of copper foils included in an item of clothing particularly for the military in conjunction with $AgPO_3$ microdosimeter rods by Bausch and Lomb.

REFERENCE

(1) E. R. Ballinger, P. S. Harris, and J. H. Larkins, Los Alamos Scientific Laboratory Report LAMS-2455 (1960), p. 206.

Gamma and Neutron Dose Measurements of [redacted] Aircrews during Kiwi-A Three Operation (E. R. Ballinger)

INTRODUCTION

Since the latter part of 1950, it has been common practice to sample the fission products of nuclear detonations and field reactor effluent by means of aircraft. Crew members have routinely worn gamma film dosimetry. Due to the fact that at the time of nuclear detonations the aircraft were considerably beyond the mean free path of neutrons and that the neutron hazard post detonation was inconsequential, no serious attempts were made to monitor aircrews for neutron dose. The sampling of the effluent of Kiwi-A and Kiwi-A Prime during full power runs was similarly monitored primarily for gamma dose.

Certain film badge discrepancies resultant of these runs suggested the possibility that thermal neutrons might be contributing in some cases to the gamma film badge reading. If, in fact, such a condition existed, then the probability that fast neutrons might be contributing a significant portion of the body dose could not be neglected. Consequently, all [redacted] aircraft and crew members on Kiwi-A Three operation were equipped with gamma and neutron dosimetry.

METHODS AND MATERIALS

All [redacted] aircrew members of the [redacted] aircraft wore gamma-neutron film packets from LASL and REECO plus gamma packets from Wright-Patterson Air Force Base, Ohio. All [redacted] aircrew members wore special lithium-shielded gamma film badges and swallowed gamma film capsules ~3 hours prior to the sampling mission. [redacted] of [redacted] crew members had base line Human Counter measurements ~1 week prior to the mission.

All aircraft were equipped with 20-kilo polyethylene jugs containing 10 times normal physiological saline solution (15 g Na/kilo H_2O). All aircraft were equipped with a gamma film packet hung in air in the after-compartment, a lithium-shielded gamma film packet at a similar position, as well as a neutron film packet. Following the mission, all films were returned to their original sources for reading. The [redacted] crew members who received Human Counter base line studies were returned to LASL and counted ~20 hours post mission.

RESULTS AND DISCUSSION

Highest gamma readings in all cases were found on the unshielded gamma film packet hung in air in the after-compartment of the [redacted] aircraft. Lowest gamma readings in all cases were on the lithium-shielded gamma film packet similarly placed and on the unshielded gamma packet on the

copilot. The lithium-shielded crew member badges were damaged to the preclusion of reading by packing procedures. Thus, for the particular configuration of the sampling passes and distance from the reactor, it would appear that the thermal neutron effect amounted to a 20 to 30 per cent exaggeration on an unshielded gamma film packet and that the shielding built in around the copilot reduced his gamma exposure over that of the pilot by ~10 per cent and over that of the in-air dose in the after-compartment by ~ 20 to 30 per cent.

Neutron dosimetry from film packets in the after-compartment of the aircraft, when uncorrected for RBE, was in reasonable agreement with Human Counter measurements, when corrected for incident neutron energy. Neutron badges worn by crew members gave unreliably low numbers. The neutron exposure, as measured in the after-compartment, amounted to ~ 1/3 to 1/4 of the gamma dose uncorrected for RBE. Actual dose and distance and velocity values are omitted for classification purposes.

DISCUSSION

Thermal neutron effect on gamma film badges cannot be disregarded on aircraft sampling missions when sampling activities are being carried out before reactor shutdown.

A pair of lithium-shielded and unshielded film badges in the after-compartment of the aircraft probably gives the most reproducible gamma value, is the simplest way to determine the presence of thermal neutrons using only gamma film, and probably represents the maximum possible exposure to a crew member. A neutron film packet in the after-compartment of the aircraft similarly gives the most reproducible and reliable value and again probably represents the maximum possible exposure to a crew member. Of the [redacted] film capsules swallowed ~3 hours prior to the mission, [redacted] were recovered and [redacted] undamaged by gastric contents. Readings were roughly 2/3 of the externally worn film badge. The polyethylene jugs filled with 10 times normal physiological saline were installed in the aircraft in anticipation of the possibility that the neutron dose to crew members would be below the measurable limits of the LASL Human Counter. This, however, was not the case, and the actual body counts of the crew members themselves were used to indicate their thermal neutron dose.

The Use of Graphite-CO_2 Ionization Chambers for the Determination of Gamma Flux and the Effective Transmission of the Front Penthouse Face of Test Cell "C" during Kiwi-A Prime and Kiwi-A Three (F. C. V. Worman)

INTRODUCTION

During the planning of Project Rover, a request was made for the fabrication of a high intensity gamma rate meter to be used for the measurement of gamma flux from the Kiwi reactors. A graphite-CO_2 ionization chamber instrument with a 6-decade range was built and is described in Los Alamos Scientific Laboratory Report LA-2361 (1). This instrumentation was used on Kiwi-A Prime and Kiwi-A Three for the purpose of measuring gamma flux in the presence of neutrons and to determine the transmission of the front test cell wall for gamma radiation.

METHODS

Two instruments were used during the high power runs of the Kiwi series. One chamber was placed in the penthouse of Test Cell "C" at a distance of ~20 ft from the center of the reactor. This chamber had the same location for Plans 116B of Kiwi-A Prime and 216B of Kiwi-A Three. Readings at this station expressed a dose rate with 4.75 ft of concrete intervened between the station and the reactor.

During Kiwi-A Prime, a second instrument was placed on the corner of the test cell roof at a distance of ~30 ft, where a free air dose was obtained. During Kiwi-A Three, it was necessary to move the outside chamber to the penthouse roof at a distance of ~25 ft. At this position, the combing of the front face of the test cell introduced 1.5 ft of concrete between instrument and reactor.

Several changes were made in the instrumentation since its description in a recent report (1). The electronics have been simplified, and the logarithmic reading ability of the instrument has been improved. The schematic diagram of the log amplifier (Fig. 1) may be compared with that shown in the previous report. The Sanborn recorders were eliminated and readings made on wide chart Brown recorders to facilitate analysis of data and eliminate the necessity of changing graph paper when the reactor running schedules were interrupted for some reason.

RESULTS AND DISCUSSION

During Plan 116B of Kiwi-A Prime, peak gamma radiation levels at full reactor power were obtained at both inside and outside stations. The reading in air at the outside station at a distance of ~30 ft was 990,000 r/hr. The reading inside the test cell through 4.75 ft of concrete was ~100 r/hr.

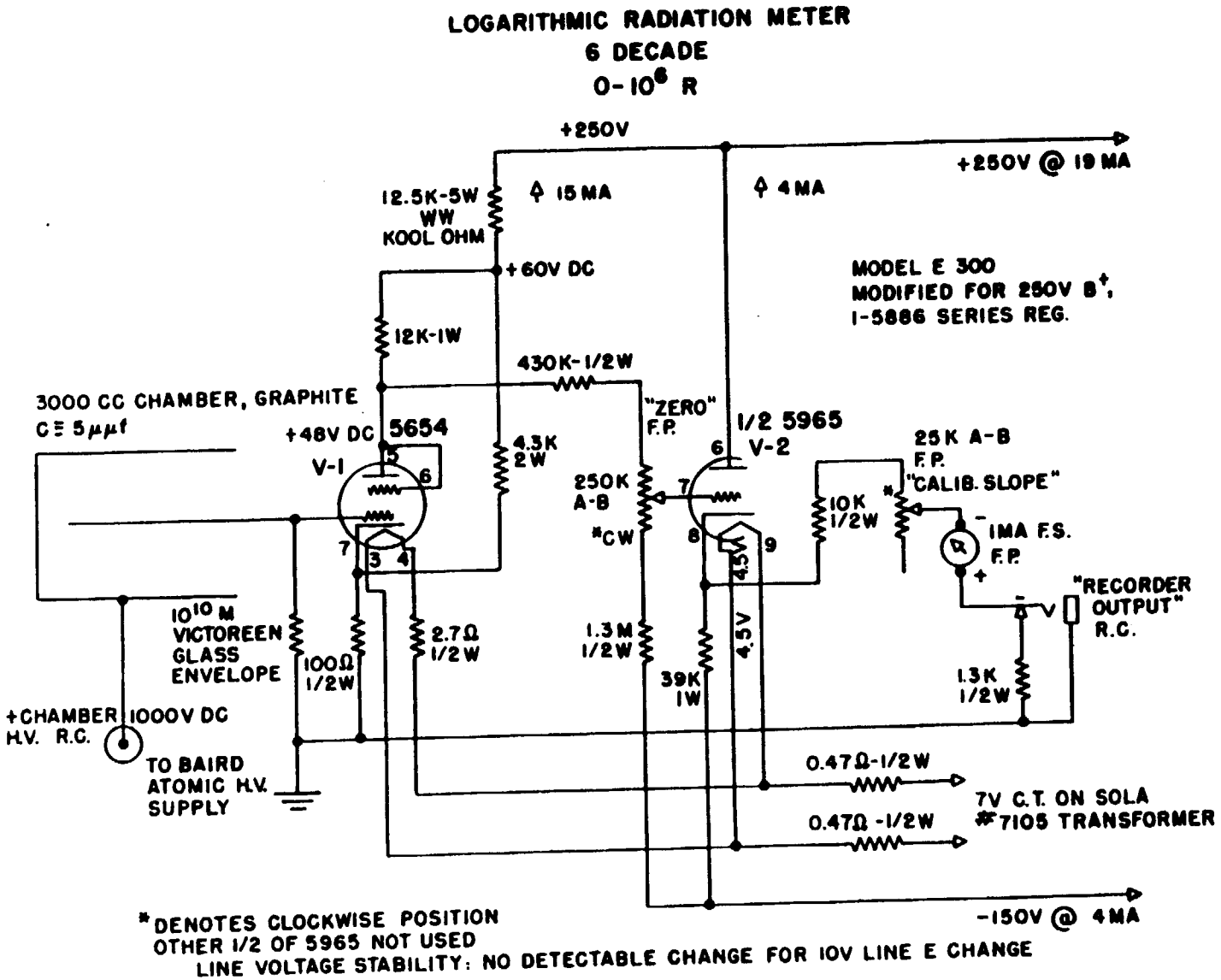

Fig. 1. Schematic drawing of logarithmic amplifier.

As the power cable to the graphite chambers was burned during the peak of the power run, it was not possible to determine an integrated dose for this plan.

On Plan 216B of Kiwi-A Three, the inside instrumentation operated very efficiently. The average reading over the full power portion of the reactor run indicated a gamma flux of ~ 400 r/hr inside the test cell. The integrated dose over the entire power run showed a total of greater than 50 r. Comparison of the inside readings with those measured by the scintillation method in free air at approximately the same distance (2) indicated a transmission factor for the front face of the penthouse on Test Cell "C" of 2.11×10^{-4}. This factor shows the effective transmission of the penthouse with no separation of sky shine (scatter) or of induced gamma radiation in the concrete penthouse wall.

Further analysis of the data and specific distances, doses, and dose rates will be reported as an LA-document.

REFERENCES

(1) F. C. V. Worman and P. S. Harris, Los Alamos Scientific Laboratory Report LA-2361 (1959).

(2) D. L. Williams, Personal communication.

Integral Neutron and Gamma Dose Measurements on Kiwi-A Prime and Kiwi-A Three (P. S. Harris, F. C. V. Worman, E. F. Montoya, and D. G. Ott)

INTRODUCTION

Considerable time was spent during this reporting period on integral dose and flux measurements on the Kiwi-A Prime and Kiwi-A Three reactors of the Rover series. Measurements were made to determine the radiation output of these reactors during operation to assess them as radiation sources for extrapolation to flyable systems. These outputs are important both insofar as launch control personnel and manning personnel are concerned. They are also important for calculation and determination of shielding efficiencies and for related radiation effects work. The information can be compared with that obtained from weapons and other high intensity nuclear sources. This work is a continuation of attempts to determine the radiation problems which exist in any use of a Rover system.

MATERIALS AND METHODS

Integral gamma ray doses at selected positions were determined using glass rod dosimeters. The glass rod system is more fully discussed elsewhere. In this use, the rods were contained in specially made Li^6 cans which eliminated the thermal neutron portion of the total response. By the judicious

use of cobalt glass plates, as well as rods, the dose range extended well into the millions of rads region. Neutron fluxes and doses were determined using the fission foil system. In addition, gold foils and sulfur pellets were utilized to extend into the thermal and high energy regions. For this work, the modified B^{10} container was used throughout. This system is more fully discussed elsewhere.

RESULTS

For classification reasons, results are not given in detail but complete data for the Kiwi-A Prime series will be found in Los Alamos Scientific Laboratory Report LA-2456 (1). Specific results on other tests will be issued as LA-documents. Both neutron and gamma ray measurements were made as a function of distance from the reactor and under a variety of shielded and unshielded conditions.

The integral gamma doses during the Kiwi-A Prime high power run varied in a predictable manner from a maximum of 2.4×10^{7} rads at close positions to 17 rads at well over 1000 ft. The over-all transmission of the penthouse on top of the test cell was found to be 5×10^{-4} for gamma rays. This was primarily due to the 4-1/2 ft concrete wall in line with the reactor. Gamma doses inside the test cell during maximum run were small but would not permit occupancy during the run. The scattered gamma ray dose at range distances

from an opaque shield was found to be 35 per cent. Integral fast neutron doses varied from a maximum of 2×10^6 to 5 rads over the distance of a few feet to over 1000 ft from the reactor. Fast neutron dose transmission through the penthouse was 1.3×10^{-4}. Fast neutron dose inside the test cell was insignificant. Scattered fast neutron doses over range distances were found to be 60 per cent of the total. As would be expected, the scattered neutron dose decrease was essentially due to energy degradation of fast neutrons in air rather than air absorption, if the unshielded condition is compared with the shadow shield.

DISCUSSION

Integral neutron and gamma ray measuring systems functioned satisfactorily. Further refinements of the methods will be expected to give better information on spectrum, some extension of the range of collection, and a continued evaluation of the radiation environment of nuclear powered rocket systems.

REFERENCE

(1) P. S. Harris, Los Alamos Scientific Laboratory Report LA-2456 (1960), (Classified).

Characteristics of the Large H-4 Fission Gamma Counter

(J. A. Sayeg, J. H. Larkins, and E. L. Carr)

INTRODUCTION

The fission threshold detector technique as proposed by Hurst and co-workers (1) has been used extensively at this Laboratory for the measurement of neutron flux, spectrum, and tissue dose (2). It has been our aim to improve the instrumentation of this method in accordance with current needs. The present paper describes the characteristics of the large H-4 fission gamma counter christened "Jumbo No. 1" (J-1) because of its size compared to other counters previously designed.

METHODS AND RESULTS

Description

This unit consists of 2 opposing 4 in. diameter, 2 in. thick, sodium iodide crystals shielded by a truncated 5/8 in. thick lead absorber to reduce the natural background of the foils used (see Fig. 1). Each crystal is connected to a DuMont No. 6363 3 in. photomultiplier tube. The entire assembly is shielded by approximately 4 in. of lead. The output of each photomultiplier is connected to a common Model 250N preamplifier, thence to a Model 250 amplifier, a

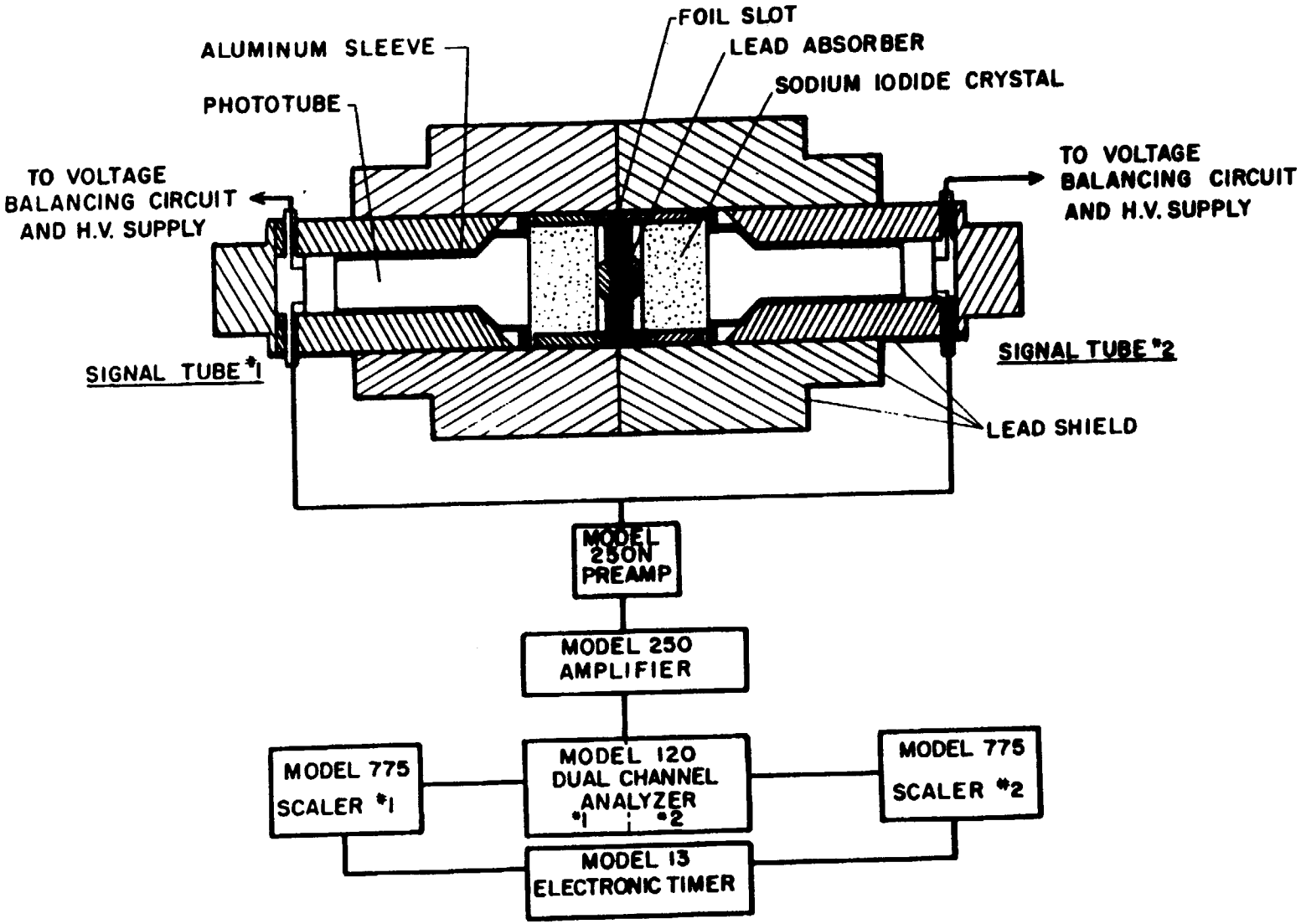

Fig. 1. Schematic of Counter J-1.

Model 120 dual channel analyzer, and finally to 2 Model 775 scalers. These electronic components provide a means of counting simultaneously at 2 different threshold counting bias values, thus permitting twice the data to be obtained in the same counting time.

Characteristics of the Counter

The counter bias versus gamma ray energy relation was obtained by using samples of Cs^{137} (0.66 Mev), Na^{22} (0.51 and 1.28 Mev), and Np^{237} (0.31 Mev). These samples were counted in 1 volt channel widths. The gamma ray energy versus integral bias relation is shown in Fig. 2. Counter bias values of 0.51 and 1.2 Mev were chosen to evaluate the fast neutron counter calibrations from a thermal neutron foil exposure.

Thermal Neutron Calibration

Equivalent foils of Pu^{239}, Np^{237}, and U^{238} (1,2) were irradiated with thermal neutrons from port S-1* of the Los Alamos Water Boiler. The foils were placed at a distance of 40-1/8 in. from the bismuth wall and each was given a separate exposure of 1 KW for 3 minutes. Each exposure was monitored by a 10 mil gold foil placed 50-1/8 in. from the bismuth wall. The gold foil monitor indicated an integral

*Port No. 1 of the south thermal column (2).

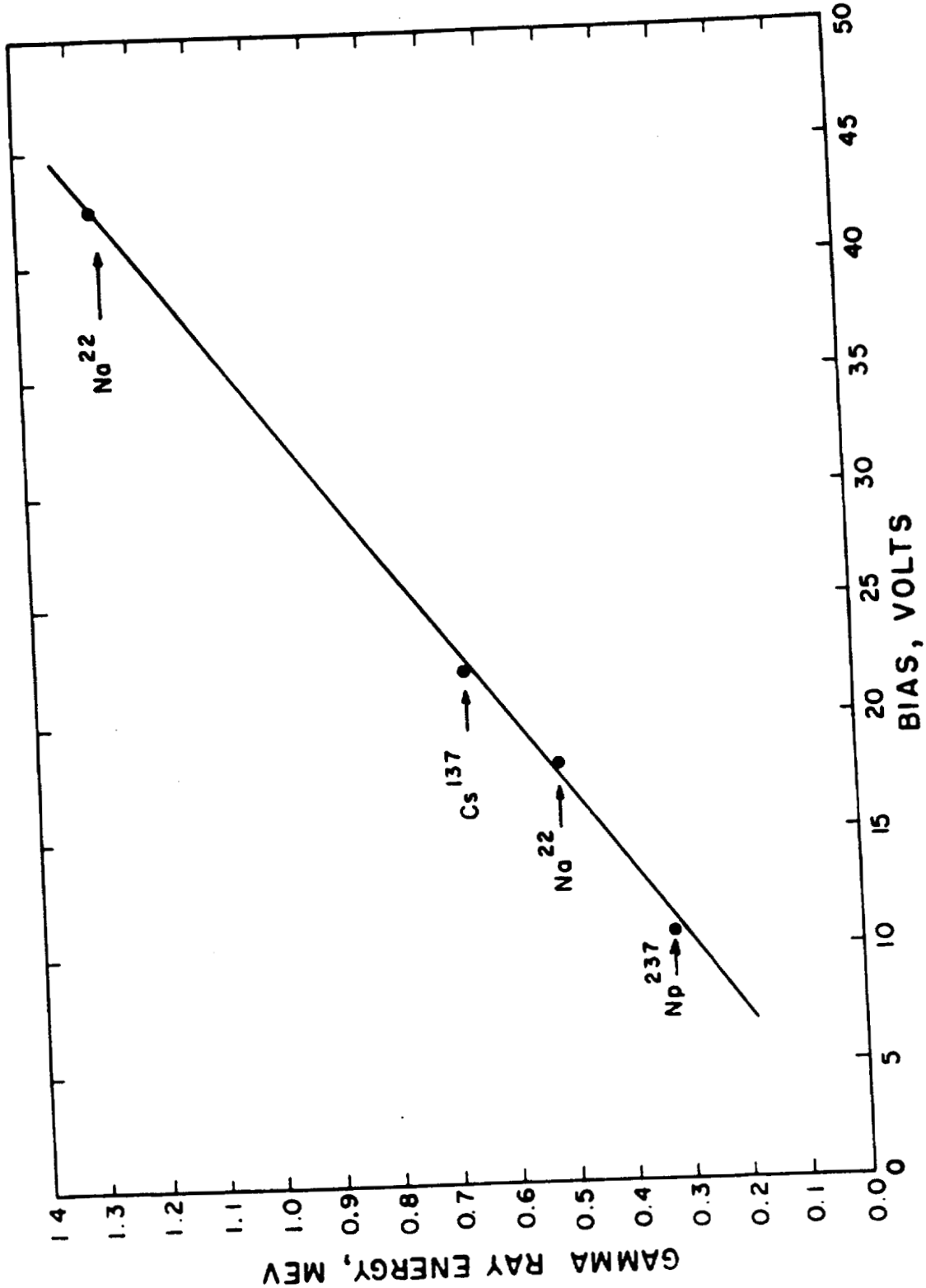

Fig. 2. Gamma Mev versus counter bias relations.

flux of 1.89×10^{10} thermal neutrons/cm^2.* The foils were then counted for a period of 8 hours. The 3-hour post exposure point was arbitrarily chosen as our calibration time. Table 1 shows the decay relations obtained, normalized to 3 hours post irradiation time. Also shown are the calibration constants for the 2 counter bias values.** The parameters used in these evaluations are discussed in detail in Ref. 2.

Foil Background

Table 2 shows the background values for the foils used at the 2 different bias levels. These foil backgrounds are dependent upon the amount of absorber used between the foil and crystal and can be varied by using a different absorber thickness and geometry. The background at 1.2 Mev for Np^{237} appears high, in view of the fact that natural Np^{237} has no gamma rays above 0.5 Mev. This high value of background is believed to be due to pulse pile-up as a result of the large counting rates at the lower energies.

---

*This value is approximately 10 per cent higher than values previously obtained. This discrepancy is being investigated.

**The data at 0.51 Mev for Np^{237} are not used because of the competing Np^{237} (n,γ) Np^{238} reaction which gives rise to a gamma ray energy of 1.0 Mev.

TABLE 1. CALIBRATION DATA FOR GAMMA FISSION COUNTER (J-1)

Post Exposure Time (hours)	Ratio of Activities to 3-Hour Activity				
	Pu^{239}		Np^{237}	U^{238}	
	0.51 Mev	1.2 Mev	1.2 Mev	0.51 Mev	1.2 Mev
1	4.51	5.18	4.07	4.41	5.30
1-1/2	2.72	2.96	2.75	2.68	2.93
2	1.83	1.93	1.82	1.81	1.90
2-1/2	1.33	1.36	1.32	1.32	1.34
3	1.00	1.00	1.00	1.00	1.00
3-1/2	0.794	0.778	0.771	0.783	0.790
4	0.647	0.626	0.608	0.635	0.641
4-1/2	0.528	0.513	0.504	0.529	0.527
5	0.440	0.423	0.426	0.448	0.437
5-1/2	0.371	0.354	0.364	0.386	0.369
6	0.325	0.300	0.312	0.333	0.317
6-1/2	0.282	0.260	0.270	0.295	0.272
7	0.253	0.226	0.233	0.257	0.239
7-1/2	0.232	0.200	0.202	0.235	0.212
8	0.211	0.177	0.175	0.212	0.187

Calibration Constants for 3 hours post irradiation time

$(n/cm^2/c/m/g)$ 3.00×10^6 1.27×10^7 1.11×10^7 9.54×10^6 4.05×10^7

Counter Standard Na^{22} Std. No. 12-7 — 0.51 Mev: 139,000 c/m; 1.2 Mev: 40,800 c/m

TABLE 2. FOIL BACKGROUND OF THE FISSION NEUTRON DETECTORS Pu^{239}, Np^{237}, AND U^{238} FOR THE LARGE GAMMA FISSION COUNTER (J-1)

Counter Bias (Mev)	Foil Background (c/m/g)		
	Pu^{239}	Np^{237}	U^{238}
0.51 (natural counter background = 385 c/m)	8238	22,560	1546
1.2 (natural counter background = 140 c/m)	1012	190	95

Comparison of the Large Fission Gamma Counter (J-1) and the Small Counter (K-2)

A small gamma fission counter (K-2) has been described in Ref. 3. Briefly, this counter employs 1-3/4 in. diameter, 1-3/4 in. thick, sodium iodide crystals shielded by 1/4 in. of lead. The foil backgrounds and 3-hour calibration constants are shown in Table 3. Comparison of the 2 counters shows that Counter J-1 is less than a factor of 2 better than Counter K-2. Stability tests, however, show that Counter J-1 is more stable. The instability of Counter K-2 is believed to be due to the large amount of radiation the phototubes are subjected to in counting a large activity sample (see background value of Np^{237} at 0.51 Mev bias). Investigations to determine the best parameters for both efficiency and stability are underway.

REFERENCES

(1) G. S. Hurst and R. H. Ritchie, Oak Ridge National Laboratory Report ORNL-2748, Part A (November 1959).

(2) J. A. Sayeg, Los Alamos Scientific Laboratory Report LA-2432 (April 1960).

(3) J. A. Sayeg, D. G. Ott, and P. S. Harris, Los Alamos Scientific Laboratory Report LA-2468 (May 1960).

TABLE 3. 3-HOUR FOIL CALIBRATION CONSTANTS AND BACKGROUND FOR THE SMALL FISSION GAMMA COUNTER (K-2)

Counter Bias (Mev)	3-Hour Calibration Constants ($n/cm^2/c/m/g$)			Foil Background (c/m/g)		
	Pu^{239}	Np^{237}	U^{238}	Pu^{239}	Np^{237}	U^{238}
0.51 (counter background = 207 c/m)	4.60×10^6	---	1.55×10^7	6970	422,230	2140
1.2 (counter background = 55 c/m)	2.25×10^7	1.93×10^7	7.40×10^7	530	145	47

Neutron Flux, Spectrum, and Tissue Dose Evaluations for the Sandia Port of the Omega West Reactor Facility (J. A. Sayeg)

INTRODUCTION

Because of the increased need for calibrated reactor sources to be used by the Biomedical Research Group, it was considered important to investigate the different Los Alamos facilities for possible applications as radiation sources. In addition, other groups within the Laboratory have expressed interest in these investigations. Since the Biomedical Research Group had acquired techniques of neutron flux, spectrum, and tissue dose evaluations (1), it was decided to make a survey of the Sandia port of the Omega West Reactor. The present report describes the preliminary neutron data obtained.

METHODS AND RESULTS

The Sandia port of the Omega West Reactor facility extends from the top of the reactor to the approximate horizontal midplane of the core. A schematic diagram is shown in Fig. 1. The threshold detector technique as proposed by Hurst and coworkers (2) was used in this investigation. This method has been used extensively by this Laboratory in making neutron flux, spectrum, and tissue dose evaluations (3,4). Briefly, this method consists of irradiating foils of Pu^{239} (surrounded by B^{10}), Np^{237}, U^{238}, and S^{32}. To facilitate ease of handling

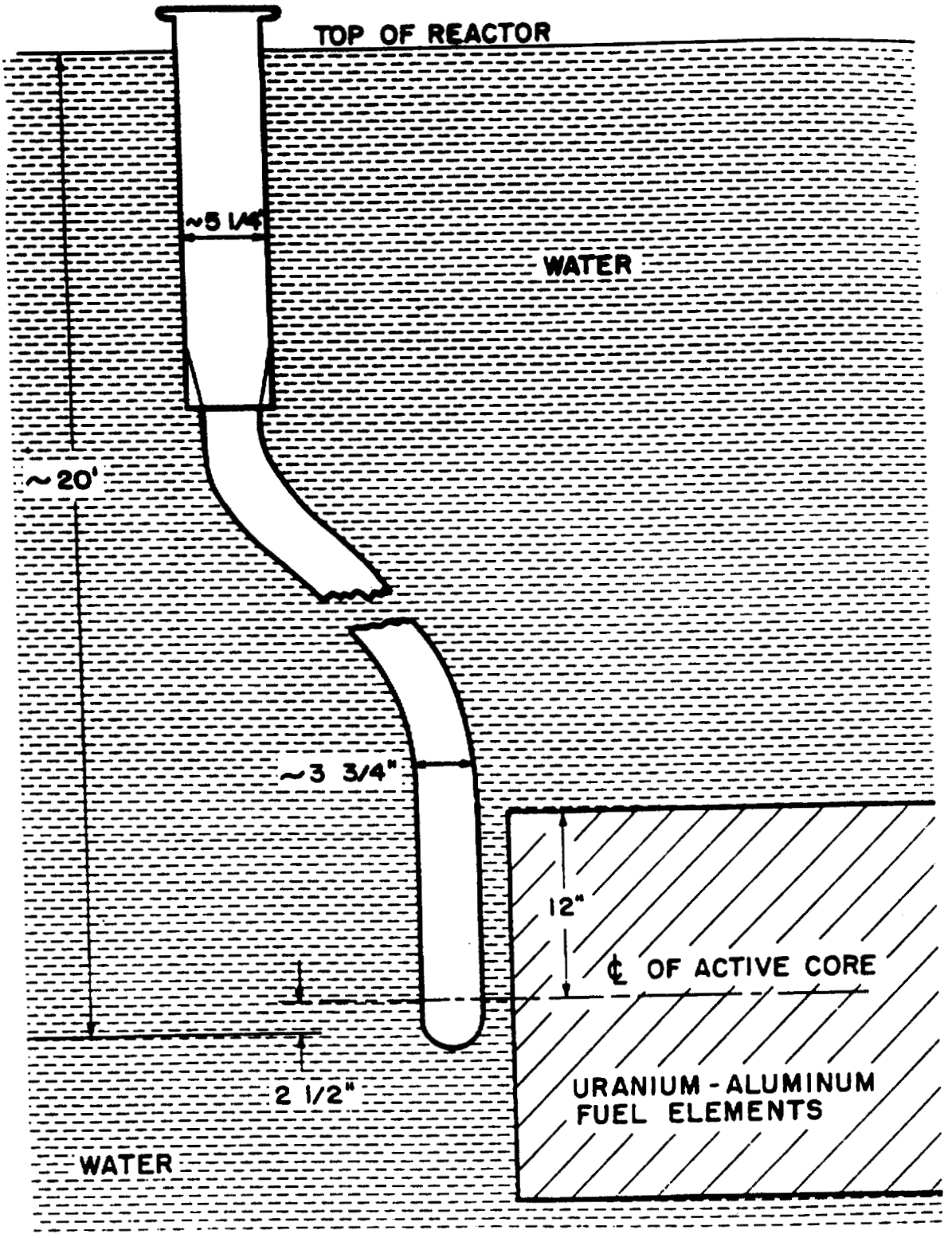

Fig. 1. Sandia port schematic diagram.

the fission foils of Pu^{239}, Np^{237}, and U^{238} were enclosed in 20 mil cadmium cans and placed inside the B^{10} sphere. The cadmium is used to absorb any thermal neutrons produced by the slowing down in the B^{10}. By suitable calibration of the counting equipment with thermal neutrons, fast neutron flux, spectrum, and first collision tissue dose can be evaluated for a fast neutron facility. The previous article described the counting equipment and calibrations used in these evaluations. References 3 and 4 present a more detailed description of the specific measurements.

The reactor was operated at 10 KW for this investigation. Each B^{10} ball was placed in a fixed position by the holder assembly shown in Fig. 2. The assembly consisted of approximately 1/16 in. thick, 3 in. diameter, aluminum cups attached to a flexible aluminum rod. The assembly was lowered into the port with piano wire. Five distances were investigated: 1, 7, 16, 31, and 46 in. from the bottom of the port. The sulfur pellets (1-1/2 in. in diameter and 3/8 in. in thickness) were placed in separate aluminum holders. These were irradiated separately from the fission foils. Both the fission foils and sulfur pellets received an integrated exposure of 30 KW-min (10 KW for 3 min).

Table 1 shows the preliminary neutron flux data obtained. The data are normalized to a working base of 5 MW. since this

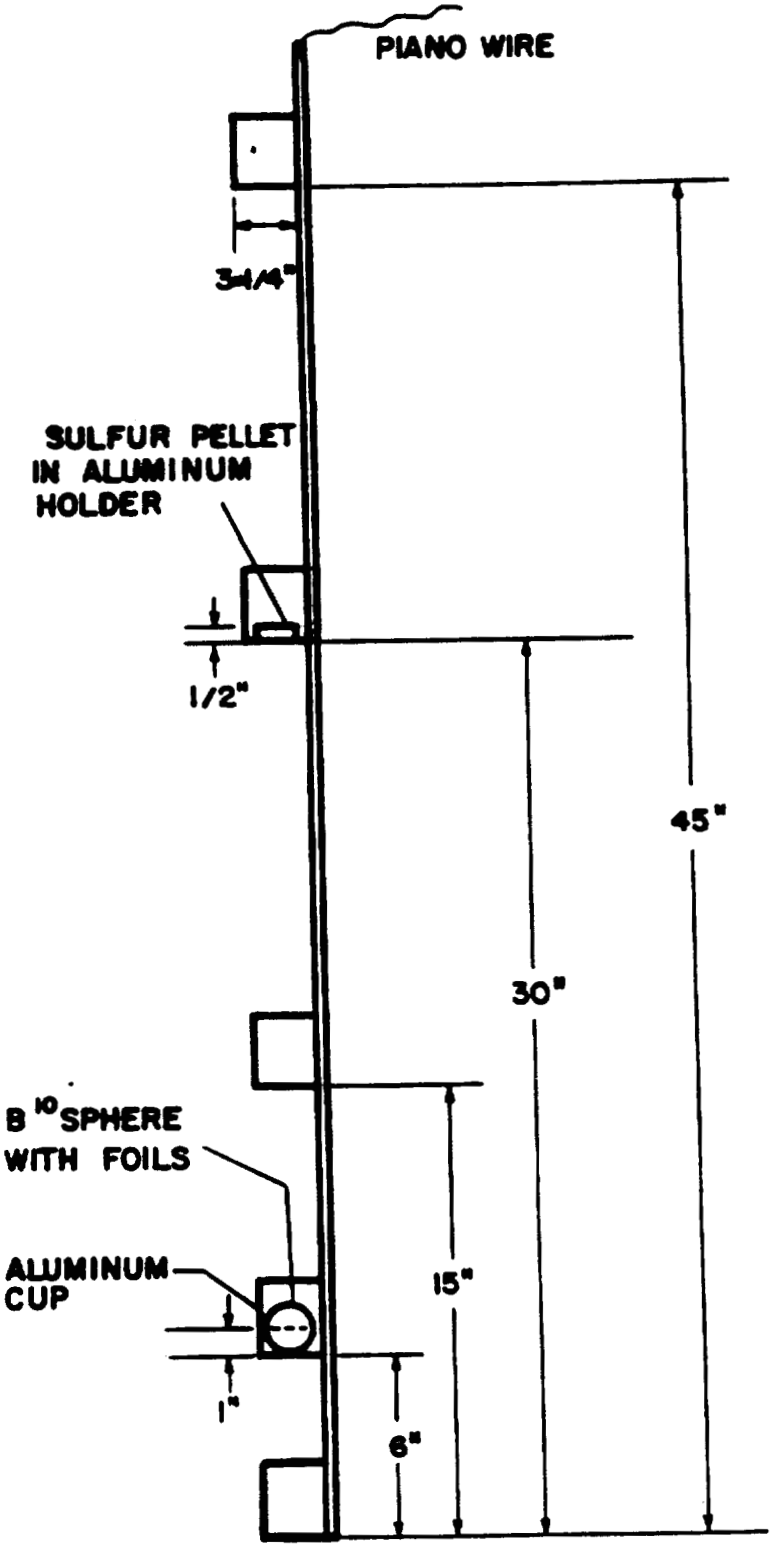

Fig. 2. Holder assembly.

TABLE 1. NEUTRON FLUX VERSUS DISTANCE RELATIONS FOR THE SANDIA PORT OF THE OMEGA WEST REACTOR FACILITY (Normalized to 5 MW-sec)

Distance from Bottom (in.)	Flux (n/cm^2/5 MW-sec x 10^{11})			
	F_{Pu} E_n > 0.004 Mev	F_{Np} E_n >0.75 Mev	F_U E_n >1.5 Mev	F_S E_n >2.5 Mev
1	25.3	15.4	10.1	4.11
7	16.5	9.78	6.78	2.78
16	3.17	1.90	1.28	0.625
31	0.0928	--	0.0300	0.0150

is the usual power at which the reactor is operated. Table 2 shows the neutron flux and tissue dose spectra, and Table 3 shows the neutron tissue dose versus distance relations. No data are reported on the 46 in. position because of the extremely low counting rates. The uncertainty of the reported measurements is approximately 18 per cent. A completion of this investigation requires the determination of the gamma contaminant, and it is hoped this phase will be completed during the next report period.

REFERENCES

(1) J. A. Sayeg, J. H. Larkins, and P. S. Harris, Los Alamos Scientific Laboratory Report LA-2174 (January 1958).

(2) G. S. Hurst and R. H. Ritchie, Oak Ridge National Laboratory Report ORNL-2748, Part A (November 1959).

(3) J. A. Sayeg, E. R. Ballinger, and P. S. Harris, Los Alamos Scientific Laboratory Report LA-2310 (March 1959).

(4) J. A. Sayeg, Los Alamos Scientific Laboratory Report LA-2432 (April 1960).

TABLE 2. NEUTRON FLUX AND TISSUE DOSE SPECTRA FOR THE SANDIA PORT OF THE OMEGA WEST REACTOR FACILITY

Energy Range (Mev)	Neutron Spectrum (per cent neutrons)	Tissue Dose Spectrum (per cent dose)
0.004 - 0.75	39.9	21.7
0.75 - 1.5	19.8	20.6
1.5 - 2.5	23.0	29.0
>2.5	17.6	28.7

TABLE 3. TISSUE DOSE VERSUS DISTANCE FOR THE SANDIA PORT OF THE OMEGA WEST REACTOR FACILITY

Distance from Bottom (in.)	Tissue Dose (rads)
	5 MW-sec
1	6026
7	3856
16	749
31	21.3

RADIOBIOLOGY SECTION PUBLICATIONS

(1) I. U. Boone, A. Murray III, and R. Des Prez, Metabolism of C^{14}-Isoniazid in Humans, Los Alamos Scientific Laboratory Report LA-2420 (August 26, 1960).

(2) M. J. Engelke, B. B. Riebe, and J. A. Sayeg, Neutron Tissue Dose Survey for the Little Eva Critical Assembly, Los Alamos Scientific Laboratory Report LA-2425 (August 5, 1960).

(3) P. S. Harris, Neutron and Gamma Integral Dose Measurements on Kiwi-A Prime, Los Alamos Scientific Laboratory Report LA-2456 (August 1960), (Classified).

(4) J. A. Sayeg, Revised Neutron Flux, Spectrum, and Tissue Dose Measurements at the Godiva II Critical Assembly -- Addendum to Los Alamos Report LA-2310, Los Alamos Scientific Laboratory Report LA-2432 (September 19, 1960).

(5) J. A. Sayeg, D. G. Ott, and P. S. Harris, Dosimetry for the Little Eva Critical Assembly. Neutron Flux, Spectrum, and Tissue Dose Evaluations, Los Alamos Scientific Laboratory Report LA-2468 (November 21, 1960).

(6) J. F. Spalding, V. G. Strang, and F. C. V. Worman, Effect of Graded Acute Exposures of Gamma Rays or Fission Neutrons on Survival in Subsequent Protracted Gamma-Ray Exposures, Rad. Res. 13, 415 (1960).

MANUSCRIPTS SUBMITTED

(1) R. Des Prez and I. U. Boone, Metabolism of C^{14}-Isoniazid in Humans, submitted to Am. Rev. Resp. Dis.

(2) J. F. Spalding, V. G. Strang, and W. L. LeStourgeon, Heritability of Radiation Damage in Mice, submitted to Genetics (in press).

(3) J. F. Spalding and V. G. Strang, Inheritance of Radiation-Induced Decrement in Ability of Mice to Withstand Protracted Gamma Radiation Stress, submitted to Rad. Res.

(4) J. F. Spalding, T. T. Trujillo, and W. L. LeStourgeon, Dependence of Recovery Half-Time on Magnitude of Conditioning Dose of Co^{60} Gamma Rays, submitted to Rad. Res.

(5) F. C. V. Worman, A Manual for Neutron Activated Foil Counting at the Nevada Test Site (December 1960), to be distributed to appropriate LASL personnel.

CHAPTER 6

RADIOPATHOLOGY SECTION

Clinical Applications of Whole Body Scintillometry. IV. Turnover Rate of Protein-Bound Iodide (C. C. Lushbaugh, D. B. Hale, and C. R. Richmond)

INTRODUCTION

This Laboratory reported previously (1,2) that whole body retention of I^{131} after oral ingestion reflected the functional status of the thyroid. A technique for determination of this retention in man and in animals was described, and the possible meanings of the two exponential regression lines were discussed. Because of erratic and irregular collection of human data after the first week of observation in this study, it was not possible to determine accurately the half-time of the second component of the retention curve, which appears to represent the turnover of bound iodide. This half-time seemed to be longer than 50 days. More recent data are reported here which seem to establish the slope of

this line accurately, while fixing the statistical limits of the level of normal iodide binding in man.

MATERIALS AND METHODS

The method of whole body counting previously described (1) was used. Twenty-six normal persons (17 women, 3 men, 3 girls, and 3 boys) were studied. Of these 26 subjects, 9 did not complete the rigid counting schedule, which demanded whole body radioactivity measurements immediately on the day of ingestion of the radioiodide and on the first, second, third, fourth, seventh, tenth, fourteenth, and eighteenth days following. These incomplete studies were not used in the first 2 methods of statistical evaluation, so each of the 9 data points consisted of 17 determinations (or subjects). Eight microcuries of I^{131} as sodium iodide was given orally 1 hour before the initial whole body count.

The statistical analysis was done by 3 different methods. The first method consisted of drawing an eye-fitted curve through the determined means for I^{131} retention on each day plotted on a semilogarithmic plot. The data comprising 6 points falling on a straight line were then analyzed by the method of least squares. They were also analyzed by a simplified IBM 704 computer line fitting program.* The third

*This analysis was done by H. Israel of Group H-6.

method consisted of a more complex line fitting IBM 704 computer program,* which took into consideration the data from the first 3 days which were ignored in the other 2 analyses and, in addition, also considered the data from the 9 subjects eliminated because of irregularities in the time schedule of data collection.

RESULTS

The results of these analyses are tabulated in Table 1 and in Fig. 1. The data in Fig. 1 are those determined by the third method, i.e., the complete line fitting 704 computer program. The figure also illustrates the parameters enumerated in the table. The 3 methods showed excellent agreement in the slope and half-time of the second component. The regression formula which represents the retention of I^{131} in normal human subjects appears to be:

$$R_t = 81.48\ e^{-2.05760\ t} + 18.47\ e^{-0.00754\ t}$$

The fiducial limits of these data are illustrated in Fig. 1 by 2 thin lines above and below the best fit line (heavy), representing 68 per cent ($\pm$ 1 standard deviation) and 95 per cent ($\pm$ 2 standard deviations) confidence areas about the mean.

---

*This analysis was performed by W. LeStourgeon of Group T-1 and C. R. Richmond of H-4.

TABLE 1. PARAMETERS OF WHOLE BODY IODINE^{131} RETENTION AFTER ORAL INGESTION BY NORMAL HUMAN SUBJECTS

Parameter	Line Fitting Methods		
	Least Squares (6 of 9 points)	IBM 704 Program 1 (6 of 9 points)	IBM 704 Program 2 (12 points)
Component I			
Slope	-2.368	---	-2.0576 ± 0.0169
Half-time	0.33 day	---	0.37 day
"0" Intercept	80.1%	---	81.48 ± 2.9%
Component II			
Slope	-0.008	-0.00837 ± 0.00115	-0.00754 ± 0.000481
Half-time	86.7 days	82.7 days	91.9 days
"0" Intercept	19.9%	19.9 ± 3.43%	18.47 ± 0.93%

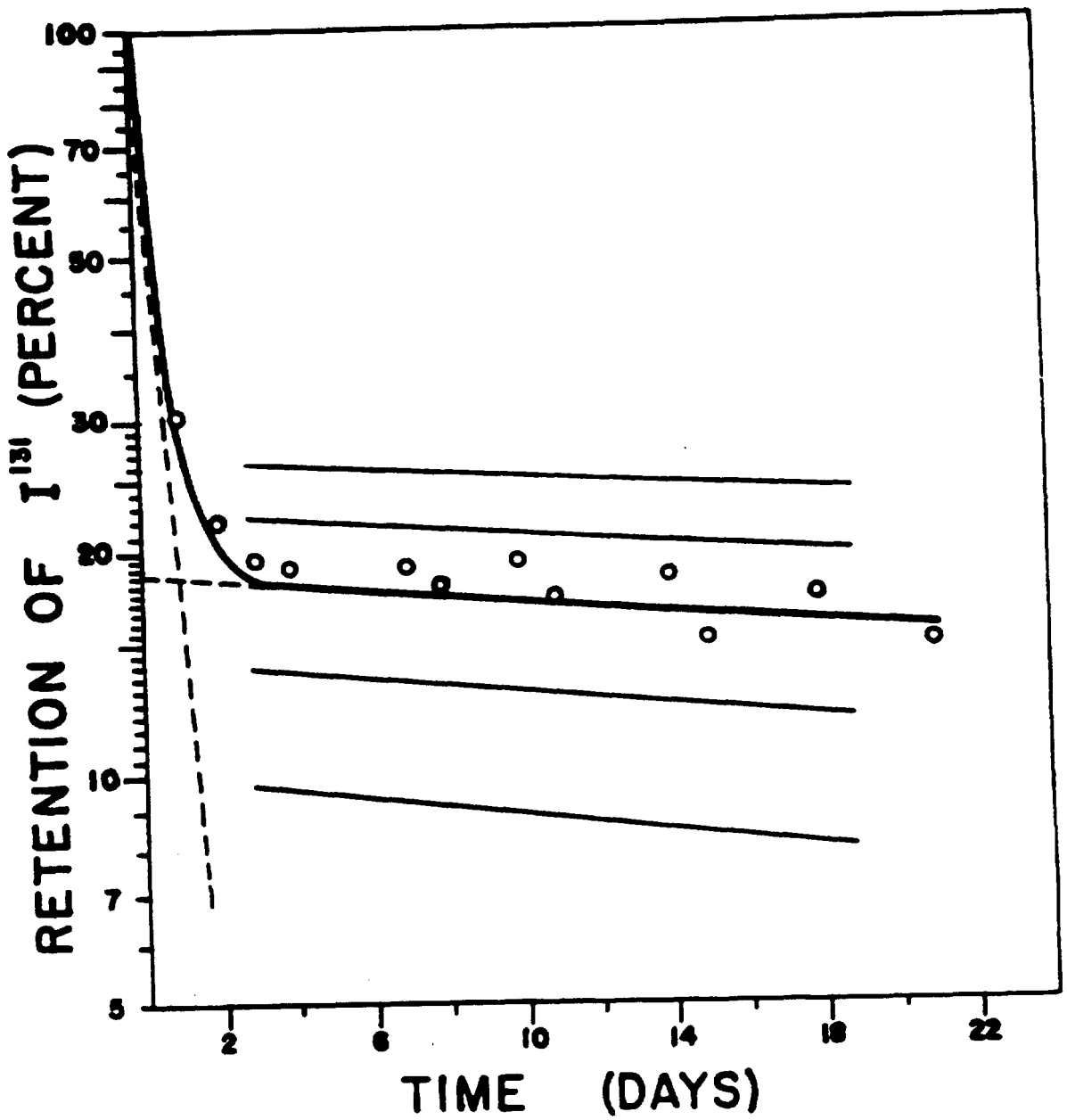

Fig. 1. Whole body retention curve of I^{131} in normal human subjects and the 2 component exponential regression lines, as determined by the IBM 704 line fitting Program 2. The thin lines parallel to the second component represent the 68 and 95 per cent fiducial limits of the fitted (heavy) line.

DISCUSSION

These data appear to determine the relative partitioning of absorbed iodide between the thyroid and the kidneys in normal human subjects. The variation that can be expected clinically in normal and diseased persons is also indicated. On the basis of this and previous studies (1-3), about 18.5 per cent of orally ingested iodide is bound by the thyroid, while 81.5 per cent is excreted by the kidneys. Variation in thyroid function in our normal persons and also in the method of study by whole body counting produces a wide range of normal uptake as defined by the 95 per cent confidence limits of the resulting data. Persons with a bound iodide retention line falling between 27.0 and 10.3 per cent can be considered, therefore, as having normal thyroid metabolism. Even with such a wide range, 3 of the "normal" individuals used in this analysis were excluded by this method as having a higher than normal thyroid iodide binding capacity. Although none of these 3 women seemed clinically hyperthyroid to us, 1 suffered from "nervousness and periodic attacks of trembling," 1 three years previously had had a subtotal thyroidectomy for Graves disease, and the other had been maintaining her slenderness by severe dietary restriction although she denied dieting during the study. We have previously shown that overnight starvation of laboratory rats (3) causes a 3 fold increase in

the average thyroid binding of I^{131}. It is apparent from that study and others (4) that increased thyroid (or whole body) retention of iodide does not necessarily mean "hyperthyroidism" any more than decreased retention in the presence of high iodide ingestion means "hypothyroidism." Pseudohyperthyroidism can obviously result from or be secondary to a low level of iodide consumption. This condition might be considered clinically as hyperthyroidism induced physiologically by hypoiodinism. Before such a diagnosis could be made with certainty, however, an iodine lack would have to be proven. This rather difficult task might be unnecessary if the patient being studied could be placed beforehand on a diet in which his daily iodine consumption was known. Since this procedure would be cumbersome routinely in all patients, we propose to restudy those patients who appear to be hyperthyroid by the whole body retention method, after a controlled period (1 week) of normal dietary iodide intake (about 300 μg of iodine).

The best information (4) available indicates that 57 to 87 μg of hormonal iodine from the 8000 μg of organic iodine in the thyroid is expended per day by normal persons, or that a little less than 1 per cent of the available iodine stores must be replaced each day. Our half-time of 91.9 days for the slope of the second exponential component (thought to be the biologic decay rate of organically-bound iodide in the

thyroid) results in a computed turnover rate of 0.755 per cent per day or a daily loss of 61 μg of iodide from the hormonal iodide pool. This seems to be remarkably precise agreement with these reported figures. The shortest half-time (82.7 days) for component II, obtained by our second analytical method, results similarly in a daily loss of 67 μg of iodide. These results seem to support strongly our conjecture that the second component of whole body iodide retention does represent the daily urinary loss of iodine from the thyroid hormonal-bound iodide pool.

REFERENCES

(1) C. C. Lushbaugh and P. S. New, Los Alamos Scientific Laboratory Report LAMS-2445 (1960), p. 348.

(2) C. C. Lushbaugh and D. B. Hale, Los Alamos Scientific Laboratory Report LAMS-2445 (1960), p. 361.

(3) C. C. Lushbaugh and D. B. Hale, Los Alamos Scientific Laboratory Report LAMS-2445 (1960), p. 375.

(4) S. C. Werner, ed., The Thyroid: A Fundamental and Clinical Text, Harper and Brothers, New York (1955).

Electronic Measurement of Cellular Volumes. I. Calibration of the Apparatus (C. C. Lushbaugh, J. A. Maddy, and N. J. Basmann)

INTRODUCTION

Diagnosis and treatment of anemia are based in part on the number and mean cellular volume (MCV) of circulating erythrocytes. Routinely these data are not obtained accurately because of inherent difficulties in the indirect hematocrit method used in determining the MCV. Fifty years ago, Price-Jones (1) showed that the frequency distribution of erythrocyte diameters varied in a diagnostically useful manner in some diseases, but this technique proved too laborious for routine use. Recently the development of electronic particle counting has enabled routine red and white blood cell counting to be done rapidly with less than 1 per cent error by unskilled persons (2). Because the amount of change in electrical resistance occurring during the passage of a cell through the counting aperture is proportional to the volume of solution displaced, this method can also be used for determining the volume of a cell directly. This report describes the progress made in combining the Coulter electronic particle counter with a LASL pulse height analyzing system affording an immediate visual display of the frequency distribution of erythrocyte volumes.

METHODS

A commercially available (Coulter) electronic particle counter and glassware with a 100-micron aperture were used in this study. The signal was obtained from the cathode follower circuit of the device and fed into a single-channel analyzer with upper and lower gate discriminators that allowed selection of pulse heights of from 4 to 104 volts. The chosen pulses were sorted in a 100-channel analyzer and their numbers collected in its memory storage unit whose capacity was limited by means of a scaler and count control unit which stopped the analysis when 100,000 cell passages were analyzed and stored. A cathode display unit allowed constant visualization of the distribution of the collected cell volumes, enabling rapid calibration of a Moseley autograph plotter to fit the frequency distribution curve being obtained. The data were graphed automatically as well as printed out on a computing tape recorder (Fig. 1).

The erythrocyte number per centimeter (RBC) of heparinized blood was determined with the Coulter counter in the accepted manner (2). Human, rabbit, and guinea pig blood were diluted 1:800,000; mouse, horse, and goat blood 1:1,600,000; reptilian and fowl blood 1:400,000 in order that a concentration of about 6000 RBC per ml of saline resulted. These high dilutions obviated correction of the

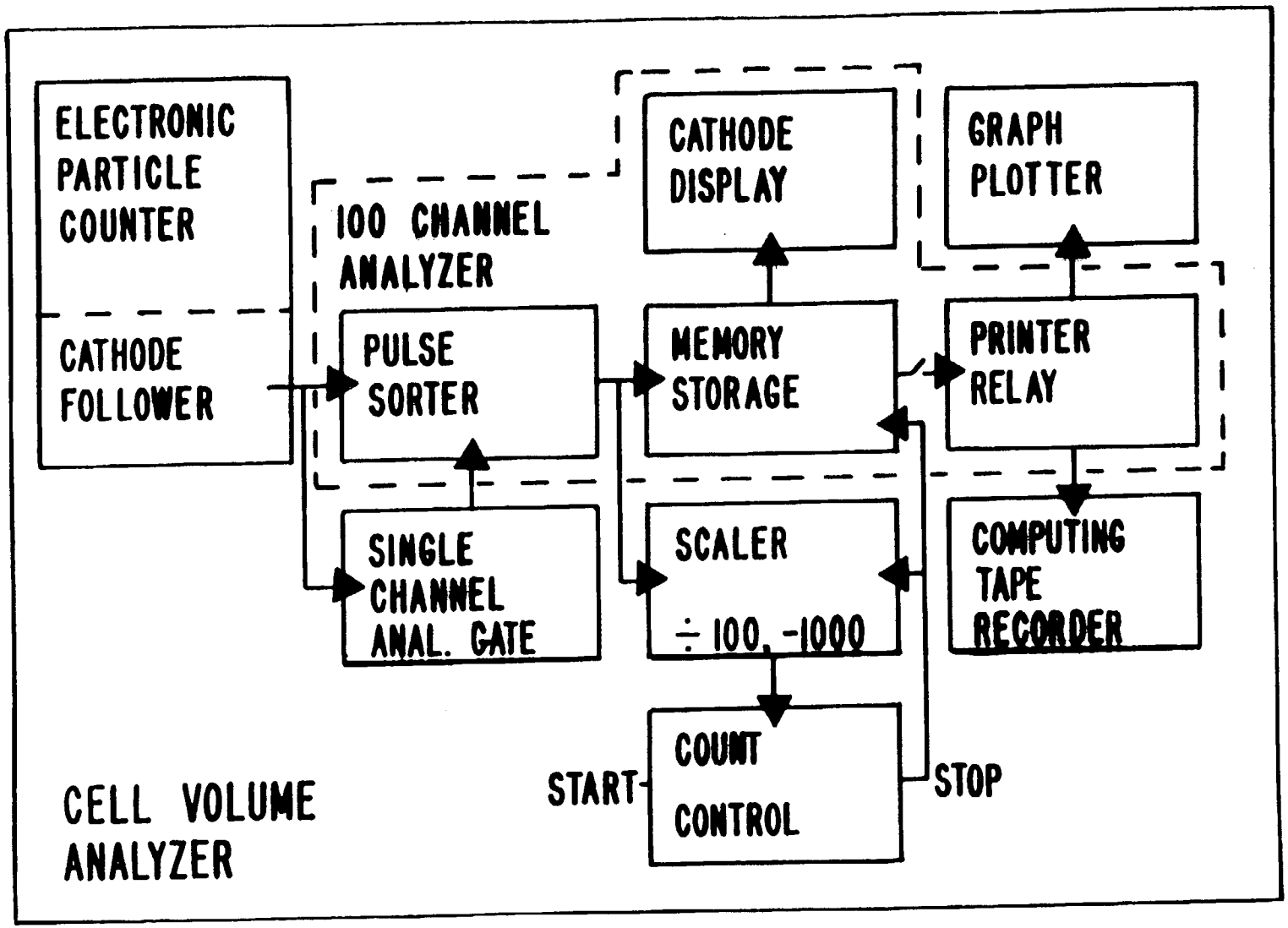

Fig. 1. Simplified scheme of arrangement of components of cell volume analyzer.

curves for coincidence error and analyzer "dead time" loss. Microhematocrits (Hmct) were done simultaneously with the RBC and the mean corpuscular volume (MCV) determined for each sample by the formula

$$\frac{\text{Hmct} \times 10}{\text{RBC}} = \text{MCV}.$$

The analyzer channel in which the mean cell volume appeared to fall electronically was found by determining mathematically the weighted mean of the frequency distribution curve (Fig. 2). This mean channel number plus 4* equalled the mean pulse height in volts (mean pulse voltage = MPv). The MCV of each sample was then plotted against the MPv to obtain best fit lines that could be used to convert pulse height voltage readings into cubic microns. In this part of the study, the blood of 8 mice, 6 rabbits, 4 guinea pigs, 25 men, 10 chickens, and 5 ducks was used because the means of the MCV of the cells of these species were widely spaced when plotted against their respective MPv (Fig. 3).

By altering the aperture current settings (ACS) of the Coulter counter, the amount of current passing through the counting aperture can be varied, so that pulses caused by

*No pulses less than 4 volts in height were measured. The first analyzer channel counted pulses of 4 volt strength, the second channel 5 volt pulses, and so on.

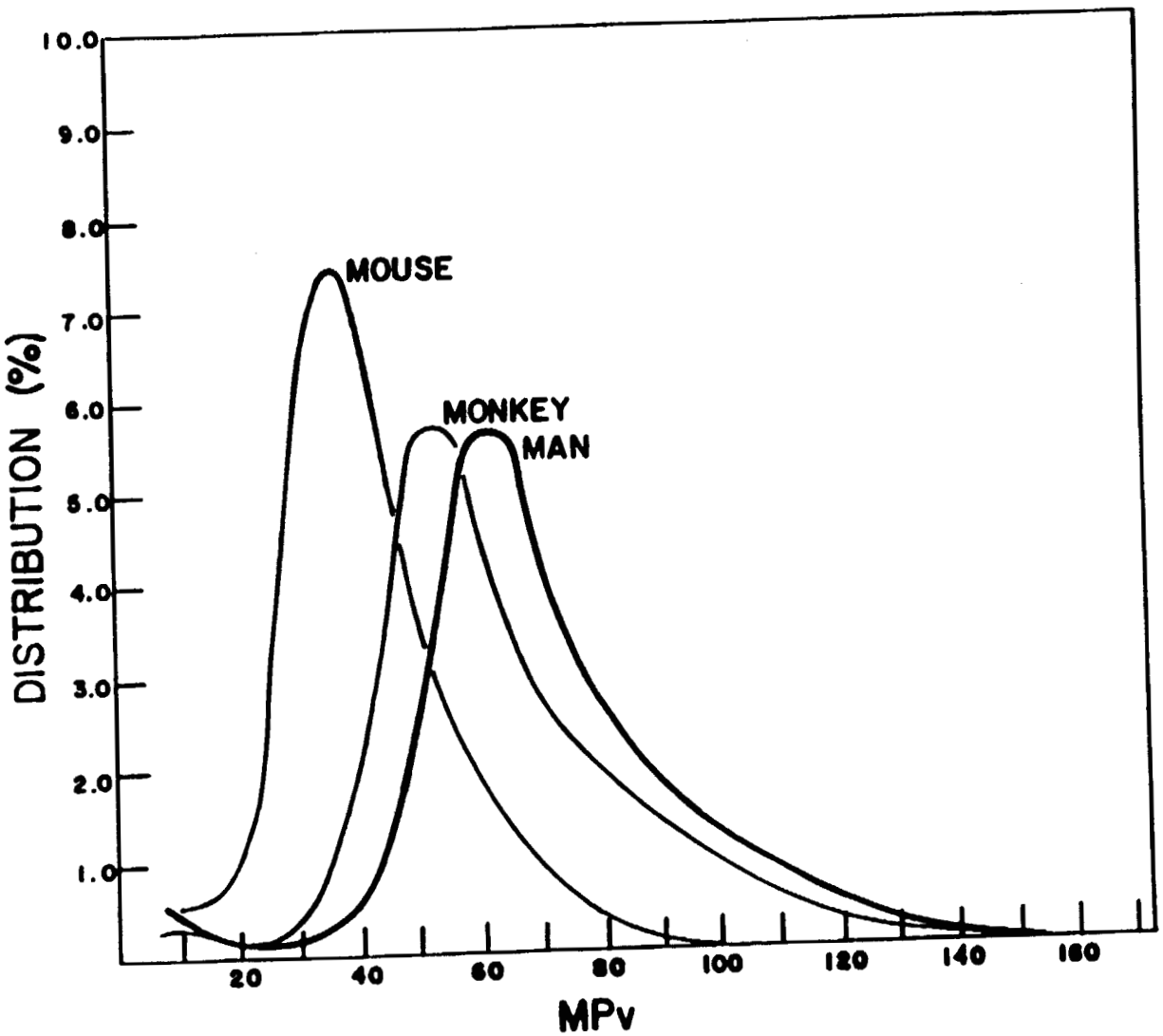

Fig. 2. Frequency distribution profiles of erythrocyte populations of mouse, monkey, and man determined electronically.

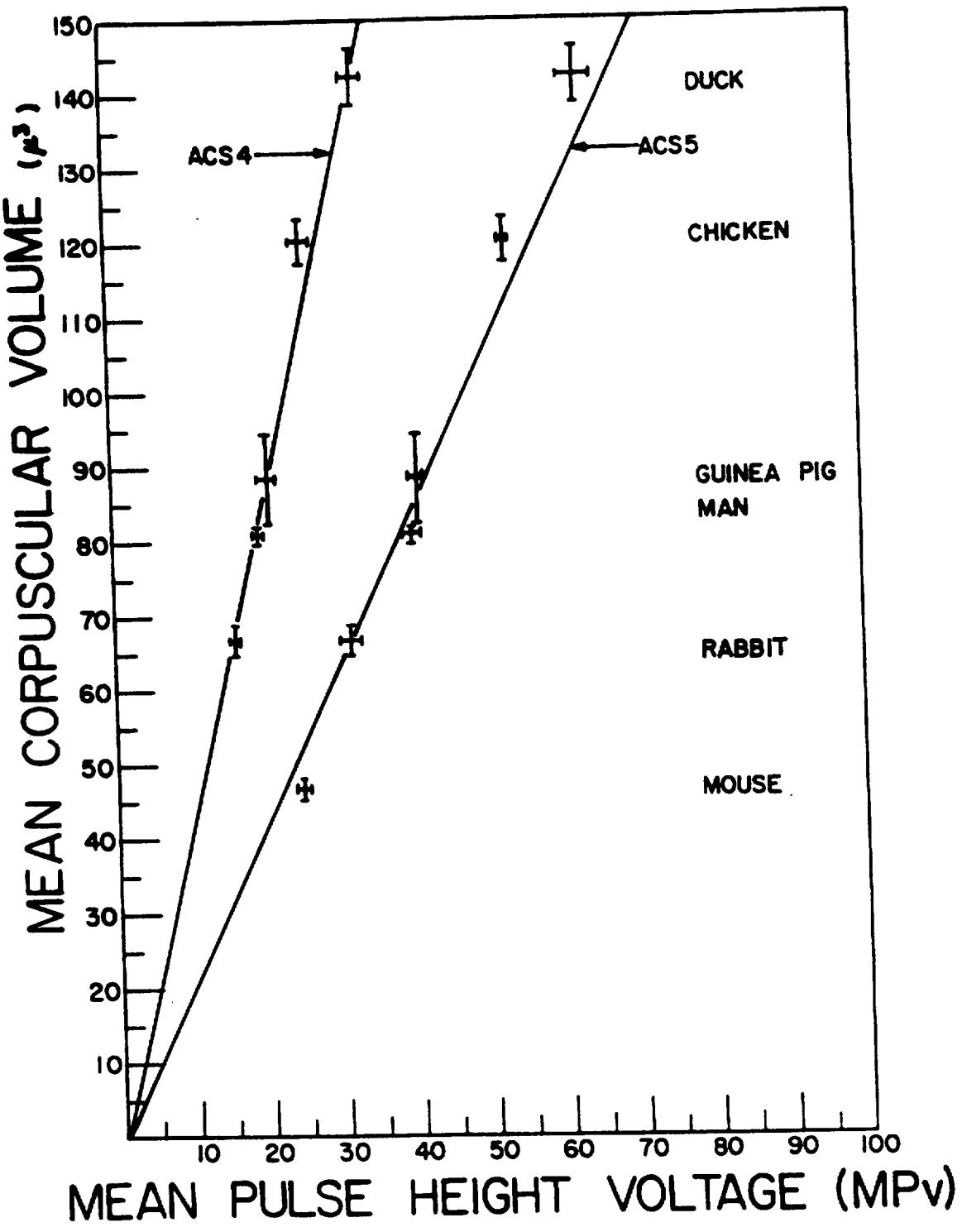

Fig. 3. Best fit lines showing relationship of MCV to MPv for ACS4 and ACS5.

populations of large cells are decreased and by populations of small cells are increased. In this manner, most cell populations can be made to produce pulses varying from 4 to 104 volts so that the entire frequency distribution profile can be contained within the limits of the 100 analyzer channels. In this calibration study, aperture current settings of 4 and 5 were used routinely to analyze each sample. When available, populations with very small cells (e.g., horses, goats, and cats) were re-analyzed at ACS6, ACS7, and ACS8, and those with very large cells (e.g., birds and reptiles) were re-analyzed with ACS1, ACS2, and ACS3. This procedure was followed to determine the alteration of apparent size caused by changes in aperture voltage and thereby relate the 8 ACS's of the Coulter counter to one another. By means of the effect of ACS on pulse heights of cells of constant volume, mathematical factors were determined for converting pulse height voltage to cubic microns for ACS1 through ACS8.

RESULTS

Typical frequency distribution profiles for the RBC of mouse, monkey, and normal man are shown in Fig. 2. The populations were found to be asymmetrical so that the mean cell volume and the most frequent cell volume (mode) were not identical, making it necessary to determine the MCV or MPv mathematically.

In Table 1, the experimental data have been tabulated in order to show the differences in the MCV of the RBC of the 6 species studied and the mean MPv obtained for these volumes with ACS4 and ACS5. The relationships of these data are shown in Fig. 3. The mouse point was omitted at ACS4 because many of the smaller mouse RBC's did not produce pulses greater than 4 volts so that an erroneously high MPv was obtained. While the mouse point was still skewed slightly to the right of the line at ACS5, the duck and chicken points were skewed to the left of the line at ACS5 because at this aperture current the largest RBC of these species created pulses greater than 104 volts and were, therefore, not analyzed. The analyzer loss of these large cells caused an apparent decrease in the mean of these populations. The modification in the relationship of cell volume to pulse height voltage affected by aperture current is shown in Fig. 4. The data illustrated in these 2 figures and in Table 1 enabled the determination of the conversion factors tabulated in Table 2. It was found that the apparent volume indicated by the channel width of the analyzer varied with amount of aperture current so that, for example, at ACS1 a single channel indicated a volume of 17.33 μ^3 while at ACS6 the indicated volume was 1 μ^3. These volumes have been designated at Factor 1 in Table 2, and can be used as factors to convert the analyzer channel

TABLE 1. RELATIONSHIP OF AVERAGE MCV OF RBC OF SIX SPECIES WITH THE AVERAGE MPv OF THEIR FREQUENCY DISTRIBUTION CURVES AT ACS4 AND ACS5

Species	No.	MCV* (μ^3)	MPv (ACS4) (volts)	MPv (ACS5) (volts)
Mouse	8	46.9 ± 1.5**	--	24.9 ± 0.6
Rabbit	6	66.9 ± 2.0	16.0 ± 0.8	31.5 ± 1.4
Man	25	81.1 ± 1.2	19.3 ± 0.6	40.0 ± 1.3
Guinea pig	4	88.6 ± 6.4	20.7 ± 1.2	40.6 ± 0.9
Chicken	10	120.3 ± 3.2	25.8 ± 1.3	53.3 ± 0.5
Duck	5	142.5 ± 3.7	33.2 ± 1.4	63.1 ± 2.7

*$\frac{\text{Hmct x 10}}{\text{RBC}}$ = MCV.

**Standard error.

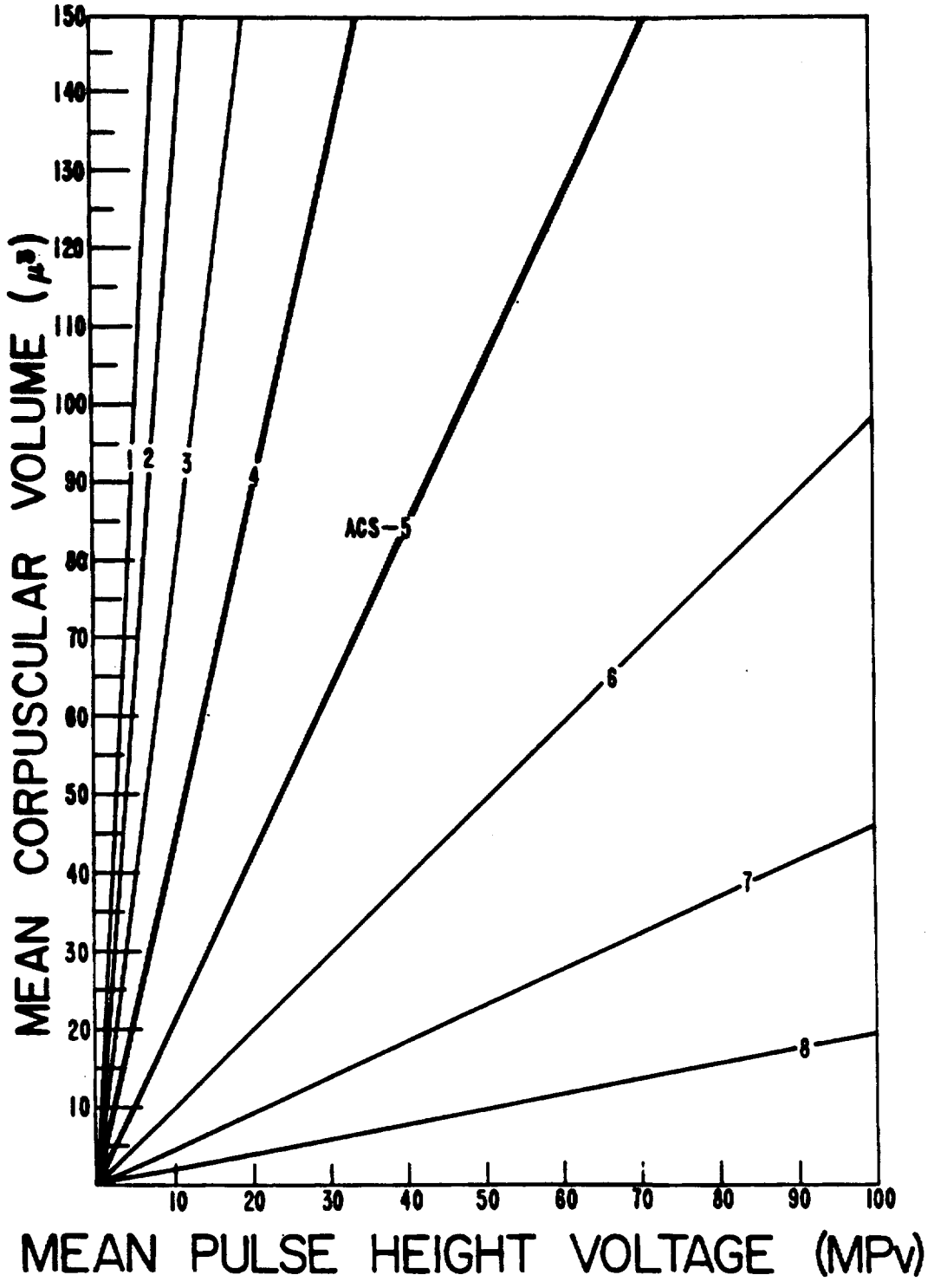

Fig. 4. The effect of aperture current setting (ACS) upon the relationship of particle volume to pulse height voltage.

TABLE 2. CONVERSION FACTORS FOR CHANNEL NUMBER TO CUBIC MICRONS (ACS5)

ACS No.	F_1 Anal. Channel Volume (μ^3)	F_2 Pulse Height $\Updownarrow$ 1 μ^3 (volts)	F_3 Channel Volume Relative to ACS5	F_4 Approximate Magnification Relative to ACS5
1	17.33	0.06	8.10	0.1
2	11.30	0.09	5.28	0.2
3	7.55	0.13	3.48	0.3
4	4.33	0.23	2.02	0.5
5	2.14	0.47	1.00	1.0
6	1.00	1.00	0.47	2.0
7	0.46	2.17	0.29	3.5
8	0.19	5.26	0.09	11.0

number or voltage into volume and to construct scales for the visual conversion of channel number (or voltage) to volume, as shown in Table 3 for ACS5. Factor 2 in Table 2 designates the pulse height voltage equivalent to 1 μ^3 at the 8 aperture current settings and can be used to compute the effect of volumetric change upon pulse height and subsequent analyses. Factor 3 in Table 3 can be used to convert the volumetric scale for ACS5 (Table 3) to a scale for any other ACS setting and thus to approximate cell volumes relative to the human erythrocyte. Similarly, Factor 4 enables the use of the aperture current settings as microscope objectives and shows the magnification produced by the apparatus in relation to human erythrocytes at ACS5. For example, an object measured at ACS8 appearing on the viewer in channel 32 is magnified 11 times relative to a human erythrocyte in that channel and, therefore, has a volume of about 7 μ^3 instead of 77 μ^3 (channel 32 + 4 = 36 volts; 36 x 2.14 = 77 μ^3, or 36 x 0.19 = 6.8, or 77/11 = 7).

DISCUSSION

Variation in resistances and internal gain adjustments produce sufficient differences in pulse heights to make it necessary to calibrate each instrument in the manner described here. Calibration of a second instrument could be greatly

TABLE 3. VISUAL CONVERSION OF PULSE HEIGHT VOLTAGE (CHANNEL NUMBER + 4) TO CUBIC MICRONS AT ACS5

Pulse (volts)	Volume (μ^3)	Pulse (volts)	Volume (μ^3)	Pulse (volts)	Volume (μ^3)	Pulse (volts)	Volume (μ^3)
1	2.1	26	55.6	51	109.1	76	162.6
2	4.3	27	57.8	52	111.3	77	164.8
3	6.4	28	59.9	53	113.4	78	166.9
4	8.6	29	62.1	54	115.6	79	169.1
5	10.7	30	64.2	55	117.7	80	171.2
6	12.8	31	66.3	56	119.8	81	173.3
7	15.0	32	68.5	57	122.0	82	175.5
8	17.1	33	70.6	58	124.1	83	177.6
9	19.3	34	72.8	59	126.3	84	179.8
10	21.4	35	74.9	60	128.4	85	181.9
11	23.5	36	77.0	61	130.5	86	184.0
12	25.7	37	79.2	62	132.7	87	186.2
13	27.8	38	81.3	63	134.8	88	188.3
14	30.0	39	83.5	64	137.0	89	190.5
15	32.1	40	85.6	65	139.1	90	192.6
16	34.2	41	87.7	66	141.2	91	194.7
17	36.4	42	89.9	67	143.4	92	196.9
18	38.5	43	92.0	68	145.5	93	199.0
19	40.7	44	94.2	69	147.7	94	201.2
20	42.8	45	96.3	70	149.8	95	203.3
21	44.9	46	98.4	71	151.9	96	205.4
22	47.1	47	100.6	72	154.1	97	207.6
23	49.2	48	102.7	73	156.2	98	209.7
24	51.4	49	104.9	74	158.4	99	211.1
25	53.5	50	107.0	75	160.5	100	214.0

simplified, however, by referring it to the first by simultaneously determined measurements of the same sample in both instruments. It would also not be necessary to compare MCV with MPv, since the comparison of the MPv or of the modal Pv in both machines would enable the conversion of the various calibration factors.

The results of this calibration study indicate that a rapid, simple calibration could be done using only human erythrocytes and treating each case separately. For standardization purposes, human red blood cells from normal young adults are more uniform and have a more constant volume distribution than any commercially available particles of this size range. Most commercially available particles are either too small, as in the case of Latex, or too small and variable, as in the case of puff balls, to be used as a standard for either finite calibration or the daily control of analyzer drift. The human red cell proved in this study to be quite adequate for this purpose.

A preliminary study of the frequency distribution curves of red blood cell populations using these calibrations and techniques is to be reported later (5).

REFERENCES

(1) C. Price-Jones, Brit. Med. J. 2, 1418 (1910).

(2) G. Brecher, M. Schneiderman, and G. Z. Williams, Am. J. Clin. Path. 26, 1439 (1956).

(3) C. F. Mattern, F. S. Brackett, and B. J. Olsen, J. Appl. Physiol. 10, 56 (1957).

(4) A. C. Peacock, G. Z. Williams, and H. F. Mengoli, J. Nat. Cancer Inst. 25, 63 (1960).

(5) C. C. Lushbaugh, N. J. Basmann, and B. Glascock, this report (1961), p. 387.

Electronic Measurement of Cellular Volumes. II. Frequency Distribution of Erythrocyte Volumes (C. C. Lushbaugh, N. J. Basmann, and B. Glascock)

INTRODUCTION

The apparatus, technique, and calibrations described previously (1) were used to study the frequency distribution of erythrocyte volumes in man and in other animals. These analyses were done in order to determine whether such population curves might vary in a manner that might prove useful either theoretically or practically in clinical or descriptive hematology.

METHODS

Blood samples were obtained in dry, heparinized capillary tubes. Five lambda of the sample was diluted with 10 ml of saline. One-half ml of this suspension was then diluted with 200 ml of saline, agitated thoroughly, and then counted in the usual manner in the Coulter counter. The second dilution was changed if the resulting count did not fall between 3000 and 4000 cells per 0.5 ml in 13 seconds. When the standard counting rate was obtained, the frequency distribution of the volumes of the cells was determined using the 100-channel pulse height analyzer unit previously described (1). The resulting curves were compared visually

and then analyzed as a spectral curve and as a composite of 2 populations of normally distributed (Gaussian) particles.

ANALYTICAL PROCEDURES

In Fig. 1, a stylized population profile (frequency distribution of volumes) for circulating mammalian erythrocytes has been drawn. It defines the terms used in the first type of analysis done in this study. In this analysis, the curve was considered a spectral peak whose resonance or resolution could be expressed mathematically by its modal frequency, mode, mean, width at half-height, and fractional width. The term "fractional width" was used because this seemed to be less confusing than the spectrographic one of "resolution" and was determined by dividing width by mode. These numbers were used as channel volts without conversion to cubic microns.

In the second mathematical analysis, a 704 IBM computer was used;* after proper programming, the computer attempted to fit 2 (or sometimes 3) normal Gaussian curves to the population profile curve as it was obtained by the 100-channel analyzer. The data obtained were then expressed graphically as in Figs. 2 and 3, and mathematically as proportional areas under the total curve with standard deviations of the Gaussian curves enclosing these areas.

---

*This computer program was arranged and operated for us by H. Israel of Group H-6.

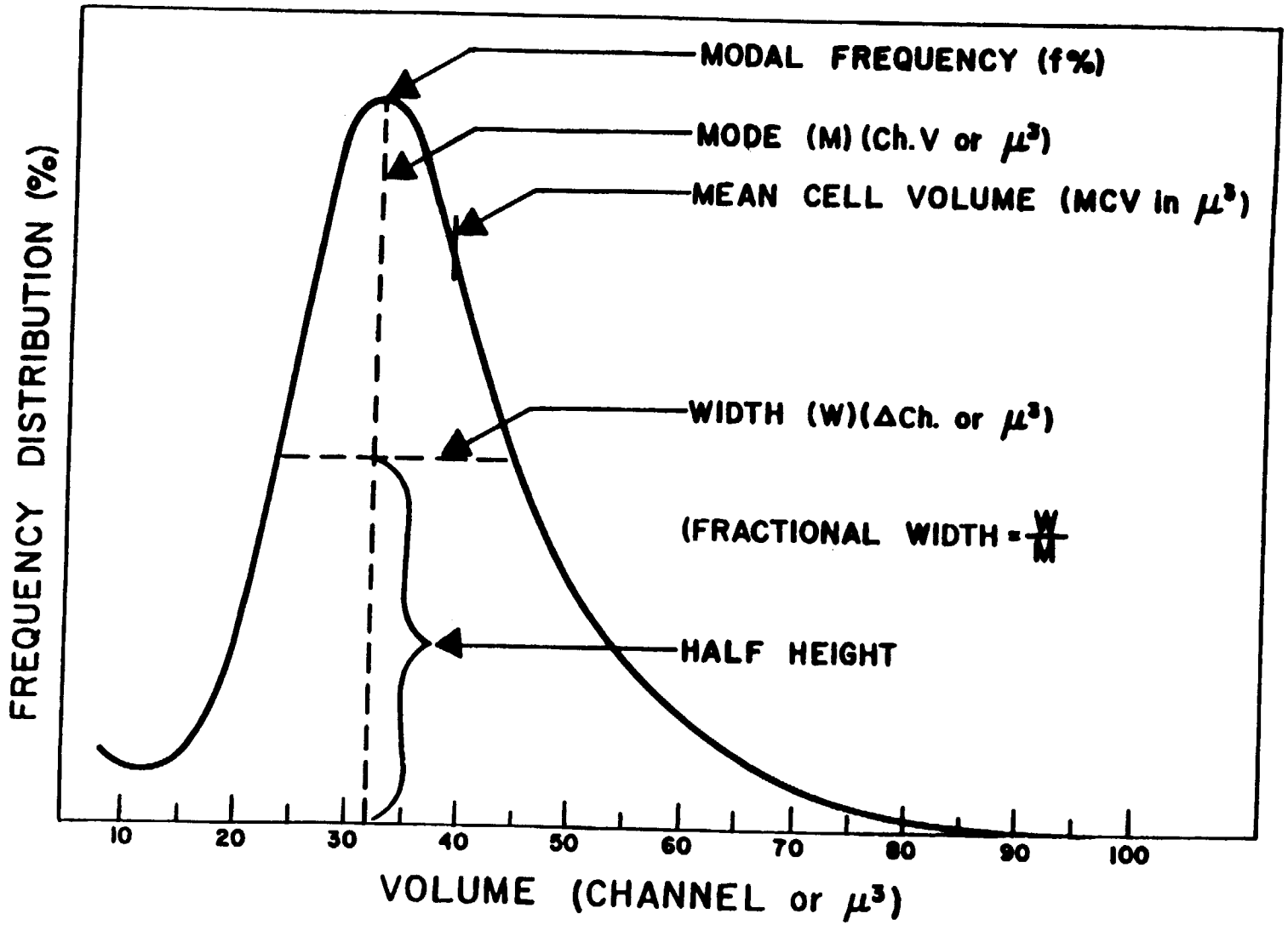

Fig. 1. Stylized frequency distribution of erythrocyte volumes defining the terms used in the "spectral" type of analysis.

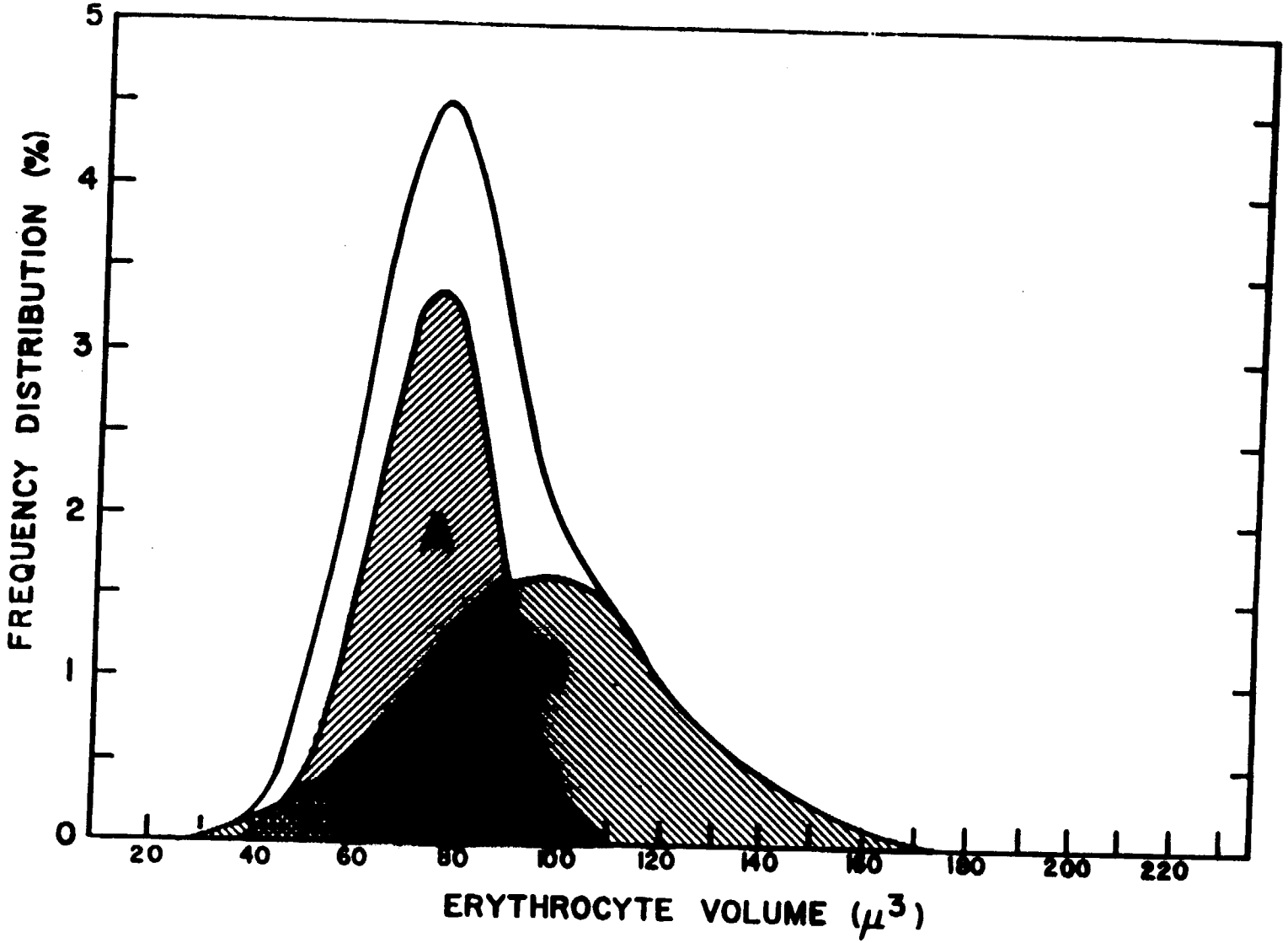

Fig. 2. Frequency distribution curve of erythrocyte volumes of human blood and its representation by 2 cell populations (A and B), each with a normal Gaussian distribution.

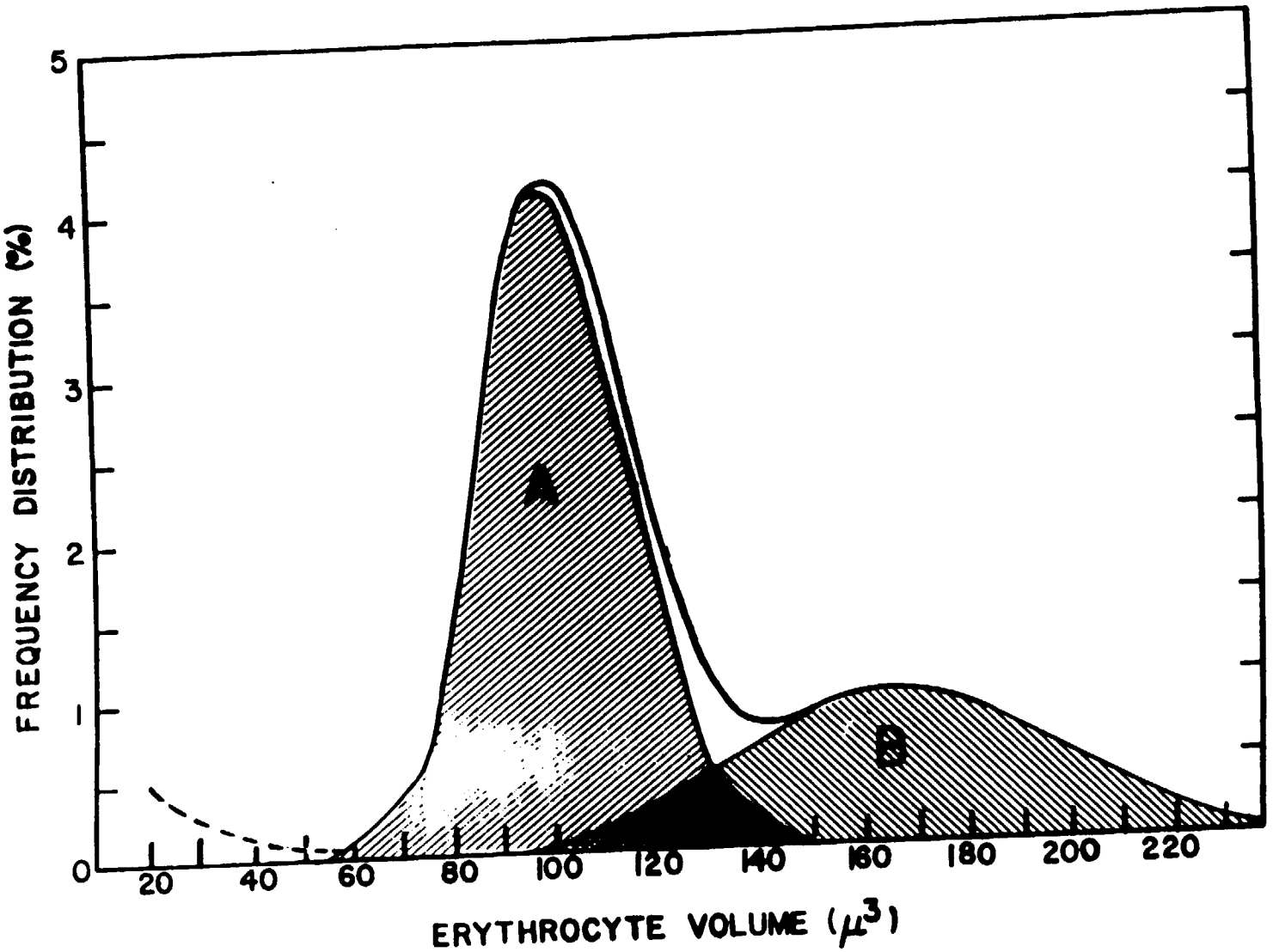

Fig. 3. Frequency distribution curve of erythrocyte volumes of chicken blood and its representation by 2 cell populations (A and B), each with a normal Gaussian distribution.

RESULTS

The results of the spectral analysis of these population profiles are tabulated in Table 1. Their fractional width was found to vary between 0.40 and 0.60 in healthy man, mouse, monkey, chicken, frog, and toad. In several questionably sick horses, as well as in 12 patients suffering from various anemias, the width of the RBC population profile was increased by a skewing of the curve to the large side of the mode so that a large increase in fractional width occurred. In man, if anemia was present, this measurement was always found to be greater than 0.6; the mean W/M was 0.80.

It was also found that as the mode became smaller its frequency increased, the width of the peak became narrower, and the mean moved closer to the mode. The mean never coincided with the mode because of the skew to the larger volume. In birds and reptiles especially but in occasional ill human beings, this skew could be seen visually to be the result of an overlapping large-volume population of cells. Examination of Wright-stained blood films of such specimens proved that if such a larger population did exist, it was not possible to determine it microscopically, although it was possible to determine that the bulge to the right was not caused by leukocytes.

It was quite gratifying, therefore, to have the IBM 704

TABLE 1. FRACTIONAL WIDTHS OF RBC POPULATION PROFILES (ACS5)

Species	No.	Frequency (per cent)	Width (ΔCh.)	Mode (Ch.)	Mode (μ^3)	Fractional Width (W/M)
Normal Man	14	4.5	17.3	33.0	70.6	0.52
Pathologic Man	12	3.6	26.2	33.3	71.6	0.80
Normal Mouse	8	7.8	11.0	18.0	38.5	0.61
Normal Chicken	13	4.0	16.3	38.6	82.6	0.42
Normal Monkey	1	5.6	16.0	27.0	57.8	0.59
Normal Frog*	1	3.1	22.0	40.0	85.6	0.55
Normal Toad*	1	3.8	18.0	39.0	83.5	0.46
Normal (?) Horse	5	6.8	12.9	12.8	27.4	1.00
	3**	4.0	21.0	28.0	28.0	0.75

*ACS = 3.

**ACS = 6.

computer analysis produce de novo perfect 2 Gaussian population fits to the curves, as shown in Figs. 2 and 3. Figure 2 shows the 2 overlapping populations of RBC in a normal young girl, a picture which has become the rule as these 704 computer analyses have continued, with population A comprising 45.6 per cent and population B 54.4 per cent of the total area or number of RBC analyzed. In Table 2, the other parameters of these 2 normal human RBC populations are listed. They show that population A is more uniform and volumetrically smaller than population B, although comprising about half of the total circulating red blood cells.

In Fig. 3, a similar analysis is depicted for the blood of a chicken. Population B is so far to the right of population A that it is rather well defined by the total curve. One can see that the 2 populations of chicken RBC have fewer cells with identical volumes than is the case with human blood.

DISCUSSION

The fact that there are 2 distinct populations of RBC circulating at 1 time in the same individual has been surmised before on the grounds of different sensitivities to various hemolysins (2) but has never obtained good morphologic support before.

If the 2 populations of red blood cells, demonstrated here

TABLE 2. AVERAGE PARAMETERS OF ERYTHROCYTE POPULATIONS IN NORMAL HUMANS

Population	(per cent)	σ (Width) (μ^3)	Mode (μ^3)
A	45.6	11.7 ± 2.4	72.8 ± 11.6
B	54.4	28.5 ± 5.4	95.0 ± 14.8

B/A = 1.36 ± 0.07.

mathematically, correspond physiologically with the 2 kinds of cells that can be differentiated by hemolysins, one would expect population A to consist of older, more fragile cells than population B, since it is well known that reticulocytes and relatively new red cells are larger than senile cells which are also hemolysin-sensitive. If so, this method should show in a hemolytic anemia a shift in favor of population B. In Figs. 4 and 5 this conjecture appears to be substantiated. It depicts 2 cases of the hemolytic anemia, erythroblastosis fetalis, that were transfused with normal adult blood. The preponderance of population B can be seen before transfusion in both cases, and its diminution afterwards. In the more severely affected case (Fig. 4), only population B appears to have been present before the exchange transfusion was done.

This hypothesis that young, newly formed cells comprise population B would seem to be susceptible to experimental verification. Such experiments are contemplated. If they support this hypothesis, the size of population B could be interpreted as the animal's response to his disease and would explain the increase in fractional width seen by us so far in all anemic disease states.

These preliminary studies of the variation and characteristics of RBC population profiles, as measured and analyzed electronically, have been sufficiently fruitful and the

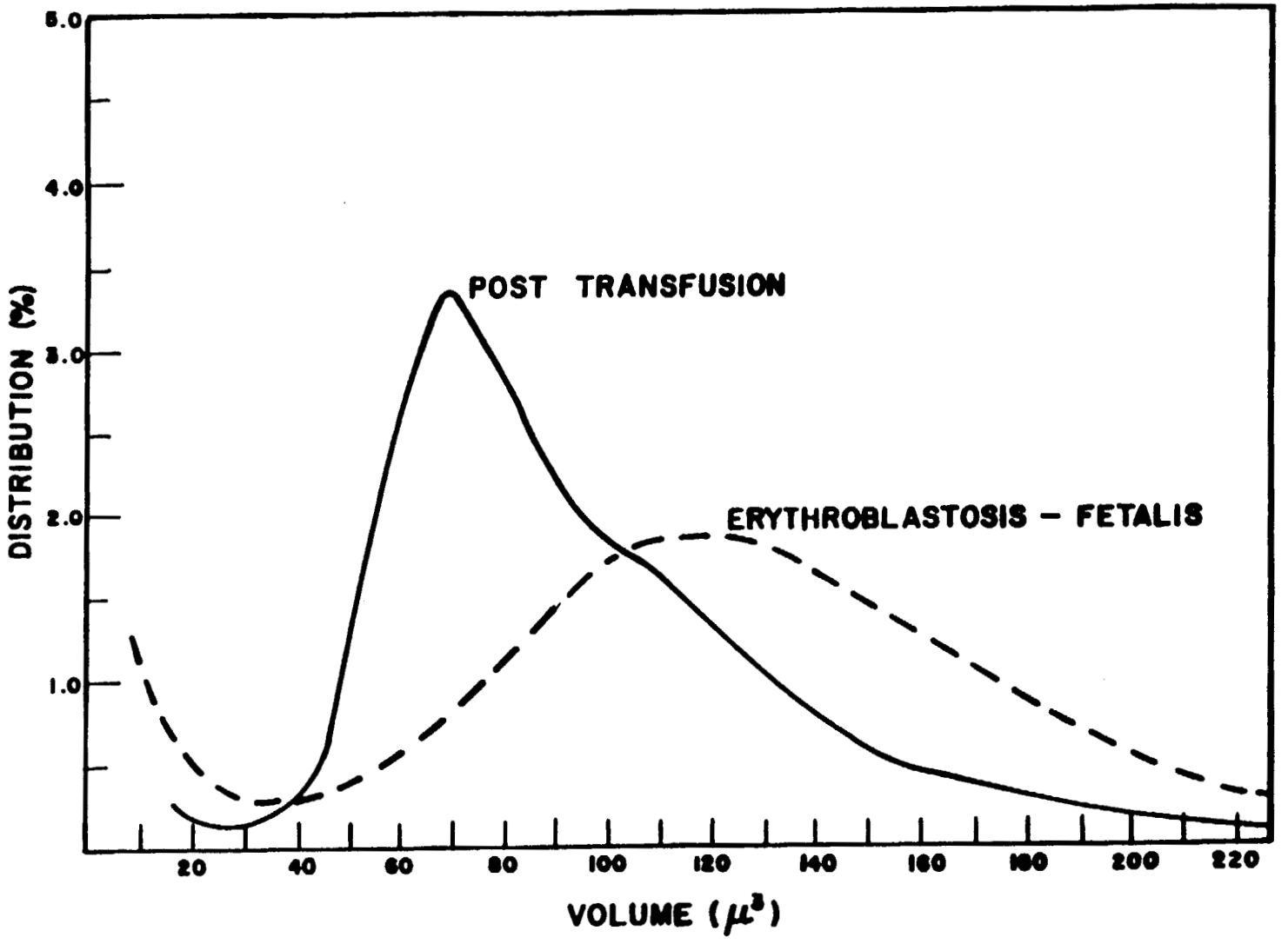

Fig. 4. Pre- and post-transfusion red blood cell profiles in a case of erythroblastosis fetalis showing the large cell preponderance in the presence of active hemolytic disease.

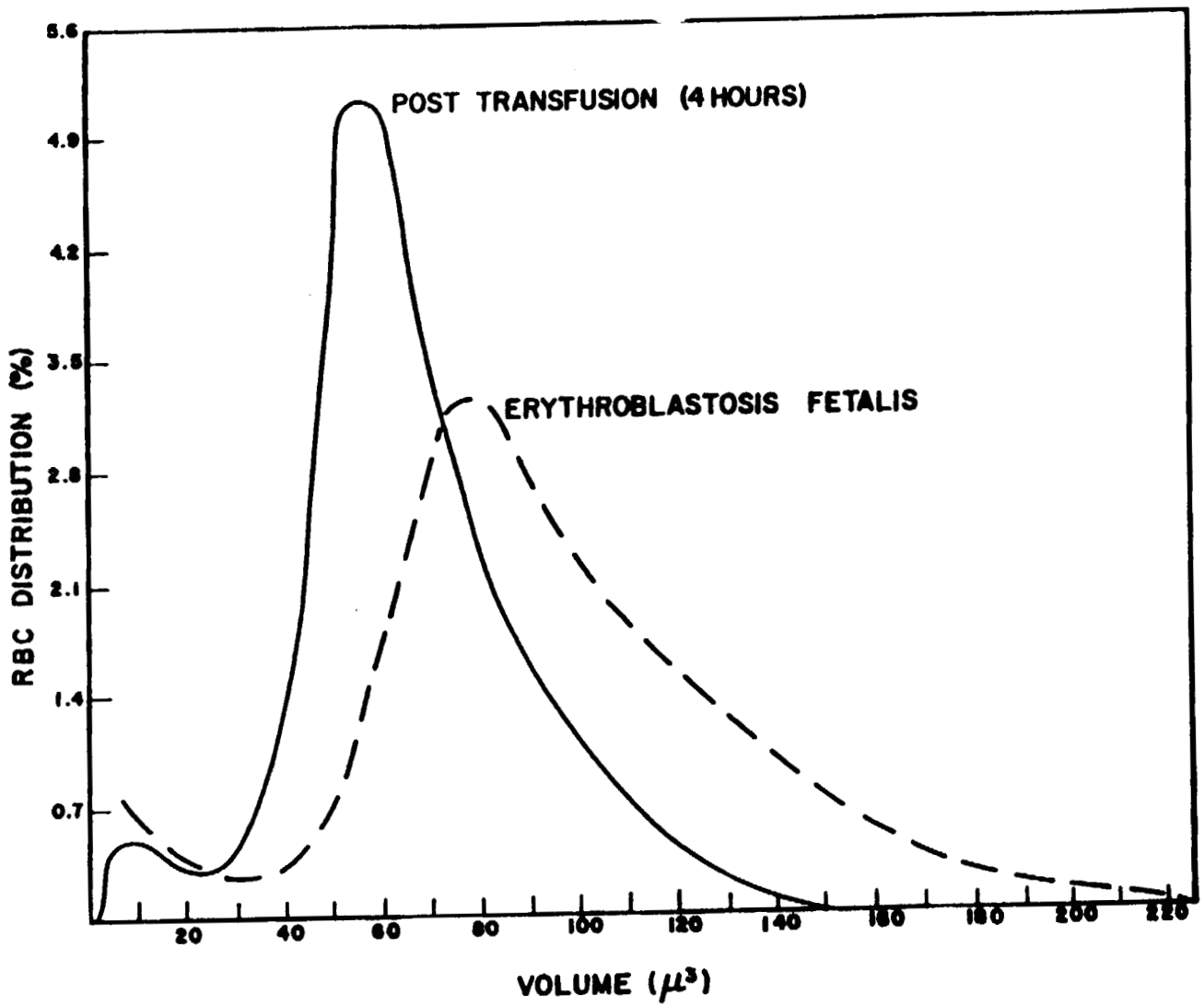

Fig. 5. Pre- and post-transfusion red blood cell profiles in a case of erythroblastosis fetalis showing the large cell preponderance in the presence of active hemolytic disease.

results provocative enough to warrant their continuation. Studies are in progress now that promise to explain as well as define the changes in RBC populations that commonly accompany various hematologic diseases.

REFERENCES

(1) C. C. Lushbaugh, J. A. Maddy, and N. J. Basmann, this report (1961), p. 372.

(2) E. Ponder, Hemolysis and Related Phenomena, Grune and Stratton, New York (1948).

RADIOPATHOLOGY SECTION PUBLICATIONS

(1) G. L. Humason and C. C. Lushbaugh, Selective Demonstration of Elastin, Reticulum and Collagen by Silver, Orcein and Aniline Blue, Stain Technol. 35, 209 (1960).

(2) C. C. Lushbaugh, J. Rose, and D. Wilson, A Practical Means for Routine Approximation of the Time of Recent Death, Police 5(1), 10 (1960).

(3) C. C. Lushbaugh, J. Sutton, and C. R. Richmond, The Question of Electrolyte Loss in the Intestinal Death Syndrome of Radiation Damage, Rad. Res. 13, 814 (1960).

CHAPTER 7

VETERINARY SERVICES SECTION

A general description of the veterinary program and the animal holding facilities of the laboratory has been given in the 2 previous semiannual reports (1,2).

Mechanization of Cage Washing Facility

During this report period, considerable effort has been expended on mechanizing the mouse cage washing operation to increase efficiency, decrease labor costs, and improve sanitation. The basic unit is an Industrial Systems continuous-feed cage washing unit with tandem washing, rinsing, and drying cycles. A mechanical disposal cycle has been added to the front of the washer to facilitate disposal of dirty wood shavings prior to inserting the cages into the washer (Fig. 1). The cages are turned upside down and the soiled bedding knocked out against 7 mechanized Neoprene rollers geared to the speed of the conveyor belt of the washing machine. The contents of the cages drop into a funnel-shaped hopper at the bottom of

Fig. 1. Wood shavings disposal unit added to the entrance of the mechanical cage washer.

which is a high-speed fan in series with an exhaust duct, terminating in a Dempster-Dumpster on the outside of the building (Fig. 2). There is an adjustable baffleplate at the bottom of the hopper to minimize throwback from the fan, which operates at 3600 RPM and is powered by a 3-HP, 440-volt, 3-phase electric motor. The unit eliminates accumulation of trash in garbage cans and transport to the outside disposal unit. After a cage washing operation, the hopper is washed down with a hose. Immediate disposal of the trash to the outside provides a much cleaner and neater washing operation and decreases the possibility of flies and other insects.

At the exit end of the washer, a "flip" bar has been added, which automatically turns the cages right side up on a set of mechanically driven rollers (Fig. 3), which transports them into the adjoining clean cage, bedding, and storage room. An automatic shavings dispenser, activated by a photocell which will mechanically dispense the proper amount of shavings into each cage, is now under construction and will be described in the next report. Once the clean cages are filled with shavings, they are stored in batches of 100 on transport carts ready to be taken to the mouse rooms.

Installation of "Quick" Disconnects in Animal Quarters

To save time and labor of the animal caretakers during

Fig. 2. Outside trash container showing exhaust duct from disposal hopper and fan.

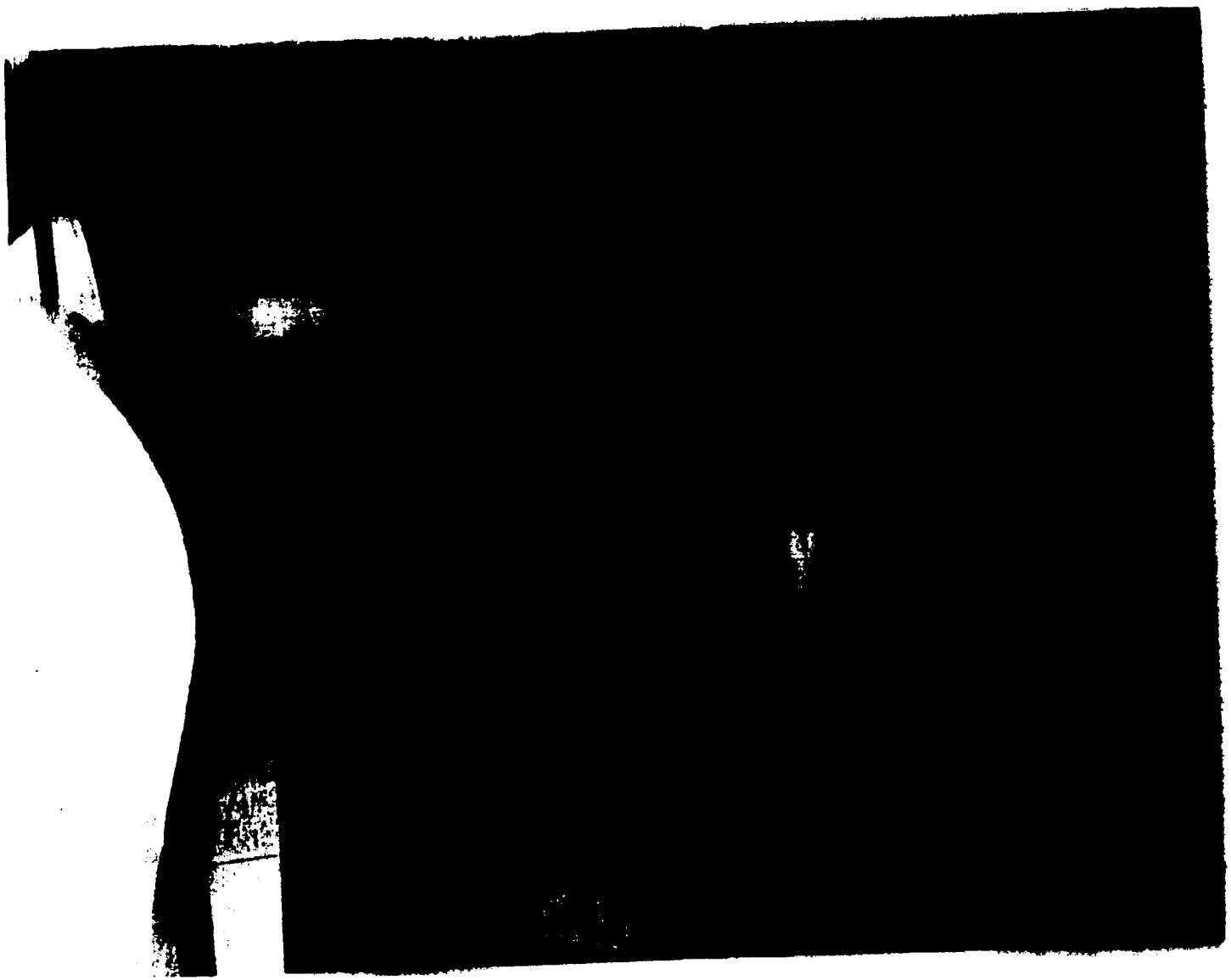

Fig. 3. "Flip" bar and mechanized roller conveyor at exit end of cage washer.

the process of washing down corridors and dog runs, "quick" disconnects or "Easy-On" connectors were installed on water and steam lines. Much time is saved by not having to screw hoses onto hose bibs. It is necessary now only to walk down the corridors and snap water and steam hoses onto the hose bibs.

Infantile Diarrhea in Mice

During the past year the mouse breeding program, especially for the RF strain, has been troubled with the appearance of diarrhea in young mice prior to weaning age. Losses ranged up to 25 to 30 per cent. Stools from the breeding mice and also from the affected young were cultured, but no bacteriological reason for the condition could be found. A review of the literature on the subject was undertaken and revealed the following.

The disease syndrome appears to be compatible with the symptoms of infantile diarrhea in suckling mice described in detail by Cheever and Mueller (3). The etiological agent for this disease is unknown, although there is evidence to support a viral etiology. Numerous other factors have been incriminated such as seasons, bedding, diet, etc. There is some feeling that more than one etiological factor may be involved. There is also some speculation that man may be the vector

carrier, although there is not enough evidence to support this hypothesis at the present time.

Control of the disease is difficult, since neither the mode of spread nor the source of infection is known. The general feeling is that first litters are the most severely affected between 10 to 15 days of age (later litters seem to build up immunity), but once weaned the animals are healthy. Therefore, it does not seem wise at this time to destroy all the animals (particularly the parents). Cheever and Mueller felt that building up a colony of multiparous females would cut down the incidence. In their studies, the disease was self-limiting and ended abruptly. This seems to be the general rule, and the disease seems to be disappearing from our colony.

Other pertinent information on the condition is given in Ref. 4 through 9.

Handling of Monkeys and Dogs in Metabolic Experiments

One of the principal projects of the Biochemistry Section is the study of interspecies correlations in the metabolism of radioisotopes using in vivo whole body counting procedures. The species being studied are mice, rats, dogs, monkeys, and man. The frequent whole body counting has necessitated adoption of routine procedures for handling monkeys and dogs.

After administration of the isotopes, the animals are placed in metabolism cages for collection of feces and urine. Periodically, they are removed from the metabolism cages and transported to the whole body counter for measurement of retained radioactivity. Feces and urine samples are collected daily and counted in the same counter to provide material balance observations. Stainless steel monkey (Fig. 4) and dog (Fig. 5) metabolism cages supplied by the Acme Sheet Metal Works are used.

During transportation and counting, animals are placed in Leverpak paper drums 26 in. in length and 16 in. in diameter. Perforations in the ends of the drums provide ample air circulation. The arrangement shown in Fig. 4 is used for loading monkeys from the metabolism cages into the Leverpak containers. The drum is placed on a cart at sufficient height to match the panel in the door of the metabolism cage and the cart fastened to the metabolism cage rack. A long chain is fastened to a short chain permanently attached to the monkey's collar. The long chain is fed through a hole in the bottom of the drum, the panel in the metabolism cage elevated, and the monkey pulled into the container. Before backing the cart away from the metabolism cage, the lid to the Leverpak is lowered into place and secured. The drum is then detached from the cart and taken to the counting room.

Fig. 4. Monkey metabolism cages and method of transferring animals to Leverpak containers for whole body counting.

Fig. 5. Dog metabolism cages.

The procedure is reversed when returning the monkey to the metabolism cage.

Beagles create no transfer and counting problems. They are merely lifted into the Leverpak drums, placed on Kardex tables, and pushed to the counting room. It is not even necessary to put lids in place (Fig. 6) until time to put the containers into the counter. The dogs seem to enjoy being counted and look forward to it as an opportunity to get some attention. The same cannot be said of the monkeys.

Receipt of Wards' Citation

A citation for humane animal quarters was awarded to the Laboratory by Wards, a national organization for the welfare of animals used for research in drugs and surgery. Ogden S. Johnson, Alternate H-4 Group Leader for Administration, accepted the award for the Health Research Laboratory at a banquet in St. Louis, Missouri, on October 27, 1960.

The citation read, "The humane citizens on Wards salute pioneering achievement toward stress-free research animal handling and housing. Through intelligent support of this kind toward a high standard of laboratory animal care, efficiency and accuracy of research are served."

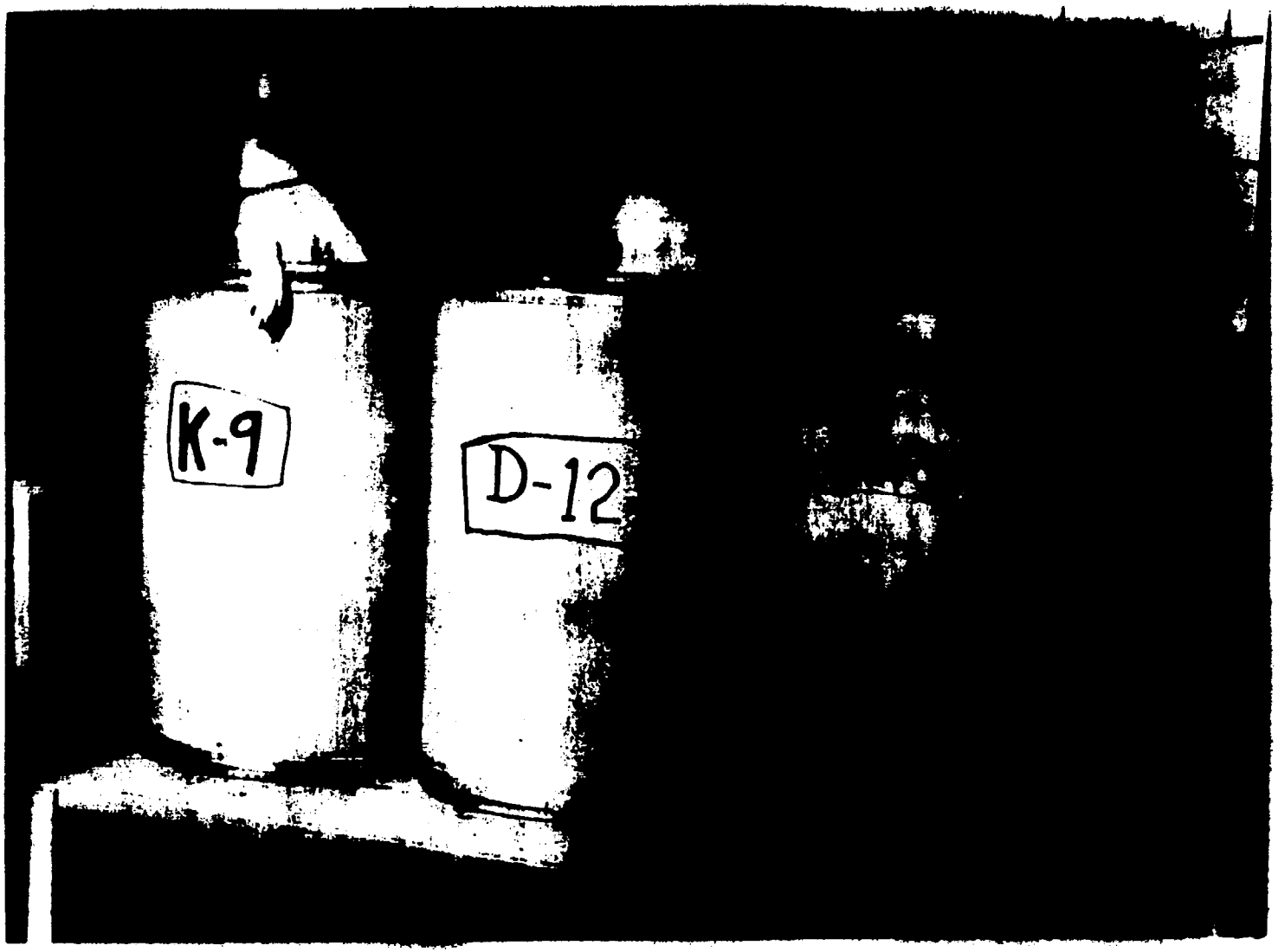

Fig. 6. Beagles awaiting their turn to be counted in the whole body counter.

Animal Production and Inventory

Mice

RFM Strain

Total number of babies born	2877
Total number of weanlings	2468
Weaning percentage	85.78
Number of breeding females	192

RF Strain

Total number of female weanlings	7467*
Number of females delivered for experimentation	5136
Number of females in stock	2318
Number of females being held for aging studies	1030
Number of breeding females	1026

AKR Strain

Total number of babies born	3002
Total number of weanlings	1837
Weaning percentage	61.19
Number of females delivered for experimentation	1174
Number of breeding females	162

CFW Strain

Total number of female weanlings	1718
Number of females delivered for experimentation	1174**
Number of breeding females	153

Sprague-Dawley Rats

Total number received	1300
Number delivered for experimentation	1029
Number of male rats in stock	725
Number of rats being held for aging studies	383

*Plus those sacrificed because of infantile diarrhea.

**Plus females saved to enlarge the breeding colony.

Beagles

Number of male beagles	32
Number of female beagles	11
Number of above females bred	2

Monkeys (rhesus)

Number in research (males)	3

Rabbits (New Zealand White)

Number of rabbits received	0
Number in stock	10

Guinea Pigs (English Short-haired)

Number of guinea pigs received	6
Number in stock	3

REFERENCES

(1) Los Alamos Scientific Laboratory Report LAMS-2445 (1960), p. 403.

(2) Los Alamos Scientific Laboratory Report LAMS-2455 (1960), p. 239.

(3) F. S. Cheever and J. H. Mueller, J. Exp. Med. 85, 405 (1947).

(4) A. M. Worden and W. Lane-Petter, eds., The UFAW Handbook on the Care and Management of Laboratory Animals, Second edition (1957), pp. 134, 243, 266.

(5) G. D. Snell, Biology of Laboratory Mouse, Second printing, Dover Publications, Inc., New York (1956).

(6) M. M. Rabstein, Proc. Animal Care Panel 8, 67 (1958).

(7) J S. Cass, Proc. Animal Care Panel 8, 13 (1958).

(8) S. M. Poiley, Proc. 3rd Annual Meeting of Animal Care Panel (1952), p. 92.

(9) H. A. Schneider, Proc. 6th Annual Meeting of Animal Care Panel (1955), p. 33.